ABSTRACT

Title of Document: DIRHODIUM CAPROLACTAMATE CATALYZED OXIDATIONS BY *TERT*-BUTYL HYDROPEROXIDE. FROM MECHANISMS TO NEW METHODOLOGIES.

Maxim Ratnikov, Ph.D., 2012

Directed By: Professor and Chair, Michael P. Doyle, Department of Chemistry and Biochemistry

Dirhodium caprolactamate, $Rh_2(cap)_4$, is a very efficient catalyst for the generation of the *tert*-butylperoxy radical from *tert*-butyl hydroperoxide, and the *tert*-butylperoxy radical is a highly effective oxidant for phenols and anilines. These reactions are performed with 70% aqueous *tert*-butyl hydroperoxide using dirhodium caprolactamate in amounts as low as 0.01 mol % in toluene and chlorobenzene to oxidize *para*-substituted phenols to 4-(*tert*-butyldioxy)cyclohexadienones. Electron rich and electron poor phenolic substrates undergo selective oxidation in good to excellent yields, but steric influences from bulky para substituents force oxidation onto the ortho position resulting in *ortho*-quinones. Comparative results with $RuCl_2(PPh_3)_3$ and CuI are provided, and mechanistic comparisons are made between these catalysts that are based on diastereoselectivity (reactions with estrone), regioselectivity (reactions with *p*-*tert*-butylphenol) and chemoselectivity in the formation of 4-(*tert*-

butyldioxy)cyclohexadienones. The data obtained are consistent with hydrogen atom abstraction by the *tert*-butylperoxy radical followed by radical combination between the phenoxy radical and the *tert*-butylperoxy radical. Under similar reaction conditions *para*-substituted anilines are oxidized to nitroarenes in good yield.

An efficient one-pot tandem sequence forming heterocycles is developed. The method consists of an efficient phenol oxidation with inexpensive T-HYDRO catalyzed by dirhodium caprolactamate followed by Brønsted acid promoted cyclization. Substrate scope includes uses of L-tyrosine ester and dipeptide derivatives. Application of chiral phosphoric acids for asymmetric cyclization is discussed. Previously unreported peroxide cleavage with $TiCl_4$ enables a rapid synthesis of cleroindidin F.

A general mechanism is proposed for transition metal catalyzed oxidative Mannich reactions of *N*-methylanilines with *tert*-butyl hydroperoxide (TBHP) as an oxidant. Kinetic data and isotope labeling of the *N*-methyl group suggest a rapid equilibrium between an iminum ion and solvent or TBHP preceding Mannich addition. Linear free-energy relationship (LFER) analysis, kinetic and product isotope effects, and utilization of radical clock substituents establish *tert*-butylperoxy radicals as an oxidant in dirhodium(II) caprolactamate [$Rh_2(cap)_4$] catalyzed oxidations of *N*,*N*-dialkylaniline by TBHP. Isotope effects measured for various transition metal salts reveal a general role of alternative catalysts as initiators of TBHP decomposition in *N*,*N*-dialkylaniline oxidations. New mechanistic insights led the development of the novel $FeCl_3$ catalyzed oxidative Mannich reaction.

DIRHODIUM CAPROLACTAMATE CATALYZED OXIDATIONS BY *TERT*-BUTYL HYDROPEROXIDE. FROM MECHANISMS TO NEW METHODOLOGIES.

By

Maxim Olegovich Ratnikov

Dissertation submitted to the Faculty of the Graduate School of the
University of Maryland, College Park, in partial fulfillment
of the requirements for the degree of
Doctor of Philosophy
2012

Advisory Committee:
Professor Michael P. Doyle, Chair
Professor Kyu Yong Choi
Professor Daniel Falvey
Professor Steven Rokita
Professor Andrei N. Vedernikov

Acknowledgements

I am exceptionally grateful to Professor Michael Doyle. My development as a scientist could not be possible without his tutelage. His guidance and leadership always kept my motivation high while his high standards constantly pushed me to new levels. Professor Michael Doyle always had research and leadership opportunities available that allowed my continuous growth. At the end of my journey for the PhD, I am proud to be a Doyle group alumni.

I am also thankful to Professors Kyu Yong Choi, Daniel Falvey, Steven Rokita, and Andrei Vedernikov for serving on my committee. Their questions were always stimulating my development. Special thanks to Andrei Vedernikov and Steven Rokita for teaching the best classes that I have ever taken.

I would like to thank my colleagues Dr. Xinfang Xu, Dr. Charles Shanahan, Dr. Dmitry Shabashov, Dr. Ryan Burgin, Dr. Yu Liu, Phong Truong, Xiaochen Wang, Xichen Xu, Deana Jabar, Yu Qian, and Derek Jendras for fruitful discussions and thoughtful feedbacks. Special thanks to Xinfang for his help with completion of my final project. I am grateful to Charles, Ryan, and Dmitry for our collaborative work.

This work would not be possible without the help of my undergraduate students, Petra Goldmann, Linda Farkas, Brendan Mallory, and Dmitry Kuznetsov. Special thanks to Petra and Linda for outstanding work ethic that found confirmation in publications and participation at the ACS National Meeting.

Finally, I would like to thank Dr. Kostya Bobyk, Fazel Fakhari, Romina Heymann, and Shrin Pal for being around through my tenure as a graduate student. Their support and positive nature were invaluable for me.

List of Abbreviations

Ac	acetyl
BINOL	1,1’-bi-2-naphthol
Boc	*tert*-butyloxycarbonyl
cap	ε-caprolactamate
Cbz	carbobezyloxy
DCE	1,2-dichloroethane
DCM	dichloromethane
dr	diastereomeric ratio
ee	enantiomeric excess
HAT	hydrogen atom transfer
IBX	2-iodoxybenzoic acid
KIE	kinetic isotope effect
LFER	linear free energy relationship
PIE	product isotope effect
PT	proton transfer
p-TsOH	p-toluenesulfonic acid
rpm	revolutions per minute
rt	room temperature
SCE	standard calomel electrode
SET	single electron transfer
TBHP	*tert*-butyl hydroperoxide
T-HYDRO	70% aqueous solutions of *tert*-butyl hydroperoxide

Table of Contents

Acknowledgements ii
Table of Contents iii
List of Abbreviations iii
List of Tables v
List of Figures viii
List of Schemes x
Chapter 1: Dirhodium Catalyzed Phenol and Aniline Oxidations with T-HYDRO. Substrate Scope and Mechanism of Oxidation
Synopsis 1
Introduction – Synthetic Methods and Mechanistic Models for Phenol Oxidation 2
Results and Discussion 15
Phenol Oxidation 15
Aniline Oxidation 28
Conclusion 32
Experimental 33
Chapter 2: Tandem Sequence of Phenol Oxidation and Intramolecular Addition as a Versatile Method in Building Heterocycles
Synopsis 50
Introduction – Transformations of 4-Substituted 2,5-Dienones 51
Results and Discussion 61
Conclusion 79
Experimental 80
Chapter 3: Mechanistic Investigation of Oxidative Mannich Reaction with *tert*-Butyl Hydroperoxide. The Role of Transition Metal Salts
Synopsis 116
Introduction -- Synthetic Methods and Mechanistic Models for Oxidative Mannich Reaction 118
Results and Discussion 140
Mechanistic Studies of the Transition Metal Salt Catalyzed Mannich Reaction with T-HYDRO 140
Oxidative Mannich Reaction by O_2 Catalyzed by $FeCl_3 \times 6\ H_2O$ 163
Conclusion 169
Experimental 170
Bibliography 214

List of Tables

Table 1-1. Comparison of transition metal complexes in the oxidation of 1-acetylcyclohexene **22** by T-HYDRO.

Table 1-2. Catalytic *tert*-butyl hydroperoxide oxidation of 4-substituted phenols and 2-naphthol.

Table 1-3. Oxidation of phenols bearing bulky 4-substituents with 4.0 equivalents of T-HYDRO in toluene.

Table 1-4. Dirhodium caprolactamate catalyzed aniline oxidation.

Table 1-5. Dirhodium caprolactamate catalyzed oxidation of primary amines by TBHP.

Table 1-6. Percent conversions for transition metal catalyzed oxidations of 2,6-di-*tert*-butyl-4-methylphenol (**27**) by T-HYDRO in DCE at 40 °C.

Table 1-7. Percent conversions for transition metal catalyzed oxidations of 2,6-di-*tert*-butyl-4-methylphenol (**27**) by T-HYDRO in chlorobenzene at 40 °C.

Table 2-1. Optimization of a catalyst for the phenol oxidation by T-HYDRO.

Table 2-2. Temperature, concentration, and solvent optimization for the $Rh_2(cap)_4$ catalyzed oxidation of **8** by T-HYDRO.

Table 2-3. Optimization of the oxidant and mode of addition of the $Rh_2(cap)_4$ catalyzed oxidation of **8.**

Table 2-4. Dirhodium caprolactamate oxidation of phenols bearing nucleophilic functional groups by T-HYDRO.

Table 2-5. Optimization of conditions for tandem phenolic oxidation - Michael addition.

Table 2-6. Tandem phenol oxidation – oxo-Michael addition.

Table 2-7. Tandem phenol oxidation – aza-Michael addition.

Table 2-8. The development of O-O bond cleavage method for conversion of the internal dialkyl peroxide **42** to cleroindicin F **(10)**.

Table 3-1. Kinetic and product isotope effects of oxidative Mannich reaction of 4-substituted *N*,*N*-dimethylanilines and *N*-phenylindole with T-HYDRO catalyzed complex **20** and with complex **23**.

Table 3-2. Kinetic isotope effects of the $Rh_2(cap)_4$ catalyzed oxidations of 4-substituted *N*,*N*-dimethylanilines by T-HYDRO.

Table 3-3. Product isotope effects of the $Rh_2(cap)_4$ catalyzed oxidations of 4-substituted *N*,*N*-dimethylanilines by T-HYDRO.

Table 3-4. Kinetic isotope effects of the $Rh_2(cap)_4$ catalyzed oxidations of 4-substituted *N*,*N*-dimethylanilines by T-HYDRO with and without N_2 flow and by O_2.

Table 3-5. Relative acidities of substituted carbon adjacent to nitrogen in *N*,*N*-dialkylaniline cation-radicals.

Table 3-6. Catalyst optimization of transition metal salt catalyzed oxidation of **5** by O_2.

Table 3-7. Conditions optimization for the $FeCl_3$ catalyzed oxidative Mannich reaction by O_2 of 4-methyl-*N*,*N*-dimethylaniline and **2**.

Table 3-8. The $FeCl_3$ catalyzed oxidative Mannich reaction by O_2 of *N*,*N*-dialkylanilines and **8**.

Table 3-9. Monitored peak pairs ^1H NMR peaks for the reaction rate determination.

Table 3-10. ^1H NMR peaks monitored for kinetic isotope effect.

Table 3-11. ^1H NMR chemical shifts of methoxy and *tert*-butylperoxy hemiaminals.

List of Figures

Figure 1-1. Conversions determined by ^{1}H NMR spectroscopy for transition metal catalyzed oxidations of 2,6-di-*tert*-butyl-4-methylphenol (**27**) by T-HYDRO in DCE at 40 °C.

Figure 1-2. Percent conversion versus time determined by ^{1}H NMR spectroscopy for $Rh_2(cap)_4$ catalyzed oxidation of **27** by T-HYDRO (4.0 equiv) at 40°C in DCE and PhCl.

Figure 1-3. Comparative time courses determined by ^{1}H NMR spectroscopy for the oxidation of **27** by T-HYDRO (4.0 equiv) in chlorobenzene catalyzed by 0.05 mol % of $Rh_2(cap)_4$, $RuCl_2(PPh_3)_3$, or CuI at 40 °C.

Figure 1-4. Comparative time courses for the oxidation of **27** by 4.0 and 2.0 equiv. of T-HYDRO in chlorobenzene catalyzed by 0.03 mol % of $Rh_2(cap)_4$ at 40 °C.

Figure 1-5. Comparative time courses determined by ^{1}H NMR spectroscopy for $Rh_2(cap)_4$ catalyzed oxidations of **27** by T-HYDRO at 40°C.

Figure 1-6. Comparative time courses determined by ^{1}H NMR spectroscopy for $RuCl_2(PPh_3)_3$ catalyzed oxidation of **27** by 4.0 equiv. of T-HYDRO at 40°C.

Figure 1-7. Comparative time courses determined by ^{1}H NMR spectroscopy for copper(I) halide catalyzed oxidation of **27** by 4.0 equiv. of T-HYDRO at 40°C.

Figure 2-1. Determination of stereochemistry of hydrobenzopyrane **46**.

Figure 2-2. NOE analysis of dihydroindols **57** and **58**.

Figure 2-3. Mechanistic model of enantioselective desymmetrization of 2,5-dienones catalyzed by chiral phosphoric acid.

Figure 3-1. The change of **15** to **16** ratio with time in the oxidation of *N*,*N*-dimethylaniline by 2 equivalents of T-HYDRO catalyzed by 0.5 mole % of $Rh_2(cap)_4$.

Figure 3-2. Equilibration of **16** to **15** in 0.14 M solution of methanol.

Figure 3-3. Kinetics of the $Rh_2(cap)_4$ catalyzed oxidative Mannich reaction in methanol by T-HYDRO of *N*,*N*-dimethylaniline and siloxyfuran **8.**

Figure 3-4. Hammett LFER analysis of the $Rh_2(cap)_4$ catalyzed oxidations by T-HYDRO of 4-substituted *N*,*N*-dimethylanilines at 40 °C in methanol. Each reaction rate was measured at least three times, and the error margins were calculated as a standard deviation of the reaction rates.

Figure 3-5. KIE and PIE measured for the $Rh_2(cap)_4$ catalyzed oxidative Mannich reaction by T-HYDRO.

List of Schemes

Scheme 1-1. Summary of transition metal salts catalyzed oxidations of phenols, nitroarenes, and primary amines having an α-C-H bond by TBHP.

Scheme 1-2. The list of selected catalysts for the allylic oxidation by TBHP of cholesteryl acetate **1**.

Scheme 1-3. Dirhodium caprolactamate oxidation of 1-acetylcyclohexene **3**.

Scheme 1-4. Benzylic oxidation of **5** by anhydrous TBHP catalyzed by $Rh_2(cap)_4$.

Scheme 1-5. Oxidation of 7-position of steroid **7** by T-HYDRO catalyzed by $Rh_2(cap)_4$.

Scheme 1-6. Oxidation of propargylic methylene position of **9** by T-HYDRO catalyzed by $Rh_2(cap)_4$.

Scheme 1-7. Relative oxidation rates of allylic, benzylic and propargylic positions.

Scheme 1-8. Dirhodium caprolactamate catalyzed oxidative Mannich addition of aniline **12** to siloxyfuran **13** and oxidation of secondary amine **15** to imine **16**.

Scheme 1-9. Conversion of phenols to 4-(*tert*-butyldioxy)cyclohexa-2,5-dienones with anhydrous TBHP under $RuCl_2(PPh_3)_3$ catalysis and the applications of 2,5-dienone **18** in syntheses of vitamins K_1 and K_3.

Scheme 1-10. Proposed mechanism for $RuCl_2(PPh_3)_3$ catalyzed phenol oxidation by anhydrous TBHP.

Scheme 1-11. Mechanism of phenol oxidation by stoichiometric $[Ru(bpy)_2(py)(O)](ClO_4)_2$.

Scheme 1-12. Dirhodium caprolactamate catalyzed conversion of *tert*-butyl hydroperoxide to the *tert*-butylperoxy radicals.

Scheme 1-13. Proposed mechanism for allylic oxidation of cyclic alkenes by TBHP catalyzed by $Rh_2(cap)_4$.

Scheme 1-14. Conversion of phenol **27** to 2,5-dienone **28**.

Scheme 1-15. Dirhodium caprolactamate oxidation of *p*-hydroxybenzoic acid **47** by T-HYDRO.

Scheme 1-16. Possible pathways of transformation of **47** into **48**.

Scheme 1-17. Dirhodium caprolactamate oxidation of bisphenol A.

Scheme 1-18. Oxidation of estrone derivatives **56** and **58** with T-HYDRO under $Rh_2(cap)_4$ catalysis.

Scheme 1-19. Oxidation of phenol **41** in *tert*-butyl alcohol by T-HYDRO catalyzed by $Rh_2(cap)_4$ and $RuCl_2(PPh_3)_3$.

Scheme 1-20. Oxidation of phenol **27** by T-HYDRO catalyzed by $[Rh_2(cap)_4]^+BF_4^-$.

Scheme 1-21. Dirhodium caprolactamate oxidation of aniline **60** by T-HYDRO.

Scheme 1-22. Plausible mechanism for $Rh_2(cap)_4$ catalyzed aniline oxidation by TBHP.

Scheme 1-23. Mechanism of Transition Metal Catalyzed Phenolic Oxidation with TBHP.

Scheme 2-1. Summary of tandem $Rh_2(cap)_4$ catalyzed phenol oxidation and Brønsted acid catalyzed intramolecular Michael addition.

Scheme 2-2. Dirhodium caprolactamate oxidation of 4-substituted phenols by T-HYDRO.

Scheme 2-3. Rearrangement of 4-(*tert*-butylperoxy)cyclohexa-2,5-dienones to 2-substituted *p*-quinones by $TiCl_4$.

Scheme 2-4. Mechanism proposed by Murahashi for rearrangement of 4-(*tert*-butylperoxy)cyclohexa-2,5-dienones to 2-substituted *p*-quinones by $TiCl_4$.

Scheme 2-5. *p*-Toluenesulfonic acid catalyzed intramolecular oxo-Michael addition of alcohols to 4-hydroperoxy-2,5-dienones **2** and **4** and 4-hydroxy-2,5-dienone **3** and **5.**

Scheme 2-6. Asymmetric intramolecular oxo-Michael addition of **7** and **8** catalyzed by chiral phosphoric acid **6**.

Scheme 2-7. Synthesis of cleroindicin F (**10**) from tyrasol (**11**).

Scheme 2-8. Ammonium salt **12** catalyzed intramolecular Michael additions of aldehydes tethered to 2,5-dienones.

Scheme 2-9. Application of secondary amine **14** catalyzed asymmetric intramolecular Michael addition of tethered aldehydes to 2,5-dienones in syntheses of *cis*-6,5-, *cis*-6,6-, and *cis*-6,7-bicyclic systems.

Scheme 2-10. Asymmetric intramolecular Michael addition of β-ketoesters to 4-alkyl-2,5-dienones.

Scheme 2-11. Cinchonine-derived urea **27** catalyzed asymmetric intramolecular Michael addition of bisphenylsulfonyl methylene to 2,5-dienone.

Scheme 2-12. Three-step removal of bisphenylsulfonyl functionality.

Scheme 2-13. Reported methods of reduction of internal peroxides.

Scheme 2-14. Possible mechanism of O-O bond cleavage of **42** by $TiCl_4$.

Scheme 3-1. Summary of mechanistic investigations of transition metal catalyzed oxidative Mannich reaction with TBHP as an oxidant.

Scheme 3-2. Summary of the ferric chloride catalyzed oxidative Mannich reaction of substituted *N*-methylanilines and siloxyfuran with O_2 as an oxidant.

Scheme 3-3. Strategies for preparation a key intermediate of the Mannich reaction.

Scheme 3-4. Selected examples of the transition metal catalyzed oxidative Mannich reaction by O_2 and DTBP.

Scheme 3-5. General scheme of oxidative Mannich reaction with TBHP.

Scheme 3-6. The $Rh_2(cap)_4$ catalyzed Mannich reaction of *N*,*N*-dialkylanilines and siloxyfurans.

Scheme 3-7. Proposed mechanism the $Rh_2(cap)_4$ catalyzed oxidative Mannich reaction with T-HYDRO.

Scheme 3-8. Preparation and interconversion of **15** and **16**.

Scheme 3-9. Kinetic and product isotope effects of *N*,*N*-dimethylanilines oxidations by anhydrous TBHP catalyzed $RuCl_2(PPh_3)_3$ and by H_2O_2 catalyzed by $RuCl_3$.

Scheme 3-10. The adopted mechanism of $RuCl_2(PPh_3)_3$ catalyzed *N*,*N*-dialkylaniline oxidation by TBHP.

Scheme 3-11. The oxidative Mannich reaction of *N*,*N*-dialkylanilines and indoles with T-HYDRO catalyzed by ruthenium complex **20**.

Scheme 3-12. The proposed mechanism for the formation of Fe oxo-complex **23** from **22** with TBHP.

Scheme 3-13. Demethylation of *N*,*N*-dimethylaniline by stoichiometric Ru oxo-complex **21** and the oxidative Mannich reaction of **3** and indole **24** with *N*-Oxide **25** catalyzed complex **20**.

Scheme 3-14. The reaction employed for LFER analysis.

Scheme 3-15. Mannich reaction of hemiaminal **16** with indole **24**.

Scheme 3-16. The oxidative Mannich reaction isoquinoline **1** and indole.

Scheme 3-17. The CuBr catalyzed oxidative Mannich reaction of tetrahydroisoquinoline **1** and nitromethane with TBHP in the presence of radical scavenger **28**.

Scheme 3-18. Two proposed mechanisms for the CuBr catalyzed oxidative Mannich reaction with TBHP as the oxidant.

Scheme 3-19. The mechanism of CuBr oxidative Mannich reaction of isoquinoline and indole with TBHP.

Scheme 3-20. Preparation of peroxy hemiaminal **35** and its reaction with nitromethane.

Scheme 3-21. Proposed mechanism for the CuBr catalyzed oxidation of tetrahydroisoquinoline by TBHP.

Scheme 3-22. Oxidation potentials of **1** and **3**.

Scheme 3-23. Dirhodium caprolactamate catalyzed *N*,*N*-dimethylaniline oxidation by T-HYDRO.

Scheme 3-24. Mechanistic implications of the observed ratio of **15** to **16** at the initial stages of the $Rh_2(cap)_4$ catalyzed N,N-dimethylaniline oxidation by T-HYDRO.

Scheme 3-25. The equilibrium of **15** and **16** in methanol.

Scheme 3-26. Isotope scrambling experiment.

Scheme 3-27. Mechanism of the loss of deuterium labeling.

Scheme 3-28. The $Rh_2(cap)_4$ catalyzed oxidative Mannich reaction of **3** and *N*-methylindole (**41**) in toluene.

Scheme 3-29. Summary of conversion of an iminium ion formed in the oxidation of *N*,*N*-dialkylanilines to the final Mannich adduct.

Scheme 3-30. Two potential rate-determining steps of the *N*,*N*-dimethylanilines oxidations by T-HYDRO.

Scheme 3-31. The rate-determining step of the $Rh_2(cap)_4$ catalyzed *N*,*N*-dimethylaniline oxidation by T-HYDRO.

Scheme 3-32. KIE and PIE experiments of the $Rh_2(cap)_4$ catalyzed oxidations of 4-substituted *N*,*N*-dimethylanilines by T-HYDRO.

Scheme 3-33. Kinetic model of the $Rh_2(cap)_4$ catalyzed oxidations of 4-substituted *N*,*N*-dimethylanilines by T-HYDRO.

Scheme 3-34. Dimerization of the *tert*-butylperoxy radicals.

Scheme 3-35. Possible mechanisms of the irreversible C-H cleavage in transition metal salt catalyzed oxidation of *N*,*N*-dimethylanilines.

Scheme 3-36. Rate of cyclopropane opening rates of radical trap substituents.

Scheme 3-37. Synthesis of **50** and **52** for radical trap experiments.

Scheme 3-38. The $Rh_2(cap)_4$ catalyzed oxidations by T-HYDRO of *N*,*N*-dialkylanilines bearing radical trap substituents.

Scheme 3-39. The $FeCl_3 \times 6\ H_2O$ catalyzed oxidative Mannich reaction by O_2 of **5** and **8**.

Chapter 1: Dirhodium Catalyzed Phenol and Aniline Oxidations with T-HYDRO. Substrate Scope and Mechanism of Oxidation

Synopsis[1]

Dirhodium caprolactamate [$Rh_2(cap)_4$] is a very efficient catalyst for the generation from *tert*-butyl hydroperoxide (TBHP) of *tert*-butylperoxy radicals (Scheme 1-1) that are a highly effective oxidants of phenols and anilines. 70% aqueous *tert*-butyl hydroperoxide (T-HYDRO) using $Rh_2(cap)_4$ as a catalyst in amounts as low as 0.03 mole % oxidize 4-substituted phenols to 4-(*tert*-butyldioxy)cyclohexa-2,5-dienones. Although these transformations have normally been performed in halocarbon solvents, there is a significant rate enhancement when the $Rh_2(cap)_4$ catalyzed phenol oxidations are performed in toluene or chlorobenzene. Electron-rich and electron-poor phenolic substrates undergo selective oxidations to afford 2,5-dienone products in 57-99% yields (Scheme 1-1). Steric hindrance of phenolic 4-substituents increases the relative amount of oxidation at the ortho position of phenol furnishing 4-substituted *ortho*-quinones. Comparative results with $RuCl_2(PPh_3)_3$ and CuI are provided, and mechanistic comparisons are made between these catalysts that are based on diastereoselectivity (reactions with estrone), regioselectivity (reactions with 4-*tert*-butylphenol) and chemoselectivity in the formation of 4-(*tert*-butylperoxy)-2,5-cyclohexadienones. The data obtained are consistent with hydrogen atom abstraction by the *tert*-butylperoxy radical followed by radical recombination between the phenoxy radical and the *tert*-butylperoxy radical (Scheme 1-1). Under similar reaction conditions anilines are

oxidized to nitroarenes in good yields, presumably through the corresponding nitrosoarenes, and primary amines having an α-C-H bond are oxidized to carbonyl compounds by TBHP in the presence of catalytic amounts of $Rh_2(cap)_4$ (Scheme 1-1).

Scheme 1-1. Summary of transition metal salts catalyzed oxidations of phenols, nitroarenes, and primary amines having an α-C-H bond by TBHP.

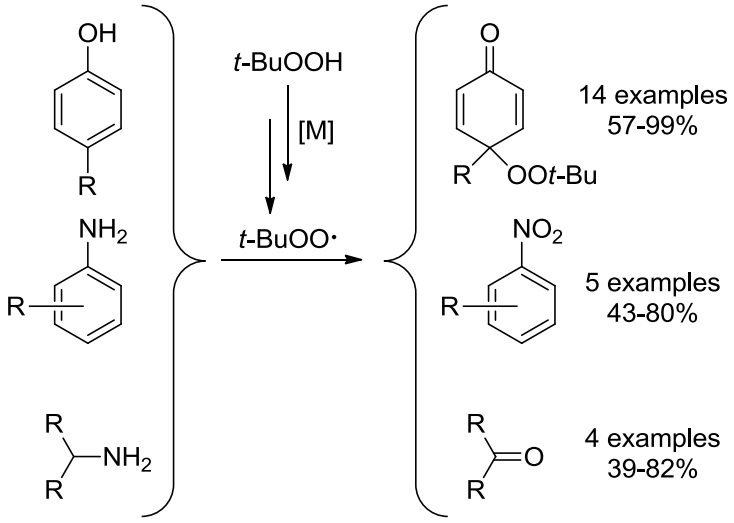

[M] = $Rh_2(cap)_4(MeCN)_2$, $RuCl_2(PPh_3)_3$

Introduction -- Synthetic Methods and Mechanistic Models for Phenol Oxidation

tert-Butyl hydroperoxide (TBHP) is an attractive terminal oxidant for development of a range of oxidative processes.[2] It poses fewer handling risks than 70% H_2O_2 in water or peracetic acid.[3] The high solubility of TBHP in organic solvents allows the preparation of anhydrous solutions of this oxidant. *tert*-Butyl hydroperoxide has a half-life of over 520 hours in refluxing benzene at 0.2 M concentration.[3] Its low acidity (pK_a = 12.8) and the formation of volatile products are the other advantages.[3] This

reagent usually allows oxidations to occur with greater selectivities than does hydrogen peroxide[4] and with higher reaction rates than do cumyl hydroperoxide or dioxygen.[5] Synthetic applications include epoxidation,[6] carbon-carbon double bond oxidations,[5d,7] oxidation of non-activated C-H bonds,[4,8] formation of internal peroxides,[5a,9] and polymerization.[10]

Despite its numerous applications in catalytic oxidative processes, *tert*-butyl hydroperoxide shows no reactivity in the absence of catalytic species.[5b,c] Kochi proposed that the active catalyst in TBHP decomposition should have a 1-electron redox pair and confirmed this proposal for iron(II), copper(I), and cobalt(II) cations.[11] The allylic oxidation by TBHP of cholesteryl acetate **1** shows that the list of potential catalysts include not only transition metal complexes of Cr,[12] Mn,[13] Ru,[14] and Pd[15] but also inorganic compounds, e.g. $BiCl_3$,[16] NaOCl,[17] and $NaClO_2$[18] (Scheme 1-2). Presumably, these 1-electron redox reagents form *tert*-butylperoxy radicals and the flux of these radicals determines the yield and selectivity of the oxidations.[19]

Scheme 1-2. The list of selected catalysts for the allylic oxidation by TBHP of cholesteryl acetate **1**.

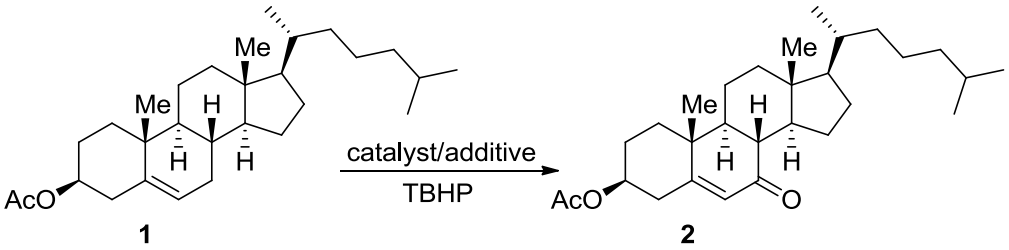

1 **2**

catalyst/additive = NaOCl (200 mol %), $BiCl_3$ (10 mol %), CuI (2.6 mol %), $RuCl_3$ (0.7 mol %), $Cr_2O_7^{2-}$ x 2 PyH^+ (2.5 mol %), $Rh_2(cap)_4$ (1.0 mol %)

The comparison of the turnover rates of the allylic oxidation of cholesteryl acetate shows greater turnover rates achieved with $Rh_2(cap)_4$ than with Fe(II),[20] Cu(I),[21] Ru(III),[14] and Cr(VI).[12] Doyle attributed this fact[22] to a higher rate of TBHP reduction by $Rh_2(cap)_4$ due to its 11 mV (vs. SCE)[23] oxidation potential that is lower than the potentials measured for Fe(II)/Fe(III),[11] Cu(I)/Cu(II),[11] Ru(III)/Ru(IV),[24] and Cr(V)/Cr(VI)[25] redox pairs. Hence, our research group investigated the ability of $Rh_2(cap)_4$ to catalyze oxidative transformations by TBHP.

Oxyfunctionalization of cyclic alkenes was the first $Rh_2(cap)_4$ catalyzed oxidation with TBHP (Scheme 1-3).[22] The initial procedure utilized an anhydrous solution of TBHP in decane and required substoichiometric amounts of potassium carbonate to increase product yields from oxidation to 70-90%. At the same time, $Rh_2(cap)_4$ loading could be lowered to 0.1 mole %.

Scheme 1-3. Dirhodium caprolactamate oxidation of 1-acetylcyclohexene **3**.

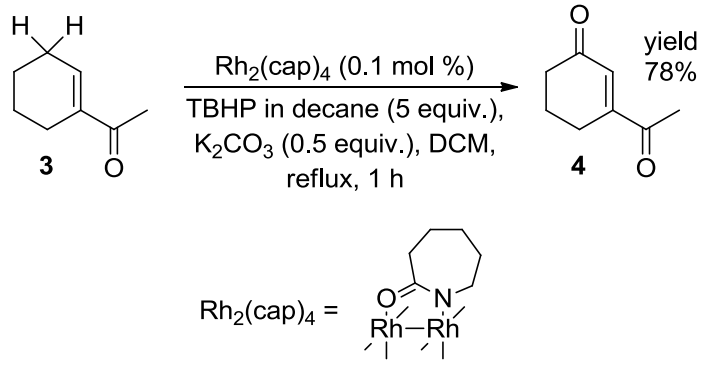

Following this initial report, our group expanded the scope of $Rh_2(cap)_4$ catalyzed oxidative transformations to benzylic oxidations (Scheme 1-4).[26] Isolated yields, obtained under optimized conditions, were generally above 80%. Oxidation of palmarumycin CP_2

precursor **6** showed that the $Rh_2(cap)_4$ catalyzed benzylic oxidation furnished higher yields and generated less waste materials than the chromium catalyzed protocol[27] or IBX based methods.[28] That no reaction occurs with aromatic rings bearing electron-withdrawing substituents (e.g., nitrile) is a limitation of the $Rh_2(cap)_4$ oxidative system.

Scheme 1-4. Benzylic oxidation of **5** by anhydrous TBHP catalyzed by $Rh_2(cap)_4$.

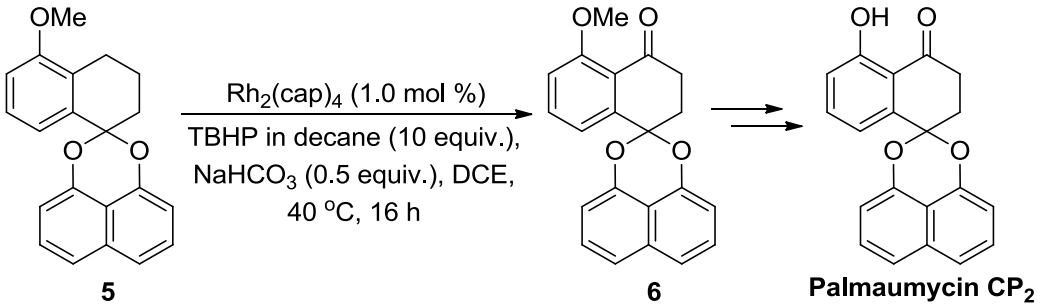

Further investigations of the synthetic potential of the $Rh_2(cap)_4$ oxidative system revealed that steroids are oxidized regioselectively at their 7-position in 38-87% yield by a 70% aqueous solution of *tert*-butyl hydroperoxide (T-HYDRO) (Scheme 1-5).[29] The replacement of anhydrous solutions of TBHP with its less expensive aqueous solution was the next step of procedure optimization. The oxidation of steroidal cores showed that steric and electronic factors contribute to the regioselectivity of oxidation. Electronic factor favors the oxidation of allylic methylene groups of the steroidal core. Presumably, steric factor affords exclusive oxidation at the less hindered 7-position the steroidal core and not at the 4-position (Scheme 1-5).

Scheme 1-5. Oxidation of 7-position of steroid **7** by T-HYDRO catalyzed by $Rh_2(cap)_4$.

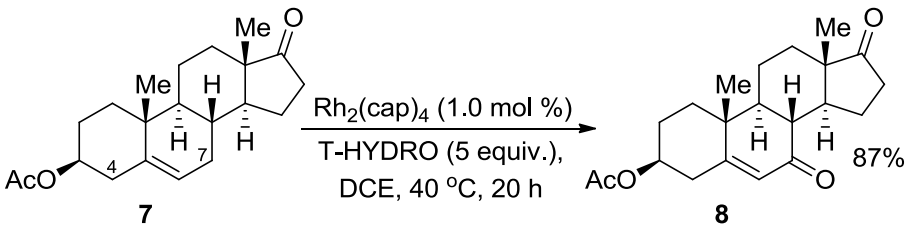

Oxyfunctionalization of propargylic methylene positions was achieved with T-HYDRO catalyzed by $Rh_2(cap)_4$ (Scheme 1-6).[30] Yields of ynones up to 80% obtained in a single step offer a synthetic advantage over the conventional two-step sequence of acetylide addition to aldehydes followed by oxidation.[31] The scope of alkynes evaluated in the propargylic oxidation revealed that the oxidation can be achieved in the presence of alcohol groups and trialkylsilane-protected acetylenes and alcohols.

Scheme 1-6. Oxidation of propargylic methylene position of **9** by T-HYDRO catalyzed by $Rh_2(cap)_4$.

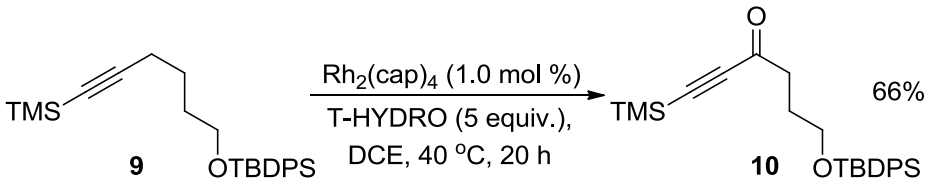

The relative rates of $Rh_2(cap)_4$ catalyzed oxyfunctionalization of allylic, benzylic and propargylic positions correlate with relative donating abilities of carbon-carbon double and triple bonds as well as a non-substituted aromatic ring. Our group found that **9** underwent oxidation at a higher rate than did **10** and **11** (Scheme 1-7). The latter two substrates underwent oxidation at a similar rate (Scheme 1-7). These competitive

experiments could be used to predict the chemoselectivity of substrates containing a combination of unsaturated functional groups.

Scheme 1-7. Relative oxidation rates of allylic, benzylic and propargylic positions.

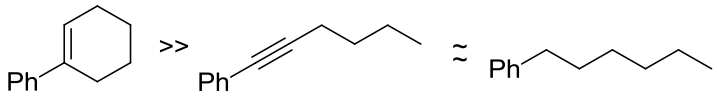

9 **10** **11**

Our group successfully applied the $Rh_2(cap)_4$ oxidative system to *N*,*N*-dialkylanilines that underwent the oxidative Mannich reaction with siloxyfurans under mild conditions in 50-89% yield (Scheme 1-8a).[32] *N*-Methyl-*N*-ethylaniline **(12)** underwent regioselective functionalization of a methyl group in 64% yield. Secondary amines were selectively converted to imines in acetonitrile by anhydrous TBHP in yields generally above 80% (Scheme 1-8b).[33] Similar to the oxidative Mannich reaction of *N*,*N*-dialkylanilines and siloxyfurans,[32] the $Rh_2(cap)_4$ catalyzed oxidation of secondary amines took place at nitrogen to form the carbon-nitrogen double bond at the less substituted α-carbon.

Scheme 1-8. Dirhodium caprolactamate catalyzed oxidative Mannich addition of aniline **12** to siloxyfuran **13** and oxidation of secondary amine **15** to imine **16**.

a)

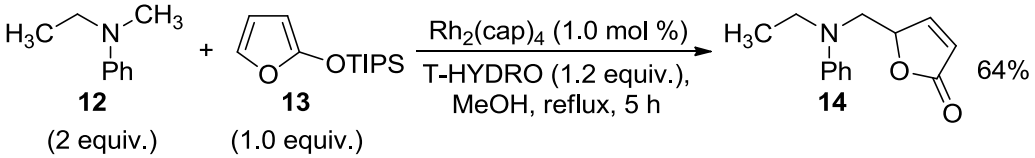

b)

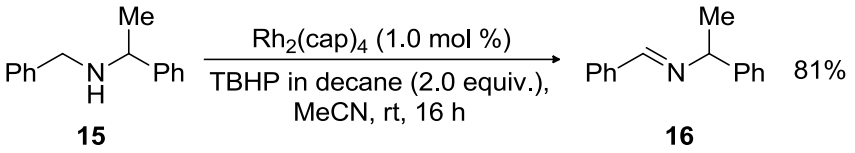

15 **16**

The reported results showed a high potential of the $Rh_2(cap)_4$ and T-HYDRO oxidative system, and an application of this oxidative method to the oxidation of phenols was pursued. In particular, 4-substituted phenols were selected because the additional substituent offers a functional handle for possible subsequent transformations.[34] Despite the numerous reports suggesting detrimental effect of free radicals in phenol oxidations,[35] Murahashi disclosed encouraging results on the oxidation of 4-substituted phenols under anhydrous conditions that prepared 4-(*tert*-butylperoxy)cyclohexa-2,5-dienones in 68-91% yields (Scheme 1-9a).[36] Murahashi used an anhydrous TBHP solution in benzene as the terminal oxidant and $RuCl_2(PPh_3)_3$ as the catalyst. Additionally, Murahashi developed a new synthetic application of 4-(*tert*-butylperoxy)cyclohexa-2,5-dienones as precursors to 2-substituted-*p*-quinones. Thus, the treatment of 2,5-dienone **18** with $TiCl_4$ afforded 2-methyl-p-quinone in 82% yield (Scheme 1-9b). Recently Murahashi applied this methodology to syntheses of vitamins K_1 and K_3 (Scheme 1-9c).[37]

Scheme 1-9. Conversion of phenols to 4-(*tert*-butyldioxy)cyclohexa-2,5-dienones with anhydrous TBHP under $RuCl_2(PPh_3)_3$ catalysis and the applications of 2,5-dienone **18** in syntheses of vitamins K_1 and K_3.

a)

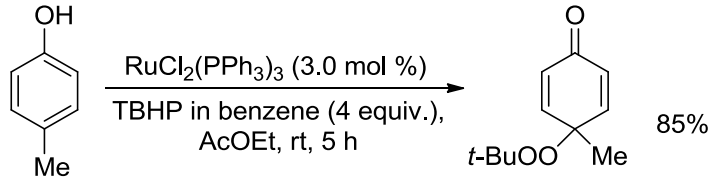

b)

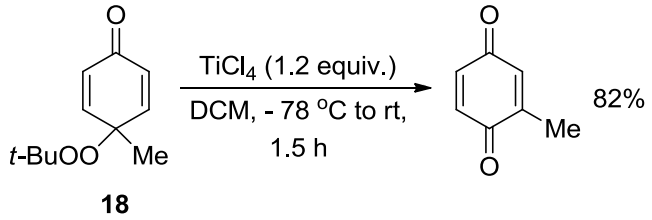

c)

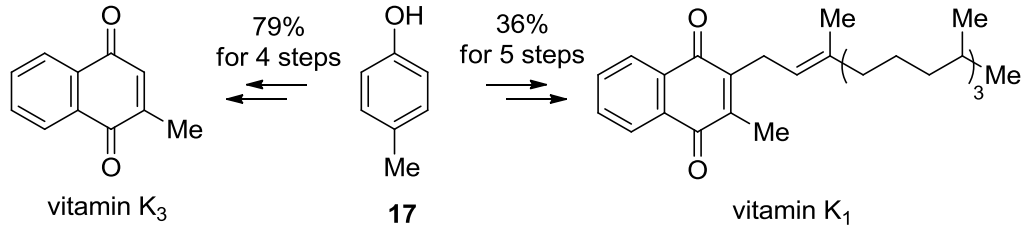

The success of Ru-catalyzed phenol oxidations by TBHP was attributed to intermediacy of phenolic cation **19** (Scheme 1-10).[38] According to the proposal of Murahashi, ruthenium oxo-complexes, presumably formed from $RuCl_2(PPh_3)_3$ or $RuCl_3$ upon treatment with TBHP, plays a central role in conversion of phenol to cation **19**. The proposed mechanism consists of a hydride abstraction from phenol in two consecutive steps, a hydrogen atom abstraction followed by electron transfer.[38] The resulting cation **19** is subsequently quenched by TBHP to afford 4-(*tert*-butylperoxy)cyclohexa-2,5-

dienones. This mechanistic proposal involving ruthenium oxo-species was extrapolated from the oxidation of *N*,*N*-dialkylanilines by TBHP catalyzed by $RuCl_2(PPh_3)_3$[39] and will be discussed in Chapter 3.

Scheme 1-10. Proposed mechanism for $RuCl_2(PPh_3)_3$ catalyzed phenol oxidation by anhydrous TBHP.

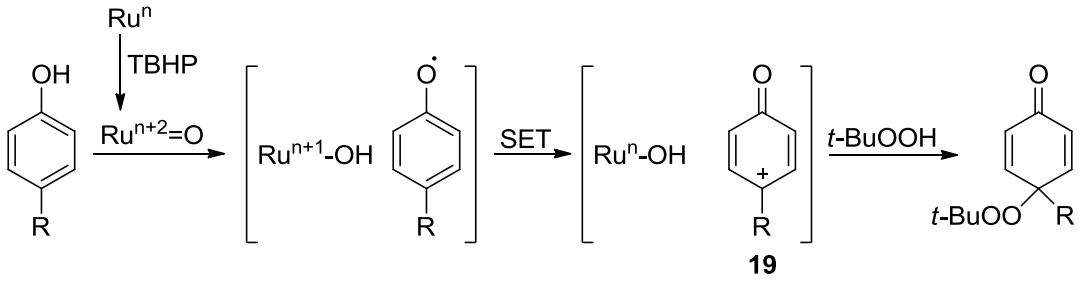

Meyer reported, however, suggests that ruthenium oxo-complex $[Ru(bpy)_2(py)(O)](ClO_4)_2$ derived from $[Ru(bpy)_2(py)OH_2](ClO_4)_2$ exhibits a different reactivity than one postulated by Murahashi.[40] According to Meyer results, the use of stoichiometric amounts of ruthenium oxo-complex affords 4-hydroxylation of phenol via an electrophilic attack of the oxo-complex on the 4-position of phenol (Scheme 1-11).

Scheme 1-11. Mechanism of phenol oxidation by stoichiometric $[Ru(bpy)_2(py)(O)](ClO_4)_2$.

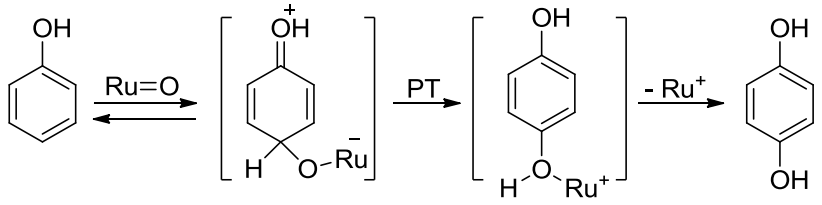

Recently the mechanistic proposal involving the formation ruthenium oxo-complexes by Murahashi was challenged by Doyle in the allylic oxidation by T-HYDRO.[19] Doyle showed that the general role of dirhodium, ruthenium, and copper salts is in generation of a flux of *tert*-butylperoxy radicals from TBHP (discussed below).

According to the mechanistic proposal of Doyle, $Rh_2(cap)_4$ converts TBHP into *tert*-butylperoxy radicals by two pathways (Scheme 1-12). The first pathway starts with the reductive cleavage of the peroxide bond of *tert*-butyl hydroperoxide by $Rh_2(cap)_4$ and the formation of the *tert*-butoxy radical and $Rh_2(cap)_4(OH)$. The *tert*-butoxy radical, in turn, rapidly abstracts a hydrogen atom from TBHP to form more thermodynamically stable *tert*-butylperoxy radical.[41] A 1-electron oxidation of TBHP by $Rh_2(cap)_4(OH)$ completes the catalyst turnover and forms the second mole of *tert*-butylperoxy radical and a mole of water while regenerating $Rh_2(cap)_4$. In summary, one $Rh_2(cap)_4$ turnover consumes three mole of TBHP (two electron oxidant) and generates one mole of *tert*-butyl alcohol, one more of water, and two moles *tert*-butyl peroxy radical (one electron oxidant) that is presumably responsible for the selectivities of the oxidation reactions.

Scheme 1-12. Dirhodium caprolactamate catalyzed conversion of *tert*-butyl hydroperoxide to the *tert*-butylperoxy radicals.

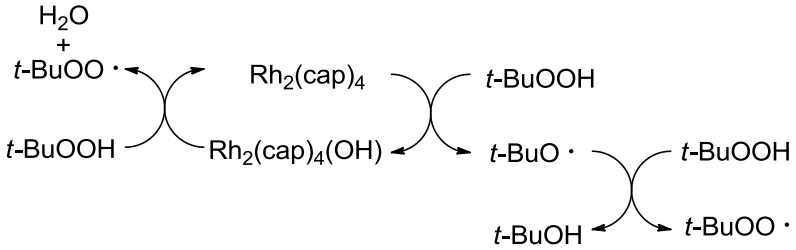

This mechanistic proposal for catalytic activity of $Rh_2(cap)_4$ was supported by studies of allylic oxidations of cyclic olefins by TBHP.[19] The oxidation occurs at the site of the least hindered position bearing the weak C-H bond that are most susceptible to hydrogen radical abstraction by a peroxy radical.[42] Similar reaction rates of $Rh_2(cap)_4$ catalyzed allylic oxidations by T-HYDRO in 1,2-dichloroethane (DCE), nitromethane, and water indicate low sensitivity of the oxidation to solvent effects that is common in radical processes.[19] UV-studies and the visual color change of dirhodium caprolactamate catalyzed oxidations indicate a 1-electron oxidation of $Rh_2(cap)_4$ to $[Rh_2(cap)_4]^+$ by TBHP.[19] The recycled $Rh_2(cap)_4$ species was observed by UV and HPLC which confirmed the proposed dirhodium turnover (Scheme 1-12).

In $Rh_2(cap)_4$ catalyzed allylic oxidations by T-HYDRO, *tert*-butylperoxy radical abstracts a hydrogen atom from the least hindered site bearing a weak carbon-hydrogen bond that the 3-position of 1-substituted cyclohexenes (Scheme 1-13a). The generated allylic radical primarily reacts with dioxygen or undergoes minor recombination with another *tert*-butylperoxy radical to yield hydroperoxides **21** or mixed peroxides **20**, respectively. The mixed peroxides were isolated in the oxidation of 1-acetylcyclohexene **22** while the intermediate hydroperoxides were isolated in the oxidation of cholesterol (Scheme 1-13a).[19] The intermediacy of an allylic radical was also confirmed for the oxidation of optically pure limonene that led to racemic carvone (Scheme 1-13b).[19]

Scheme 1-13. Proposed mechanism for allylic oxidation of cyclic alkenes by TBHP catalyzed by $Rh_2(cap)_4$.

a)

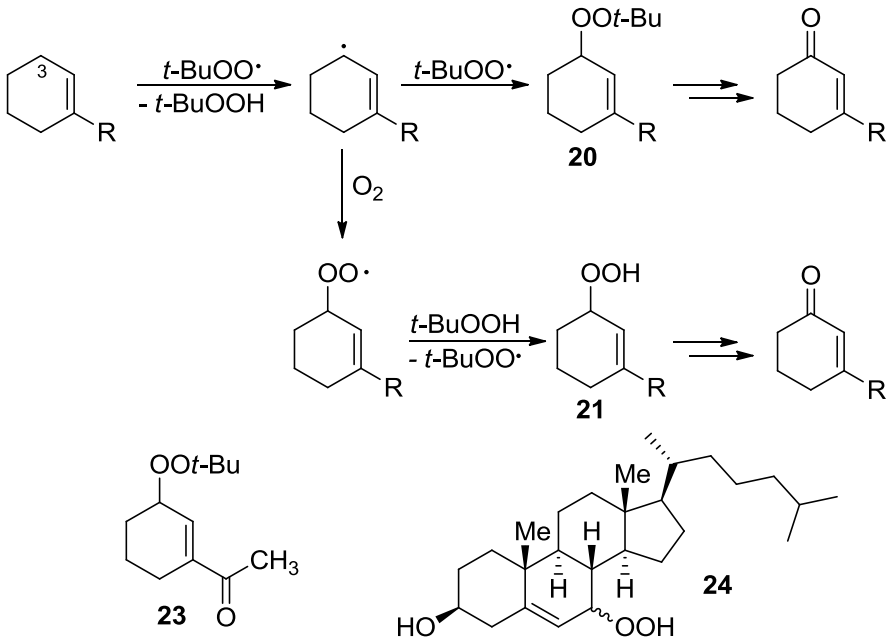

b)

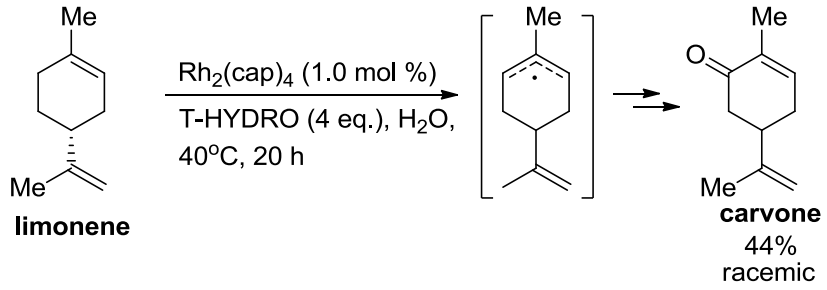

The generality of the mechanism involving the *tert*-butylperoxy radical for allylic oxidations was established in the oxidation of 1-acetylcyclohexene **22** (Table 1). Hydrogen abstraction from the 3-position forms the allylic radical that can react at the 1- and 3-positions. The observed 1.9 ± 0.3 ratio of oxidation products at the 3-position (**23** + **25**) and the 1-position (**26**) is identical within an experimental error among $Rh_2(cap)_4$, $RuCl_3$, CuI, and $Pd(OH)_2$ catalyzed oxidations of **22**. Thus, Doyle postulated the

formation of identical reaction intermediates in the allylic oxidation by TBHP catalyzed by these transition metal salts.[19] Furthermore, the comparison of catalysts revealed that dirhodium caprolactamate is the more efficient for TBHP decomposition than are $RuCl_3$, CuI, and $Pd(OH)_2$.

Table 1-1. Comparison of transition metal complexes in the oxidation of 1-acetylcyclohexene **22** by T-HYDRO.

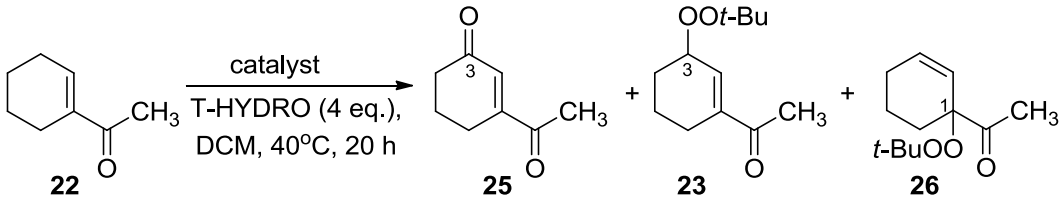

entry	catalyst	catalyst loading, mole %	Combined yield of **23**, **25**, **26**, %	ratio (**23** + **25**) / **26**
1	$Rh_2(cap)_4$	0.5	71	1.6
2	$Rh_2(cap)_4$	0.1	63	2.3
3	$RuCl_3$	2.0	42	1.5
4	CuI	2.0	51	1.6
5	$Pd(OH)_2$	5.0	36	2.0

In summary, the $Rh_2(cap)_4$ and T-HYDRO catalytic system should be evaluated to the oxidation of 4-substituted phenols and, if successful, mechanistic investigations of phenol oxidation by T-HYDRO could elaborate on the role of transition metal salts. In

this chapter turnover number and rate, product yield, catalyst loading, and required amounts of T-HYDRO have been thoroughly investigated for oxidations of phenols by *tert*-butyl hydroperoxide with dirhodium caprolactamate in comparison with other transition metal catalysts.

Results and Discussion

Phenol oxidation

The development of the phenol oxidation was begun with four equivalents of T-HYDRO in 1,2-dichloroethane (DCE) at 40 °C, the conditions developed for the $Rh_2(cap)_4$ catalyzed allylic oxidation (Scheme 1-14).[19,22,29] The $Rh_2(cap)_4$ catalytic activity was compared to one of $RuCl_2(PPh_3)_3$, the catalyst developed by Murahashi,[36] and to Cu(I) salts, inexpensive transition metal salts frequently used for the oxidations by TBHP.[21,43] The catalysts for the phenol oxidation with T-HYDRO were compared using 2,6-di-*tert*-butyl-4-methylphenol (BHT, **27**), known radical scavenger, that was expected to furnish 2,5-dienone products in quantitative yields.

Scheme 1-14. Conversion of phenol **27** to 2,5-dienone **28**.

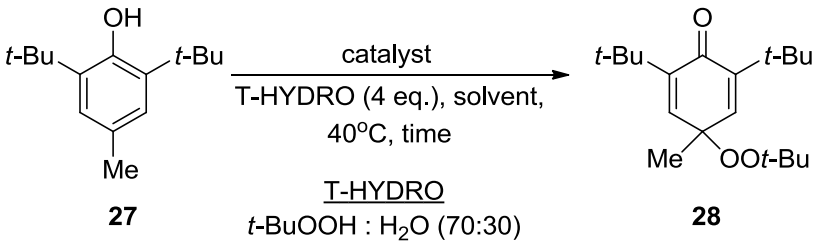

The use of DCE as a solvent and a 70% aqueous solution of TBHP (T-HYDRO) led to a heterogeneous mixture due immiscibility of water content with the organic

solvent. Copper iodide (1.0 and 0.1 mole %), $RuCl_2(PPh_3)_3$ (0.1 mole %), and $Rh_2(cap)_4$ (0.1 mole %) were evaluated in DCE with four equivalents of T-HYDRO at 40 °C in the oxidation of BHT (**27)** (Figure 1-1). The ruthenium complex showed the highest turnover rate, providing complete conversion of **27** to **28** in 3 hours while oxidations of **27** catalyzed by 0.1 mole % of either copper iodide or $Rh_2(cap)_4$ achieved the full conversion after 48 hours (Figure 1-1).

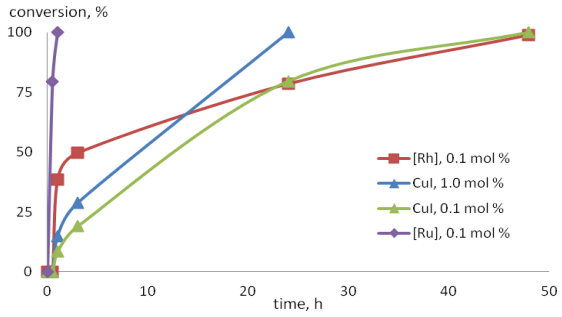

Figure 1-1. Conversions determined by ^{1}H NMR spectroscopy for transition metal catalyzed oxidations of 2,6-di-*tert*-butyl-4-methylphenol (**27**) by T-HYDRO in DCE at 40 °C.

Solvent effects were investigated for $Rh_2(cap)_4$, $RuCl_2(PPh_3)_3$, and CuI catalyzed phenol oxidation by T-HYDRO. Reaction rate of $Rh_2(cap)_4$ catalyzed oxidation of phenol **27** was increased in chlorobenzene over that in dichloroethane (Figure 1-2). In chlorobenzene the % conversion of $Rh_2(cap)_4$ catalyzed oxidation of **27** reached 100% after 3 hours at just 0.03 mole % catalyst loading (Figure 1-2). The reaction time for the $Rh_2(cap)_4$ catalyzed oxidation was lowered from 48 hours in DCE to just 10 minutes in chlorobenzene with only 0.05 mole % catalyst loading. Furthermore, the turnover rate achieved for $Rh_2(cap)_4$ catalyzed oxidation in chlorobenzene was higher than turnover

rates for the same transformation catalyzed by either $RuCl_2(PPh_3)_3$ or CuI (Figure 1-3). Thus, $Rh_2(cap)_4$ was established as a preferred catalyst for phenol oxidation by T-HYDRO in chlorobenzene. At the initial stages chlorobenzene was selected as an alternative of benzene that would not undergo oxidation under the reaction conditions. Later phenol oxidations were found to work equally well in toluene without detectable amounts of solvent oxidation. Toluene was selected the solvent of choice for preparative phenol oxidations.

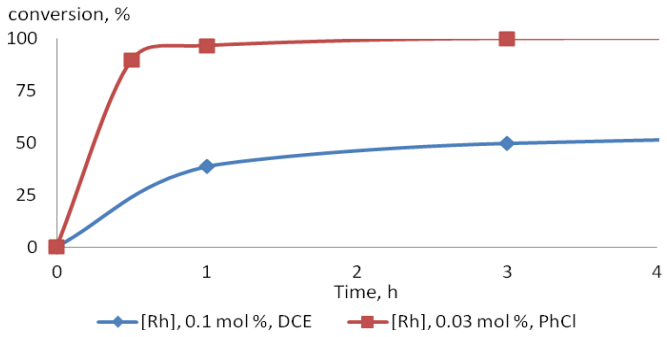

Figure 1-2. Percent conversion versus time determined by ^1H NMR spectroscopy for $Rh_2(cap)_4$ catalyzed oxidation of **27** by T-HYDRO (4.0 equiv) at 40°C in DCE and PhCl.

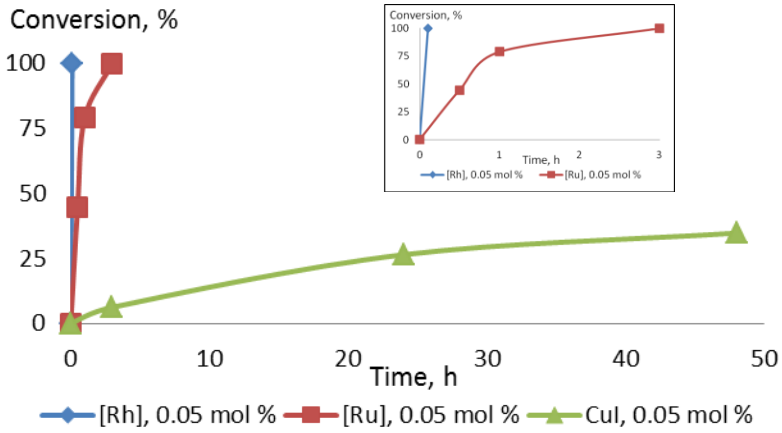

Figure 1-3. Comparative time courses determined by ^{1}H NMR spectroscopy for the oxidation of **27** by T-HYDRO (4.0 equiv) in chlorobenzene catalyzed by 0.05 mol % of $Rh_2(cap)_4$, $RuCl_2(PPh_3)_3$, or CuI at 40 °C.

Lowering the number of molar equivalents of T-HYDRO from four to two resulted in incomplete conversion (Figure 1-4) due to competing dimerization of *tert*-butyl peroxy radicals with subsequent formation of di-*tert*-butyl peroxide and molecular oxygen (eq. 1-1).[44]

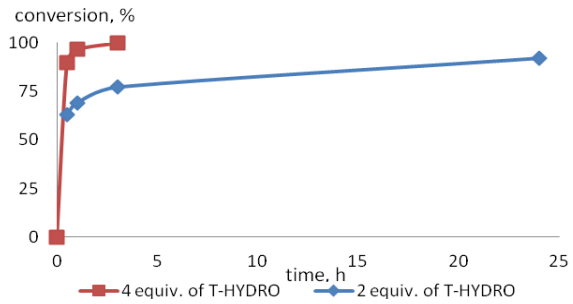

Figure 1-4. Comparative time courses for the oxidation of **27** by 4.0 and 2.0 equiv. of T-HYDRO in chlorobenzene catalyzed by 0.03 mol % of $Rh_2(cap)_4$ at 40 °C.

Eq. 1-1 $$2\ t\text{-BuOO}\cdot \longrightarrow t\text{-BuOO}t\text{-Bu} + O_2$$

Application of $Rh_2(cap)_4$ catalyzed T-HYDRO oxidations to representative phenols is reported in Table 1-2. Reactions were performed at 40 °C in the indicated solvent. 2,6-Di-*tert*-butyl-4-methylphenol (**27**) was a standard substrate from which optimal conditions for oxidations, catalyzed by various transition metal complexes, could be determined. 4-Substituted phenols gave the expected dienone products in yields generally above 70%; *p*-quinones are produced from phenols without 4-alkyl or 4-aryl substituents.[45] The oxidations of phenols **29**, **31**, **33**, **35**, **37**, and **39** were performed in DCE prior to the discovery of rate enhancement in aromatic solvents and was not repeated. In some cases an increase in T-HYDRO from four to ten equivalents was necessary to significantly improve yields (entries 5, 6, 8). Presumably, a greater excess of T-HYDRO makes the high flux of *tert*-butyl peroxy radicals independent of a level of phenol conversion. Thus, intermolecular reactions between phenol radicals are minimized even at high conversions. A similar yield increase with greater excess of T-HYDRO was reported for the allylic oxidation of electron poor alkenes.[19]

Murahashi's use of anhydrous TBHP in benzene (4.0 equiv) with 0.3 mol % $RuCl_2(PPh_3)_3$ at room temperature produced higher yields of **40** and **42** than $Rh_2(cap)_4$ with T-HYDRO for two phenols only (entries 7 and 8). On the other hand, 4 or10 equivalents of T-HYDRO in the presence of 1.0 mole % of T-HYDRO furnished comparable or better yields of 2,5-dienones **28**, **30**, **32**, **34**, and **36** to those of reported by Murahashi (entries 1-6). Thus, similar yields of phenol oxidation products, lower catalyst loading, and the use inexpensive T-HYDRO rather than the anhydrous solution of TBHP

suggested that the developed $Rh_2(cap)_4$ catalytic system was superior than one reported by Murahashi.[36]

Table 1-2. Catalytic *tert*-butyl hydroperoxide oxidation of 4-substituted phenols and 2-naphthol.

entry	phenol	catalyst	catalyst loading, mole %	equiv. of T-HYDRO	solvent	product	isolated yield, %[a]
1	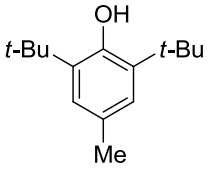 **27**	$Rh_2(cap)_4$	1.0	4	DCE	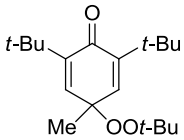 **28**	99
		$Rh_2(cap)_4$	0.03	4	PhMe		98
		CuI	0.1	4	PhMe		97[b]
		$RuCl_2$-$(PPh_3)_3$	0.05	4	PhMe		94
2	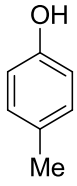 **29**	$Rh_2(cap)_4$	1.0	10	DCE	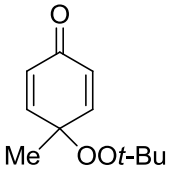 **30**	82
		$RuCl_2$-$(PPh_3)_3$	3.0	4[c]	PhH		85[36]
3	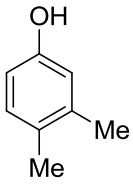 **31**	$Rh_2(cap)_4$	1.0	10	DCE	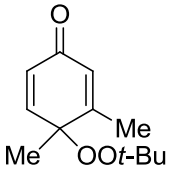 **32**	88
		$RuCl_2$-$(PPh_3)_3$	3.0	4[c]	PhH		77[36]

4	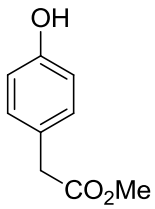 **33**	$Rh_2(cap)_4$	1.0	10	DCE	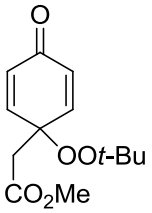 **34**	87
		$RuCl_2$-$(PPh_3)_3$	3.0	4[c]	PhH		82[36]
5	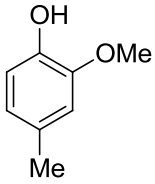 **35**	$Rh_2(cap)_4$	1.0	4	DCE	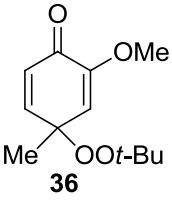 **36**	71
			1.0	10	DCE		90
6	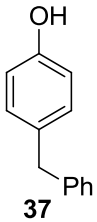 **37**	$Rh_2(cap)_4$	1.0	4	DCE		72
			1.0	10	DCE	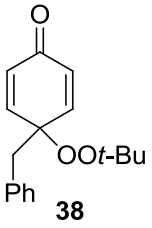 **38**	91
		$RuCl_2$-$(PPh_3)_3$	3.0	4[c]	PhH		78[36]
7	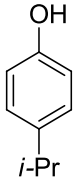 **39**	$Rh_2(cap)_4$	1.0	4	DCE		35
			1.0	10	DCE	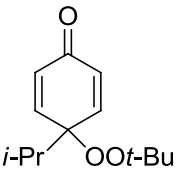 **40**	58
		$RuCl_2$-$(PPh_3)_3$	3.0	4[c]	PhH		86[36]
8	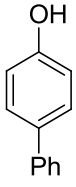 **41**	$Rh_2(cap)_4$	0.05	8	PhMe	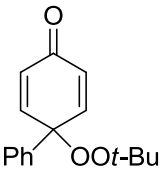 **42**	57[d,e]
		$RuCl_2$-$(PPh_3)_3$	3.0	4[c]	PhH		91[36]

9	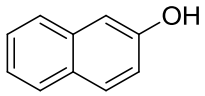 **43**	$Rh_2(cap)_4$	0.05	4	PhMe	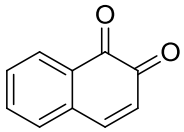 **44**	57[f,g]
10	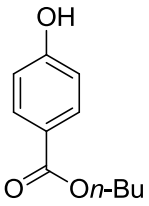 **45**	$Rh_2(cap)_4$	2.0	10	PhCl	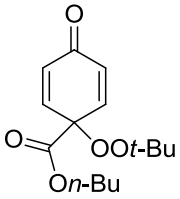 **46**	66

[a] Weight yield after column chromatography (silica gel). [b] The reaction was performed at 40 °C with an anhydrous 5 M solution of TBHP in benzene. [c] The reaction time was 24 hours. [d] Four equiv. of T-HYDRO were added all at once at 0°C at the beginning of the reaction followed after one hour by another four equiv. of T-HYDRO and then allowing reaction to warm to room temperature. [e] Neutral alumina was used for column chromatography. [f] A solution of 2-naphthol was added dropwise to a solution of $Rh_2(cap)_4$ and T-HYDRO. [g] Yield was determined by ^{1}H NMR spectroscopy using compound **2** as an internal standard.

Although isolated product yields are usually above 70%, and the 2,5-dienones are generally stable to the reaction conditions, the peroxidation process has limitations. The product from oxidation of **41** (entry 8) undergoes slow decomposition; keeping pure **42** in a DCE solution at 40 °C overnight resulted in complete decomposition of peroxide **42** to unknown products. However, lowering the reaction temperature from 40 °C to 0 °C minimized decomposition of **42**. ^{1}H NMR spectrum of the reaction mixture of 2-naphthol oxidation contained a 6.6-7.8 ppm broad absorption that indicated possible formation of oligomerization products. A dropwise of addition of a 2-naphthol solution in toluene to a mixture of $Rh_2(cap)_4$ and T-HYDRO in toluene formed 1,2-naphthoquinone in 57% yield. Presumably, the dropwise addition of 2-naphthol keeps TBHP in a large excess

relative to 2-naphthol throughout the reaction that minimizes oligomerization of the naphthyl radicals.

Phenols bearing electron-withdrawing carboxylate groups in the 4-position underwent oxidation in chlorobenzene using 1-2 mol % of dirhodium caprolactamate (Table 1-2, entry 10 and Scheme 1-15). The oxidation of a common antifungal preservative in cosmetic products,[46] butyl paraben, (entry 10) afforded peroxide product **46** in 66% yield. However, oxidation of 4-hydroxybenzoic acid resulted in the formation of *p*-benzoquinone as a major product along with a minor ortho oxidation product (**49**) that were detected by ^{1}H NMR and GC/MS (Scheme 1-15). Presumably, the presence of a carbonyl group on the α-position and an acidic hydrogen on the β-position to the peroxide group lead to the decomposition of 4-carboxylate substituted 4-(*tert*-butyldioxy)cyclohexa-2,5-dienone (Scheme 1-16). Such decomposition could be either a concerted reaction (Scheme 1-16a) or a stepwise loss of a proton followed a cascade bond breaking reactions (Scheme 1-16b).

Scheme 1-15. Dirhodium caprolactamate oxidation of *p*-hydroxybenzoic acid **47** by T-HYDRO.

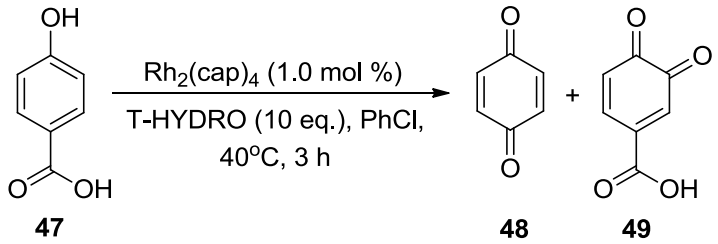

47 **48** **49**

Scheme 1-16. Possible pathways of transformation of **47** into **48**.

a) Concerted route

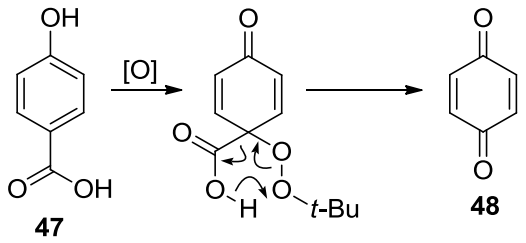

b) Stepwise route

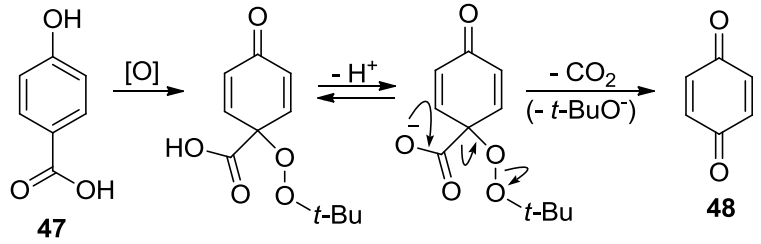

Phenolic oxidation by T-HYDRO catalyzed by $Rh_2(cap)_4$ usually occurs with functionalization of its 4-position (Table 1-2, entries 1-8, and 10). This result is consistent with the greater spin density at the para position than in the ortho position of a delocalized π-system of phenolic radicals.[47] However, bulky substituents in the para position hinder the phenol para position from the reaction with *tert*-butylperoxy radical and inhibit the reaction at the para position (Table 1-3). Functionalization at the ortho position increases with a size of a para substituent, as is evident from comparison of regioselectivities of oxidations of **30**, **40**, and **53** (Table 1-3). Similar outcomes were obtained with the use of $Rh_2(cap)_4$ and $RuCl_2(PPh_3)_3$ (entries 3 and 4), suggesting the similarity in reaction pathway with these two catalysts.

Table 1-3. Oxidation of phenols bearing bulky 4-substituents with 4.0 equivalents of T-HYDRO in toluene.

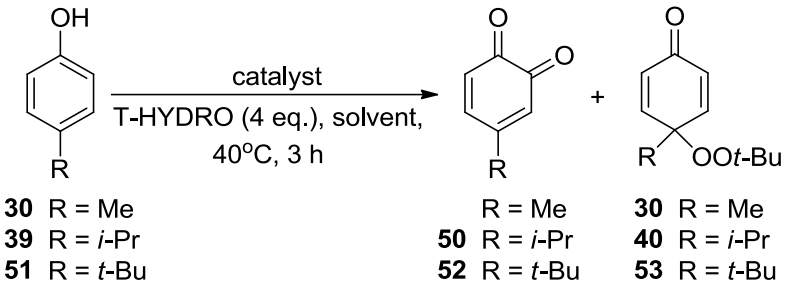

entry	phenol	catalyst	solvent	catalyst loading, mol %	ratio of *o*-/*p*-oxidation products	yield, %
1	**29**	$Rh_2(cap)_4$	DCE	1.0	< 1:99	82
2	**39**	$Rh_2(cap)_4$	toluene	0.05	27:73[a]	51[b]
3	**51**	$Rh_2(cap)_4$	toluene	0.05	39:61	53[c]
4		$RuCl_2(PPh_3)_3$		0.1	43:57[a]	46[a]

[a] Determined by ^{1}H NMR with **28** as an internal standard. [b] Yield of product **40** after chromatography (silica gel). [c] Combined yield of products **52** and **53** after chromatography.

The oxidation of bisphenol A (BPA) reveals another dimension of selectivity. This compound underwent oxidation of just one phenol ring to produce ortho-quinone **55** in 44% yield along with unidentified products (Scheme 1-17). This selectivity presumably arises from hindrance at the 4-position of the phenol radical by the large 4-substituent that favors the oxidation at the 2-position of phenol. The greater solubility of **55** in the aqueous layer than in the organic layer provides protection of **55** from further oxidation. The rate of phenol oxidation is greater in the organic layer, especially in aromatic solvents, than in the aqueous layer (nucleophilic solvents inhibit ligand

exchange of dirhodium complexes).[33] As a result, BPA presumably undergoes oxidation of one phenolic ring in the organic phase or at the aqueous-organic interface, and this product migrates to the aqueous layer where **55** is preserved from subsequent oxidation. Higher concentration of **55** in aqueous layer is consistent with a greater intensity of the spots on TLC corresponding to **55** from aqueous layer than from toluene layer.

Scheme 1-17. Dirhodium caprolactamate oxidation of bisphenol A.

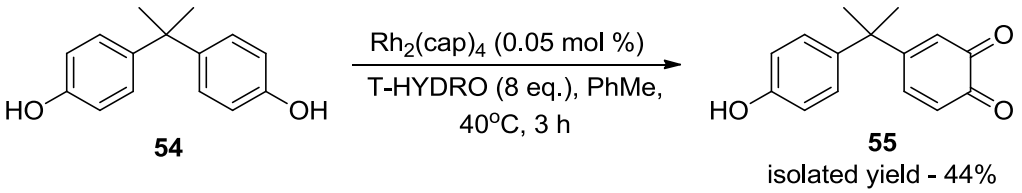

Investigations of the peroxidation of estrone provided an opportunity to evaluate selectivity in product formation and through this study to better understand the mechanism of oxidation. Murahashi has reported that the oxidation of estrone **56** catalyzed by $RuCl_2(PPh_3)_3$ yielded dienone **57** in 89% yield with a diastereomeric ratio 56:44. We found an identical diastereomer ratio when the oxidation of estrone by T-HYDRO is catalyzed by $Rh_2(cap)_4$ indicating the same intermediates for both catalysts (Scheme 1-18a). An essential role of the phenolic O-H bond for peroxidation is indicated in the result from oxidation of acetylated estrone **58** (Scheme 1-18b).

Scheme 1-18. Oxidation of estrone derivatives **56** and **58** with T-HYDRO under $Rh_2(cap)_4$ catalysis.

a)

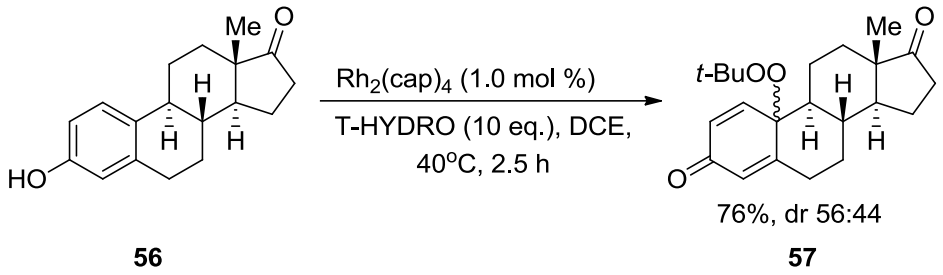

56 **57**

b)

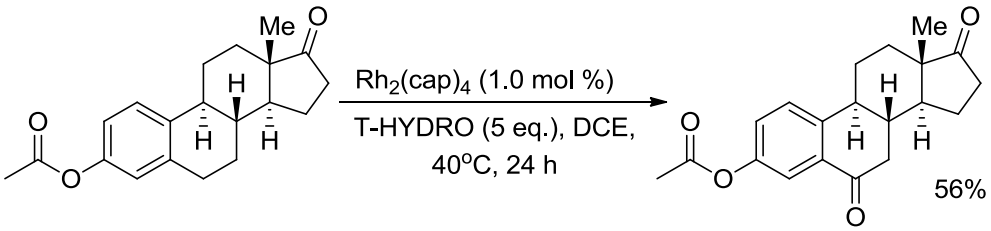

58 **59**

Similar to $Rh_2(cap)_4$ catalyzed allylic oxidation by T-HYDRO (Schemes 1-12 and 1-13a),[19] a radical mechanism was expected for phenolic oxidation. However, Murahashi, using anhydrous TBHP, postulated the formation of a dienyl cation **19** after interaction of 4-substituted phenol and ruthenium oxo-complex (Scheme 1-10).[36,38] High yields of mixed peroxides **28**, **32**, **34**, **36**, **38** (Table 1, entries 1, 3, 4, 5, 6) and no formation of corresponding 4-hydroxy-2,5-dienones in $Rh_2(cap)_4$ and $RuCl_2(PPh_3)_3$ catalyzed oxidations by T-HYDRO, however, support the radical mechanism. In addition, the Rh- and Ru-catalyzed oxidations of **41** in *tert*-butyl alcohol did not furnish products that could arise from trapping of *tert*-butyl alcohol or water by **19** (Scheme 1-19). The formation of **42** as the only product of $Rh_2(cap)_4$ and $RuCl_2(PPh_3)_3$ catalyzed oxidations of **41** by T-HYDRO is another evidence supporting the radical mechanism.

Scheme 1-19. Oxidation of phenol **41** in *tert*-butyl alcohol by T-HYDRO catalyzed by $Rh_2(cap)_4$ and $RuCl_2(PPh_3)_3$.

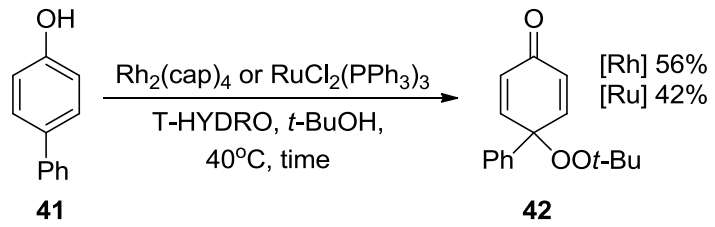

To validate the mechanistic proposal for $Rh_2(cap)_4$ turnover (Scheme 1-12), the involvement of the $[Rh_2(cap)_4]^+$ species was evaluated. A complete conversion of phenol **27** to 2,5-dienone **28** with four equivalents of T-HYDRO was achieved in one hour with 0.05 mole % of $[Rh_2(cap)_4]^+BF_4^-$ (Scheme 1-20). This reaction time is similar to one observed for neutral $Rh_2(cap)_4$ (Figure 1-2). Hence, the data are consistent with the involvement of the $[Rh_2(cap)_4]^+$ species that was shown by 507 and 974 nm absorptions in the UV spectrum of the allylic oxidation reaction mixture (Scheme 1-12).[19]

Scheme 1-20. Oxidation of phenol **27** by T-HYDRO catalyzed by $[Rh_2(cap)_4]^+BF_4^-$.

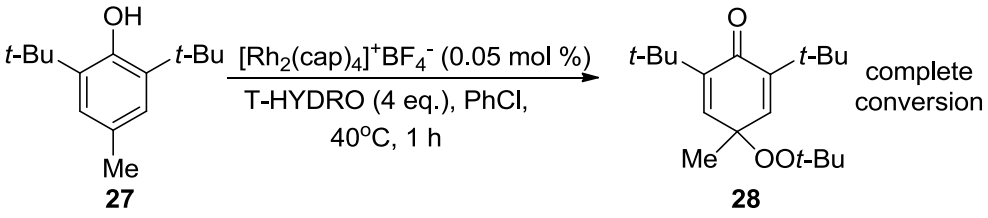

Aniline Oxidation

Having proposed the operating mechanism consistent with the experimental data for the phenol oxidation by T-HYDRO, this mechanism could be general for any

heteroatom bearing a hydrogen atom adjacent to the aromatic ring. Anilines were used as isolobal analogs of phenols to test this hypothesis.

The dirhodium caprolactamate/T-HYDRO catalytic oxidative system converted anilines preferentially to nitro compounds (Table 3) rather than to 2,5-dieneimines that by hydrolysis would result in 2,5-dienones. *p*-Toluidine is oxidized to *p*-nitrotoluene in 75% yield, but with detectable amounts of dienone **30** (Scheme 1-21). *tert*-Butyl hydroperoxide gave nearly identical yields of **61** in the oxidation of **60** as a 5 M anhydrous solution in decane and as a 70% aqueous solution (Table 1-4, entries 1 and 2). Nitro compounds were readily obtained from anilines bearing strong or weak electron-donating substituents (entries 1-4). The presence of an aromatic ring in the ortho position (entry 5), or a strongly electron-withdrawing group in the para position (entry 6), significantly decreases product yield. The low yields of **67** and **69** were caused by the formation of unknown by-products that were observed as colored products on TLC.

Scheme 1-21. Dirhodium caprolactamate oxidation of aniline **60** by T-HYDRO.

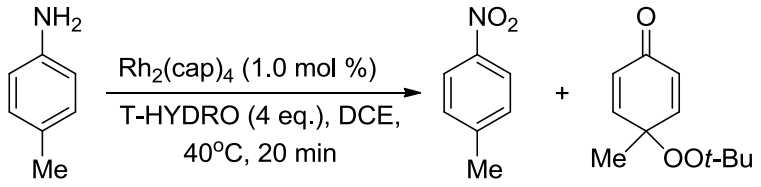

60 **61** 75% **30** 20%

Table 1-4. Dirhodium caprolactamate catalyzed aniline oxidation.

entry	aniline	method[a]	product	isolated yield, %
1	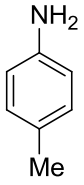 **60**	A	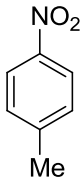 **61**	79
2		B		75
3	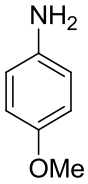 **62**	A	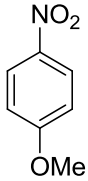 **63**	60
4	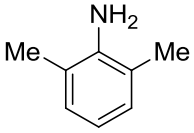 **64**	A	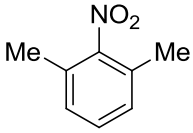 **65**	80
5	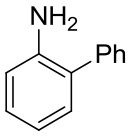 **66**	B	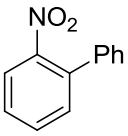 **67**	43
6	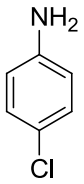 **68**	A	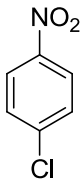 **69**	51

[a] **Method A:** $Rh_2(cap)_4$ (0.1 mol %), DCM (0.27 M), TBHP in decane (4 eq.), $NaHCO_3$ (0.5 eq.), rt, 16 h; **Method B:** $Rh_2(cap)_4$ (1.0 mol %), DCE (0.5 M), T-HYDRO (4 eq.), 40°C, 20 min

Monitoring the oxidation of aniline **60** with GC/MS revealed the presence of an intermediate with a M+14 mass that is, most likely, the corresponding nitroso compound.

Detection of dienone **30** in the reaction mixture from oxidation of **60** indicates that, similar to phenolic oxidation, aniline oxidation includes hydrogen atom abstraction from an amino group followed by trapping by the peroxy radical or dioxygen at nitrogen or at the 4-position (Scheme 1-22). A similar radical mechanism was proposed by Rieker and Nishinaga for a series of cobalt Schiff base complexes catalyzed aniline oxidations to nitroarenes by TBHP in DCE.[48] A stepwise single electron transfer followed by proton transfer (discussed in Chapter 3) is an alternative mechanism.

Scheme 1-22. Plausible mechanism for $Rh_2(cap)_4$ catalyzed aniline oxidation by TBHP.

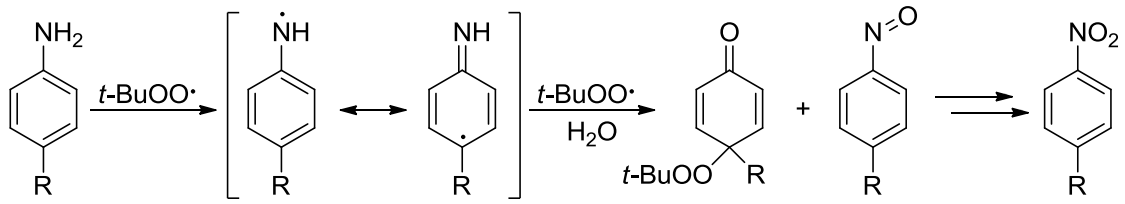

In contrast to reactions of secondary amines that form imines[33] and with tertiary amines that form iminium ions,[32] dirhodium catalyzed oxidations of benzylic and homobenzylic primary amines by TBHP oxidatively remove the amino group in moderate to good yields (Table 1-5). The reaction has greater efficiency for amines whose adjacent C-H bond has a lower bond dissociation energy (e.g., entry 2).

Table 1-5. Dirhodium caprolactamate catalyzed oxidation of primary amines by TBHP.

entry	reactant[a]	product	isolated yield, %
1	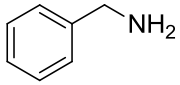 **70**	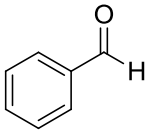 **71**	39[b]
2	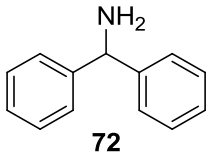 **72**	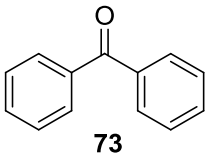 **73**	82
3	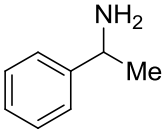 **74**	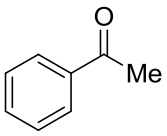 **75**	41

[a] Reactions were performed on 1.34 mmol scale using 4.0 eq. TBHP in decane and 1.0 % mol $Rh_2(cap)_4$ in DCM (0.27 M) for 16 h. [b] Two equiv TBHP were used.

Conclusion

In summary, $Rh_2(cap)_4$ is an efficient catalyst for the peroxidation of phenols by T-HYDRO. Toluene and chlorobenzene media boost the rate of TBHP conversion to the *tert*-butylperoxy radicals by $Rh_2(cap)_4$ thus allowing catalyst loadings of 0.05 mole % or lower. The efficiency of the phenol oxidation is determined by the flux of the *tert*-butylperoxy radical generated according to the higher yields achieved in the oxidations with four and ten equivalents of T-HYDRO (Table 1-2, entries 5-7). Identical product ratios in the oxidation of estrone **56** by TBHP and the ortho and para selectivity

in the oxidation of phenol **51** catalyzed by $Rh_2(cap)_4$ and $RuCl_2(PPh_3)_3$ indicate a formation of a common intermediate. The absence of products of nucleophilic trapping by a cationic intermediate suggests the radical mechanism initiated and terminated by *tert*-butylperoxy radical (Scheme 1-22) for the phenol oxidations by TBHP catalyzed by $Rh_2(cap)_4$, $RuCl_2(PPh_3)_3$ and, possibly, CuI. A similar mechanistic scheme is applicable to the oxidation of anilines.

Scheme 1-22. Mechanism of Transition Metal Catalyzed Phenolic Oxidation with TBHP.

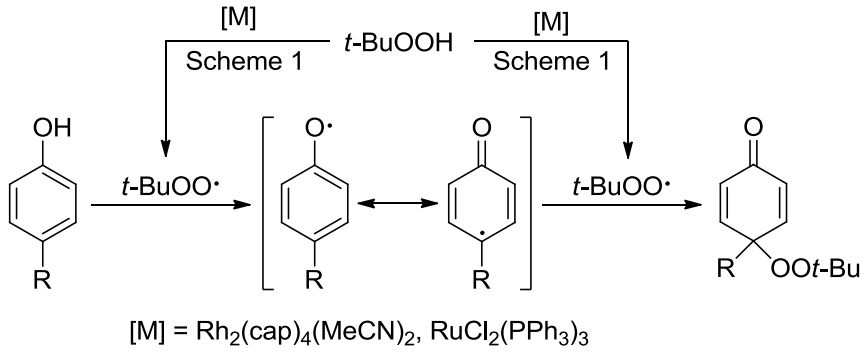

Experimental

General Information. All reactions were performed under atmospheric conditions unless the conditions are specified. Infrared spectra were recorded on a JASCO FT/IR 4100 spectrometer. ^{1}H NMR spectra were recorded on 400 MHz and 600 MHz spectrometers. Tetramethylsilane (TMS) (0.00 ppm) was used as the internal standard for all ^{1}H and ^{13}C spectra. Data are reported as follows: chemical shift (in ppm, δ), integration, multiplicity (s = singlet, d = doublet, t = triplet, q = quartet, sept = septet, br = broad, m = multiplet, comp = composite) and coupling constants (in Hz). ^{13}C NMR spectra were recorded on a 125 MHz spectrometer operated with complete proton

decoupling. Chemical shifts are reported in ppm utilizing a central absorption of $CDCl_3$ as a reference (77.0 ppm). Thin layer chromatography was performed on silica gel coated on a glass plates (250 μm, F-254), and spots were visualized with 254 nm ultraviolet light. Flash chromatography used silica gel (32-63 μm) and neutral alumina (50-200 μm) as stationary phases. High resolution mass spectra (HRMS) were acquired on a ESI-TOF spectrometer using CsI as a standard. $Rh_2(cap)_4$ was prepared according to the literature procedure.[49]

All previously unreported products were characterized by ^1H and ^{13}C NMR spectroscopy and HRMS. Spectra of peroxides **28**, **30**, **32**, **34**, **38**, **40, 50, 57** are in agreement with published chemical shifts and masses of molecular ions.[36] Spectra of carbonyl compounds **41**,[50] **59**,[51] **71**,[52] **73**,[53] and **75**[53] and nitro arenes **61**,[54] **63**,[55] **65**,[54] **67**,[56] and **69**[54] were identical to reported spectra.

General Procedure for Transition Metal Complex Catalyzed Phenolic Oxidation in DCE. The phenol derivative (2.0 mmol), a catalyst, and DCE (4.0 mL) were placed in a 6-dram screw-cap vial containing a magnetic stirring bar. The suspension containing a small amount of undissolved $Rh_2(cap)_4$ was heated to 40 °C in an oil bath at 250 rpm, and T-HYDRO was added to the suspension all at once via syringe. The reaction mixture was loosely capped to allow release of pressure built-up and stirred at 40 °C. After 45 minutes the reaction mixture was transferred to a 100-mL round-bottom flask, concentrated under reduced pressure, and the residue was purified by column chromatography (silica gel, DCM:AcOEt:hexane). Fractions containing the product were combined, and the solvent was evaporated under reduced pressure. The

resulting peroxide products were dried under high vacuum (0.09 Torr) for 20 minutes at room temperature.

General Procedure for Transition Metal Complex Catalyzed Phenolic Oxidation in an Aromatic Solvent. The phenol derivative (3.0 mmol), a catalyst, and a solvent (6.0 mL) were placed in a 6-dram screw-cap vial containing a magnetic stirring bar. The suspension containing a small amount of undissolved $Rh_2(cap)_4$ was heated to 40 °C in an oil bath at 250 rpm, and T-HYDRO was added to the suspension all at once via syringe. The reaction mixture was loosely capped to allow release of pressure built-up and stirred at 40 °C. After three hours the reaction mixture was transferred to a 100-mL round-bottom flask, concentrated under reduced pressure, and the residue was purified by column chromatography (silica gel, DCM:AcOEt:hexane). Fractions containing the product were combined; the solvent was evaporated under reduced pressure. A fraction of the peroxide products were dried under high vacuum (0.09 Torr) for 20 minutes at room temperature.

4-(*tert*-Butylperoxy)-2-methoxy-4-methylcyclohexa-2,5-dien-1-one (36): R_f = 0.32 [hexane/AcOEt (10:1)]; colorless oil; ^{1}H NMR (500 MHz, $CDCl_3$) δ 6.91 (dd, *J* = 10.1, 2.7 Hz, 1 H), 6.23 (d, *J* = 10.1 Hz, 1 H), 5.77 (d, *J* = 2.7 Hz, 1 H), 3.70 (s, 3 H), 1.45 (s, 4 H), 1.20 (s, 9 H); ^{13}C NMR (125 MHz, $CDCl_3$) δ 181.0, 151.4, 150.7, 127.7, 117.5, 79.8, 77.8, 54.8, 26.3, 24.2; HR-MS (ESI) calcd. for $C_{12}H_{19}O_4$ 227.12834, found 227.12928 (M+H); IR (thin film) cm^{-1}: 2980, 1678, 1646, 1619, 1455.

***n*-Butyl 1-(*tert*-Butylperoxy)-4-oxocyclohexa-2,5-diene-1-carboxylate (46):** R_f = 0.40 [hexane/AcOEt/DCM (10:1:1)]; pale yellow oil; ^{1}H NMR (500 MHz, $CDCl_3$) δ

7.08 (d, *J* = 10.1 Hz, 2 H), 6.36 (d, *J* = 10.1 Hz, 2 H), 4.20 (t, *J* = 6.5 Hz, 2 H), 1.70 – 1.60 (comp, 2 H), 1.43 – 1.34 (comp, 2 H), 1.25 (s, 9 H), 0.93 (t, *J* = 7.4 Hz, 3 H); ^{13}C NMR (125 MHz, $CDCl_3$) δ 184.9, 167.0, 142.7, 130.8, 81.4, 79.3, 66.3, 30.4, 26.3, 18.9, 13.6; HR-MS (ESI) calcd. for $C_{15}H_{23}O_5$ 283.15455, found 283.15216 (M+H).

4-*tert*-Butylbenzo-1,2-quinone (52): R_f = 0.28 [hexane/AcOEt/DCM (4:1:1)]; brown oil; ^{1}H NMR (400 MHz, $CDCl_3$) δ 7.19 (dd, *J* = 10.4, 2.4 Hz, 1 H), 6.40 (d, *J* = 10.4 Hz, 1 H), 6.29 (d, *J* = 2.4 Hz, 1 H), 1.24 (s, 9 H). ^{13}C NMR (125 MHz, DMSO) δ 180.3, 180.2, 162.1, 140.0, 129.4, 123.8, 35.6, 27.8; HR-MS (ESI) calcd. for $C_{10}H_{13}O_2$ 165.09155, found 165.09168 (M+H).

4-*tert*-Butyl-4-(*tert*-butylperoxy)cyclohexa-2,5-dien-1-one (53): R_f = 0.26 [hexane/AcOEt/DCM (8:1:1)]; pale yellow oil; ^{1}H NMR (500 MHz, $CDCl_3$) δ 7.03 (d, *J* = 10.4 Hz, 2 H), 6.31 (d, *J* = 10.4 Hz, 2 H), 1.22 (s, 9 H), 1.03 (s, 9 H); ^{13}C NMR (125 MHz, DMSO) δ 185.5, 150.5, 130.6, 82.6, 80.1, 40.0, 26.4, 26.0; HR-MS (ESI) calcd. for $C_{14}H_{22}O_3$ - 238.15689, found 238.15372 (M^+).

4-[1-(4-Hydroxyphenyl)-1-methylethyl]benzo-1,2-quinone (55): R_f = 0.48 [hexane/AcOEt/DCM (8:1:1)]; dark brown oil; ^{1}H NMR (500 MHz, $CDCl_3$) δ 7.16 (d, *J* = 8.8 Hz, 2 H), 6.87 (m, *J* = 8.8 Hz, 2 H), 6.65 (dd, *J* = 10.3, 2.1 Hz, 1 H), 6.50 (d, *J* = 2.1 Hz, 1 H), 6.22 (d, *J* = 10.3 Hz, 1 H), 5.28 (s, 1 H), 1.54 (s, 6 H); ^{13}C NMR (150 MHz, $CDCl_3$) δ 180.4 (2 C), 161.4, 154.8, 141.5, 136.1, 129.0, 127.8, 123.8, 115.9, 43.0, 27.3; HR-MS (ESI) calcd. for $C_{15}H_{15}O_3$ 243.10212, found 243.10110 (M+H).

Procedure for Kinetic Measurements of Transition Metal Catalyzed Oxidations of 2,6-di-*tert*-Butyl-4-methylphenol (27) by T-HYDRO. Phenol **27** (13.63

mmol, 3.00 g), catalyst and solvent (27.0 mL) were placed in a 125-mL Erlenmeyer flask containing a magnetic stirring bar. The mixture containing a small amount of undissolved catalyst was heated to 40°C on a stirrer-hotplate, and T-HYDRO was added to the suspension all at once via syringe. The flask was equipped with a septum containing a needle to release any pressure built-up and was stirred at 40 °C. The catalyst was completely dissolved within one minute after T-HYDRO addition. Immediately after the T-HYDRO addition the mixture became cloudy due to formation of an aqueous layer, the color of the reaction mixture became red for the $Rh_2(cap)_4$ catalyzed reaction, dark green for the $RuCl_2(PPh_3)_3$ catalyzed reaction, and yellow after 4 hours for the Cu salts catalyzed reaction. After the specified time an aliquot (about 0.10 mL) of the organic layer was removed from the reaction mixture, and the solvent was rapidly evaporated under high vacuum (0.09 Torr) for 5 minutes at room temperature. The residue was dissolved in $CDCl_3$ and analyzed by ^1H NMR spectroscopy. Percent conversion was measured as the ratio of absorption of product **28** (s, 6.56 ppm) to absorption of phenol **27** (s, 6.98 ppm).

Table 1-6. Percent conversions for transition metal catalyzed oxidations of 2,6-di-*tert*-butyl-4-methylphenol (**27**) by T-HYDRO in DCE at 40 °C.

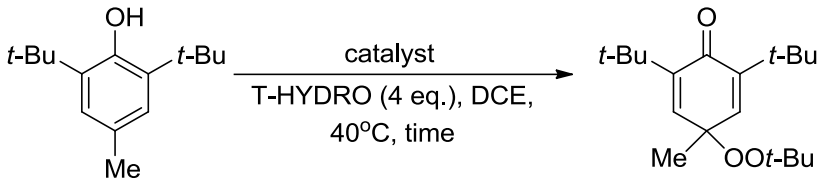

27 **28**

entry	catalyst	loading, mole %	equiv. of T-HYDRO	conversion, %					
				0 h	0.5 h	1 h	3 h	24 h	48 h
1	$Rh_2(cap)_4$	0.1	4	0	—	39	50	79	99
2	CuI	1.0	4	0	—	15	29	100	—
3	CuI	0.1	4	0	—	8.3	19	80	100
4	$RuCl_2(PPh_3)_3$	0.1	4	0	79	100	—	—	—

Table 1-7. Percent conversions for transition metal catalyzed oxidations of 2,6-di-*tert*-butyl-4-methylphenol (**27**) by T-HYDRO in chlorobenzene at 40 °C.

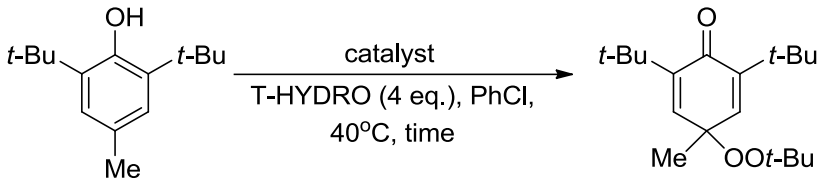

27 **28**

entry	catalyst	loading, mol %	equiv. of T-HYDRO	conversion, %						
				0 h	0.1 h	0.5 h	1 h	3 h	24 h	48 h
1	$Rh_2(cap)_4$	0.05	4	0	100	—	—	—	—	—
2	$Rh_2(cap)_4$	0.01	4	0	—	—	32	50	79	99
3	$Rh_2(cap)_4$	0.03	4	0	—	90	97	100	—	—
4	$Rh_2(cap)_4$	0.03	2	0	—	63	69	77	92	—
5	CuI	1.0	4	0	—	—	28	61	100	—
6	CuI	0.1	4	0	—	—	18	35	100	—
7	CuI	0.05	4	0	—	—	0.7	6.3	27	35
8	CuBr	0.1	4	0	—	—	0.1	8.0	80	—
9	CuCl	0.1	4	0	—	—	0.1	1.7	79	—
10	$RuCl_2(PPh_3)_3$	0.1	4	0	—	—	100	—	—	—
11	$RuCl_2(PPh_3)_3$	0.05	4	0	—	45	79	100	—	—

Figure 1-5. Comparative time courses determined by ^{1}H NMR spectroscopy for $Rh_2(cap)_4$ catalyzed oxidations of **27** by T-HYDRO at 40°C.

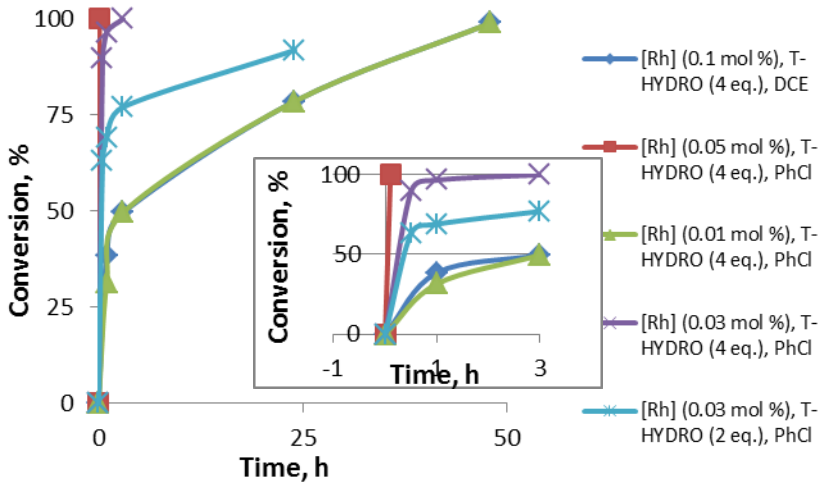

Figure 1-6. Comparative time courses determined by ^{1}H NMR spectroscopy for $RuCl_2(PPh_3)_3$ catalyzed oxidation of **27** by 4.0 equiv. of T-HYDRO at 40°C.

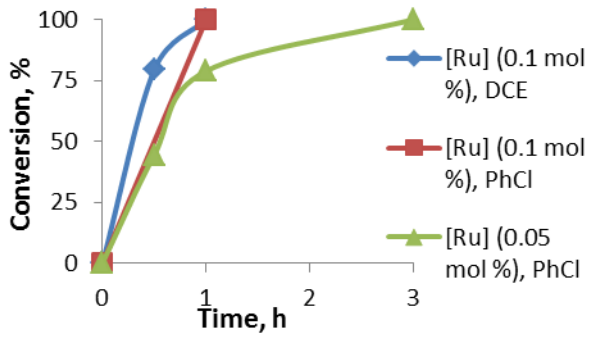

Figure 1-7. Comparative time courses determined by ^{1}H NMR spectroscopy for copper(I) halide catalyzed oxidation of **27** by 4.0 equiv. of T-HYDRO at 40°C.

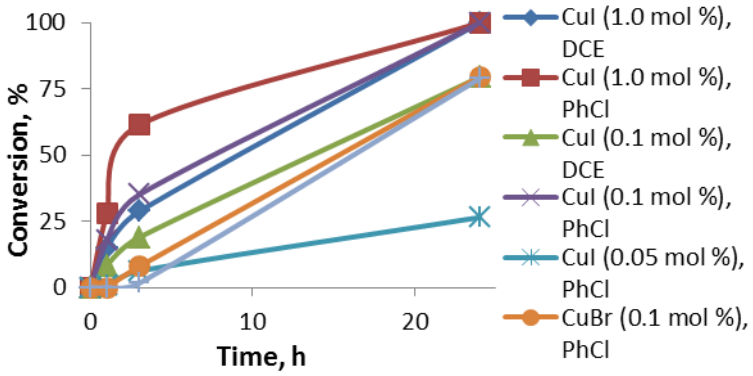

Oxidation of 4-Phenylphenol (41) in Toluene. 4-Phenylphenol **41** (3.0 mmol, 510 mg), $Rh_2(cap)_4(MeCN)_2$ (1.5 µmol, 1.1 mg) or $RuCl_2(PPh_3)_3$ (3.0 µmol, 2.9 mg), and toluene (6.0 mL) were placed in 6-dram screw-cap vial containing a magnetic stirring bar. The mixture was sonicated to ensure maximal concentration of the phenol in a resulting suspension. The vial containing the suspension was placed in an ice bath and stirred for about three minutes to allow the temperature to equilibrate to 0 °C. T-HYDRO (12.0 mmol, 1.66 mL, 4.0 equiv.) was added via syringe dropwise over the period of one minute of stirring at 400 rpm. After one hour of stirring at 250 rpm at 0 °C, another 4.0 equiv. of T-HYDRO were added via syringe all at once. The vial was removed from the ice bath, and the reaction mixture was allowed to warm to room temperature. The reaction solution remains heterogeneous throughout the reaction due to the formation of an aqueous layer. After three hours of stirring (250 rpm) at room temperature, the reaction mixture contained a single spot with R_f = 0.31 in hexane/AcOEt (10:1) according to TLC analysis, and the mixture was transferred to a 100-mL round-bottom flask and concentrated on a rotary evaporator (20 Torr, room temperature). The residue was

dissolved in DCM and was purified by column chromatography [neutral alumina, 18 mm diameter, 18 cm height, EtOAc/DCM/hexane (1:1:16, 250 mL)]. Fractions containing product **42** were combined, and the solvent was removed on a rotary evaporator (60 Torr, room temperature). The residue was further dried under high vacuum (0.09 Torr) for 20 minutes at room temperature to yield 441 mg (57%) of mixed peroxide **42** as a pale yellow oil from the $Rh_2(cap)_4$ catalyzed oxidation and 278 mg (36%) of mixed peroxide **42** as a pale yellow oil from the $RuCl_2(PPh_3)_3$ catalyzed reaction; R_f = 0.31 [hexane/AcOEt (10:1)]; ^{1}H NMR (500 MHz, $CDCl_3$) δ 7.42 – 7.33 (comp, 5 H), 7.01 (d, *J* = 10.2 Hz, 2H), 6.33 (d, *J* = 10.2 Hz, 2H), 1.29 (s, 9 H). ^{13}C NMR (125 MHz, $CDCl_3$) δ 185.9, 150.0, 136.9, 128.9, 128.8, 125.8, 80.6, 79.6, 26.5; HR-MS (ESI) calcd. for $C_{16}H_{19}O_3$ 259.13342, found 259.13258 (M+H).

Oxidation of 4-Phenylphenol (41) in *tert*-Butyl Alcohol. 4-Phenylphenol **41** (1.0 mmol, 170 mg), $Rh_2(cap)_4(MeCN)_2$ (10.0 μmol, 7.4 mg) or $RuCl_2(PPh_3)_3$ (20.0 μmol, 19.2 mg), and *tert*-butyl alcohol (5.0 mL) were placed in 6-dram screw-cap vial containing a magnetic stirring bar. The mixture was sonicated to facilitate a complete dissolution of the phenol. The vial with the resulting solution was placed in an oil bath and warmed to 40 °C. T-HYDRO (10.0 mmol, 1.38 mL, 10 equiv.) was added via syringe all at once, and the reaction solution was stirred at 40 °C until complete consumption of **41** according to TLC. The reaction mixture contained two spots with R_f = 0.31 and 0.00 in hexane/AcOEt (10:1) according to TLC analysis. The mixture was transferred to 100-mL round-bottom flask and concentrated on a rotary evaporator (20 Torr, room temperature). The residue was dissolved in DCM and purified by column chromatography [neutral alumina, 18 mm diameter, 18 cm height, EtOAc/DCM/hexane

(1:1:16, 250 mL)]. Fractions containing **42** were combined, and the solvent was evaporated on a rotary evaporator (60 Torr, room temperature). The residue was further dried under high vacuum (0.09 Torr) for 20 minutes at room temperature to yield 433 mg (56%) of mixed peroxide **42** as a pale yellow oil for $Rh_2(cap)_4$ catalyzed oxidation and 124 mg (16%) mixed peroxide **42** as a pale yellow oil for $RuCl_2(PPh_3)_3$ catalyzed reaction.

Oxidation of 2-Naphthol (43). $Rh_2(cap)_4(MeCN)_2$ (0.50 μmol, 1.1 mg) and toluene (10.0 mL) were placed in a 50-mL Erlenmeyer flask and the suspension was warmed to 40 °C. T-HYDRO (12.0 mmol, 1.66 mL, 4.0 equiv.) was added via syringe dropwise followed immediately by dropwise addition over five minutes of a solution of 2-naphthol **43** (3.0 mmol, 432 mg) and peroxide **28** (1.0 mmol, 308 mg) in toluene (20.0 mL). Peroxide **28** was used as the internal standard. After completion of addition the reaction mixture was stirred for 20 minutes at 40 °C, then an aliquot (about 0.10 mL) was removed from the organic layer and concentrated under high vacuum (0.09 Torr) for five minutes at room temperature. The residue was dissolved in $CDCl_3$ and analyzed by ^1H NMR spectroscopy. Percent yield was determined from the integral values of internal standard **28** (s, 6.56 ppm) and alkene proton of **44** (d, 6.44 ppm): R_f = 0.16 (hexane/AcOEt/DCM (8:1:1)); ^1H NMR (600 MHz, $CDCl_3$) δ 8.11 (d, *J* = 7.6 Hz, 1 H), 7.66 (t, *J* = 7.5 Hz, 1 H), 7.52 (t, *J* = 7.6 Hz, 1 H), 7.46 (d, *J* = 10.1 Hz, 1 H), 7.38 (d, *J* = 7.5 Hz, 1 H), 6.44 (d, *J* = 10.1 Hz, 1 H); ^{13}C NMR (150 MHz, $CDCl_3$) δ 180.9, 178.9, 145.3, 135.8, 134.8, 131.6, 130.8, 130.2, 129.8, 127.9.

General Procedure for $Rh_2(cap)_4$-Catalyzed Oxidation of Anilines with 5 M TBHP in Decane or with T-HYDRO. The substituted aniline (2.0 mmol),

$Rh_2(cap)_4(MeCN)_2$ (14.8 mg, 0.020 mmol), and DCE (4.0 mL) were placed in a 4-dram screw-cap vial containing a magnetic stirring bar. The vial was place in an oil bath and the suspension was stirred at 250 rpm at 40 °C. Five molar TBHP solution in decane (1.6 mL, 8.0 mmol, 4.0 equiv.) or T-HYDRO (1.1 mL, 8.0 mmol, 4.0 equiv.) was added to the suspension all at once via syringe. The reaction mixture was loosely capped to release any pressure built-up and stirred for 20 minutes at 40 °C. Then the reaction mixture was transferred to a 100-mL round-bottom flask, concentrated under reduced pressure, and the residue was purified by column chromatography (silica gel, DCM:AcOEt:hexane). Fractions containing the product were combined, and the solvent was evaporated on a rotary evaporator. The residue was additionally dryed under high vacuum (0.09 Torr) for 20 minutes at room temperature.

^{1}H and ^{13}C Spectra of New Compounds

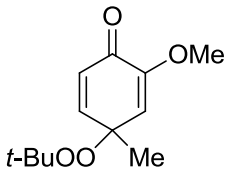

36

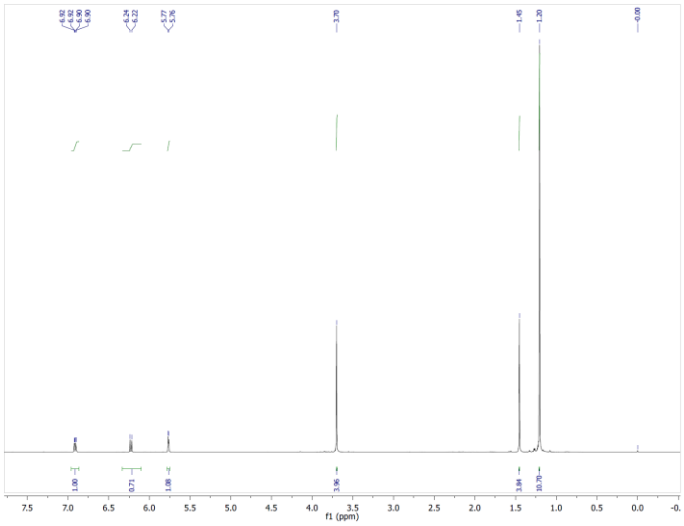

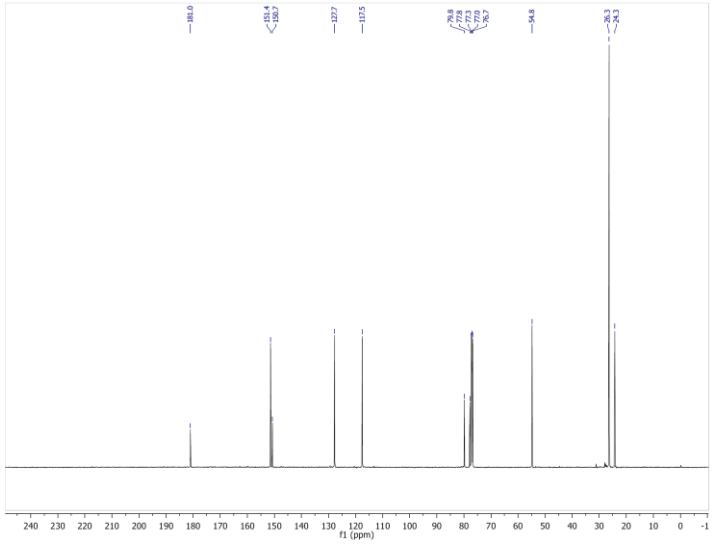

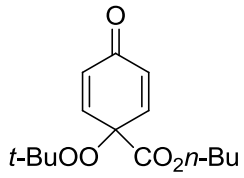
O
t-BuOO
CO2n-Bu

46

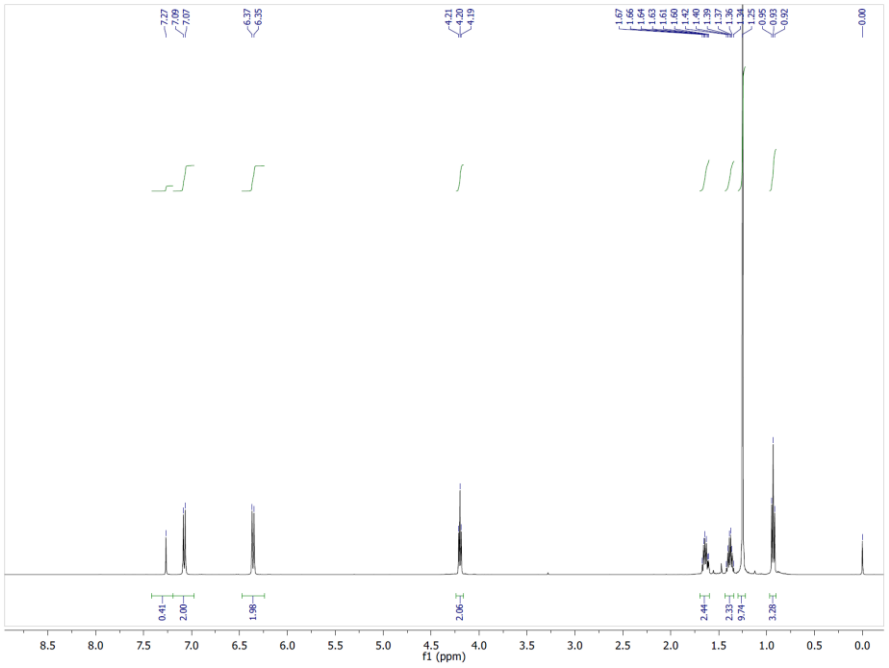
7.27
7.09
7.07
6.37
6.35
4.21
4.20
4.19
1.67
1.66
1.64
1.63
1.61
1.60
1.42
1.40
1.39
1.37
1.36
1.34
1.25
0.95
0.93
0.92
0.00
0.41
2.00
1.98
2.06
2.44
2.33
9.74
3.28
8.5 8.0 7.5 7.0 6.5 6.0 5.5 5.0 4.5 4.0 3.5 3.0 2.5 2.0 1.5 1.0 0.5 0.0
f1 (ppm)

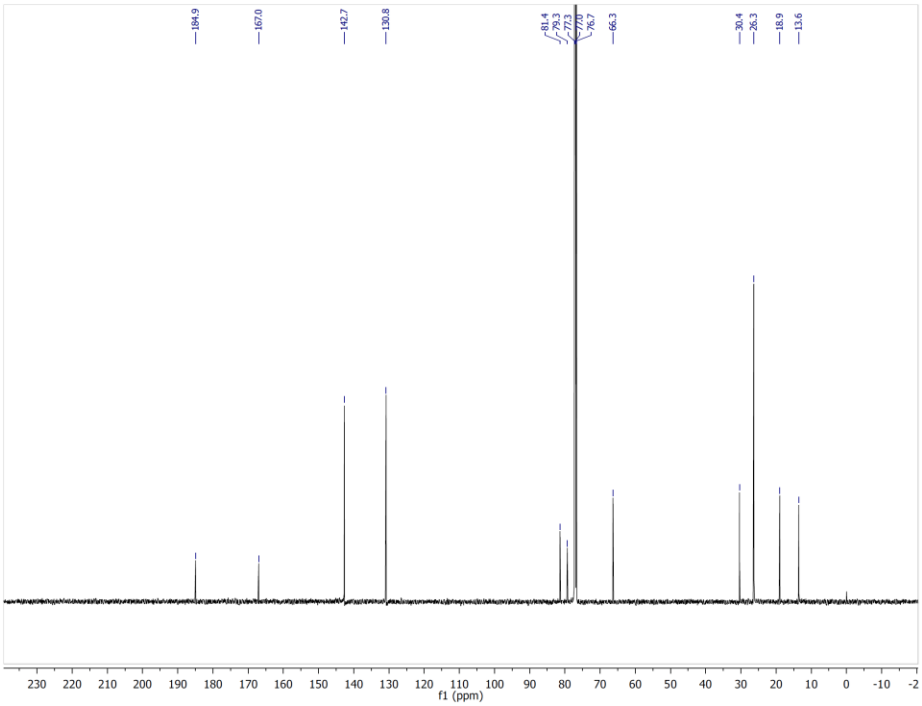
184.9
167.0
142.7
130.8
81.4
79.3
77.3
77.0
76.7
66.3
30.4
26.3
18.9
13.6
230 220 210 200 190 180 170 160 150 140 130 120 110 100 90 80 70 60 50 40 30 20 10 0 -10 -2
f1 (ppm)

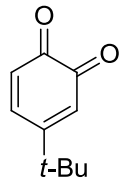
O
O
t-Bu

52

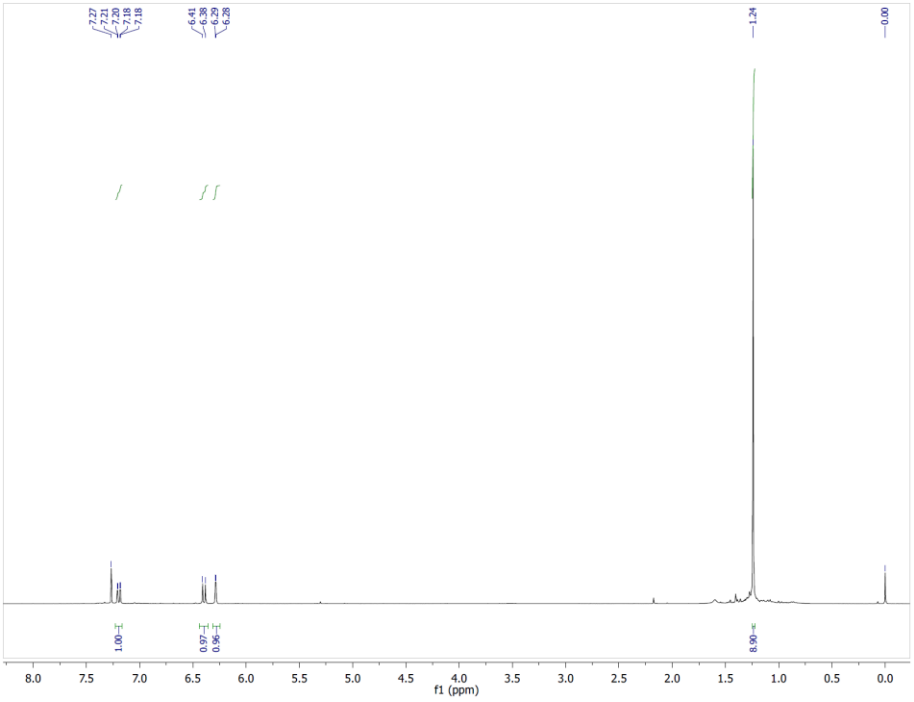
7.27
7.21
7.20
7.18
7.18
6.41
6.38
6.29
6.28
1.24
0.00
1.00
0.97
0.96
8.90
f1 (ppm)

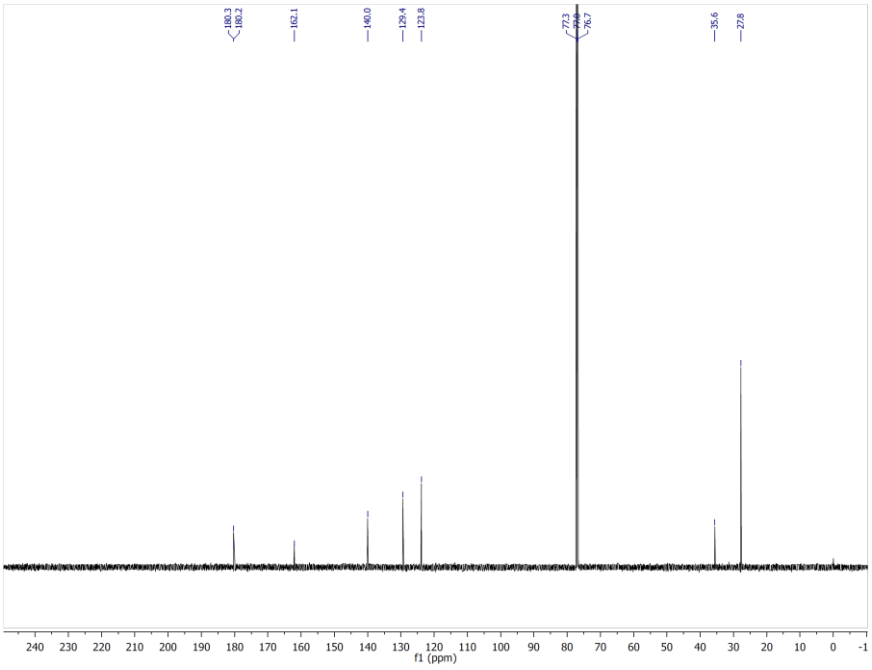
180.3
180.2
162.1
140.0
129.4
123.8
77.3
77.0
76.7
35.6
27.8
f1 (ppm)

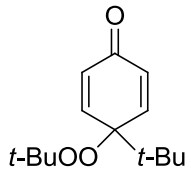
O
t-BuOO
t-Bu

53

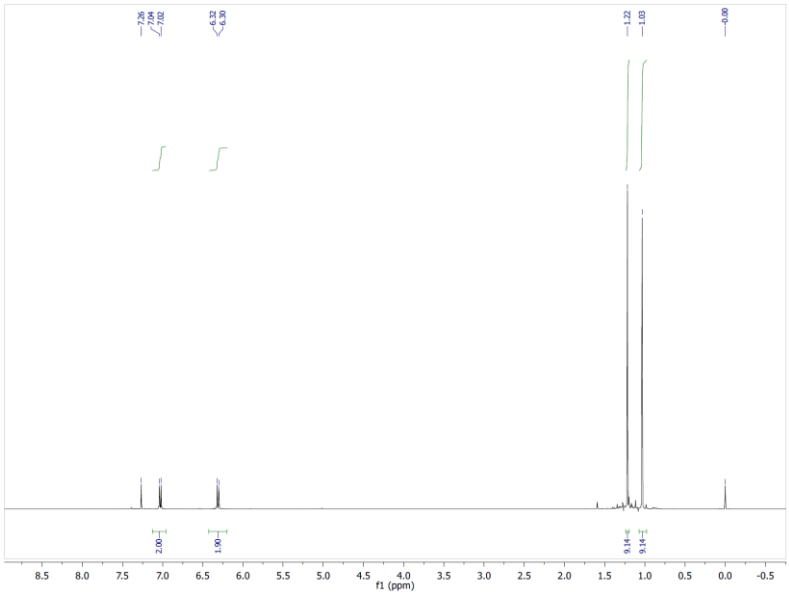
7.26
7.04
7.02
6.32
6.30
1.22
1.03
0.00
2.00
1.90
9.14
9.14
f1 (ppm)

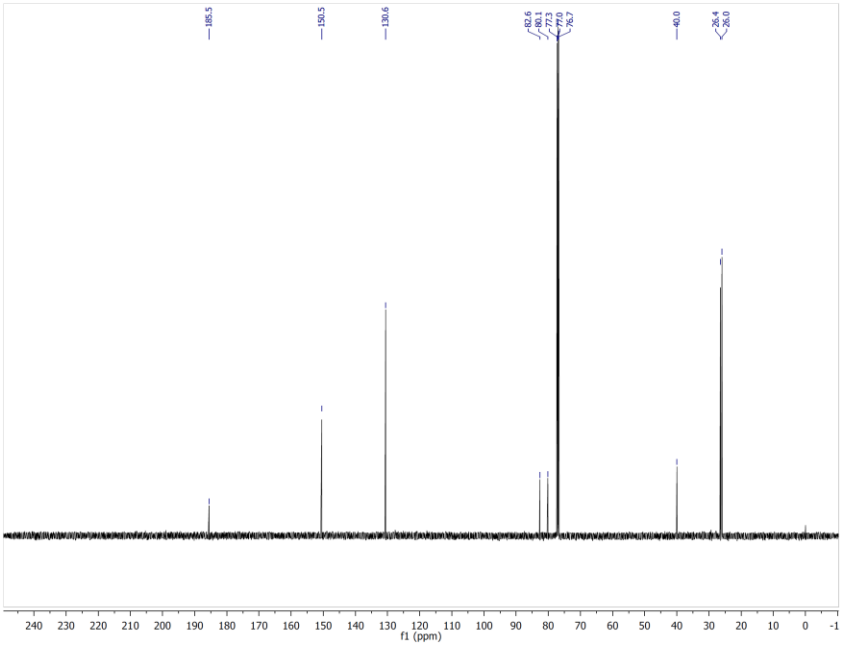
185.5
150.5
130.6
82.6
80.1
77.3
77.0
76.7
40.0
26.4
26.0
f1 (ppm)

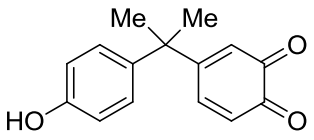
Me
Me
O
O
HO

55

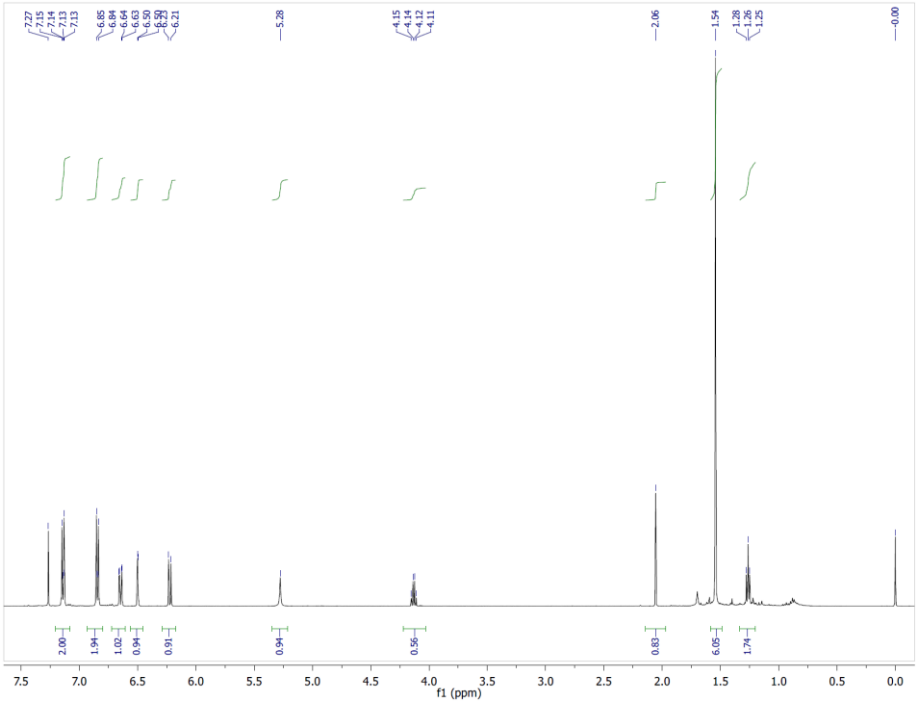
7.27
7.15
7.14
7.13
7.13
6.85
6.84
6.64
6.63
6.50
6.50
6.21
5.28
4.15
4.14
4.12
4.11
2.06
1.54
1.28
1.26
1.25
0.00
2.00
1.94
1.02
0.94
0.91
0.94
0.56
0.83
6.05
1.74
7.5
7.0
6.5
6.0
5.5
5.0
4.5
4.0
3.5
3.0
2.5
2.0
1.5
1.0
0.5
0.0
f1 (ppm)

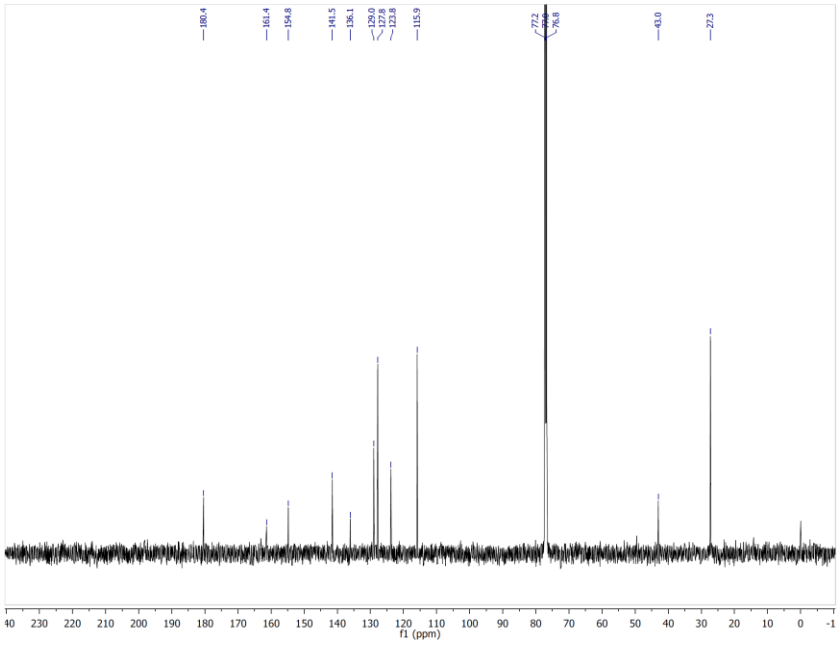
180.4
161.4
154.8
141.5
136.1
129.0
123.8
115.9
77.2
76.8
43.0
27.3
40
230
220
210
200
190
180
170
160
150
140
130
120
110
100
90
80
70
60
50
40
30
20
10
0
-1
f1 (ppm)

Chapter 2: Tandem Sequence of Phenol Oxidation and Intramolecular Addition as a Versatile Method in Building Heterocycles

Synopsis

This chapter will focus on the development of a tandem phenol - Michael addition that furnishes a number of oxo- and -aza-heterocycles. The scope of the $Rh_2(cap)_4$ catalyzed phenol oxidation by T-HYDRO that was presented in Chapter 1 is expanded to include alcohols, ketones, amides, carboxylic acids, and *N*-Boc protected amines tethered to the 4-position of phenol. The presence of alcohols, carboxylic acids, and *N*-Boc protected amines opened a new synthetic application for products of phenol oxidation by T-HYDRO, 4-(*tert*-butylperoxy)cyclohexa-2,5-dienones. It was found that Brønsted acids catalyze intramolecular Michael addition of alcohols, carboxylic acid, and *N*-Boc protected amines to 2,5-dienone scaffolds in the phenol oxidation reaction mixture. A series of 4-substituted phenols were converted into oxo- and aza-heterocycles in one-pot according to the developed tandem protocol of phenol oxidation - Michael addition (Scheme 2-1). The scope of the developed methodology includes dipeptides Boc-Tyr-Gly-OEt and Boc-Tyr-Phe-Me. A novel method of selective cleavage of O-O bond in hindered internal peroxide using $TiCl_4$ was discovered. To exemplify its synthetic versatility this methodology was used to complete the synthesis of cleroindicin F from tyrosol in 50% yield over 3 steps.

Scheme 2-1. Summary of tandem $Rh_2(cap)_4$ catalyzed phenol oxidation and Brønsted acid catalyzed intramolecular Michael addition.

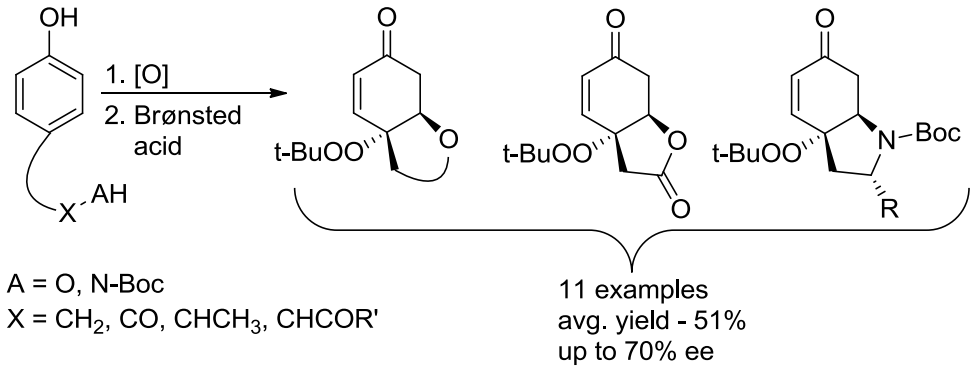

Introduction -- Synthetic Methods and Mechanistic Models for Phenol Oxidation

The development of the dirhodium caprolactamate [$Rh_2(cap)_4$] catalyzed oxidation of 4-substituted phenols by T-HYDRO (Chapter 1) provided access to 4-(*tert*-butylperoxy)cyclohexa-2,5-dienones in yields generally above 70% (Scheme 2-2).[1] The phenol oxidation by T-HYDRO enabled access a variety of alkyl, aryl, and carboxylate groups in the presence of nucleophiles and oxygen. The versatility of this methodology and the commercial availability of 4-substituted phenols prompted us to explore the synthetic applications of phenol oxidation.

Scheme 2-2. Dirhodium caprolactamate oxidation of 4-substituted phenols by T-HYDRO.

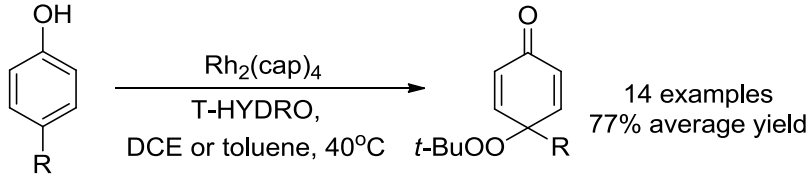

Murahashi has shown 4-(*tert*-butyldioxy)cyclohexa-2,5-dienones afford 2-substituted *p*-quinones upon treatment with $TiCl_4$ (Scheme 2-3).[36] The range of 4-substituents of 4-(*tert*-butyldioxy)cyclohexa-2,5-dienones includes alkyl, cycloalkyls, and allyl substituents. Presumably, the mechanism of this rearrangment starts with the binding of a Lewis acid to carbonyl group of the 2,5-dienone (Scheme 2-4).[36] Coordination by an electron deficient $TiCl_4$ facilicates migration of the substituent at the 4-position in the order Ph ~ $PhCH_2$ > *i*-Pr > Me > CH_2CO_2Me. The resulting intermediate **1** furnishes 2-substituted *p*-quinones after the loss of *tert*-butyl alcohol and $TiCl_4$. Recently Murahashi applied this protocol to the syntheses from *p*-cresol of vitamin K_1 (36% yield, 5 steps) and vitamin K_3 (79% yield, 4 steps).[37]

Scheme 2-3. Rearrangement of 4-(*tert*-butylperoxy)cyclohexa-2,5-dienones to 2-substituted *p*-quinones by $TiCl_4$.

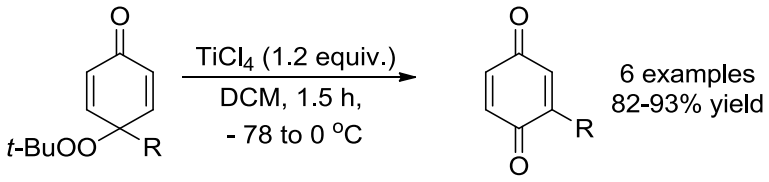

Scheme 2-4. Mechanism proposed by Murahashi for rearrangement of 4-(*tert*-butylperoxy)cyclohexa-2,5-dienones to 2-substituted *p*-quinones by $TiCl_4$.

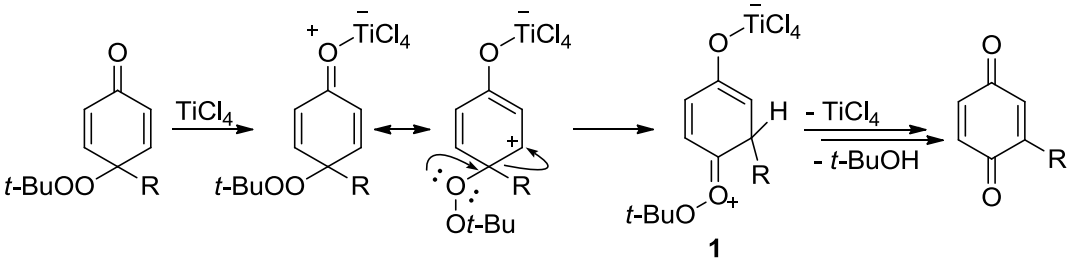

A number of transformations were reported for 2,5-dienone scaffolds that did not contain the 4-*tert*-butylperoxy group. These methods include regioselective reduction of the carbonyl group of 2,5-dienones,[57] expoxidation of a carbon-carbon double bond,[58] intermolecular Diels-Alder cycloaddition,[59] and the Baylis-Hillman reaction.[60] However, I found intramolecular transformations of 2,5-dienone scaffold the most promising because of the range of functional groups that can be tethered to the 4-position of 4-substituted phenols. Furthermore, I decided to focus on intramolecular Michael addition because the $Rh_2(cap)_4$ catalyzed phenol oxidation by T-HYDRO is insensitive to the nucleophilic functional groups (discussed in Chapter 1)

Carreno reported a strategy for activation of 2,5-dienones by *p*-toluenesulfonic acid (TsOH) to promote intramolecular oxo-Michael addition with tethered alcohols.[34c] This protocol affords *cis*-furan and *cis*-pyran-fused cyclohexenones in 47-91% yields. The cyclization of racemic 4-hydroperoxy-2,5-dienone **2** afforded the tetrahydrofuran ring in 47% yield and a 85:15 diastereomeric ratio (Scheme 2-5a). However, reduction of the hydroperoxide to the hydroxyl group improved the yield of the cyclization step for 4-hydroxy-2,5-dienone **3** to 82% but the diastereomeric ratio decreased to 70:30 (Scheme 2-5b). The similar difference in yield between cyclization of 4-hydroperoxy- (**4**) and 4-hydroxy-2,5-dienones (**5**) was observed for the formation of the pyran ring from secondary alcohols (Scheme 2-5c-d).

Scheme 2-5. *p*-Toluenesulfonic acid catalyzed intramolecular oxo-Michael addition of alcohols to 4-hydroperoxy-2,5-dienones **2** and **4** and 4-hydroxy-2,5-dienone **3** and **5**.[34c]

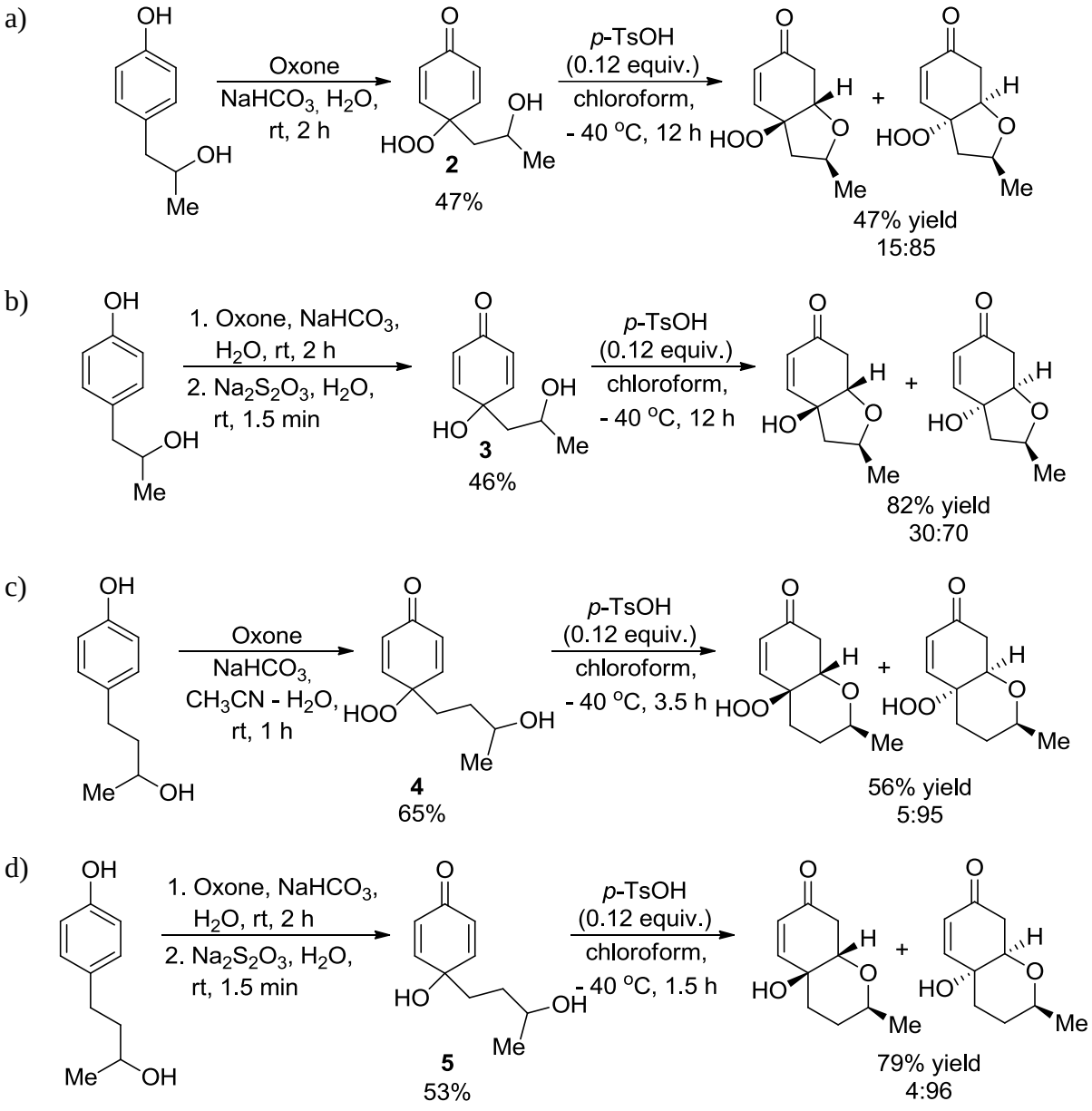

You reported a chiral version of 2,5-dienones desymmetrization via an oxo-Michael reaction catalyzed by BINOL-derived chiral phosphoric acids.[34a] The method forms *cis*-fused 1-oxo- and 1,4-dioxo-heterocycles in 71-92% yield and 61-95% ee. You found that a sterically encumbered phosphoric acid (**6**) afforded the highest

degree of enantiomeric excess with 2,5-dienone **7** (Scheme 2-6a). A series of 4-aryl-2,5-dinones underwent cyclization in higher than 81% yield and above 90% ee while the most sterically encumbered 2,5-dienone **8** furnished the lowest yield and ee value of 71% and 61%, respectively (Scheme 2-6b). The unfavorable steric interaction between bulky 4-substituents of 2,5-dienones and **8** indicates a potential limitation of this protocol. Chiral phosphoric acid derivative **6** catalyzed intramolecular oxo-Michael addition of **9** afforded the tetrahydrofuran ring in 57% yield and 80% ee (Scheme 2-7). This transformation was a key step in the synthesis of optically pure cleroindicin F **(10)** from tyrasol **(11)** (3 steps, 22% overall yield, 80% ee).[34a]

Scheme 2-6. Asymmetric intramolecular oxo-Michael addition of **7** and **8** catalyzed by chiral phosphoric acid **6**.[34a]

a)

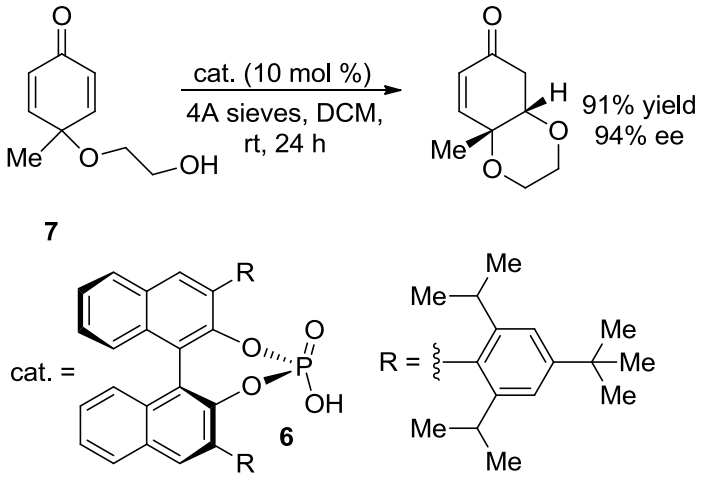

b)

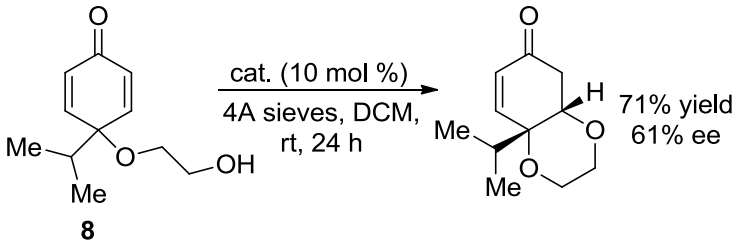

Scheme 2-7. Synthesis of cleroindicin F (**10**) from tyrasol (**11**).

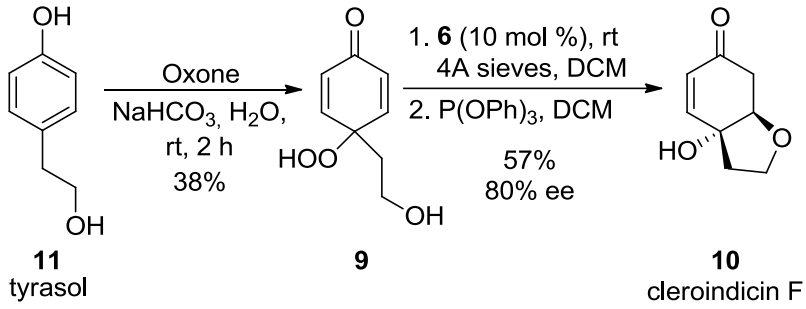

I considered several protocols developed for chiral desymmetrization of 4,4-disubstituted 2,5-dienones via intramolecular Michael reaction. Hayashi stereoselective intramolecular Michael addition of aldehydes to 4,4-disubstituted 2,5-dienones was one of them (Scheme 2-8a).[61] The use of 10 mole % of cysteine-derived ammonium salt **12** furnished *cis*-6,5-fused carbocycles from corresponding 2,5-dienones in 89-99% yield, 82-92% de, and 90-95% ee. However, Hayashi applied this protocol to just four substrates. Furthermore, 4,4-dialkyl-2,5-dienones are derived from cyclohexenone **13** via the 6 step synthesis (Scheme 2-8b)[61] rather than from 4-substituted phenols.

Scheme 2-8. Ammonium salt **12** catalyzed intramolecular Michael additions of aldehydes tethered to 2,5-dienones.

a)

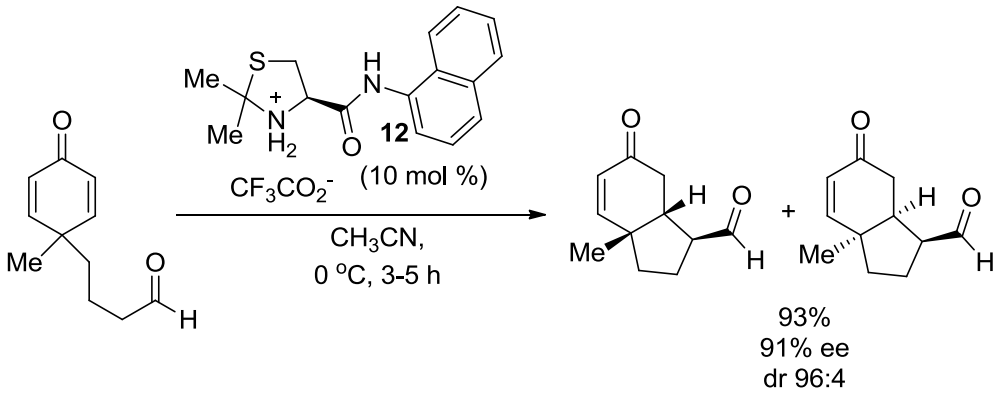

b)

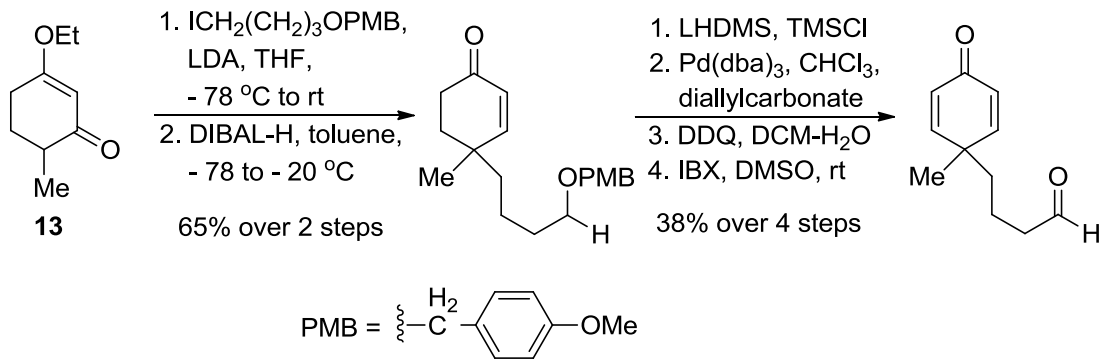

Gaunt found that *L*-proline-derived secondary amine **14** catalyzes the intramolecular Michael addition of an aldehyde to 2,5-dienone in **15** in 91% yield, 99% ee, and > 20:1 dr (Scheme 2-9a).[34b] Further investigations revealed that intramolecular Michael addition of aldehydes tethered to 4-methoxy-2,5-dineones could be conducted simultaneously with the oxidation of 4-substituted phenol by one equivalent of $PhI(OAc)_2$ in methanol in the one-pot procedure (Scheme 2-9b). This methodology afforded *cis*-6,5- and *cis*-6,6-fused ring systems in 52-75% yield, 97-99% ee, and dr up to > 20:1 for aldehydes tethered to phenol with hydrocarbon chains.[34b] The use of oxygen (**16**) or tosylated nitrogen (**17**) as an attachment point of an aldehyde tether to phenol furnished **18** in 84% yield, 99% ee, > 20:1 dr and **19** in 68% yield, 99% ee, > 20:1 dr (Scheme 2-9c). 2,6-Dimethyl substitution in the phenol ring decreased enantiomeric excess to 40% and diastereomeric ratio to 2:1 of the *cis*-6,5-carbocycle from 97% ee, and 15:1. The erosion of diastereoselectivity was observed from > 20:1 for the oxo-heterocycle **18** (Scheme 2-9c) to 6.7:1 for the *cis*-6,7-membered oxo-heterocycle **20**, however, the ee value reached 97% (Scheme 2-9d). Presumably, the decrease of diastereoselectivity is caused by a competing epimerization of methine group adjacent to the aldehyde in the product of phenol oxidation – intramolecular Michael addition.

Scheme 2-9. Application of secondary amine **14** catalyzed asymmetric intramolecular Michael addition of tethered aldehydes to 2,5-dienones in syntheses of *cis*-6,5-, *cis*-6,6-, and *cis*-6,7-bicyclic systems.

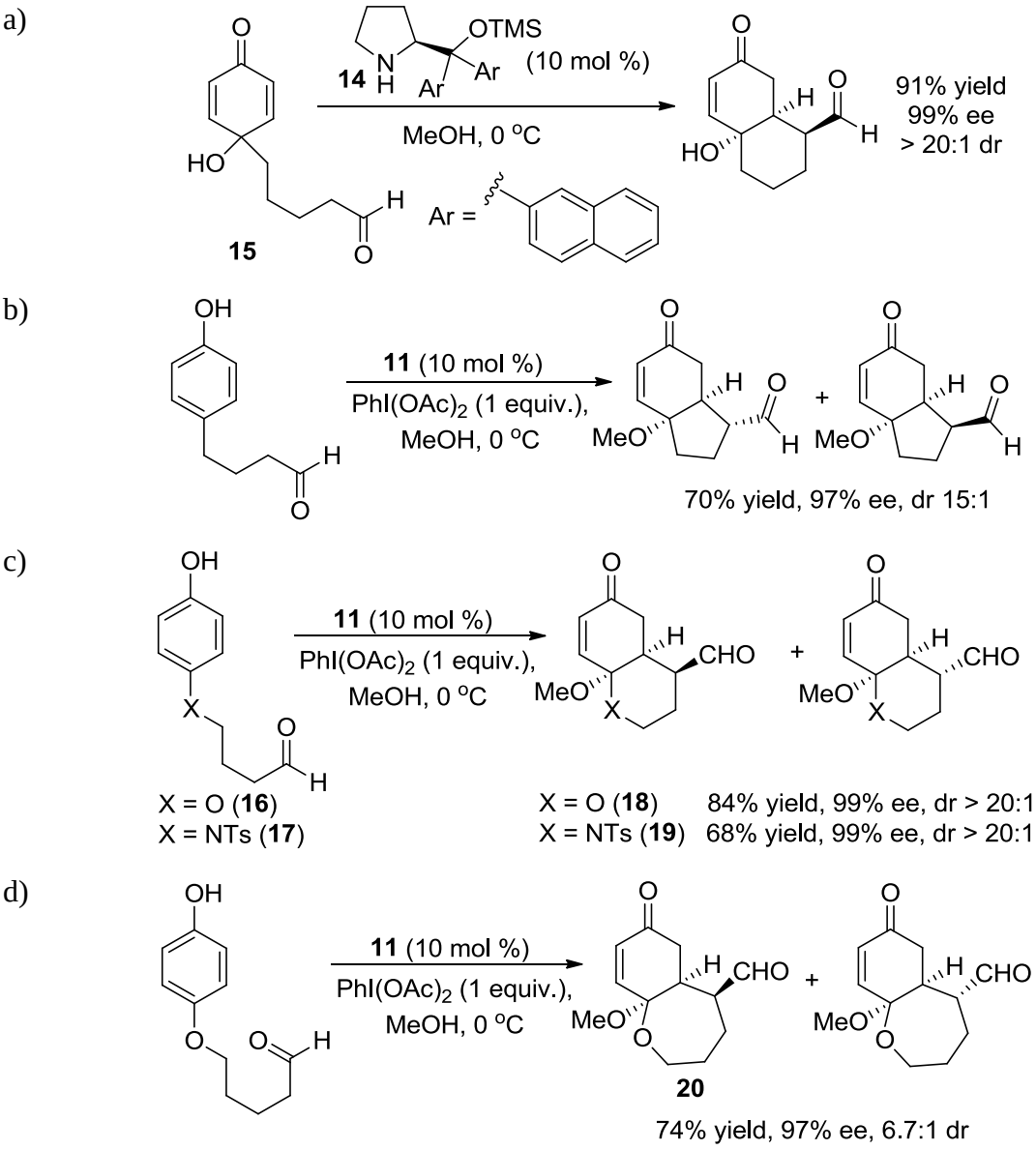

β-Ketoesters tethered to the 4-position of 4-alkyl-2,5-dienones were employed for the intramolecular Michael addition of 2,5-dienones under phase transfer catalysis **21** (Scheme 2-10a).[62] This strategy furnished *cis*-furan-fused cyclohexenes in 77-89% yields and 50-74% ee from 2,5-dienones bearing methyl, *iso*-propyl or phenyl groups. The more

sterically encumbered 2,5-dienones **22** and **23** afforded *cis*-furan-fused cyclohexenes **25** in 44% yield, 54% ee and **26** in 52% yield, 50% ee (Scheme 2-10a). 2,6-Dimethyl substitution on the 2,5-dienone decreased the yield and the enantiomeric excess to 67% and 38%, respectively (Scheme 2-10b). Noteworthy, this protocol allows no tether variations and requires two chromatographic purifications during a two-step synthesis of β-ketoesters tethered to 2,5-dienones.

Scheme 2-10. Asymmetric intramolecular Michael addition of β-ketoesters to 4-alkyl-2,5-dienones.

a)

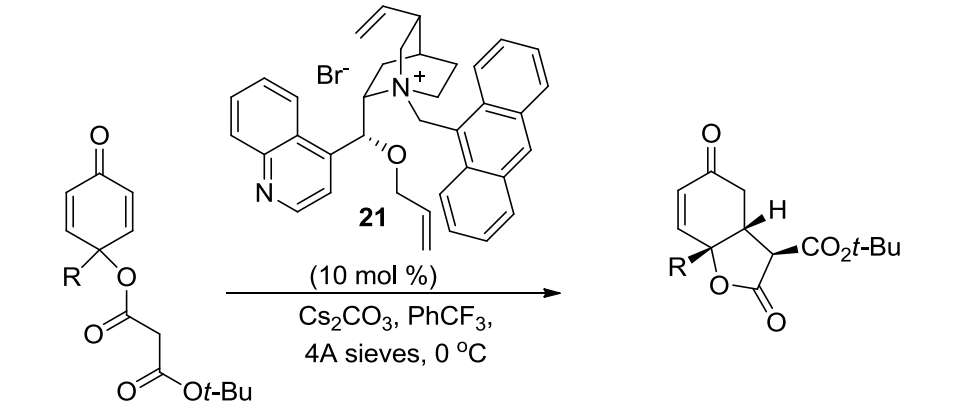

b)

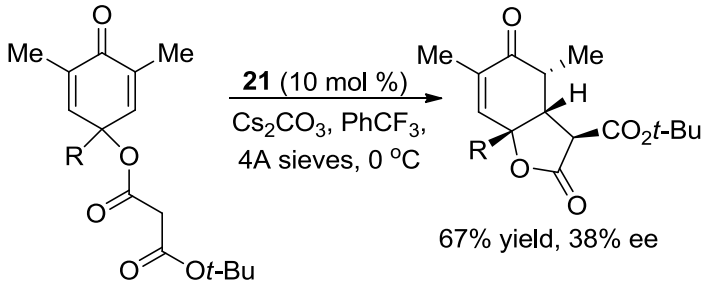

Bisphenylsulfonyl methylene is an alternative nucleophilic scaffold for β-ketoesters in their intramolecular Michael addition to 2,5-dienones.[63] You studied cinchonine-derived ureas as catalysts for the chiral desymmetrization of 2,5-dienones

tethered to bisphenylsulfonyl methylene at 4-position (Scheme 2-11) and found urea **27** to be an optimal catalyst. The use of **27** furnished *cis*-6,5- and *cis*-6,6-carbocycles from 4-alkoxy-2,5-dienones in 82-97% yield and 84-91% ee.[63] The bisphenylsulfonyl methylene tether can be varied from two methylene units to *o*-substituted aromatic ring thus offering more structural diversity in comparison to the protocol developed for β-ketoesters. The removal of bisphenylsulfonyl functionality requires a three-step procedure (Scheme 2-12).[63]

Scheme 2-11. Cinchonine-derived urea **27** catalyzed asymmetric intramolecular Michael addition of bisphenylsulfonyl methylene to 2,5-dienone.

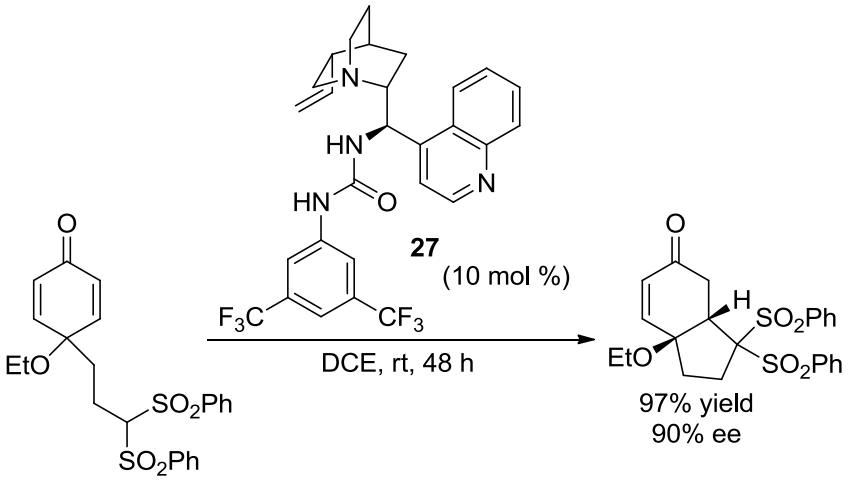

Scheme 2-12. Three-step removal of bisphenylsulfonyl functionality.

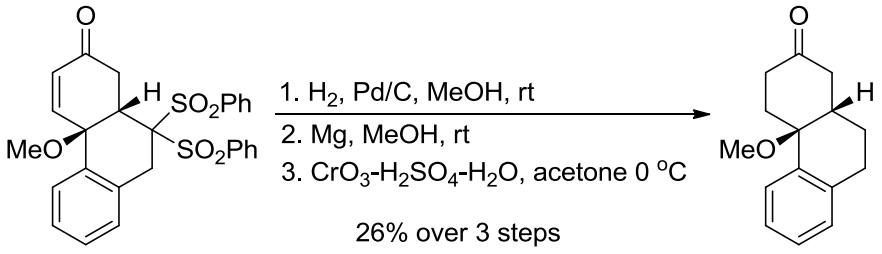

The analysis of reported protocols for the chiral desymmetrization of 4-substituted 2,5-dienones showed that the Brønsted acid catalyzed intramolecular oxo-Michael addition was the most promising. This methodology afforded up to 91% yield and 95% ee for a scaffold that is closely related to 4-(*tert*-butylperoxy)cyclohexa-2,5-dienones.[34a] Thus, I envisioned combining the $Rh_2(cap)_4$ catalyzed phenol oxidation by T-HYDRO and the Brønsted acid catalyzed intramolecular Michael addition in a one-pot protocol. The higher yields of the phenol oxidation than those reported for oxone (Scheme 2-7)[34a] would enable stereoselective synthesis of oxo-heterocycles in higher overall yields. Additionally, I planned to explore nitrogen-containing nucleophiles in Brønsted acid catalyzed intramolecular aza-Michael addition to 2,5-dienones.

Results and Discussion

The development of the phenol oxidation - Michael addition tandem transformation was started with the oxidation of tyrosol **8**, the precursor to a potential treatment for malaria and rheumatism, cleroindicin F (**10**) [Scheme 2-7].[64] Initial phenol oxidation experiments were conducted under conditions previously developed for the $Rh_2(cap)_4$ oxidation of 4-substituted phenols [4 equivalents of T-HYDRO in 1,2-dichloroethane (DCE) at 40 °C].[1] The evaluation of the most active catalysts for 4-substituted phenol oxidation with T-HYDRO [$RuCl_3$, $RuCl_2(PPh_3)_3$, and $Rh_2(cap)_4$][1] at 1.0 mole % loading revealed that dirhodium caprolactamate provides the best yield in the conversion of **8** to **28** (Table 2-1, entries 1-3). The use of 2.0 mole % of $Rh_2(cap)_4$ eroded the yield of 2,5-dienone **28** (entry 4) while 0.5 mole % of $Rh_2(cap)_4$ gave incomplete conversion. Thus, I inferred 4 equivalents of T-HYDRO in 1,2-dichloroethane (DCE) at

40 °C using 1.0 mole % of $Rh_2(cap)_4$ as the first generation of optimal conditions. The oxidation of **8** under these conditions furnished **28** in 66% isolated yield (eq. 2-1).

Table 2-1. Optimization of a catalyst for the phenol oxidation by T-HYDRO.

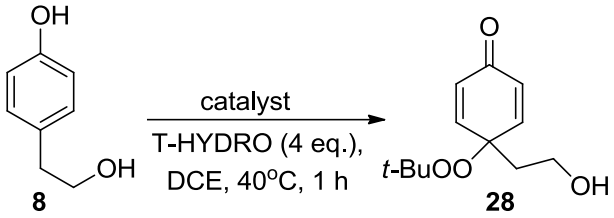

entry	catalyst	catalyst loading, mol %	yield, %[a]
1	$RuCl_3$	1.0	23
2	$RuCl_2(PPh_3)_3$	1.0	48
3	**$Rh_2(cap)_4$**	**1.0**	**66**
4	$Rh_2(cap)_4$	2.0	48

[a] Determined by ^{1}H NMR spectroscopy from the ratio of peak (6.32 ppm, d, J = 10.2 Hz, 2H) corresponding to **28** and biphenyl peak (7.60 ppm, d, J = 7.2 Hz, 4H) that was used as an internal standard.

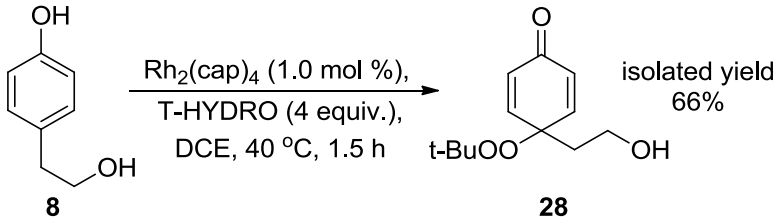

(eq. 2-1)

Although ^{1}H NMR spectroscopy and TLC showed that the sample contained only 2,5-dienone **28** after 1.5 hour in the reaction mixture of $Rh_2(cap)_4$ catalyzed phenol oxidation by T-HYDRO, the isolated yield was non-quantitative $Rh_2(cap)_4$. The reaction temperature was lowered to room temperature in an attempt to improve yield and ^{1}H NMR spectroscopy revealed the formation of transient *o*-quinone **29** along with 53%

yield of 2,5-dienone **28** (eq. 2-2)**.** However, because of *o*-quinone **29** instability under the reaction conditions, its decomposition products were insoluble in the reaction mixture after 1.5 hour at 40 °C.

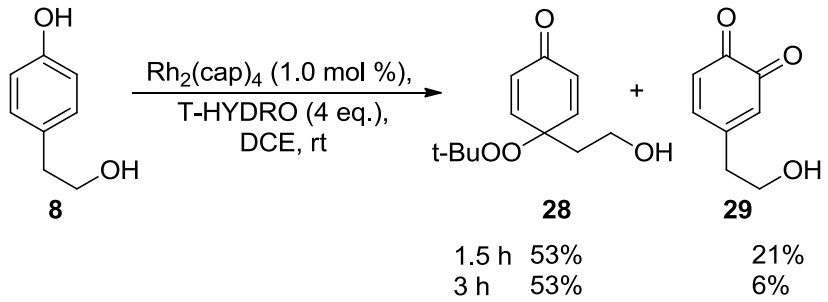

(eq. 2-2)

To improve the yield of the $Rh_2(cap)_4$ catalyzed phenol oxidation by T-HYDRO factors that could increase the of 2,5-dienone **28** (temperature, solvent, etc.) were evaluated. Temperature and concentration had minimal effects on the yield of **28** (Table 2-2, entries 1-4). Solvent screening confirmed the initial choice of DCE as the optimal solvent (entries 5-15). Other common organic solvents gave 24-60% yields of **28** that are not higher than the 66% yield achieved in DCE.

Table 2-2. Temperature, concentration, and solvent optimization for the $Rh_2(cap)_4$ catalyzed oxidation of **8** by T-HYDRO.

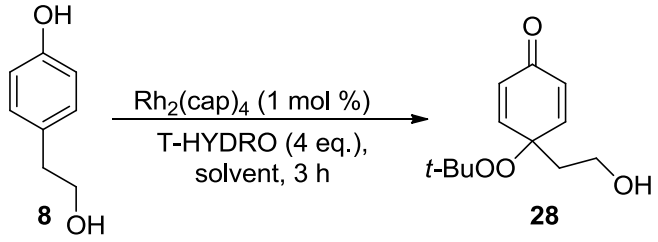

entry	solvent	concentration, M	temperature, °C	yield, %[a]
1	**DCE**	**0.5**	**40**	**66**
2	DCE	0.5	room temperature	53
3	DCE at 0 °C	0.5	0	61[b]
4	DCE (0.01 M)	0.01	40	55
5	DCM	0.5	room temperature	58
6	Et_2O	0.5	40	52
7	THF	0.5	40	28
8	AcOEt	0.5	40	60
9	DCE / MeOH (1:1)	0.5	40	50
10	MeCN	0.5	40	42
11	MeOH	0.5	40	37
12	EtOH	0.5	40	34
13	MeOH / H_2O (1:1)	0.5	40	37
14	H_2O	0.5	40	24
15	DCE / water (2:1)	0.5	40	58

[a] Determined by ^1H NMR spectroscopy from the ratio of peak (6.32 ppm, d, J = 10.2 Hz, 2H) corresponding to **28** and biphenyl peak (7.60 ppm, d, J = 7.2 Hz, 4H) that was used as an internal standard. [b] Adjusted for 55% conversion.

The use of 2.5, 3.0 and 10 equivalents of T-HYDRO had a detrimental effect on the yield of **28** (Table 2-3, entries 1-3). Anhydrous TBHP in decane and cumyl hydroperoxide afforded the corresponding 2,5-dienone **28** in 45% and 48 % yield (entries 4-5), respectively. Similarly, different modes of reactant addition showed no improvement in the yield of **28** (entries 6-10). Thus, the initial set of conditions were concluded to be optimal for the phenol oxidation bearing an alcohol group, and all of the subsequent phenol oxidations were conducted using 1 mole % of $Rh_2(cap)_4$ with 4 equiv. of T-HYDRO in DCE (0.5 M) at 40 °C. Although I was unable to further improve the yield of **28**, the 66% yield of oxidation of **8** by T-HYDRO under $Rh_2(cap)_4$ catalysis was higher than 22% yield reported with oxone (Scheme 2-7).[34a]

Table 2-3. Optimization of the oxidant and mode of addition of the $Rh_2(cap)_4$ catalyzed oxidation of **8.**

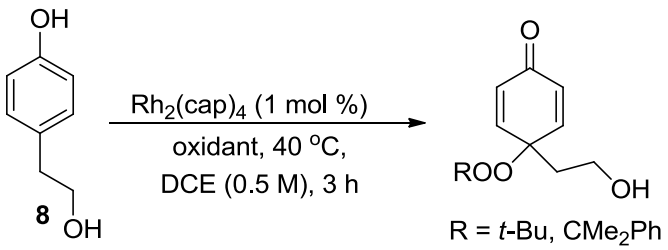

entry	oxidant	number of equivalents of TBHP	modification to standard conditions	yield, %[a]
1	T-HYDRO	2.5	—	42
2	T-HYDRO	3.0	—	53
3	T-HYDRO	10	—	53
4	TBHP in decane	4.0	—	45
5	$PhMe_2COOH$	4.0	—	48
6	T-HYDRO	4.0	stirring at 600 rpm	61
7	T-HYDRO	4.0	N_2 bubbling	52
8	T-HYDRO	4.0	preheat to 40 °C prior to T-HYDRO addition	64
9	T-HYDRO	4.0	no sonication of phenol suspension	63
10	T-HYDRO	4.0	the oxidation is quenched with $Na_2S_2O_3$	54

[a] Determined by ^1H NMR spectroscopy from the ratio of peak (6.32 ppm, d, J = 10.2 Hz, 2H) corresponding to **28** and biphenyl peak (7.60 ppm, d, J = 7.2 Hz, 4H) that was used as an internal standard.

The versatility of $Rh_2(cap)_4$ catalyzed phenol oxidation by T-HYDRO was examined for 4-substituted phenol bearing alcohol groups, carboxylic acids, methyl ketone, and the Boc-protected amine. The corresponding 2,5-dienones were isolated in 45-65% yields (Table 2-4). Similar to the oxidation of **8** phenol oxidations presented in Table 2-4 contained only 2,5-dienone products in their reaction mixtures. Pure 2,5-dienone products can be rapidly isolated by filtration of the reaction mixture through a silica gel plug. Although product yields vary, phenol oxidation by T-HYDRO, catalyzed by $Rh_2(cap)_4$ is not restricted by carboxylic acid, alcohol, and ketone substituents that could serve as potential nucleophiles in subsequent reactions. Likewise, the presence of the *N*-Boc group in tyramine **38** does not alter the oxidation pathway and furnished 2,5-dienone **39** in 59% yield (entry 5). The oxidation *p*-hydroxybenzyl alcohol **41,** however, produced *p*-quinone presumably due to fragmentation of peroxides bearing an acidic hydrogen on β-atom (entry 6) according to the mechanism discussed in Chapter 1 (Scheme 1-16).[1]

Table 2-4. Dirhodium caprolactamate oxidation of phenols bearing nucleophilic functional groups by T-HYDRO.

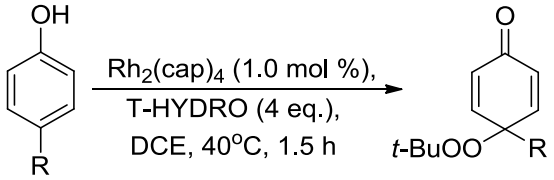

entry	phenol	product	isolated yield,[a] %
1	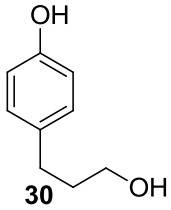 **30**	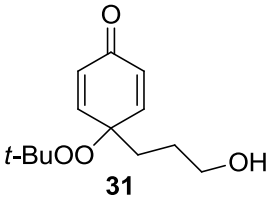 **31**	65
2	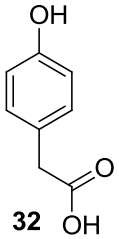 **32**	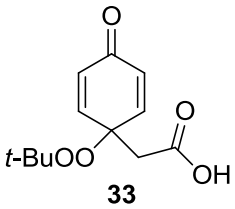 **33**	45[b]
3	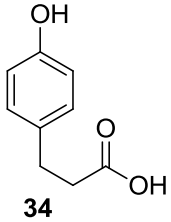 **34**	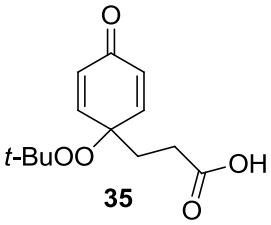 **35**	46[b]
4	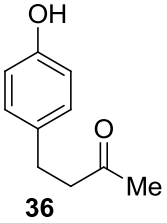 **36**	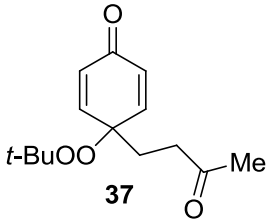 **37**	62

5	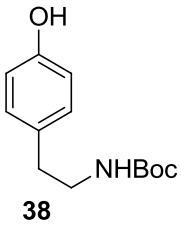 **38**	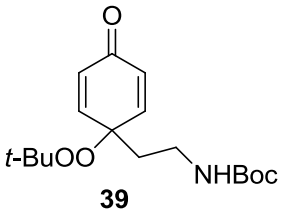 **39**	59
6	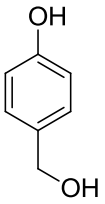 **40**	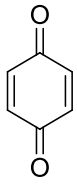 **41**	55[c]

[a] Yield after the silica gel plug. [b] 2 mole % of $Rh_2(cap)_4$ were used [c] The yield of volatile *p*-quinone (6.70 ppm, s, 4H) was determined by ^1H NMR spectroscopy using biphenyl (0.033 mmol) as internal standard.

The development of a phenol oxidation - Michael addition tandem transformation started with the simultaneous catalysis of phenolic oxidation by $Rh_2(cap)_4$ and oxo-Michael addition by BINOL-based phosphoric acid **43**. The addition of a Brønsted acid inhibited the oxidation step (Table 2-5, entries 1 and 2). However, the introduction of **43** after completion of the phenol oxidation furnished **42** with > 20:1 diastereoselectivity after 16 hours at room temperature (entry 3). The stereochemistry of the bicyclic ring junction was extrapolated from the analogous Brønsted acid catalyzed intramolecular oxo-Michael addition of 4-hydroperoxy-2,5-dienones (Scheme 2-5a).[34c] Furthermore, the addition of drying reagents improves the conversion of oxo-Michael reaction (entries 4-6). The addition of anhydrous Na_2SO_4 was considered to be the optimal procedure for the stepwise $Rh_2(cap)_4$ phenol oxidation by T-HYDRO followed by Brønsted acid catalyzed oxo-Michael addition.

Table 2-5. Optimization of conditions for tandem phenolic oxidation - Michael addition.

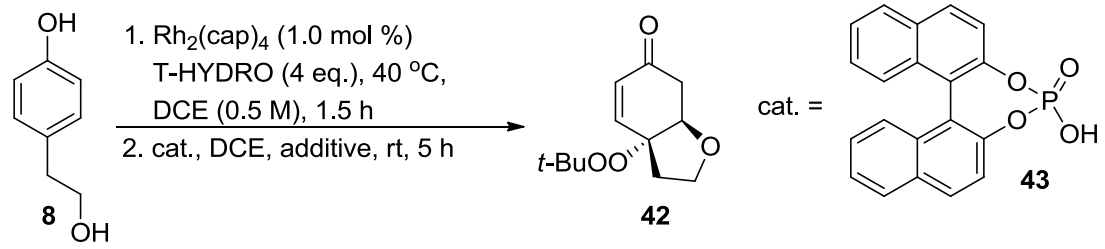

entry	loading of acid **30**, %	mode of addition	additive	conversion of phenol oxidation, %[a]	conversion of Michael addition, %[a]
1	10	simultaneous	—	45	nd[b]
2	2	simultaneous	—	70	nd
3	10	stepwise	—	100	78
4	10	stepwise	4 Å sieves	100	85
5	2	stepwise	4 Å sieves	100	17
6	**10**	**stepwise**	**Na_2SO_4**	**100**	**91**

[a] Determined by ^{1}H NMR spectroscopy from the ratio of peak (6.09 ppm, d, J = 10.3 Hz, 1H) corresponding to **42** and biphenyl peak (7.60 ppm, d, J = 7.2 Hz, 4H) that was used as an internal standard. [b] nd - not determined.

The isolated yields of cyclic products of the tandem $Rh_2(cap)_4$ catalyzed phenol oxidation and Brønsted acid catalyzed oxo-Michael addition were identical within experimental error to the yields for the tandem sequence that include purification of 2,5-dienone products in the phenol oxidation step. Hydrobenzofuran **42** and hydrobenzopyran **44** were prepared by tandem transformation in 62% and 52% isolated yields, respectively, as single diastereomers (Table 2-6, entries 1 and 2). oxo-Michael addition could also be catalyzed by TsOH (entry 2). Secondary alcohol **45** formed a mixture of only two out of possible four diastereomers (7.4:1) that were separated by

column chromatography in 59% isolated yield (entry 4). The major diastereomer (**46**) was determined by a NOESY experiment that showed a cross-peak of two axial protons in the α-positions to the ether oxygen of **46** (Figure 2-1). The formation of lactone **48** showed the developed tandem protocol could be applied to phenols with carboxylic acids tethered to the 4-position (entry 5). The division of the isolated yields of **42**, **44**, **48** for the tandem phenol oxidation - Michael transformation (Table 2-6, entries 1, 2, 3, and 5) by the isolated yields of **28**, **31** and **33** for just phenol oxidation (eq. 2-2 and Table 2-4, entries 1 and 2) suggests that oxo-Michael addition occurs in yields above 80%.

Table 2-6. Tandem phenol oxidation – oxo-Michael addition.

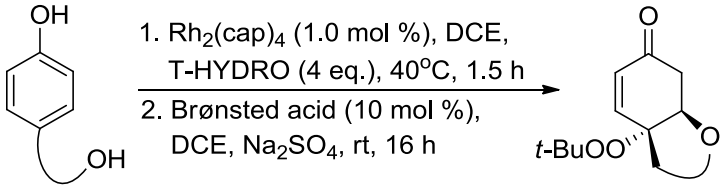

entry	phenol	product[a]	Brønsted acid	diastereomer ratio	isolated yield, %[b]
1	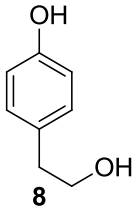 **8**	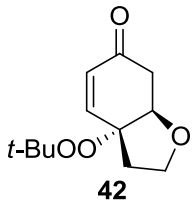 **42**	**30**	> 20:1	62[c]
2			TsOH	> 20:1	60
3	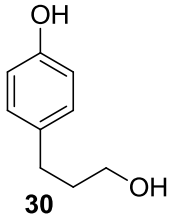 **30**	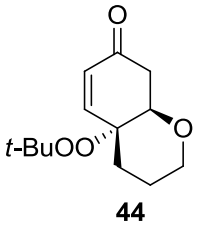 **44**	**30**	> 20:1	52

4	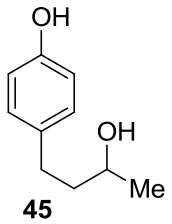	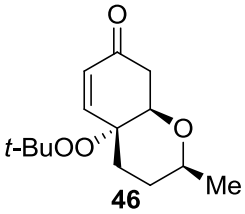 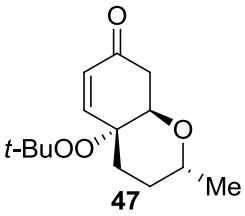	**30**	> 20:1[d]	59[e]
5	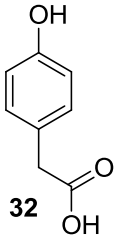	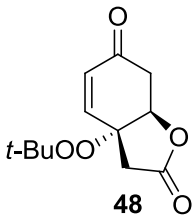	**30**	> 20:1	40

[a] Major diastereomer is shown. [b] After flash chromatography through silica gel. [c] Phenolic oxidation forms 21% *o*-quinone that undergoes decomposition under reaction conditions. [d] The ratio of **46**:**48** is 7.4:1. [e] Each diastereomer is isolated as an individual compound.

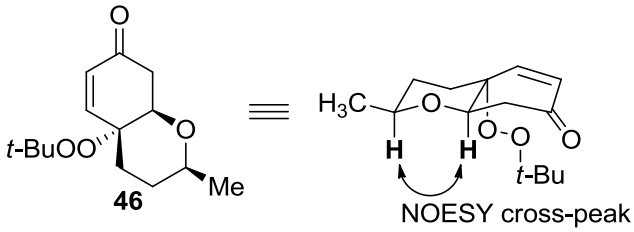

Figure 2-1. Determination of stereochemistry of hydrobenzopyrane **46**.

Having elaborated the optimum conditions and potential for generality of the tandem phenol oxidation - oxo-Michael addition, I moved to the development of a novel tandem oxidation - aza-Michael addition. L-Tyrosine derivatives were chosen as the initial substrates due to their biological relevance.[65] In agreement with the phenol oxidations reported in Tables 2-4 and 2-6, the oxidation of L-tyrosine derivatives furnished single 2,5-dienone products along with polar unidentified materials that did not

interfere with the subsequent Brønsted acid catalyzed cyclization. Carbamates **49** and **51** afforded dihydroindol derivatives **50** and **52** in 42% and 31% isolated yield, respectively (Table 2-7, entries 1 and 2). No cyclization was observed with acetyl protected amine **53** (entry 3). The highest yield in the tandem reaction of L-tyrosine derivative **49**, **51**, and **53** was achieved with **50** suggesting the use of the Boc-group for amine protection in the following phenol oxidation - aza-Michael addition transformations. The isolated yields of bicyclic products were improved if L-tyrosine derivatives lacked the carboxylic acid group (entry 4) or contained ester functionality (entries 5 and 6). The lower yield in the absence of carboxylic acid is presumably caused by the lower yield on the phenol oxidation step (Table 2-4, compare entries 1 and 5 with entries 2 and 3). Diastereomers formed from **57** and **58** were completely separable on silica gel and were isolated as individual isomers. The diastereochemistry of the ester group was determined by NOE experiments for diastereomers **57** and **58** (Figure 2-2). The phenol oxidation – aza-Michael addition occurred in the presence of the amide group (entry 7). Furthermore, the oxidation of dipeptide **62** could occur at the benzylic position of a phenylalanine residue and at the phenol group of a tyrosine residue but only the latter process was observed (entry 8).

Table 2-7. Tandem phenol oxidation – aza-Michael addition.

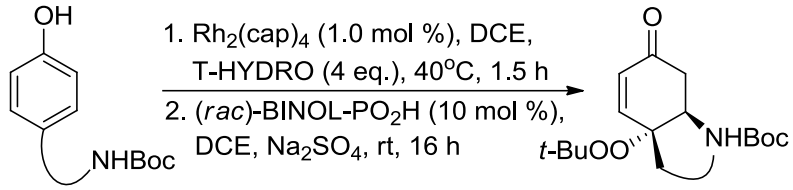

entry	phenol		product[a,b]		isolated yield, % (dr)[c]
1	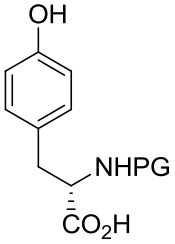	PG = Boc **49**	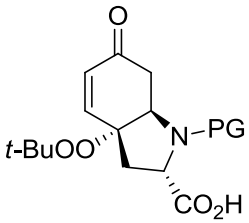	PG = Boc **50**	42 (2.8 : 1.0)
2		PG = Cbz **51**		PG = Cbz **52**	31[d]
3		PG = Ac **53**		PG = Ac **54**	N.R.[e]
4	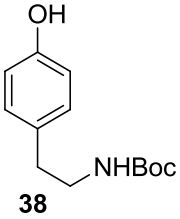 **38**		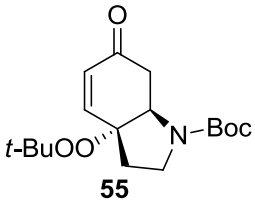 **55**		55
5	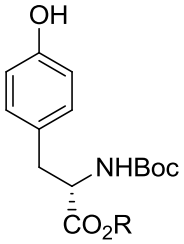	R = Me **56**	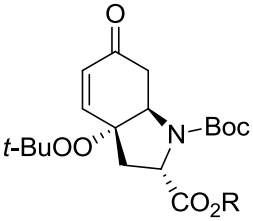	R = Me **57**	53 (1.6 : 1.0)
6		R = *t*-Bu **59**		R = *t*-Bu **60**	62 (2.0 : 1.0)
7	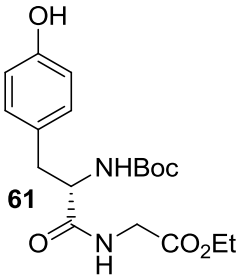 **61**		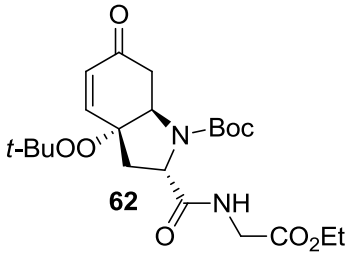 **62**		43[f] (2.3 : 1.0)

8	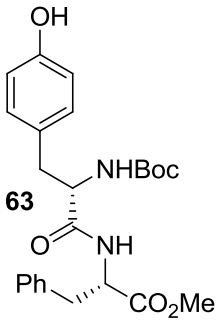	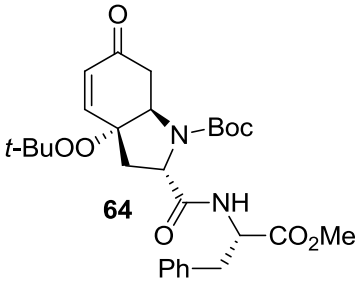	39[f]	(1.4 : 1.0)

[a] Major diastereomer is shown. [b] *cis*-Diastereomer of the bicyclic scaffold is formed in > 20:1 ratio. [c] Each diastereomer is isolated as an individual compound. [d] Determined by ^{1}H NMR spectroscopy from the ratio of peak (6.09 ppm, d, J = 10.4 Hz, 1H) corresponding to **52** and biphenyl peak (7.60 ppm, d, J = 7.2 Hz, 4H) that was used as an internal standard. [e] N.R. - no intramolecular aza-Michael addition. [f] Cyclization was achieved with TsOH (1.5 eq.).

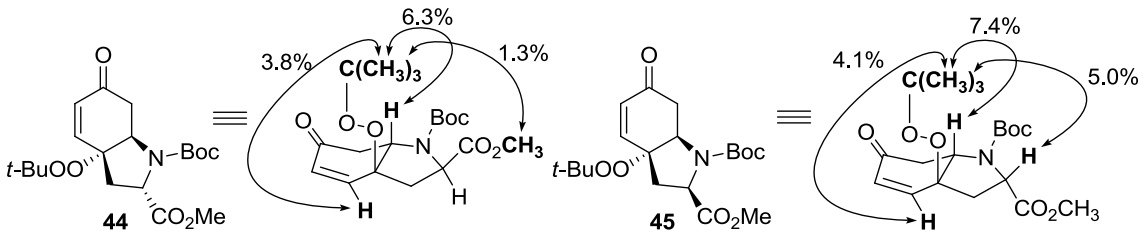

Figure 2-2. NOE analysis of dihydroindols **57** and **58**.

The enantioselective version of intramolecular oxo-Michael addition was also investigated. According to the mechanistic proposal by You, phosphoric acid **6** binds to the carbonyl group and the alcohol groups with the hydroperoxy group positioned away from the phosphoric acid (Figure 2-3, X = H).[34a] The substitution of a hydrogen atom of hydroperoxide for a *tert*-butyl group was expected to have no interaction with the phosphoric acid. Thus, a comparable level of enantioselectivity was anticipated for the cyclization of **28** and **30** (X = *t*-Bu). However, the cyclization of **30** catalyzed by **6** afforded only moderate enantioselectivity (up to 59% ee) and took a considerably longer time (eq. 2-3) than cyclization of 4-hydroperoxy-2,5-dienone **9**. A shorter alcohol linker gave a greater degree of enantiocontrol, reaching 70% ee for cyclization of **28** (eq. 2-4).

Phosphoric acid **6** showed no catalytic activity with 2,5-dienone **39**. The less sterically encumbered triphenylsilyl functionalized phosphoric acid **65** catalyzed the cyclization of **39,** albeit at the expense enantiomeric excess (eq. 2-5).

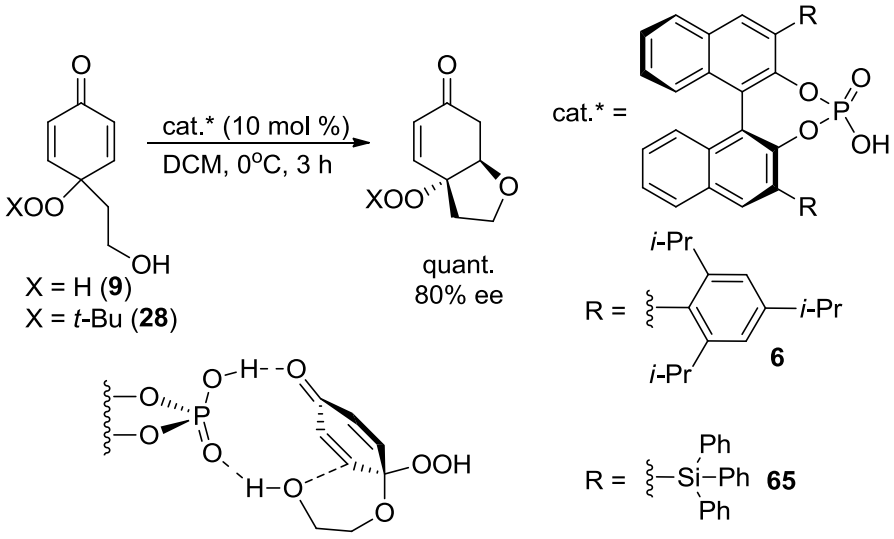

Figure 2-3. Mechanistic model of enantioselective desymmetrization of 2,5-dienones catalyzed by chiral phosphoric acid.[34a]

(eq. 2-3)

(eq. 2-4)

(eq. 2-5)

You reported synthesis of cleroindicin F (**10**) from phenol **8** in 22% overall yield over 3 steps (Scheme 2-7).[34a] The oxidation of phenol **8** afforded only 38% of 2,5-dienone **9** that decreased the overall yield of this synthetic route. The replacement of phenol oxidation by oxone with the $Rh_2(cap)_4$ catalyzed phenol oxidation by T-HYDRO followed by Brønsted acid catalyzed Michael addition was expected to improve the overall yield of cleroindicin F synthesis. However, the tandem sequence phenol oxidation by T-HYDRO followed by Michael addition furnished 4-(*tert*-butylperoxy) functionalized cleroindicin F (**42**) that required the development of selective reduction of the internal peroxide group.

Several reductive systems of internal peroxide **66** (Scheme 2-13)[66] were employed for the reduction of the *tert*-butylperoxy group of **42**. However, the treatment of **42** with zinc in acetic acid and magnesium or thiourea in methanol afforded no cleavage of the sterically hindered O-O bond of **42** (Table 2-8, entries 1-3). Catalytic hydrogenation in presence of palladium on carbon or Lindlar catalyst furnished primarily the reduction of the carbon-carbon double bond (entries 4 and 5). The dropwise addition of $TiCl_4$ solution in DCM to an anhydrous solution of pure peroxide **42** in DCM afforded **10** in 81% yield as a single product (entry 6). Thus, the cleroindicin F was synthesized from tyrosol **8** in 50% overall yield over 3 steps that is superior to cleroindicin F syntheses of You (3 steps,

22% overall yield),[34a] of Pettus (10 steps, 18% overall yield),[64a] and of Hoveyda (9 steps, 17% overall yield).[58a]

Scheme 2-13. Reported methods of reduction of internal peroxides.

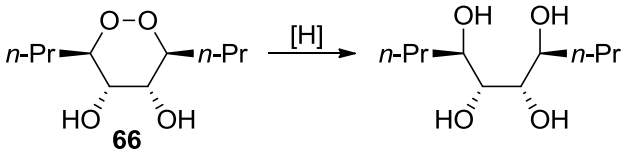

[H] = Pd/C (10 wt. %), H_2, MeOH, rt 72%
[H] = Zn (5 equiv.), AcOH, rt 84%
[H] = Mg (5 equiv.), MeOH, rt 77%
[H] = thiourea (5 equiv.), MeOH, rt 66%

Table 2-8. The development of O-O bond cleavage method for conversion of the internal dialkyl peroxide **42** to cleroindicin F **(10)**.

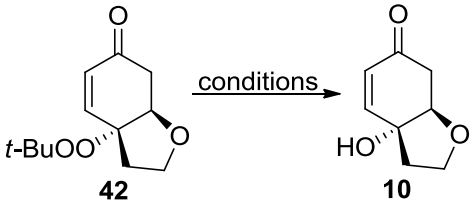

entry	reductant	conditions	yield, %
1	Zn (5 equiv.)	AcOH, rt	N.R.[a]
2	Mg (5 equiv.)	MeOH, rt	decomp.[b]
3	thiourea (5 equiv.)	MeOH, rt	N.R.[a]
4	H_2 (1 atm.), Pd/C (10 wt. %)	MeOH, rt	0[c]
5	H_2 (1 atm.), Lindlar cat. (10 wt. %)	MeOH, rt	47[d]
6	**$TiCl_4$ (2.0 equiv.)**	**DCM (dry), rt**	**81[e]**
7	$ZnCl_2$ (1.5 equiv.)	DCM (dry), rt	N.R.
8	$AlCl_3$ (1.5 equiv.)	DCM (dry), rt	N.R.
9	$Ti(Oi\text{-}Pr)_3Cl$ (1.5 equiv.)	DCM (dry), rt	0[f]
10	BF_3 x OEt_2 (1.5 equiv.)	DCM (dry), rt	decomp.

[a] No reaction. [b] Decomposition. [c] The reduction of the C=C bond. [d] The mixture contained 53% C=C bond reduction product. [e] Isolated yield after flash chromatography on silica gel. [f] Reverse Michael reaction was observed.

The O-O cleavage activity was unique to $TiCl_4$. Zinc chloride and aluminum chloride were unreactive under these conditions while $Ti(O\textit{i}\text{-}Pr)_3Cl$ catalyzed the reverse Michael addition (Table 2-8, entry 9) and the use of BF_3 x OEt_2 led to the decomposition of **42** to unknown products (entry 10). Treatment of peroxides **48** and **55** with $TiCl_4$ led to decomposition of these materials.

A possible mechanism of O-O bond cleavage of peroxide **42** upon treatment with $TiCl_4$ is proposed in Scheme 2-14. The binding of titanium chloride to an oxygen atom of peroxide polarizes the O-O bond for a subsequent nucleophilic attack by chloride furnishing titanium alkoxy complex **67**. The subsequent aqueous work-up hydrolyses complex **67** affording **10**.

Scheme 2-14. Possible mechanism of O-O bond cleavage of **42** by $TiCl_4$.

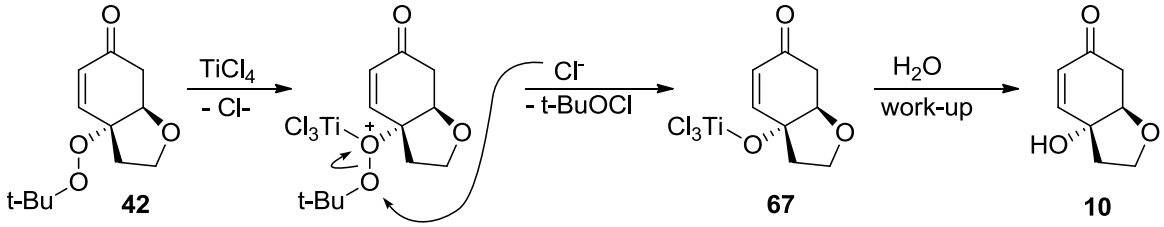

Conclusion

In conclusion, the scope of $Rh_2(cap)_4$ catalyzed phenol oxidation was expanded to phenols bearing carboxylic acids, alcohols, methyl ketone, Boc-protected amines. The one-pot stepwise tandem sequence of the phenol oxidation followed by Brønsted acid Michael addition was developed (Scheme 2-1). This protocol improves the overall yield of racemic cleroindicin F from phenol **8** from 22%[34a] to 50%. The scope of Brønsted acid catalyzed intramolecular Michael addition to 2,5-dienones was expanded to include

carboxylates and Boc-protected amines. The developed tandem protocol includes multifunctional dipeptides. Finally, the selective cleavage of a hindered internal peroxide bond of **29** upon the treatment with $TiCl_4$ was discovered.

Experimental

General Information. All reactions were performed under atmospheric conditions unless the conditions are specified. ^{1}H NMR spectra were recorded on 400 MHz and 600 MHz spectrometers. Tetramethylsilane (TMS) (0.00 ppm) was used as a reference for all spectra. Data are reported as follows: chemical shift (in ppm, δ), integration, multiplicity (s = singlet, d = doublet, t = triplet, q = quartet, sept = septet, br = broad, m = multiplet, comp = composite) and coupling constants (in Hz). ^{13}C NMR spectra were recorded on a 125 MHz spectrometer operated with complete proton decoupling. Chemical shifts are reported in ppm utilizing the central resonance of $CDCl_3$ peak as a reference (77.0 ppm). Thin layer chromatography was performed on silica gel coated on a glass plates (250 μm, F-254), and spots were visualized with either 254 nm ultraviolet light or $KMnO_4$ stain. Flash chromatography used silica gel (32-63 μm). High resolution mass spectra (HRMS) were acquired on a ESI-TOF spectrometer using CsI as a standard. $Rh_2(cap)_4$ was prepared according to the literature procedure.[67] Enantiomeric exesses were determined using a HPLC AD-H column and *i*-PrOH-hexane mixture as the eluting solvent. The concentration of TBHP in a received T-HYDRO reagent was determined by iodometric titration to be 70% by weight.

Spectra of peroxide **37** are in agreement with published information.[36] Phosphoric acids **6, 43, 65** were prepared according to the published procedure.[68] Compounds **56**,[69] **59**[69] and **61**,[70] **63**[70] were prepared according to published procedures.

General Procedure for Transition Metal Complex Catalyzed Phenolic Oxidation. The phenol derivative (2.0 mmol), $Rh_2(cap)_4$ (0.02 mmol, 1 mol%), and DCE (4.0 mL) were placed in a 4-dram screw-cap vial containing a magnetic stirring bar. The suspension containing a small amount of undissolved phenol derivative and $Rh_2(cap)_4$ was heated to 40°C at 250 rpm, and T-HYDRO (8.0 mmol, 4 equiv., 110 µL) was added all at once via syringe. The vial containing the suspension was loosely capped to allow release of pressure built-up, and its contents were stirred using a magentic stirring bar at 40°C. All solid materials dissolved within 10 minutes after T-HYDRO addition. After 1.5 hour the reaction mixture was transferred to a 100-mL round-bottom flask, concentrated under reduced pressure, and the residue was purified by column chromatography (silica gel, DCM:AcOEt:hexane). Fractions containing the product were combined, and the solvent was evaporated under reduced pressure. The peroxide product were dried under high vacuum for 20 minutes (0.09 Torr, room temperature).

4-(*tert*-Butylperoxy)-4-(2-hydroxyethyl)cyclohexa-2,5-dien-1-one (28): R_f 0.30 (EtOAc/DCM/hexane (1:1:1)); colorless oil; ^{1}H NMR (500 MHz, $CDCl_3$) δ 7.03 (d, J = 10.2 Hz, 2H), 6.32 (d, J = 10.2 Hz, 2H), 3.77 (t, J = 6.2 Hz, 2H), 2.03 (t, J = 6.2 Hz, 2H), 1.22 (s, 9H); ^{13}C NMR (126 MHz, $CDCl_3$) δ 186.0, 150.3, 129.5, 80.6, 78.2, 58.0, 39.3, 26.2; IR (neat, cm^{-1}): 3432, 3048, 2979, 2930, 1669, 1627, 1363, 1193, 1079, 1045, 984, 927, 857; EI-HRMS: calculated for $C_{12}H_{18}O_4$ (M+H) 227.12834 found 227.12667.

4-(*tert*-Butylperoxy)-4-(3-hydroxypropyl)cyclohexa-2,5-dien-1-one (31): R_f 0.24 (EtOAc/DCM/hexane (1:1:1)); colorless oil; ^{1}H NMR (500 MHz, $CDCl_3$) δ 6.89 (d, *J* = 10.2 Hz, 2H), 6.28 (d, *J* = 10.2 Hz, 2H), 3.63 (t, *J* = 6.3 Hz, 2H), 1.89 – 1.71 (comp, 2H), 1.66 – 1.44 (comp, 3H), 1.20 (s, 9H); ^{13}C NMR (126 MHz, $CDCl_3$) δ 185.8, 150.4, 129.9, 80.2, 78.9, 62.4, 32.9, 26.6, 26.4; EI-HRMS: calculated for $C_{13}H_{20}O_4$ (M+H) 241.14399, found 241.14334.

[1-(*tert*-Butylperoxy)-4-oxocyclohexa-2,5-dien-1-yl]acetic acid (33): R_f 0.20 (EtOAc/DCM/hexane (1:1:1)); colorless oil; ^{1}H NMR (500 MHz, $CDCl_3$) δ 7.05 (d, *J* = 10.0 Hz, 2H), 6.31 (d, *J* = 10.0 Hz, 2H), 2.79 (s, 2H), 1.21 (s, 9H); ^{13}C NMR (126 MHz, $CDCl_3$) δ 195.0, 185.3, 147.5, 130.2, 80.9, 75.9, 31.2, 26.3; EI-HRMS: calculated for $C_{12}H_{16}O_5$ (M+H) 241.10760, found 241.10911.

3-[1-(*tert*-Butylperoxy)-4-oxocyclohexa-2,5-dien-1-yl]propanoic acid (35): R_f 0.26 (EtOAc/DCM/hexane (1:1:1)); colorless oil; ^{1}H NMR (500 MHz, $CDCl_3$) δ 6.89 (d, *J* = 10.2 Hz, 2H), 6.32 (d, *J* = 10.2 Hz, 2H), 2.39 (t, *J* = 7.9 Hz, 2H), 2.10 (t, *J* = 7.9 Hz, 2H), 1.22 (s, 9H); ^{13}C NMR (126 MHz, $CDCl_3$) δ 185.5, 177.4, 149.3, 130.4, 80.4, 78.1, 31.0, 28.1, 26.3; EI-HRMS: calculated for $C_{13}H_{18}O_5$ (M+H) 255.12325, found 255.12305.

4-(*tert*-Butylperoxy)-4-(3-oxobutyl)cyclohexa-2,5-dien-1-one (37): R_f 0.50 (EtOAc/DCM/hexane (1:1:1)); colorless oil; ^{1}H NMR (400 MHz, $CDCl_3$) δ 6.83 (d, *J* = 10.2 Hz, 2H), 6.28 (d, *J* = 10.2 Hz, 2H), 2.39 (t, *J* = 7.7 Hz, 2H), 2.12 (s, 3H), 2.01 (t, *J* = 7.7 Hz, 2H), 1.20 (s, 9H); ^{13}C NMR (100 MHz, $CDCl_3$) δ 206.9, 186.1, 150.3, 130.6,

80.7, 78.9, 37.7, 30.5, 29.8, 26.8; EI-HRMS: calculated for $C_{14}H_{20}O_4$ (M+H) 253.14399, found 253.14494.

***tert*-Butyl [2-[1-(*tert*-Butylperoxy)-4-oxocyclohexa-2,5-dien-1-yl]ethyl]carbamate (39):** R_f 0.30 (EtOAc/DCM/hexane (1:1:1)); colorless oil; ^{1}H NMR (500 MHz, $CDCl_3$) δ 6.91 (d, *J* = 10.1 Hz, 2H), 6.28 (d, *J* = 10.1 Hz, 2H), 4.68 (s, 1H), 3.18 (br d, *J* = 6.3 Hz, 2H), 1.93 (t, *J* = 7.1 Hz, 2H), 1.43 (br s, 9H), 1.20 (s, 9H); ^{13}C NMR (126 MHz, $CDCl_3$) δ 185.5, 149.5, 130.0, 80.8, 80.4, 79.5, 78.0, 36.9, 35.9, 28.4, 26.3; EI-HRMS: calculated for $C_{17}H_{27}O_5N$ (M+H) 326.19675, found 326.19541.

General Procedure for Tandem Phenol Oxidation – Michael Addition Sequence. 4-(*tert*-butyldioxy)cyclohexa-2,5-dienone (2.0 mmol), [Rh_2(cap)$_4$] (0.02 mmol, 0.01 eq.), and DCE (4.0 mL) were placed in a 4-dram screw-cap vial containing a magnetic stirring bar. The suspension containing a small amount of undissolved phenol derivative and Rh_2(cap)$_4$ was heated to 40 °C in an oil bath at 250 rpm, and T-HYDRO was added all at once via syringe. The vial containing the reaction mixture was loosely capped to allow release of pressure built-up, and its contents were stirred using a magentic stirring bar at 40°C. All solid materials dissolved within 10 minutes of T-HYDRO addition. After 90 minutes the reaction mixture was allowed to cool to room temperature, and anhydrous Na_2SO_4 (600 mg) followed by TsOH or (*rac*)-BINOL-PO_2H (0.20 mmol, 0.1 eq.) were added to the mixture. The suspension was stirred overnight at room temperature and then transferred to a 100-mL round-bottom flask, concentrated under reduced pressure; and the residue was purified by column chromatography (silica gel, DCM:AcOEt:hexane). Fractions containing the product were combined, and the

solvent was evaporated under reduced pressure. The peroxide product was dried under high vacuum for 20 minutes (0.09 Torr, room temperature).

(3a*R*,7a*R*)-3a-(*tert*-Butylperoxy)-3,3a,7,7a-tetrahydro-1-benzofuran-6(2*H*)-one (42): R_f 0.14 (EtOAc/DCM/hexane (1:1:8)); colorless oil; ^{1}H NMR (500 MHz, $CDCl_3$) δ 6.77 (dd, *J* = 10.3, 1.6 Hz, 1H), 6.09 (d, *J* = 10.3 Hz, 1H), 4.46 (td, *J* = 5.0, 1.6 Hz, 1H), 3.96 (dd, *J* = 7.8, 6.7 Hz, 2H), 2.87 (dd, *J* = 16.9, 5.0 Hz, 1H), 2.68 (dd, *J* = 16.9, 4.4 Hz, 1H), 2.32 (dt, *J* = 13.5, 6.7 Hz, 1H), 2.08 (dt, *J* = 13.5, 7.8 Hz, 1H), 1.23 (s, 9H); ^{13}C NMR (126 MHz, $CDCl_3$) δ 196.7 (C), 147.4 (CH), 129.7 (CH), 84.2 (C), 80.2 (C), 79.2 (CH), 66.0 (CH_2), 41.3 (CH_2), 36.9 (CH_2), 26.4 (CH_3); IR (neat, cm^{-1}): 3034, 2877, 2932, 2881, 1688, 1386, 1363, 1190, 1067, 1017, 877; ESI-HRMS: calculated for $C_{12}H_{18}O_4$ (M+H) 217.12841, found 217.12817. The enantiomeric excess was determined by HPLC AD-H column (80:20 hexanes/*i*-PrOH, 1.0 mL/min): t_R (major) = 4.13 min; t_R (minor) = 4.75 min.

(4a*R*,8a*R*)-4a-(*tert*-Butylperoxy)-2,3,4,4a,8,8a-hexahydro-7*H*-chromen-7-one (44): R_f 0.08 (EtOAc/DCM/hexane (1:1:4)); colorless oil; ^{1}H NMR (500 MHz, $CDCl_3$) δ 6.53 (dd, *J* = 10.2, 2.0 Hz, 1H), 6.15 (d, *J* = 10.2 Hz, 1H), 4.06 (td, *J* = 3.9, 2.0 Hz, 1H), 3.92 – 3.80 (m, 1H), 3.44 (td, *J* = 11.1, 2.7 Hz, 1H), 3.00 (dd, *J* = 16.8, 3.5 Hz, 1H), 2.57 (dd, *J* = 16.8, 4.2 Hz, 1H), 2.10 – 1.93 (comp, 2H), 1.79 – 1.67 (m, 1H), 1.68 – 1.54 (m, 1H), 1.21 (s, 9H); ^{13}C NMR (126 MHz, $CDCl_3$) δ 197.6 (C), 147.1 (CH), 132.5 (CH), 79.9 (C), 75.7 (C), 75.3 (CH), 66.3 (CH_2), 41.1 (CH_2), 31.9 (CH_2), 26.5 (CH_3), 22.9 (CH_2); EI-HRMS: calculated for $C_{13}H_{20}O_4$ (M+H) 241.14394, found 241.14362. The enantiomeric excess was determined by separation on a HPLC AD-H column (90:10 hexanes/*i*-PrOH, 1.0 mL/min): t_R (major) = 4.51 min; t_R (minor) = 5.35 min.

(2*S*,4a*R*,8a*R*)-4a-(*tert*-Butylperoxy)-2-methyl-2,3,4,4a,8,8a-hexahydro-7*H*-chromen-7-one (46): R_f 0.26 (EtOAc/DCM/hexane (1:1:16)); colorless oil; ^{1}H NMR (500 MHz, $CDCl_3$) δ 6.46 (dd, *J* = 10.1, 2.4 Hz, 1H), 6.16 (d, *J* = 10.1 Hz, 1H), 4.01 (dd, *J* = 5.5, 2.4 Hz, 1H), 3.50 (dtd, *J* = 12.1, 6.1, 4.2 Hz, 1H), 3.03 (dd, *J* = 16.9, 3.3 Hz, 1H), 2.50 (dd, *J* = 16.9, 2.5 Hz, 1H), 2.13 – 1.92 (comp, 2H), 1.69 (dt, *J* = 13.6, 4.6 Hz, 1H), 1.38 – 1.24 (m, 1H), 1.20 (s, 9H), 1.12 (d, *J* = 6.2 Hz, 3H); ^{13}C NMR (126 MHz, $CDCl_3$) δ 197.7 (C), 146.1 (CH), 133.0 (CH), 79.9 (C), 75.8 (CH), 75.1 (C), 73.2 (CH), 41.5 (CH_2), 32.8 (CH_2), 30.6 (CH_2), 26.5 (CH_3), 21.3 (CH); EI-HRMS: calculated for $C_{14}H_{22}O_4$ (M+H) 255.15972, found 255.15941.

(2*R*,4a*R*,8a*R*)-4a-(*tert*-Butylperoxy)-2-methyl-2,3,4,4a,8,8a-hexahydro-7*H*-chromen-7-one (47): R_f 0.09 (EtOAc/DCM/hexane (1:1:16)); colorless oil; ^{1}H NMR (500 MHz, $CDCl_3$) δ 6.91 (d, *J* = 10.3 Hz, 1H), 5.99 (d, *J* = 10.3 Hz, 1H), 4.60 (dd, *J* = 12.2, 5.1 Hz, 1H), 3.90 – 3.72 (m, 1H), 2.94 (dd, *J* = 16.1, 12.2 Hz, 1H), 2.70 (dd, *J* = 16.2, 5.1 Hz, 1H), 2.14 – 1.99 (m, 1H), 1.83 – 1.70 (m, 1H), 1.67 – 1.53 (m, 1H), 1.49 (dd, *J* = 13.2, 3.3 Hz, 1H), 1.23 (s, 9H), 1.21 (t, *J* = 6.3 Hz, 3H); ^{13}C NMR (126 MHz, $CDCl_3$) δ 198.3, 153.5, 129.2, 80.0, 77.3, 70.1, 65.3, 40.1, 27.9, 27.2, 26.5, 26.4, 21.07; EI-HRMS: calculated for $C_{14}H_{22}O_4$ (M+H) 255.15972, found 255.15974.

(3a*R*,7a*R*)-3a-(*tert*-Butylperoxy)-3,3a,7,7a-tetrahydro-1-benzofuran-2,6-dione (49): R_f 0.30 (EtOAc/DCM/hexane (1:1:4)); colorless oil; ^{1}H NMR (500 MHz, $CDCl_3$) δ 6.75 (dd, *J* = 10.3, 1.2 Hz, 1H), 6.24 (d, *J* = 10.3 Hz, 1H), 5.11 (dd, *J* = 8.2, 1.2 Hz, 1H), 3.24 – 2.97 (comp, 2H), 2.89 – 2.65 (comp, 2H), 1.24 (s, 9H); ^{13}C NMR (126 MHz, $CDCl_3$) δ 193.5, 171.4, 144.0, 131.5, 81.4, 80.4, 78.7, 40.4, 38.7, 26.3; EI-HRMS: calculated for $C_{12}H_{16}O_5$ (M+H) 241.10760, found 241.10701.

***tert*-butyl (3a*R*,7a*R*)-3a-(*tert*-Butylperoxy)-6-oxo-2,3,3a,6,7,7a-hexahydro-1*H*-indole-1-carboxylate (55):** R_f 0.34 (EtOAc/DCM/hexane (1:1:4)); colorless oil; ^{1}H NMR (500 MHz, $CDCl_3$) δ 7.08 – 6.79 (m, 1H), 6.06 (d, *J* = 10.4 Hz, 1H), 4.77 – 4.50 (m, 1H), 3.70 – 3.41 (m, 2H), 3.24 – 2.96 (m, 1H), 2.51 – 2.31 (m, 1H), 2.31 – 2.19 (m, 1H), 2.19 – 2.02 (m, 1H), 1.46 (s, 9H), 1.21 (s, 9H); ^{13}C NMR (126 MHz, $CDCl_3$) δ 197.0, 154.1, 148.9, 130.1, 86.1, 80.4, 80.1, 77.2, 58.7, 44.7, 42.7, 32.6, 28.4, 26.4; EI-HRMS: calculated for $C_{17}H_{27}NO_5$ (M+H) 326.19685, found 326.19641. The enantiomeric excess was determined by HPLC AD-H column (97:3 hexanes/*i*-PrOH, 1.0 mL/min): t_R (major) = 7.04 min; t_R (minor) = 8.84 min.

(2*S*,3a*R*,7a*R*)-1-(*tert*-Butoxycarbonyl)-3a-(*tert*-butylperoxy)-6-oxo-2,3,3a,6,7,7a-hexahydro-1*H*-indole-2-carboxylic acid (50): R_f 0.36 (DCM/MeOH (9:1)); colorless oil; ^{1}H NMR (500 MHz, $CDCl_3$) δ 10.14 (br s, 1H), 6.98 – 6.81 (m, 1H), 6.09 (d, *J* = 10.4 Hz, 1H), 4.82 – 4.63 (m, 1H), 4.63 – 4.43 (m, 1H), 3.43 – 3.14 (m, 1H), 2.85 – 2.56 (m, 1H), 2.55 – 2.26 (comp, 2H), 1.54 – 1.40 (comp, 9H), 1.23 – 1.18 (comp, 9H); ^{13}C NMR (126 MHz, $CDCl_3$) δ 196.0, 195.8, 175.8, 172.9, 155.6, 153.0, 148.2, 146.7, 130.5, 130.3, 85.2, 84.4, 82.6, 81.0, 80.8, 80.7, 59.6, 59.2, 58.5, 58.1, 42.2, 41.5, 37.5, 35.8, 28.4, 28.1, 26.7, 26.3; EI-HRMS: calculated for $C_{18}H_{27}NO_7$ (M+H) 370.18668, found 370.18606.

1-*tert*-Butyl 2-Methyl (2*S*,3a*R*,7a*R*)-3a-(*tert*-Butylperoxy)-6-oxo-2,3,3a,6,7,7a-hexahydro-1*H*-indole-1,2-dicarboxylate (57): R_f 0.23 (EtOAc/DCM/hexane (1:1:4)); colorless oil; ^{1}H NMR (600 MHz, $CDCl_3$) δ 6.94 – 6.85 (m, 1H), 6.09 – 6.03 (m, 1H), 4.85 – 4.61 (m, 1H), 4.55 – 4.39 (m, 1H), 3.81 – 3.71 (comp, 3H), 3.28 – 3.03 (m, 1H), 2.81 – 2.56 (comp, 2H), 2.27 – 2.11 (m, 1H), 1.47 – 1.39 (comp, 9H), 1.24 – 1.19 (comp,

9H); ^{13}C NMR (126 MHz, $CDCl_3$) δ 196.3, 196.1, 171.4, 170.5, 153.5, 153.0, 147.7, 146.9, 130.4, 130.1, 129.5, 125.7, 85.5, 84.3, 80.9, 80.8, 80.6, 80.5, 59.2, 58.2, 57.8, 52.1, 52.0, 42.7, 41.5, 37.6, 36.7, 28.4, 28.2, 26.3; EI-HRMS: calculated for $C_{19}H_{29}NO_7$ (M+H) 384.20222, found 384.20319.

1-*tert*-Butyl 2-Methyl (2*R*,3a*R*,7a*R*)-3a-(*tert*-Butylperoxy)-6-oxo-2,3,3a,6,7,7a-hexahydro-1*H*-indole-1,2-dicarboxylate (58): R_f 0.31 (EtOAc/DCM/hexane (1:1:4)); colorless oil; ^{1}H NMR (600 MHz, $CDCl_3$) δ 6.92 – 6.82 (m, 1H), 6.12 – 6.05 (m, 1H), 4.79 – 4.61 (m, 1H), 4.61 – 4.41 (m, 1H), 3.82 – 3.72 (comp, 3H), 3.40 – 3.14 (m, 1H), 2.67 – 2.51 (m, 1H), 2.51 – 2.42 (m, 1H), 2.41 – 2.27 (m, 1H), 1.53 – 1.40 (comp, 9H), 1.25 – 1.18 (comp, 9H); ^{13}C NMR (126 MHz, $CDCl_3$) δ 196.6, 196.2, 172.9, 172.8, 153.6, 153.0, 147.6, 146.9, 130.6, 130.4, 129.6, 125.8, 85.8, 85.0, 80.9, 80.6, 59.7, 59.6, 59.5, 59.0, 52.5, 52.3, 42.6, 42.2, 38.0, 37.3, 28.4, 28.2, 26.4, 26.3; EI-HRMS: calculated for $C_{19}H_{29}NO_7$ (M+H) 384.20222, found 384.20352.

Di-*tert*-butyl (2*S*,3a*R*,7a*R*)-3a-(*tert*-Butylperoxy)-6-oxo-2,3,3a,6,7,7a-hexahydro-1*H*-indole-1,2-dicarboxylate (60): R_f 0.27 (EtOAc/hexane (1:5)); colorless oil; ^{1}H NMR (500 MHz, $CDCl_3$) δ 6.90 – 6.80 (m, 1H), 6.11 – 6.02 (m, 1H), 4.83 – 4.63 (m, 1H), 4.45 – 4.26 (m, 1H), 3.39 – 3.11 (m, 1H), 2.65 – 2.38 (comp, 2H), 2.39 – 2.28 (m, 1H), 1.52 – 1.40 (comp, 18H), 1.27 – 1.19 (comp, 9H); ^{13}C NMR (126 MHz, $CDCl_3$) δ 196.6, 196.4, 169.1, 168.8, 153.3, 153.3, 148.3, 147.7, 130.2, 130.0, 85.5, 84.4, 81.3, 81.0, 80.8, 80.7, 80.5, 80.3, 59.4, 59.3, 58.5, 58.4, 42.6, 41.7, 37.9, 37.0, 28.4, 28.2, 28.1, 26.4, 26.4; EI-HRMS: calculated for $C_{22}H_{35}NO_7$ (M+H) 426.24896, found 426.24793.

Di-*tert*-butyl (2*R*,3a*R*,7a*R*)-3a-(*tert*-Butylperoxy)-6-oxo-2,3,3a,6,7,7a-hexahydro-1*H*-indole-1,2-dicarboxylate (68): R_f 0.37 (EtOAc/hexane (1:5)); colorless oil; ^{1}H NMR (500 MHz, $CDCl_3$) δ 6.96 – 6.83 (m, 1H), 6.14 – 5.99 (m, 1H), 4.91 – 4.59 (m, 1H), 4.43 – 4.26 (m, 1H), 3.27 – 3.01 (m, 1H), 2.83 – 2.53 (comp, 2H), 2.25 – 2.07 (m, 1H), 1.53 – 1.40 (comp, 18H), 1.25 – 1.18 (comp, 9H); ^{13}C NMR (126 MHz, $CDCl_3$) δ 196.9, 196.5, 171.3, 171.2, 153.3, 153.2, 147.8, 147.3, 130.7, 130.4, 85.8, 84.9, 81.8, 81.7, 80.6, 80.5, 60.2, 60.1, 59.6, 42.5, 42.1, 38.2, 37.2, 28.3, 28.2, 27.9, 27.9, 26.3, 26.2; EI-HRMS: calculated for $C_{22}H_{35}NO_7$ (M+H) 426.24896, found 426.24793.

***tert*-Butyl (2*S*,3a*R*,7a*R*)-3a-(*tert*-Butylperoxy)-2-[[(2-ethoxy-2-oxoethyl) amino]carbonyl]-6-oxo-2,3,3a,6,7,7a-hexahydro-1*H*-indole-1-carboxylate (62):** R_f 0.16 (EtOAc/DCM/hexane (1:1:1)); colorless oil; ^{1}H NMR (500 MHz, $CDCl_3$) δ 7.22 (s, 1H), 7.01 – 6.82 (m, 1H), 6.76 (s, 1H), 6.07 (d, *J* = 10.4 Hz, 1H), 4.95 – 4.62 (m, 1H), 4.59 – 4.36 (m, 1H), 4.30 – 3.79 (comp, 4H), 3.53 – 3.16 (m, 1H), 2.88 – 2.13 (comp, 3H), 1.49 (comp, 9H), 1.28 (t, *J* = 7.1 Hz, 3H), 1.19 (s, 9H); ^{13}C NMR (126 MHz, $CDCl_3$) δ 195.9, 195.5, 171.9, 170.8, 169.4, 168.4, 154.7, 153.2, 148.7, 147.5, 130.5, 130.0, 85.7, 85.2, 81.9, 81.5, 80.5, 61.4, 60.4, 59.9, 42.0, 41.7, 41.4, 40.7, 37.6, 35.9, 29.7, 28.3, 27.9, 26.4, 26.3, 14.1; EI-HRMS: calculated for $C_{22}H_{34}N_2O_8$ (M+H) 455.23947, found 455.24020.

***tert*-Butyl (2*S*,3a*R*,7a*R*)-3a-(*tert*-Butylperoxy)-2-[[(2-methoxy-1-benzyl-2-oxo-ethyl)amino]carbonyl]-6-oxo-2,3,3a,6,7,7a-hexahydro-1*H*-indole-1-carboxylate (64):** R_f 0.35 (EtOAc/DCM/hexane (1:1:1)); colorless oil; ^{1}H NMR (500 MHz, $CDCl_3$) δ 7.69 – 6.64 (comp, 7H), 6.14 – 5.97 (m, 1H), 5.02 – 4.26 (comp, 3H), 3.76 – 3.59 (comp, 3H), 3.49 – 2.74 (comp, 4H), 2.59 – 2.13 (comp, 2H), 1.55 – 1.32 (comp, 9H), 1.30 – 1.06

(comp, 9H); ^{13}C NMR (126 MHz, $CDCl_3$) δ 195.9, 195.7, 171.7, 171.5, 170.9, 170.3, 155.0, 154.9, 148.9, 148.8, 147.8, 147.5, 136.3, 136.0, 85.7, 85.2, 81.8, 80.6, 80.5, 60.1, 60.0, 59.8, 56.1, 54.0, 53.8, 52.0, 51.8, 42.4, 41.9, 38.4, 38.3, 37.8, 37.7, 35.6, 35.3, 28.4, 28.3, 28.0, 26.7, 26.4, 26.3; EI-HRMS: calculated for $C_{28}H_{38}N_2O_8$ (M+H) 531.27079, found 531.26927.

***tert*-Butyl (2*R*,3a*R*,7a*R*)-3a-(*tert*-Butylperoxy)-2-[[(2-methoxy-1-benzyl-2-oxoethyl)amino]carbonyl]-6-oxo-2,3,3a,6,7,7a-hexahydro-1*H*-indole-1-carboxylate (69):** R_f 0.46 (EtOAc/DCM/hexane (1:1:1)); colorless oil; ^{1}H NMR (500 MHz, $CDCl_3$) δ 7.65 – 6.65 (comp, 5H), 6.17 – 6.03 (m, 1H), 4.94 – 4.29 (comp, 3H), 3.77 – 3.58 (comp, 3H), 3.48 – 3.25 (comp, 2H), 3.19 – 2.86 (comp, 2H), 2.62 – 2.25 (comp, 2H), 1.59 – 1.53 (m, 1H), 1.51 – 1.37 (comp, 9H), 1.29 – 1.20 (comp, 9H); ^{13}C NMR (126 MHz, $CDCl_3$) δ 197.0, 196.8, 168.6, 167.5, 153.7, 153.4, 147.4, 146.5, 130.6, 130.1, 129.3, 128.4, 84.8, 83.3, 80.9, 80.7, 80.6, 80.1, 60.1, 59.6, 58.9, 56.2, 52.0, 46.2, 43.5, 42.0, 40.0, 38.6, 38.2, 37.2, 28.4, 28.3, 26.4, 25.6, 24.6; EI-HRMS: calculated for $C_{28}H_{38}N_2O_8$ (M+H) 531.27079, found 531.26875.

General Procedure for Asymmetric Intramolecular Michael Addition. 4-(*tert*-butyldioxy)cyclohexa-2,5-dienones (0.10 mmol), chiral phosphoric acid (0.010 mmol, 0.1 eq.), and dry DCM (0.25 mL) were added under nitrogen to an oven-dry 1-dram screw-cap vial containing a magnetic stirring bar, and the reaction was stirred for 20 hours at room temperature. The suspension was stirred overnight at room temperature and then transferred to a 100-mL round-bottom flask, concentrated under reduced pressure; and the residue was purified by column chromatography (silica gel, DCM:AcOEt:hexane). Fractions containing the product were combined, and the solvent was evaporated under

reduced pressure. The peroxide product was dried under high vacuum for 20 minutes (0.09 Torr, room temperature).

General Procedure for Dialkylperoxide 28 Cleavage by Lewis acids. Peroxide **28** (0.30 mmol, 68 mg) and dry DCM (1.5 mL) were placed under nitrogen in an oven-dried 5-ml round-bottom flask capped with a septum. The Lewis acid (0.60 mmol) was slowly added to the solution at room temperature, and the reaction was stirred for four hours at room temperature. A light brown precipitate formed after 30 seconds. The suspension was poured into an aqueous 5% solution of Na_2SO_3 (9 mL), the organic layer was separated, and the aqueous layer was washed with AcOEt (3 x 15 mL). The organic layers were combined, dried over Na_2SO_4 and the solvent evaporated on rotary evaporator to yield cleroindicin F **10** as a colorless liquid (38 mg, 81%) that matched previously reported ^{1}H NMR spectrum.[64a]

^{1}H and ^{13}C Spectra of New Compounds

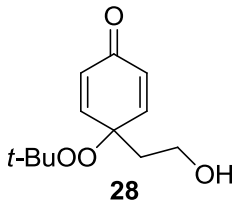

28

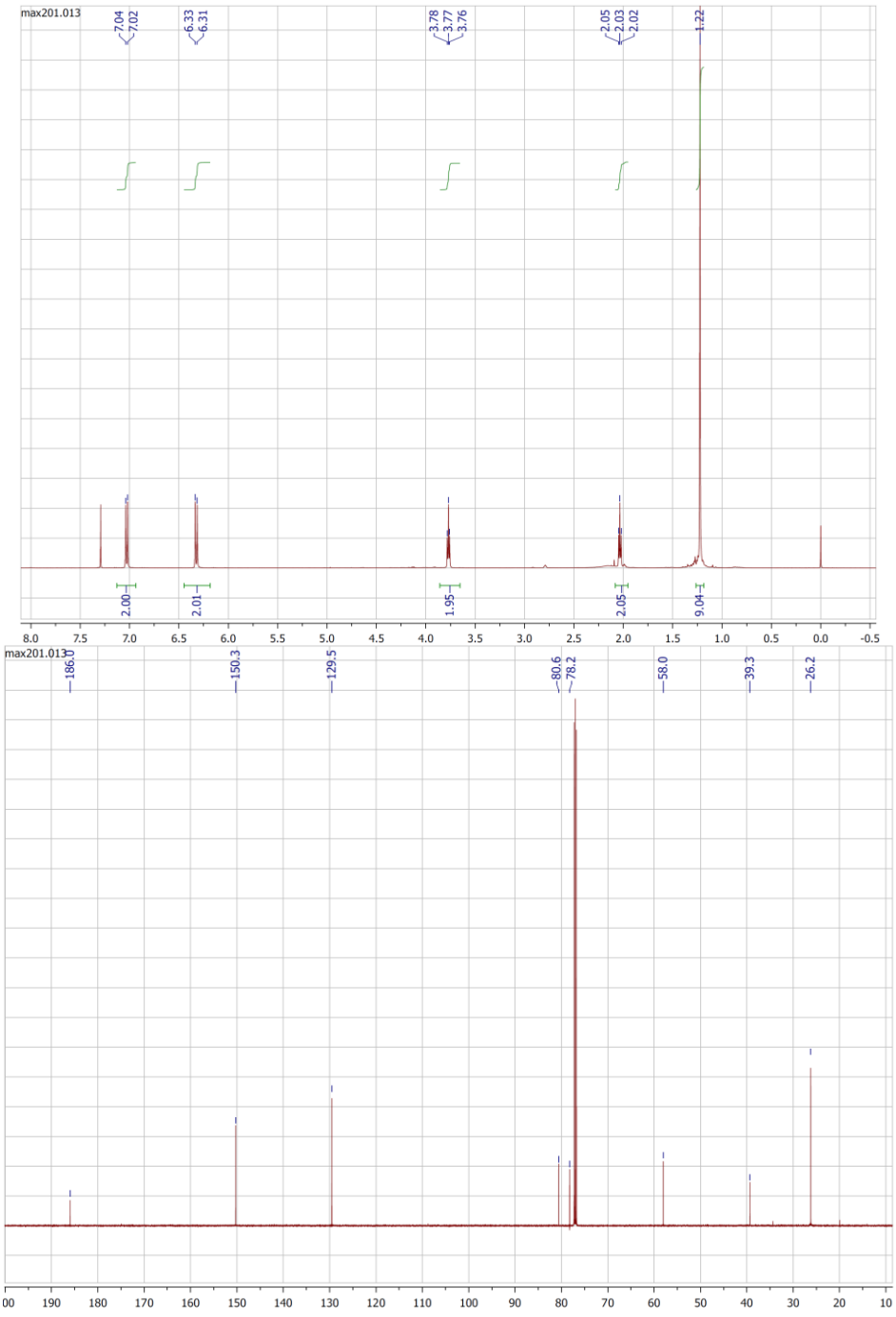

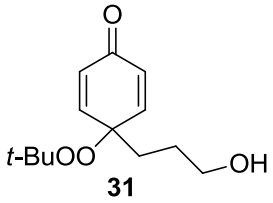
O
t-BuOO
OH

31

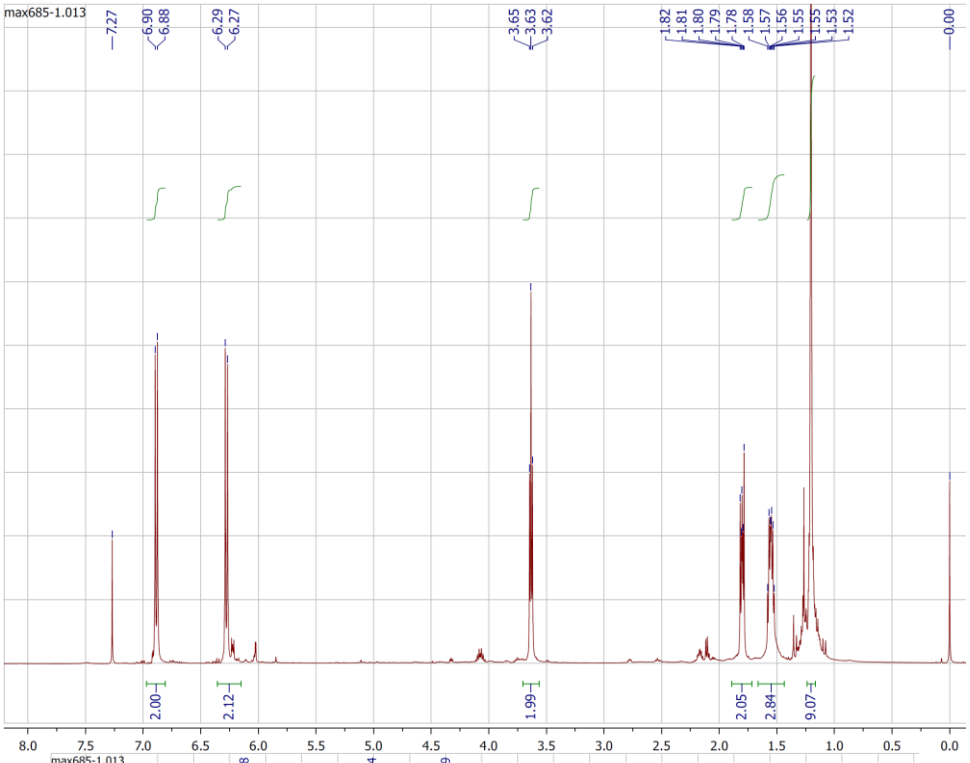
max685-1.013
7.27
6.90
6.88
6.29
6.27
3.65
3.63
3.62
1.82
1.81
1.80
1.79
1.78
1.58
1.57
1.56
1.55
1.55
1.53
1.52
0.00
2.00
2.12
1.99
2.05
2.84
9.07

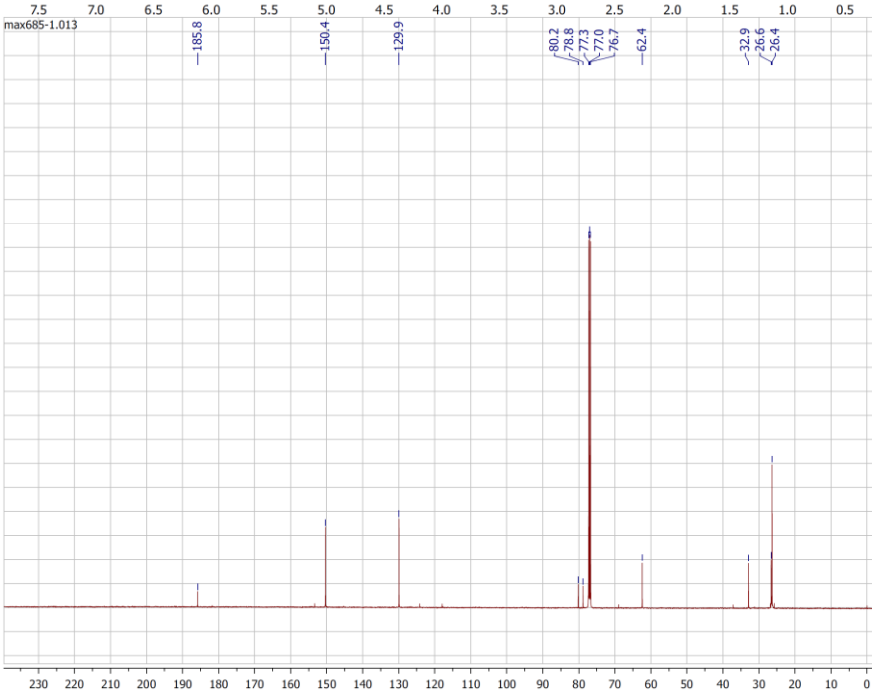
max685-1.013
185.8
150.4
129.9
80.2
78.8
77.3
77.0
76.7
62.4
32.9
26.6
26.4

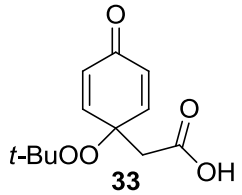
O
O
t-BuOO
OH

33

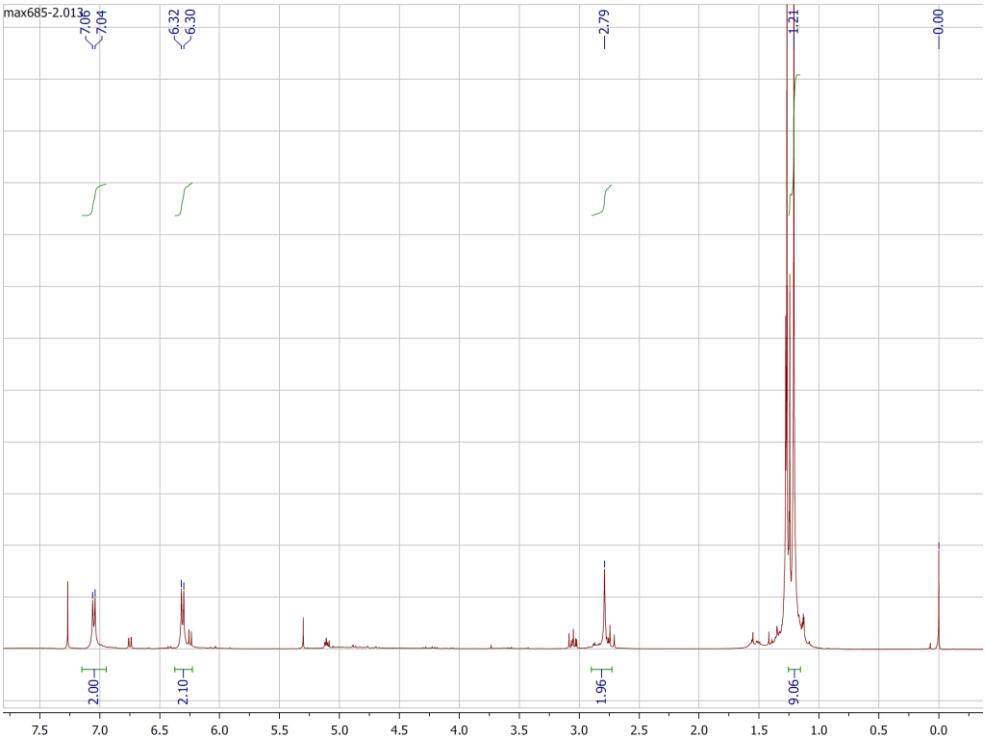
max685-2.013
7.06
7.04
6.32
6.30
2.79
1.21
0.00
2.00
2.10
1.96
9.06
7.5
7.0
6.5
6.0
5.5
5.0
4.5
4.0
3.5
3.0
2.5
2.0
1.5
1.0
0.5
0.0

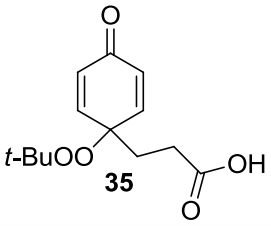
O
t-BuOO
OH
O

35

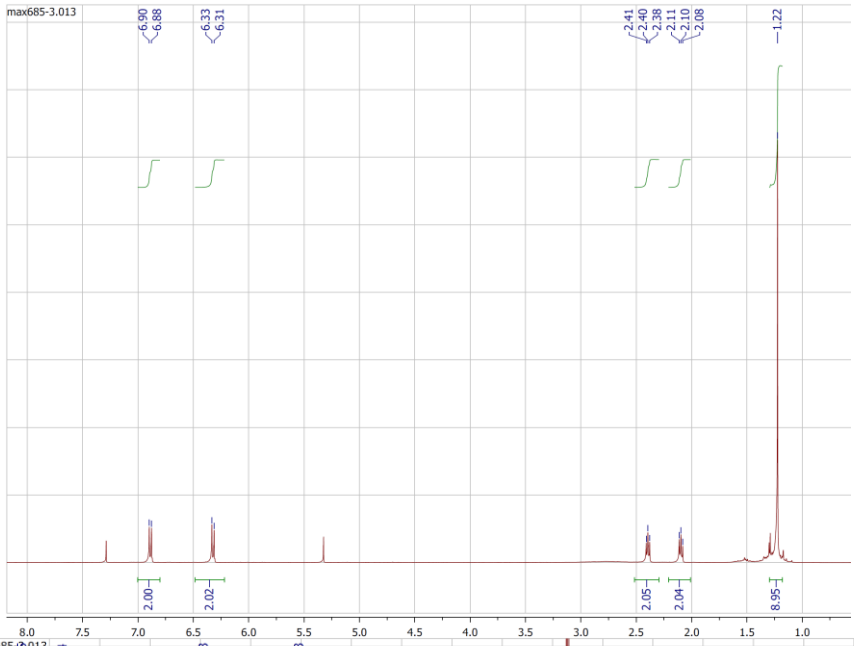
max685-3.013
6.90
6.88
6.33
6.31
2.41
2.40
2.38
2.11
2.10
2.08
1.22
2.00
2.02
2.05
2.04
8.95
8.0
7.5
7.0
6.5
6.0
5.5
5.0
4.5
4.0
3.5
3.0
2.5
2.0
1.5
1.0

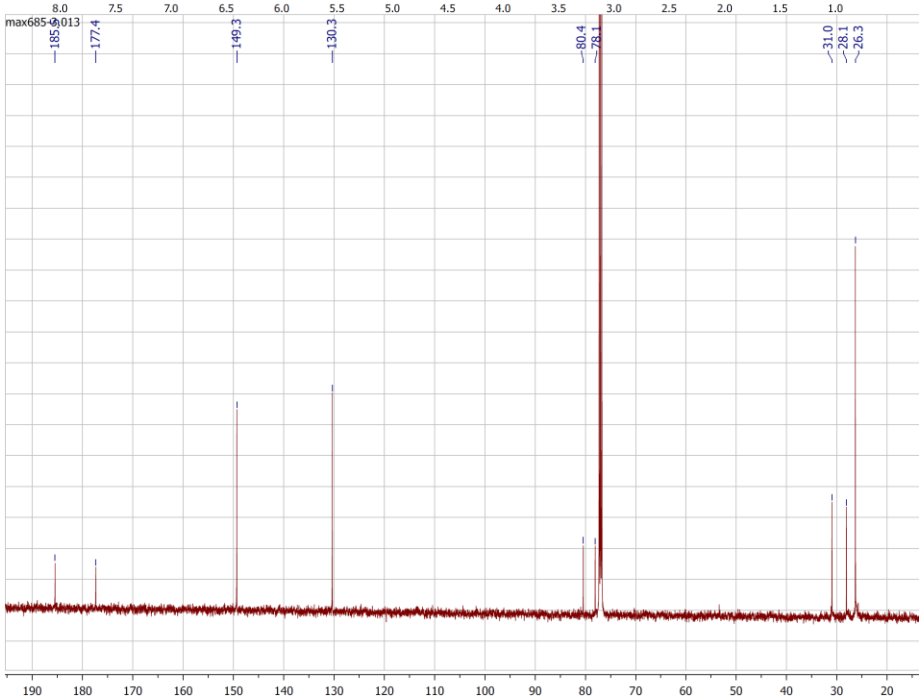
max685-3.013
185.9
177.4
149.3
130.3
80.4
78.1
31.0
28.1
26.3
190
180
170
160
150
140
130
120
110
100
90
80
70
60
50
40
30
20

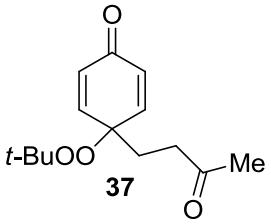
O
t-BuOO
Me
O

37


max442.013
6.84
6.81
6.29
6.27
2.00
1.96
2.02
2.98
2.07
8.94
7.5 7.0 6.5 6.0 5.5 5.0 4.5 4.0 3.5 3.0 2.5 2.0 1.5 1.0 0.5

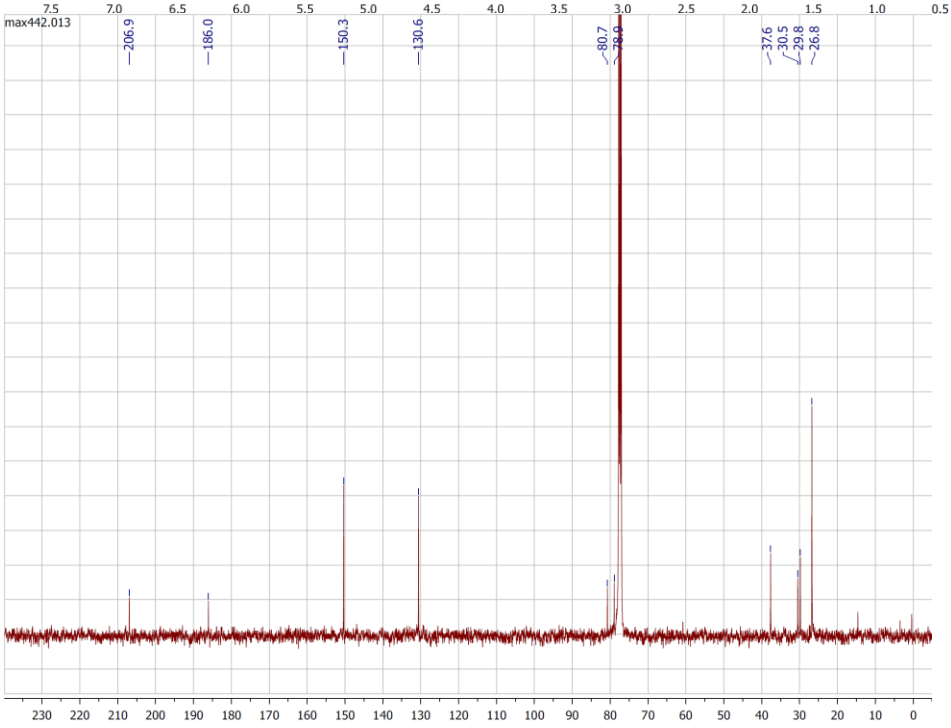
max442.013
206.9
186.0
150.3
130.6
80.7
78.9
37.6
30.5
29.8
26.8
230 220 210 200 190 180 170 160 150 140 130 120 110 100 90 80 70 60 50 40 30 20 10 0

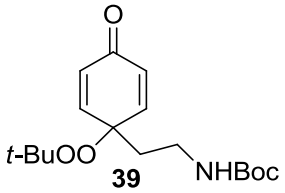
O
t-BuOO
NHBoc

39

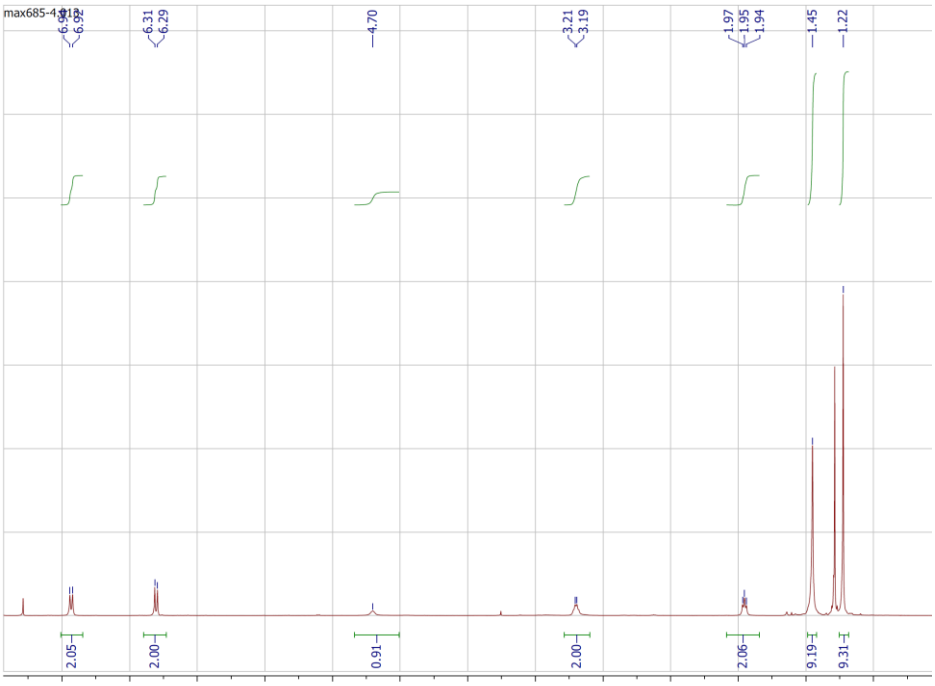
6.31
6.29
4.70
3.21
3.19
1.97
1.95
1.94
1.45
1.22
2.05
2.00
0.91
2.00
2.06
9.19
9.31
7.0
6.5
6.0
5.5
5.0
4.5
4.0
3.5
3.0
2.5
2.0
1.5
1.0

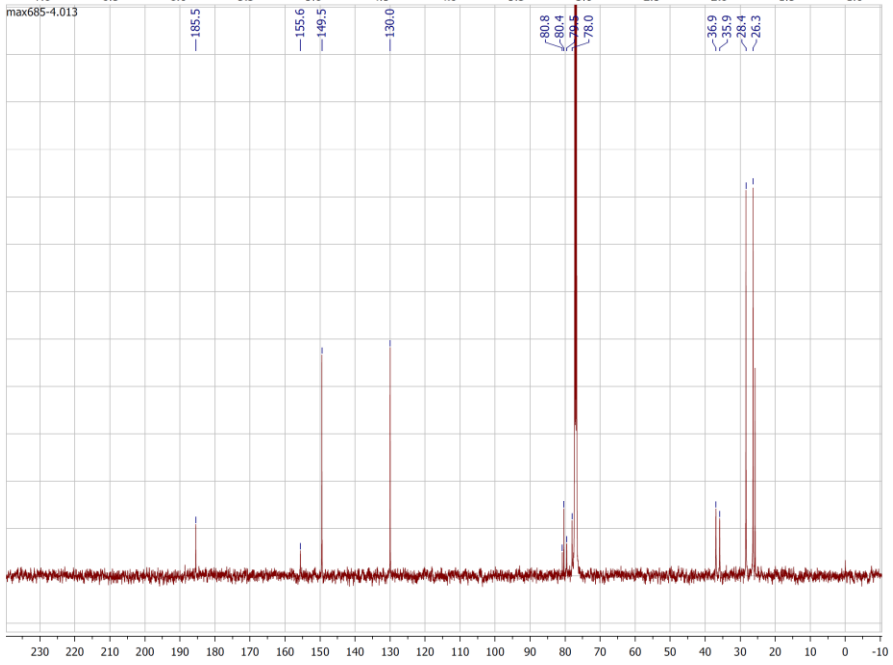
max685-4.013
185.5
155.6
149.5
130.0
80.8
80.4
78.0
36.9
35.9
28.4
26.3
230
220
210
200
190
180
170
160
150
140
130
120
110
100
90
80
70
60
50
40
30
20
10
0
-10

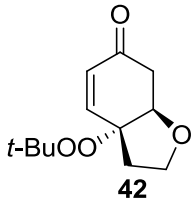

42

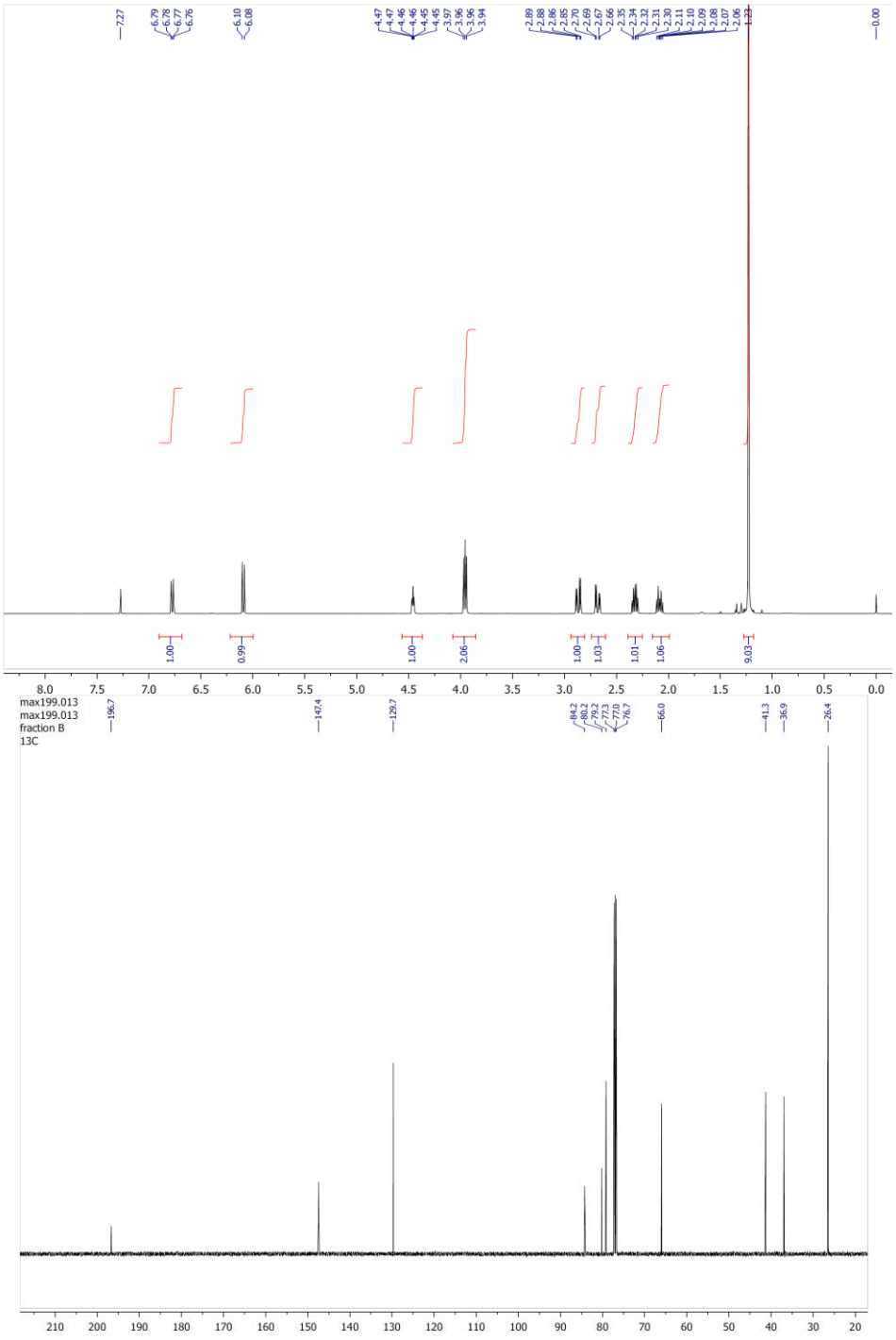

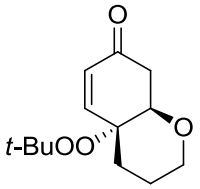
O
O
t-BuOO

44

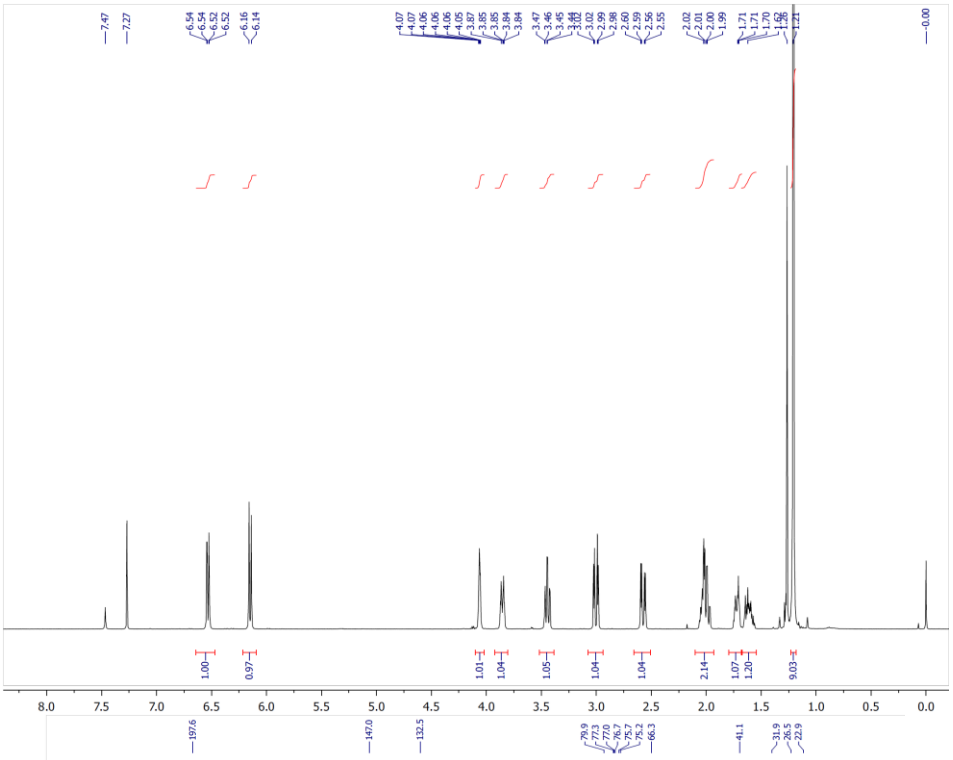
7.47
7.27
6.54
6.54
6.53
6.52
6.16
6.14
4.07
4.07
4.06
4.06
4.06
4.05
3.87
3.85
3.85
3.84
3.84
3.47
3.46
3.45
3.44
3.44
3.02
3.01
2.99
2.98
2.60
2.59
2.56
2.55
2.02
2.01
2.00
1.99
1.71
1.71
1.70
1.58
1.56
1.21
0.00
1.00
0.97
1.01
1.04
1.05
1.04
1.04
2.14
1.07
1.20
9.03
8.0
7.5
7.0
6.5
6.0
5.5
5.0
4.5
4.0
3.5
3.0
2.5
2.0
1.5
1.0
0.5
0.0

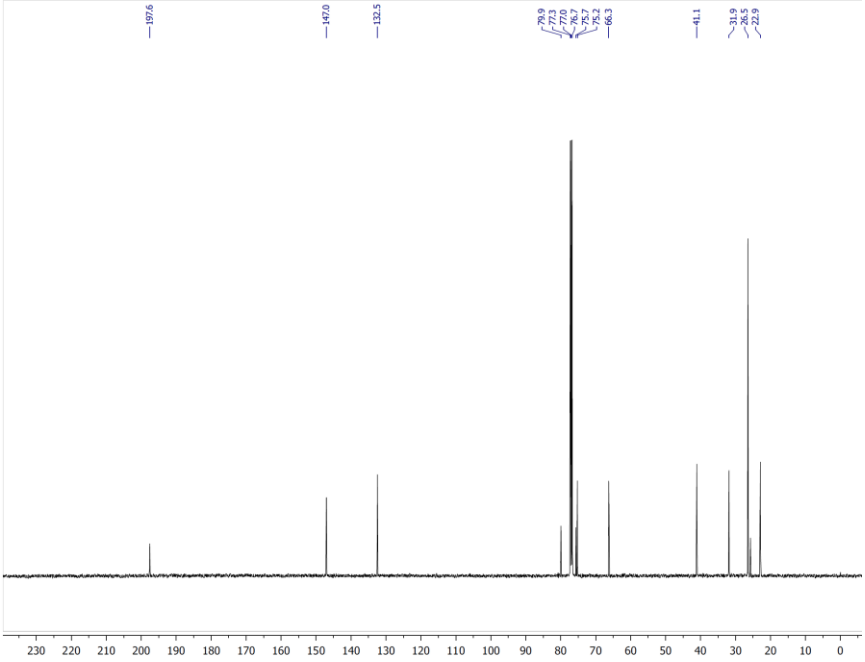
197.6
147.0
132.5
79.9
77.3
77.0
76.7
75.7
75.2
66.3
41.1
31.9
26.5
20.9
230
220
210
200
190
180
170
160
150
140
130
120
110
100
90
80
70
60
50
40
30
20
10
0

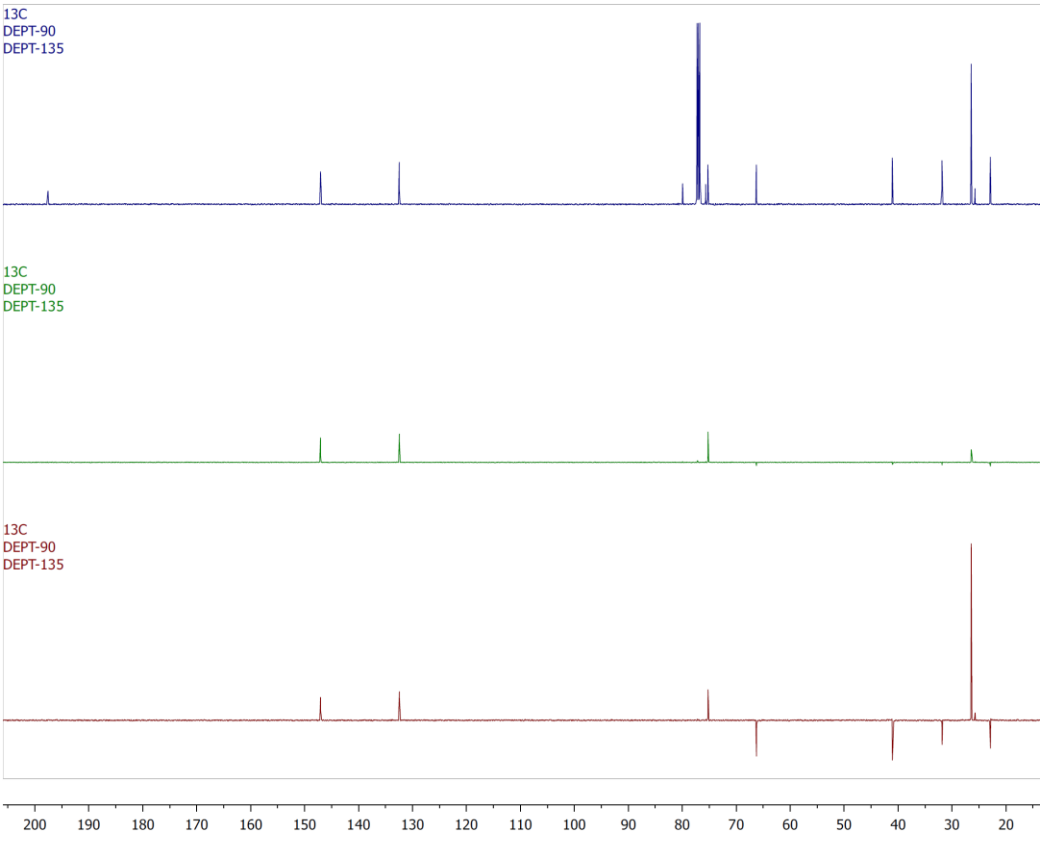
13C
DEPT-90
DEPT-135
13C
DEPT-90
DEPT-135
13C
DEPT-90
DEPT-135
200
190
180
170
160
150
140
130
120
110
100
90
80
70
60
50
40
30
20

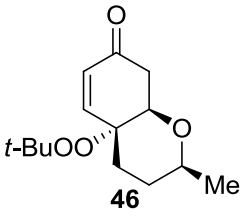
O
O
t-BuOO
Me

46

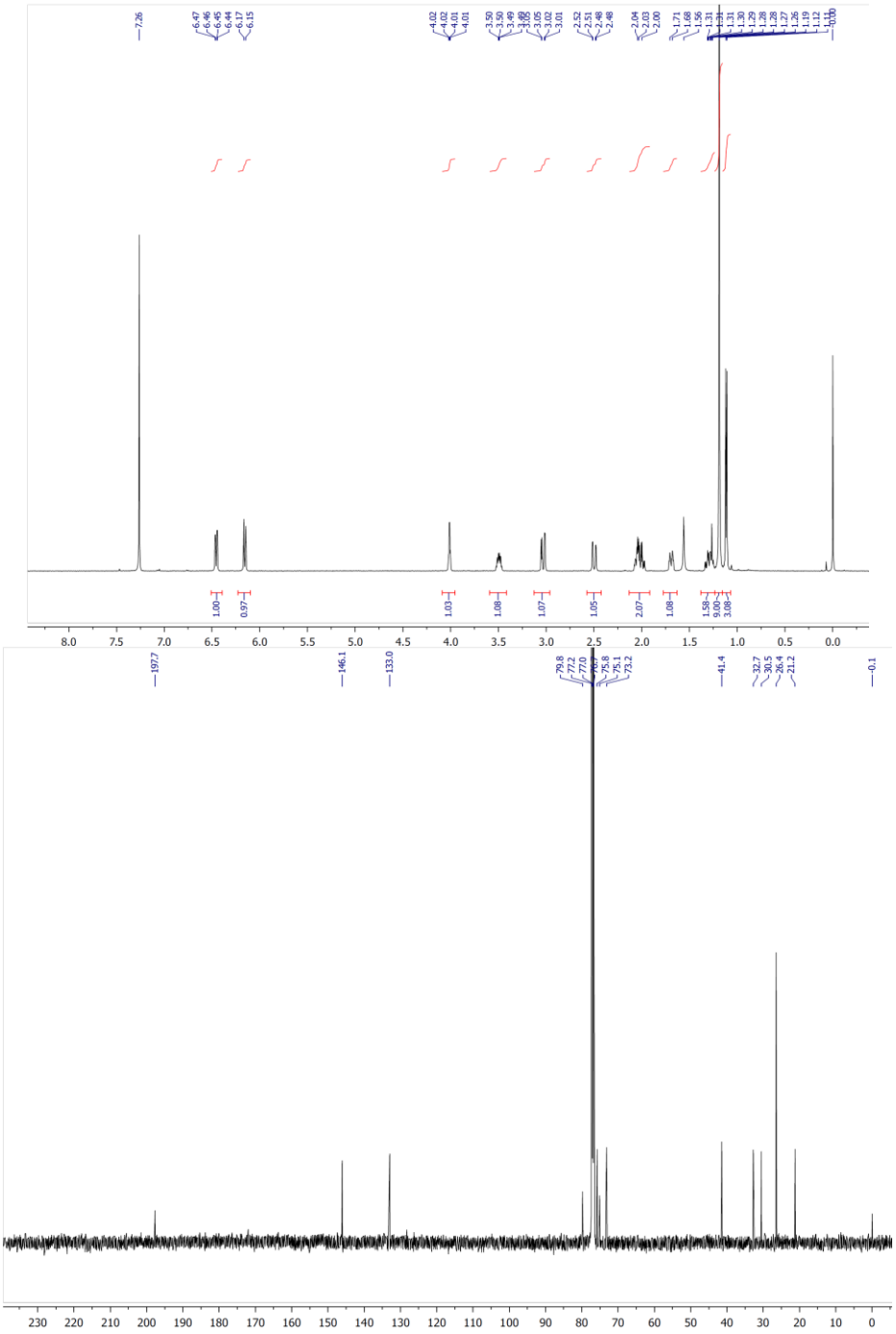
7.26
6.47
6.46
6.45
6.44
6.17
6.15
4.02
4.02
4.01
4.01
3.50
3.50
3.49
3.49
3.05
3.02
3.01
2.52
2.51
2.48
2.48
2.04
2.03
2.00
1.71
1.68
1.56
1.31
1.30
1.29
1.28
1.28
1.27
1.26
1.19
1.12
1.11
0.00
1.00
0.97
1.03
1.08
1.07
1.05
2.07
1.08
1.58
9.00
3.08
8.0
7.5
7.0
6.5
6.0
5.5
5.0
4.5
4.0
3.5
3.0
2.5
2.0
1.5
1.0
0.5
0.0
197.7
146.1
133.0
79.8
77.2
77.0
76.7
75.8
75.1
73.2
41.4
32.7
30.5
26.4
21.2
-0.1
230
220
210
200
190
180
170
160
150
140
130
120
110
100
90
80
70
60
50
40
30
20
10
0

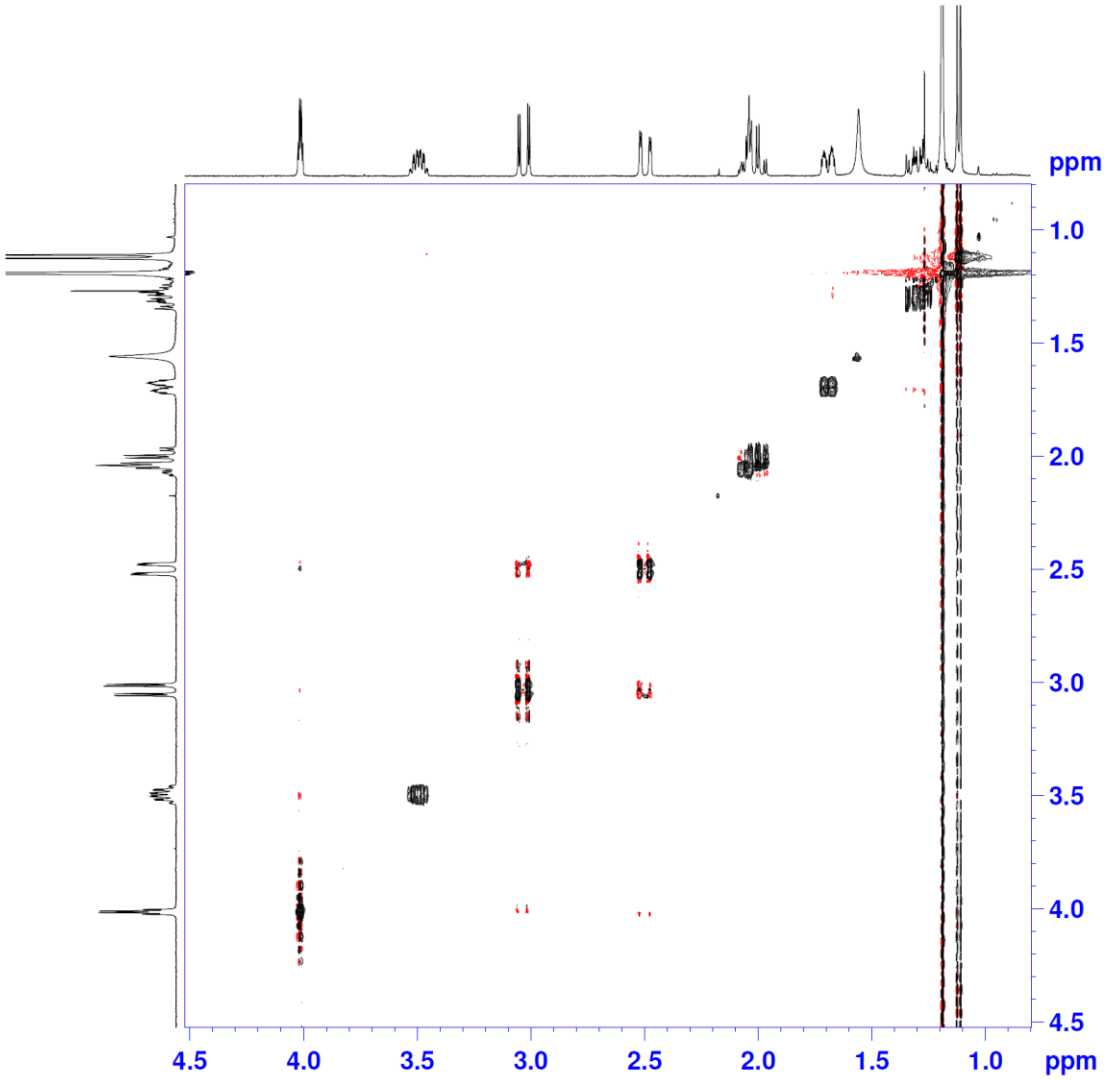
ppm
1.0
1.5
2.0
2.5
3.0
3.5
4.0
4.5
4.5
4.0
3.5
3.0
2.5
2.0
1.5
1.0
ppm

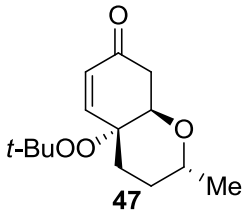
O
t-BuOO
O
Me

47

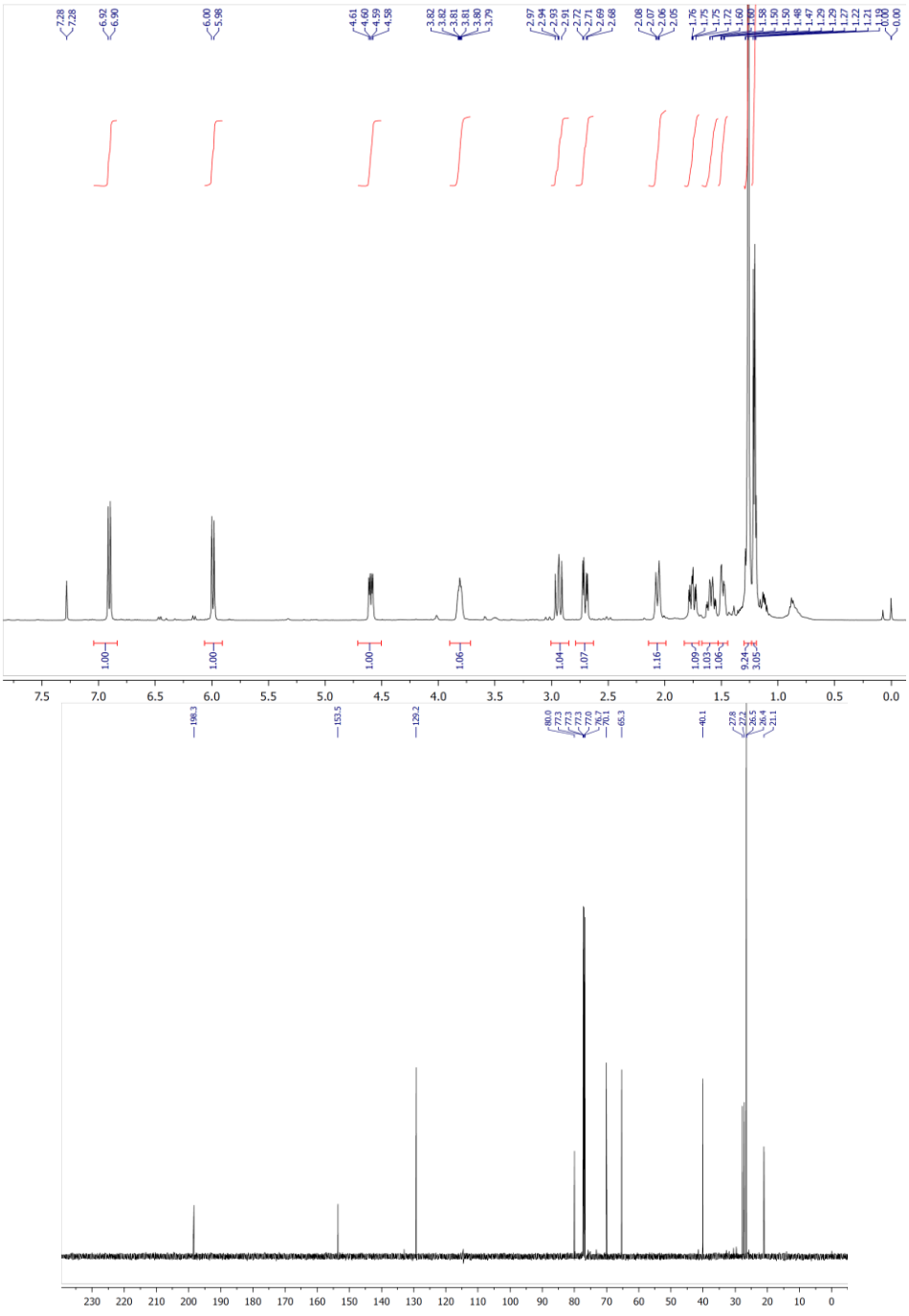
7.28
7.28
6.92
6.90
6.00
5.98
4.61
4.60
4.59
4.58
3.82
3.82
3.81
3.81
3.80
3.79
2.97
2.94
2.93
2.91
2.72
2.71
2.69
2.68
2.08
2.07
2.06
2.05
1.76
1.75
1.75
1.72
1.60
1.58
1.58
1.50
1.50
1.48
1.47
1.29
1.29
1.27
1.27
1.22
1.21
0.00
0.00
1.00
1.00
1.00
1.06
1.04
1.07
1.16
1.09
1.03
1.06
9.24
3.05
7.5
7.0
6.5
6.0
5.5
5.0
4.5
4.0
3.5
3.0
2.5
2.0
1.5
1.0
0.5
0.0
198.3
153.5
129.2
80.0
77.3
77.1
76.8
76.7
70.1
65.3
40.1
27.8
27.2
26.5
26.4
21.1
230
220
210
200
190
180
170
160
150
140
130
120
110
100
90
80
70
60
50
40
30
20
10
0

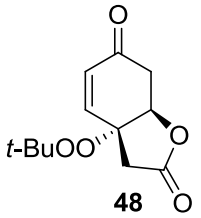
O
t-BuOO
O
O

48

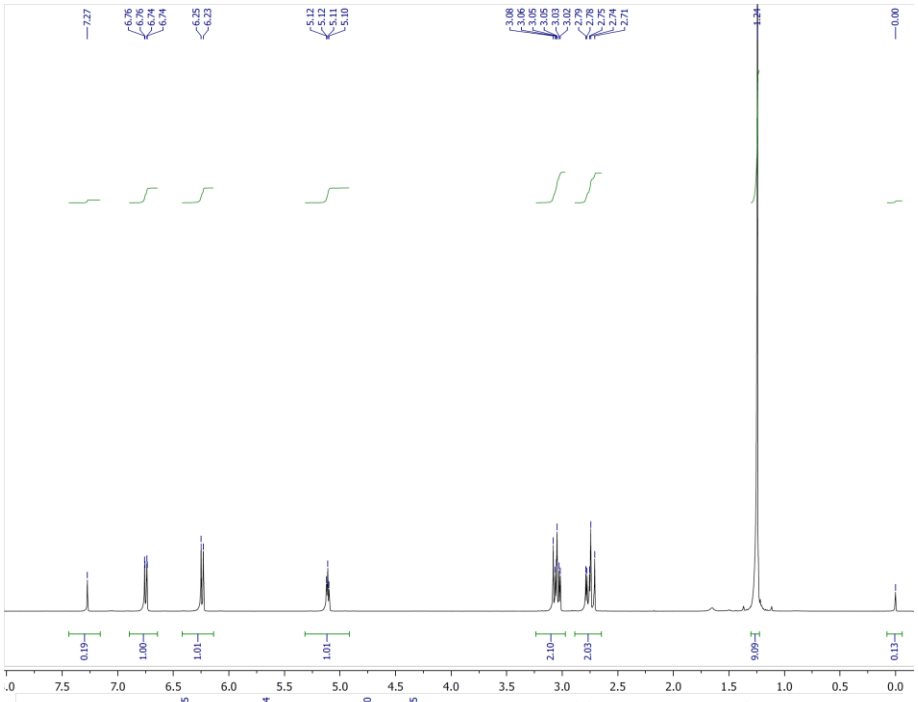
7.27
6.76
6.76
6.75
6.74
6.74
6.25
6.23
5.12
5.12
5.11
5.10
3.08
3.06
3.05
3.05
3.03
3.02
2.79
2.78
2.75
2.74
2.71
1.34
0.00
0.19
1.00
1.01
1.01
2.10
2.03
9.09
0.13
.0
7.5
7.0
6.5
6.0
5.5
5.0
4.5
4.0
3.5
3.0
2.5
2.0
1.5
1.0
0.5
0.0

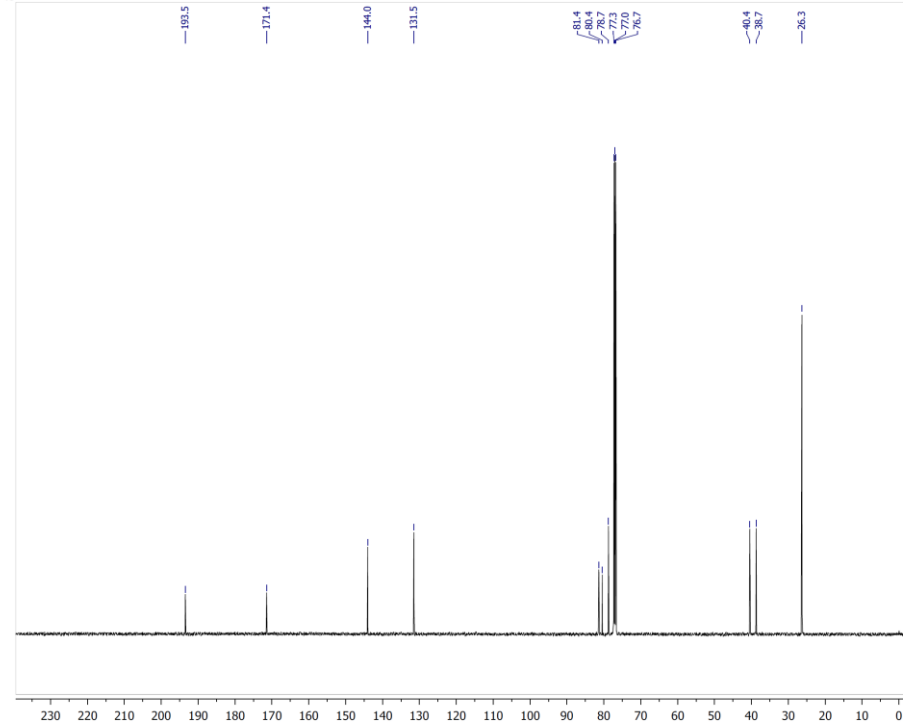
193.5
171.4
144.0
131.5
81.4
80.4
77.3
77.0
76.7
40.4
38.7
26.3
230
220
210
200
190
180
170
160
150
140
130
120
110
100
90
80
70
60
50
40
30
20
10
0

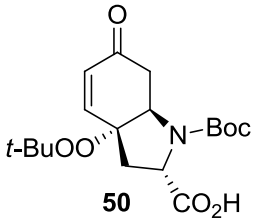

50

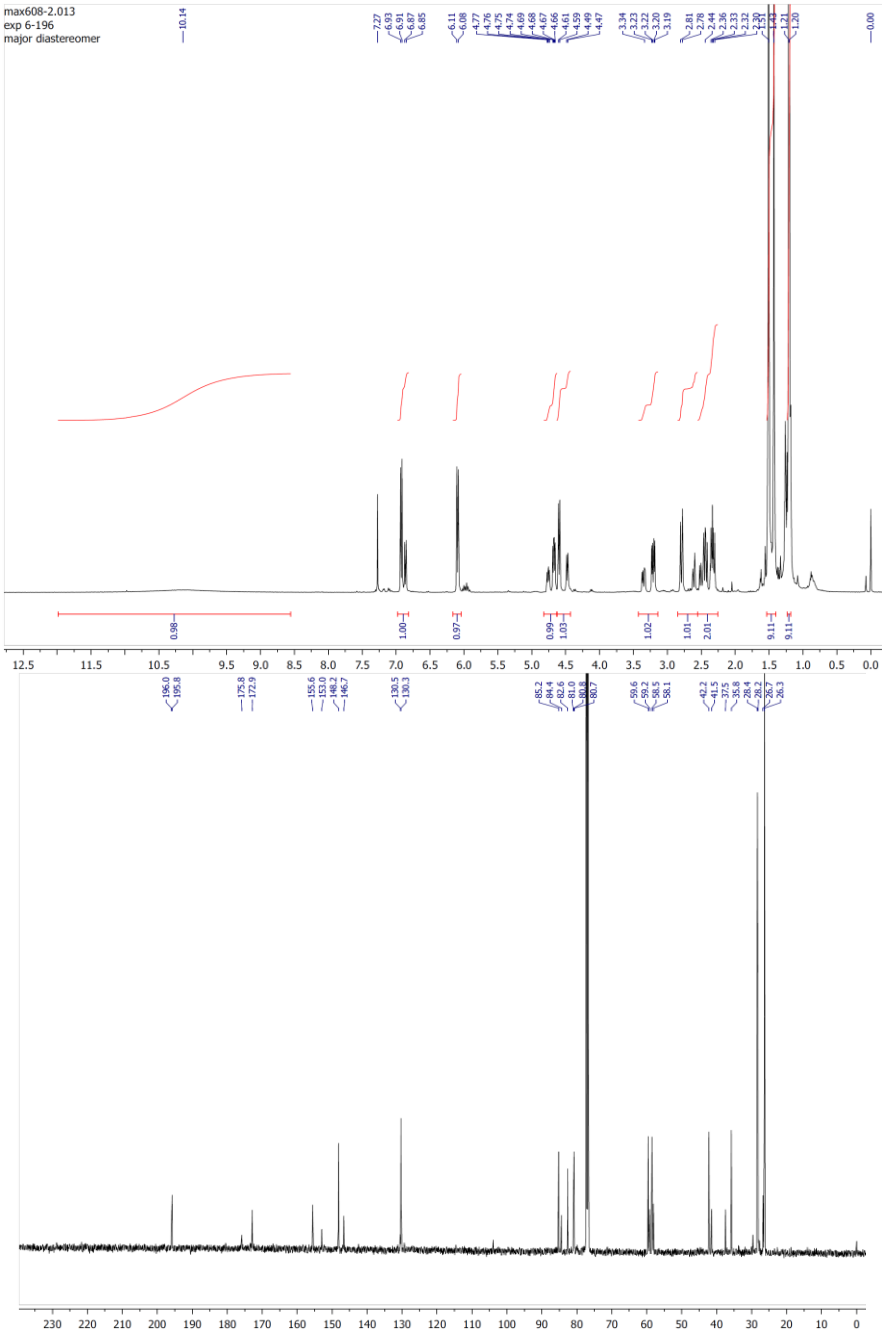

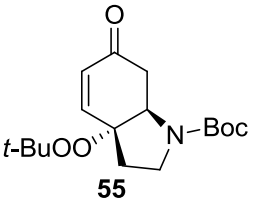

55

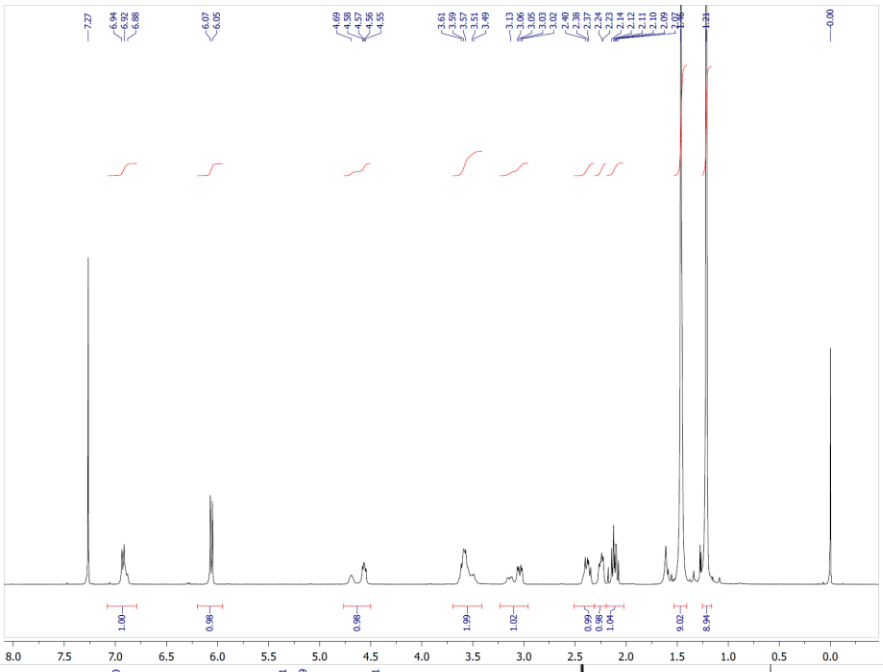

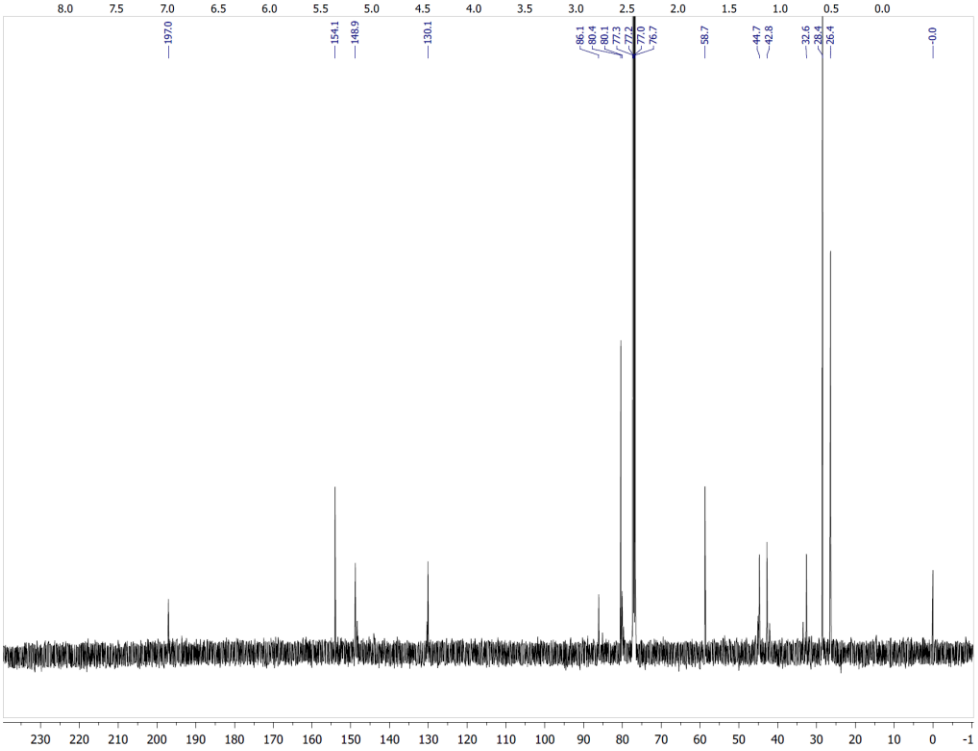

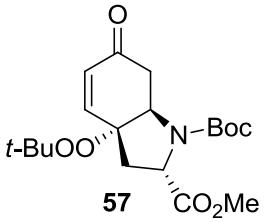
O
N–Boc
t-BuOO
CO2Me

57

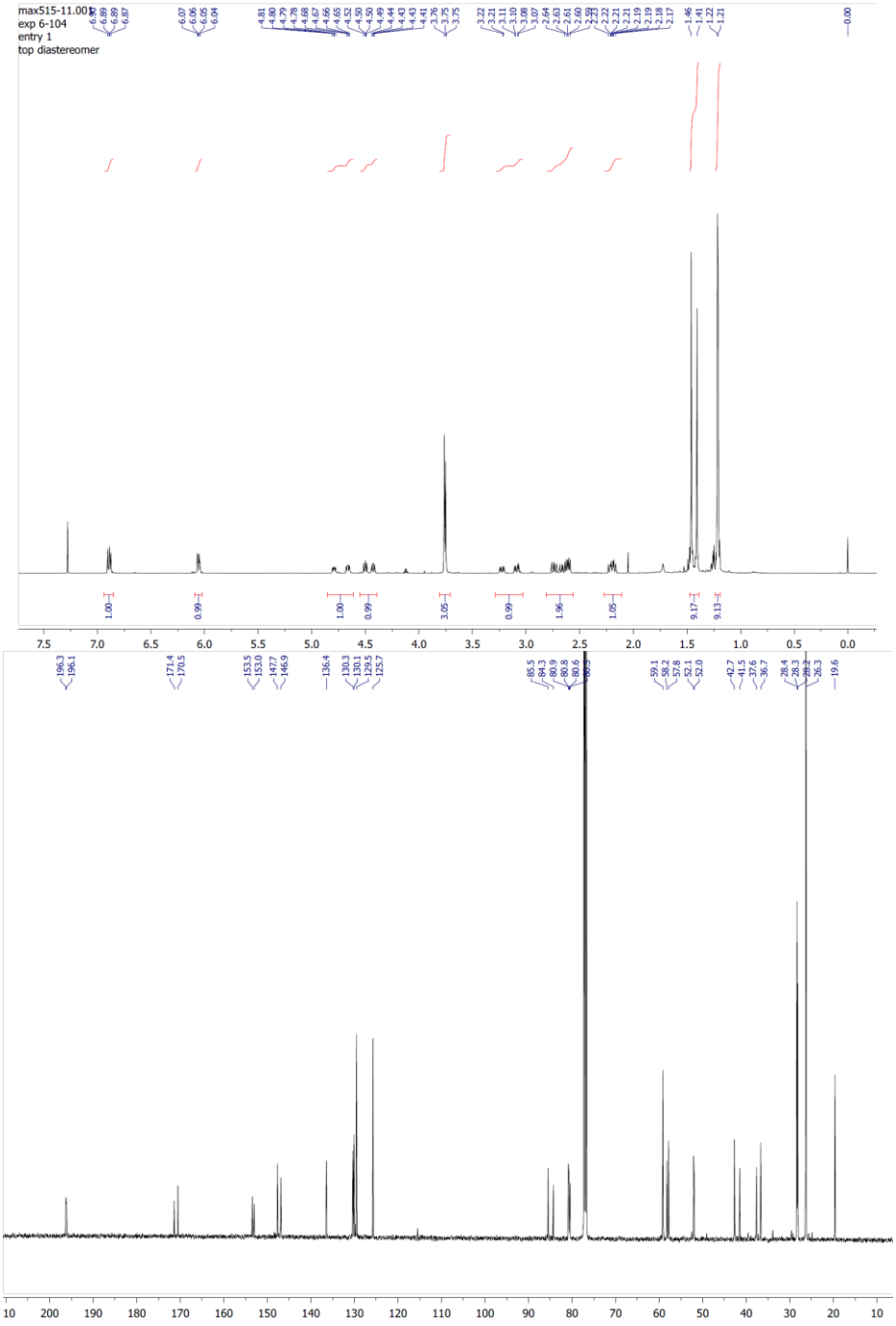
max515-11.001
exp 6-104
entry 1
top diastereomer

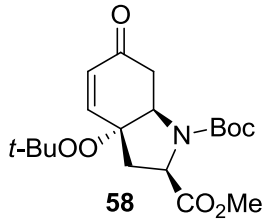

58

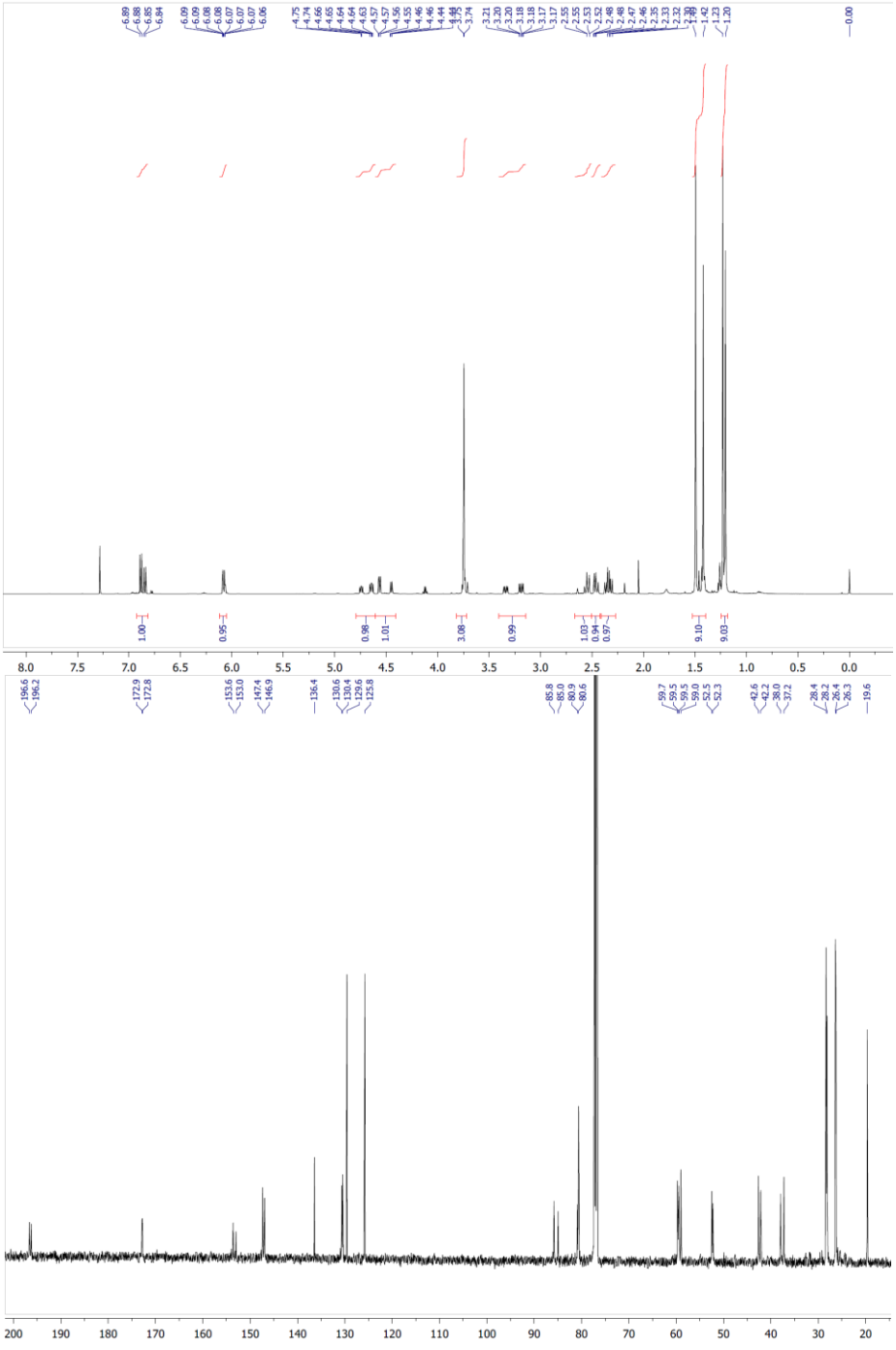

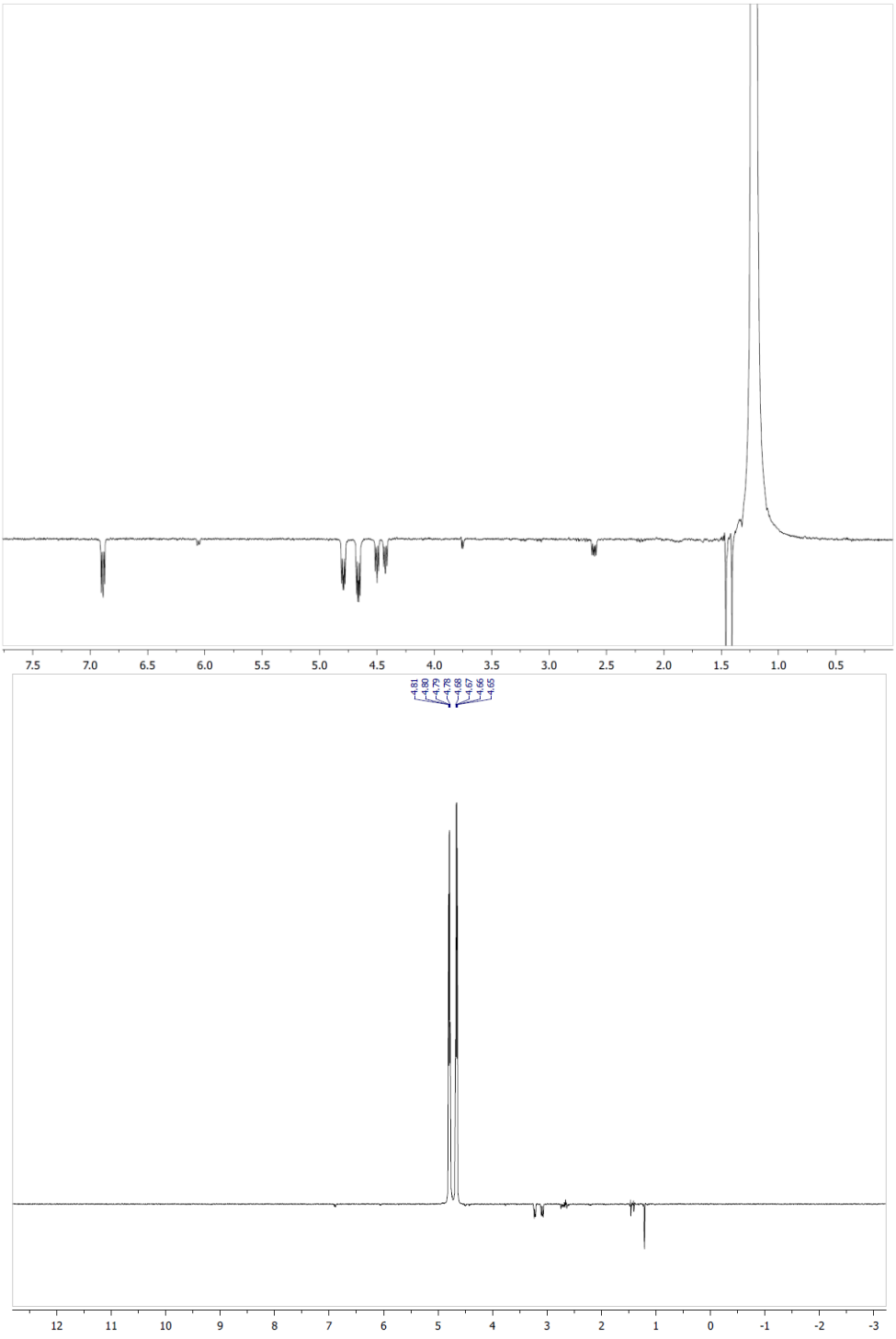
7.5
7.0
6.5
6.0
5.5
5.0
4.5
4.0
3.5
3.0
2.5
2.0
1.5
1.0
0.5
-4.81
-4.80
-4.79
-4.78
-4.68
-4.67
-4.66
-4.65
12
11
10
9
8
7
6
5
4
3
2
1
0
-1
-2
-3

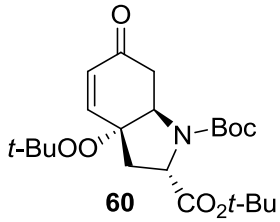
O
t-BuOO
N–Boc
CO2t-Bu

60

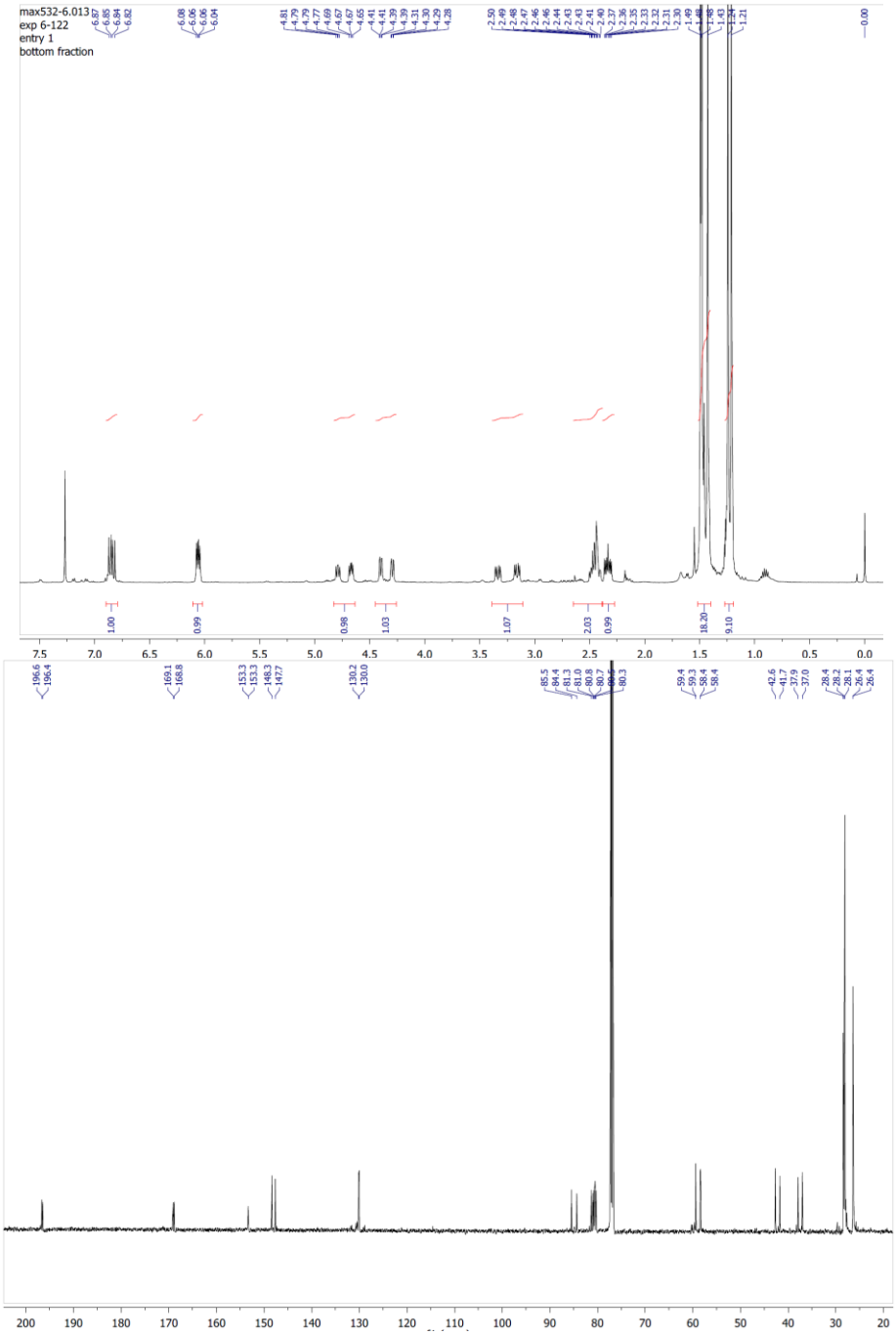
max532-6.013
exp 6-122
entry 1
bottom fraction

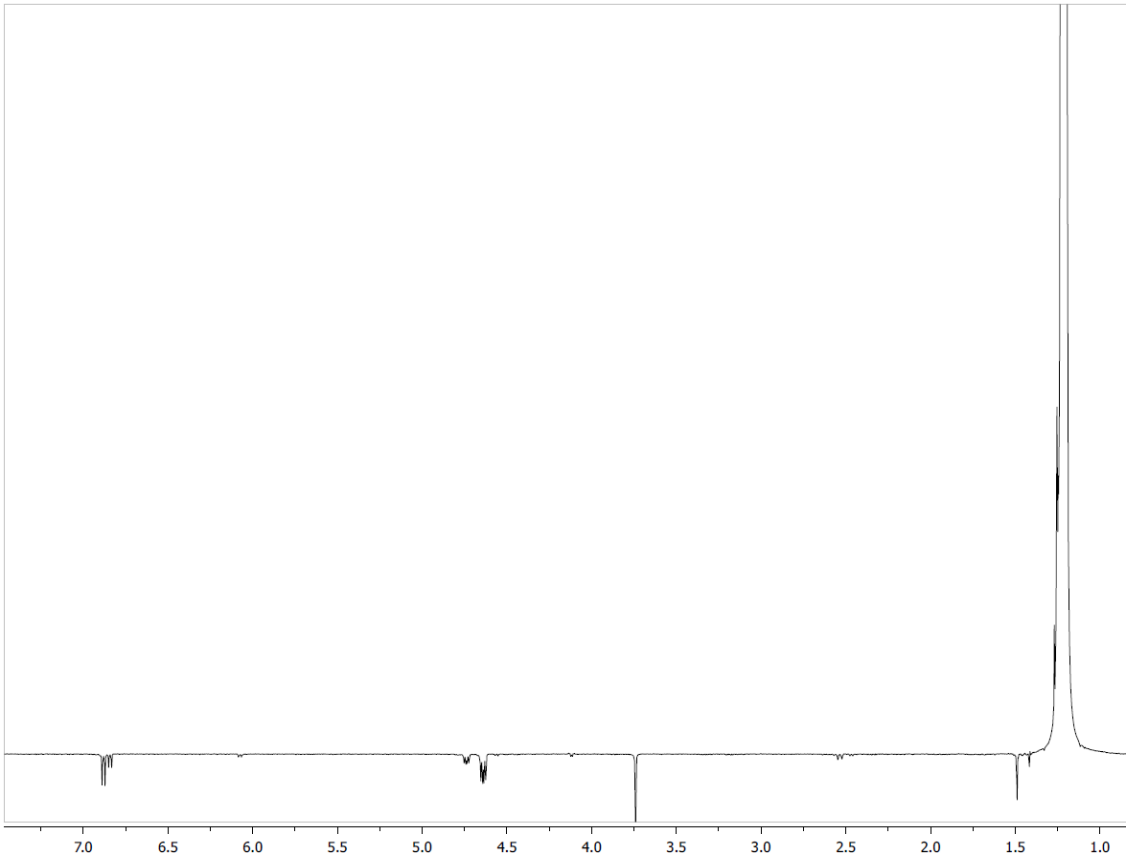
7.0
6.5
6.0
5.5
5.0
4.5
4.0
3.5
3.0
2.5
2.0
1.5
1.0

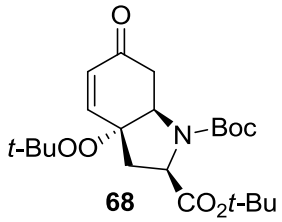
O
N–Boc
t-BuOO
CO2t-Bu

68

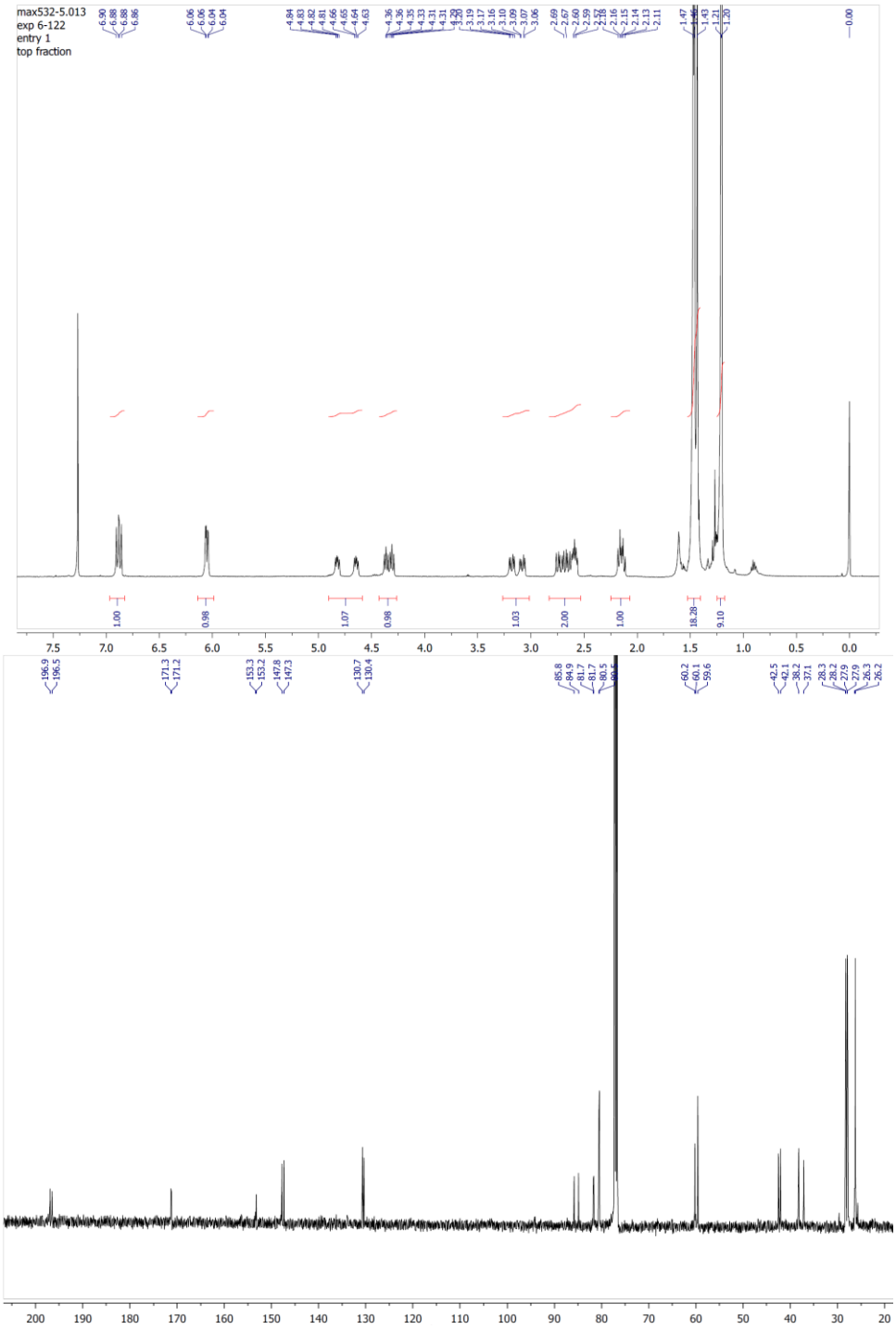
max532-5.013
exp 6-122
entry 1
top fraction

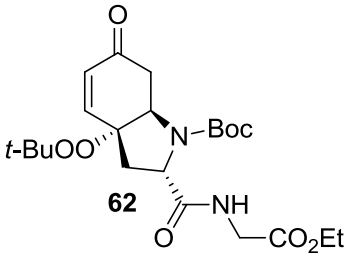

62

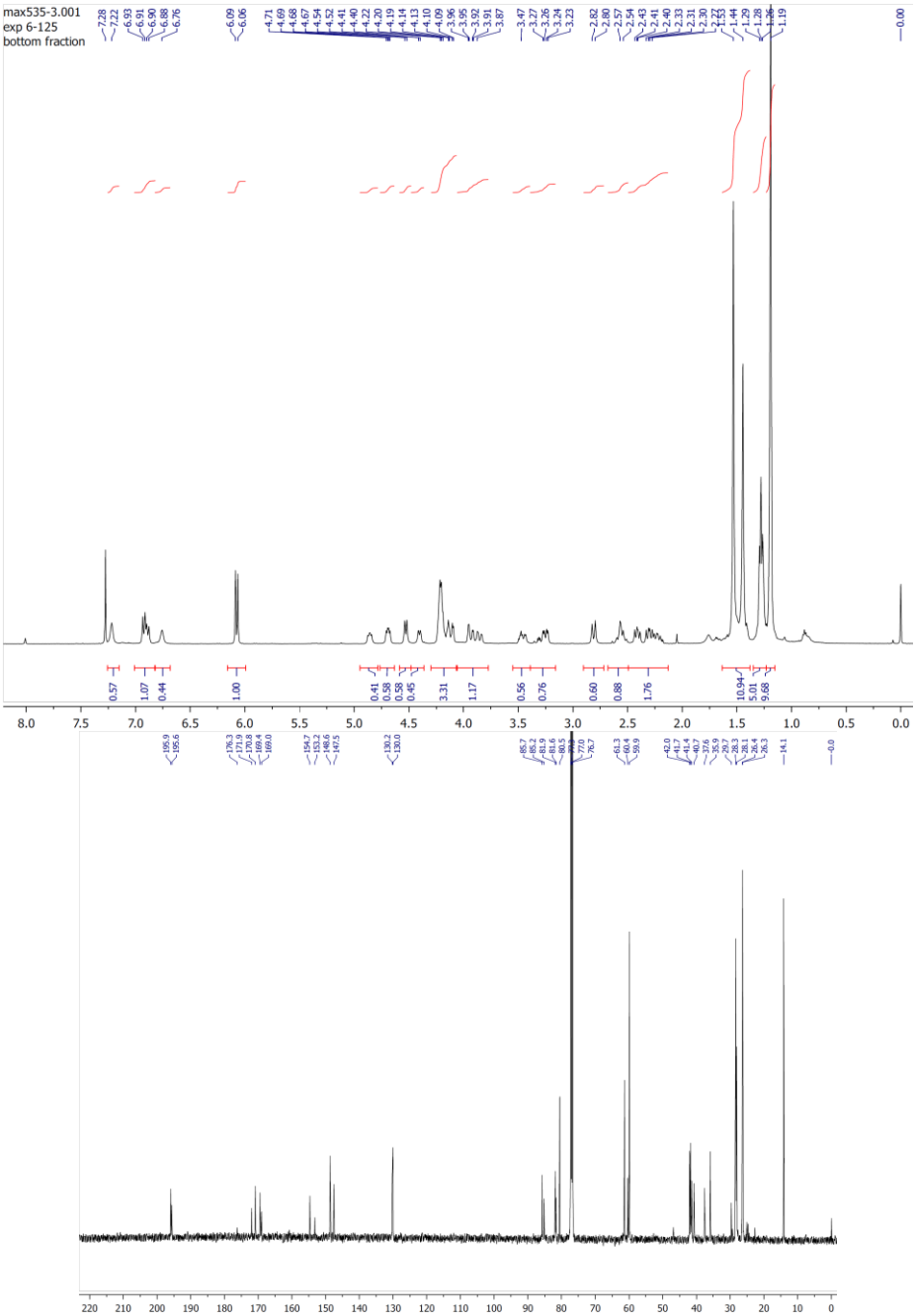

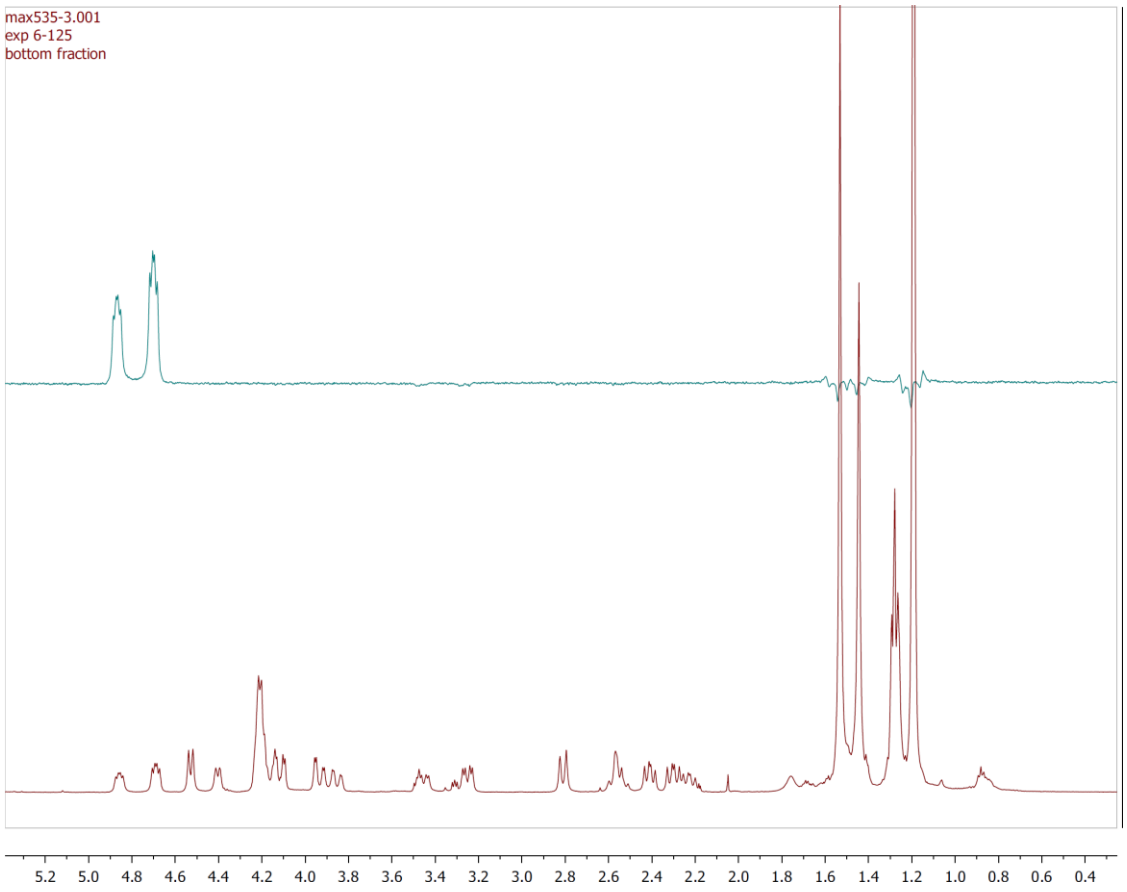
max535-3.001
exp 6-125
bottom fraction
5.2 5.0 4.8 4.6 4.4 4.2 4.0 3.8 3.6 3.4 3.2 3.0 2.8 2.6 2.4 2.2 2.0 1.8 1.6 1.4 1.2 1.0 0.8 0.6 0.4

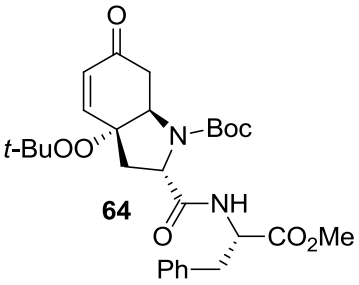

64

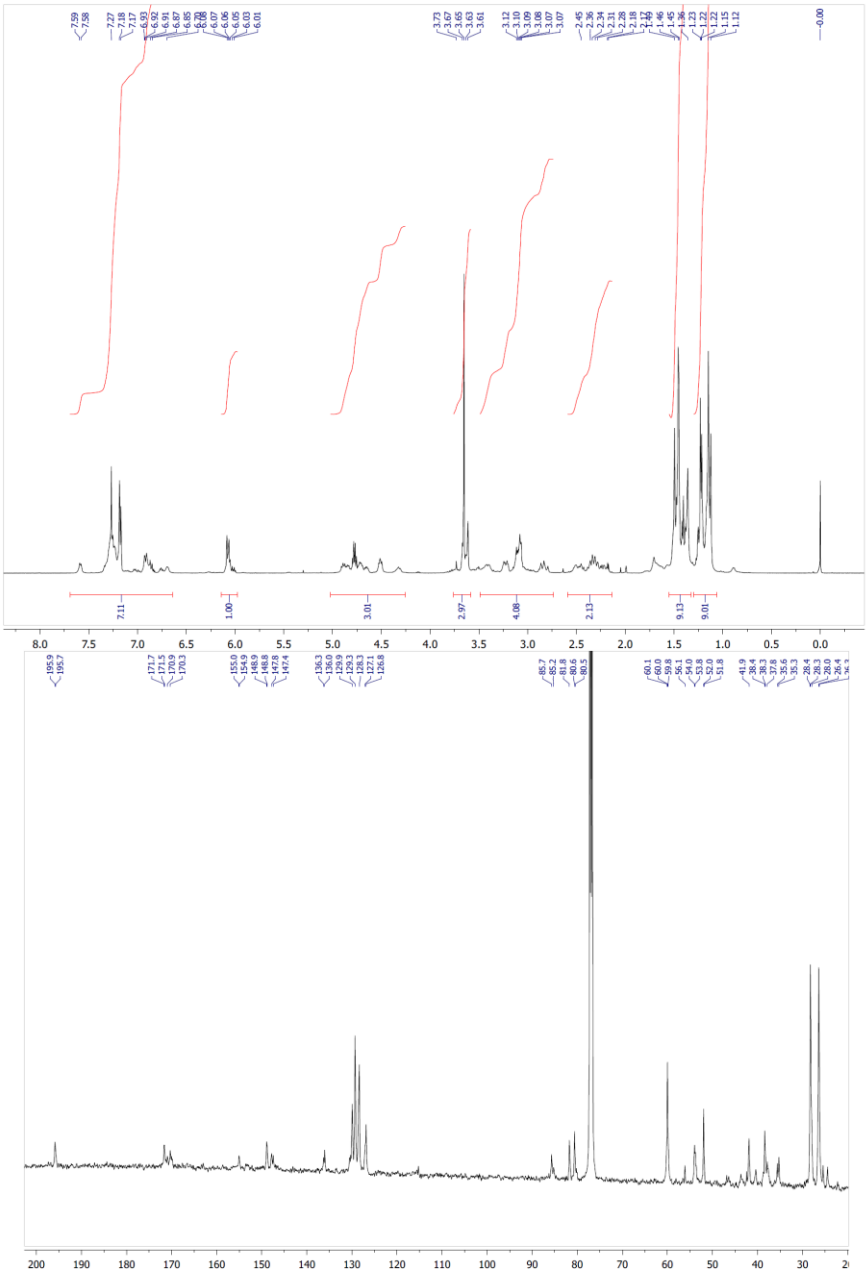

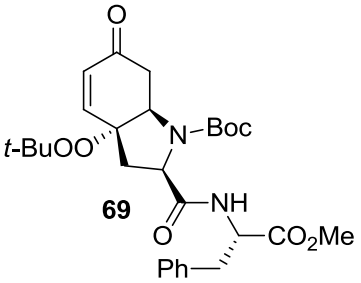

69

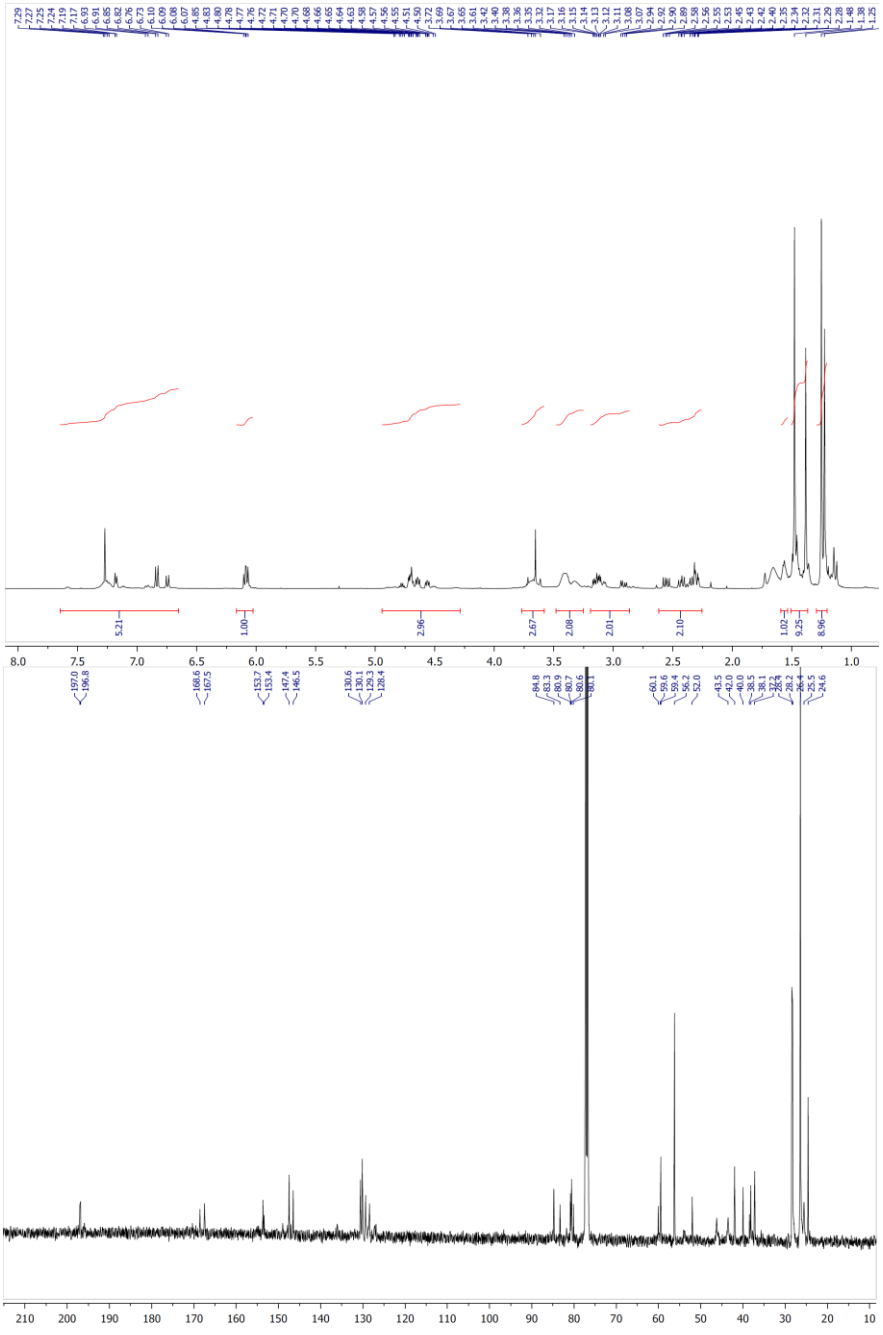

Chapter 3: Mechanistic Investigation of Oxidative Mannich Reaction with *tert*-Butyl Hydroperoxide. The Role of Transition Metal Salts

Synopsis

A general mechanism is proposed for transition metal catalyzed oxidative Mannich reactions of *N,N*-dialkylanilines with *tert*-butyl hydroperoxide (TBHP) as the oxidant (Scheme 3-1). The mechanism consists of a rate-determining single electron transfer (SET) that is uniform for *N,N*-dimethylanilines bearing 4-substituents ranging from methoxy to cyano groups. *tert*-Butylperoxy radical is the major oxidant in the rate-determining SET step that is followed by competing backward SET and irreversible heterolytic cleavage of the carbon-hydrogen bond at the α-position to nitrogen. The conversion of *N,N*-dimethylaniline to an iminium ion is completed with the second SET. The resulting iminium ion is subsequently trapped by the nucleophilic solvent or the oxidant prior to formation of the Mannich adduct. The general role of $Rh_2(cap)_4$, $RuCl_2(PPh_3)_3$, CuBr, $FeCl_3$, and $Co(OAc)_2$ in *N,N*-dialkylaniline oxidations by T-HYDRO is to initiate the conversion of TBHP to *tert*-butylperoxy radicals. A second pathway involving O_2 as the oxidant exists for copper, iron, and cobalt salts.

Results from the linear free-energy relationship (LFER) analysis, kinetic and product isotope effects (KIE and PIE), radical trap experiments of the transition metal salt catalyzed *N,N*-dimethylaniline oxidation by T-HYDRO are discussed. The kinetic studies of the oxidative Mannich reaction in methanol and toluene are reported.

New mechanistic insights revealed that $FeCl_3$ is a potential catalyst for the *N*,*N*-dialkylaniline oxidations by O_2. Based on this discovery, a novel protocol for oxidative Mannich reaction of *N*,*N*-dialkylanilines and siloxyfuran was developed using a commodity catalyst ($FeCl_3$) and atom efficient oxidant (O_2) (Scheme 3-2).

Scheme 3-1. Summary of mechanistic investigations of transition metal catalyzed oxidative Mannich reaction with TBHP as an oxidant.

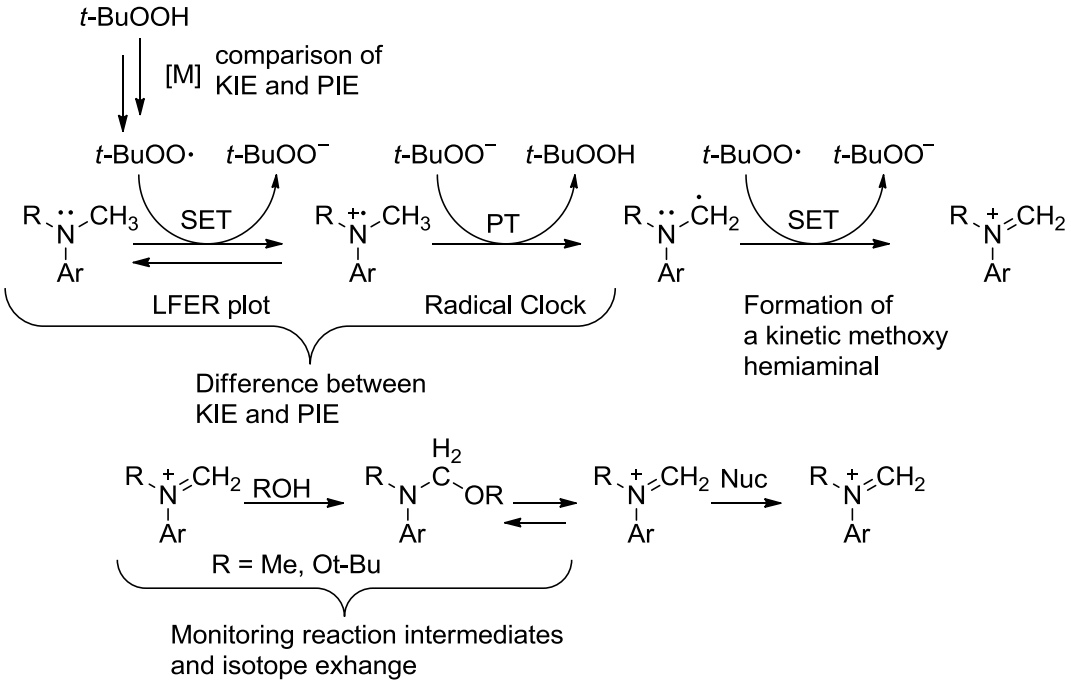

Scheme 3-2. Summary of the ferric chloride catalyzed oxidative Mannich reaction of substituted *N*-methylanilines and siloxyfuran with O_2 as an oxidant.

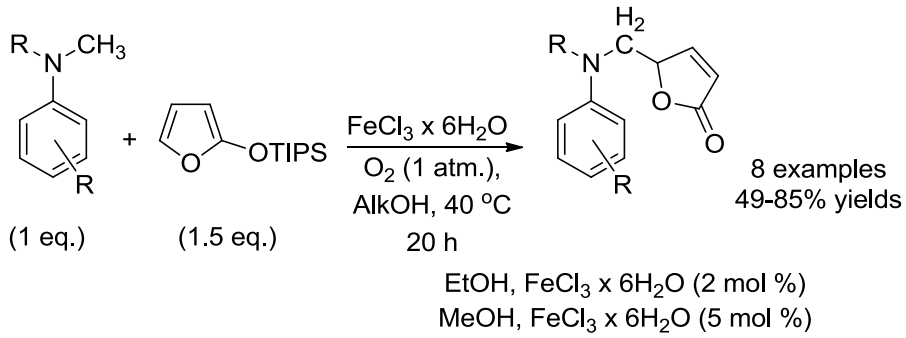

Introduction - Synthetic Methods and Mechanistic Models for Oxidative Mannich Reaction

The Mannich reaction is a powerful transformation for the syntheses of nitrogen-containing natural products and active pharmaceutical ingredients.[71] Iminium ions, key intermediates of the Mannich reaction, react with a large variety of nucleophiles.[43,72] However, despite their synthetic value, only simple *N*,*N*-dimethylmethylideneammonium halides (Eschenmoser's salts) are commercially available iminium ions. Hence, the iminium ions have to be prepared in situ by methods that limit the scope of nucleophiles that are compatible. Strategies allowing access to Mannich reaction intermediates include condensation of secondary amines with aldehydes,[71a] α-fragmentation of iminium ion precursors,[71b] and the oxidation of tertiary amines (Scheme 3-3).[32,43,72a,b,73] The latter method directly and under mild conditions functionalizes otherwise inert C-H bonds that are adjacent to nitrogen.

Scheme 3-3. Strategies for preparation a key intermediate of the Mannich reaction.

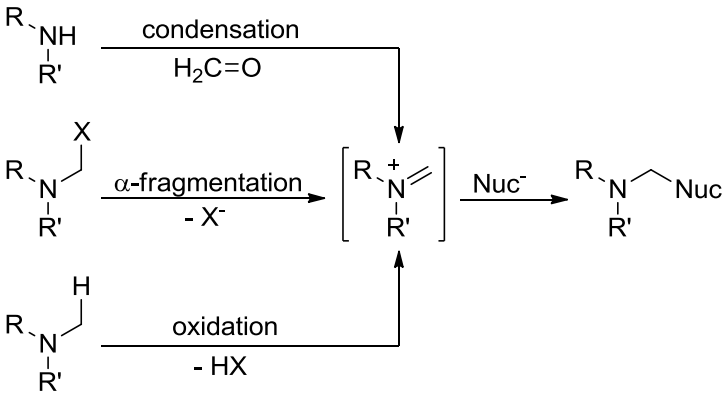

In the last decade several catalytic systems were developed for the conversion of *N*,*N*-dialkylanilines to their corresponding iminium ions. The scope of catalysts for this

transformation include Ru,[73-74] Rh,[32] Cu,[43,72b,75] Fe,[76] Mo,[77] and V[78] complexes. Recent advances in the oxidative Mannich reaction of *N*,*N*-dialkylanilines enabled the use of dioxygen[73,75a,b] or di-*tert*-butylperoxide (DTBP) as oxidants.[79] However, the copper(II) chloride catalyzed Mannich reaction by O_2 is limited to *N*,*N*-dialkylanilines with low oxidation potential, *N*-aryl-tetrahydroisoquinolines (Scheme 3-4a).[75a,b] The $RuCl_3$ catalyzed transformation, on the other hand, is applicable to *N*,*N*-dimethylanilines and *N*-aryl-tetrahydroisoquinolines but was reported only with cyanide and requires 5 mole % of a catalyst loading (Scheme 3-4b).[73] The reaction temperature of 100 °C in the ferrous chloride catalyzed oxidative Mannich reaction of *N*,*N*-dimethylanilines and alkynes with DTBP poses a risk of explosion under neat conditions (Scheme 3-4c).[79] Moreover, without electron-donating substituent at the 4-position of *N*,*N*-dimethylaniline, the iron-catalyzed protocol furnished only 32% yield (Scheme 3-4c). Thus, the mild conditions[32] and often higher yields[72b,75a,76c] of the oxidative Mannich reaction by *tert*-butyl hydroperoxide (TBHP) support TBHP as the oxidant of choice.

Scheme 3-4. Selected examples of the transition metal catalyzed oxidative Mannich reaction by O_2 and DTBP.

a)

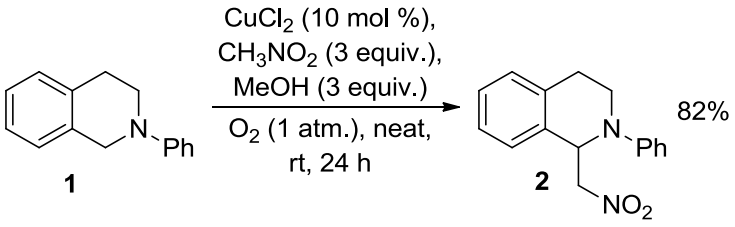

b)

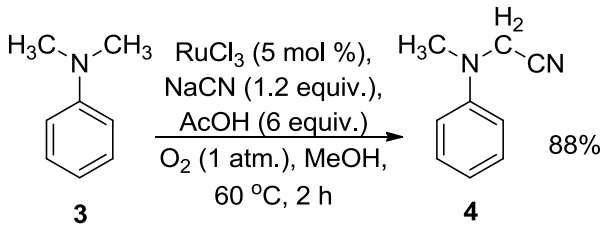

c)

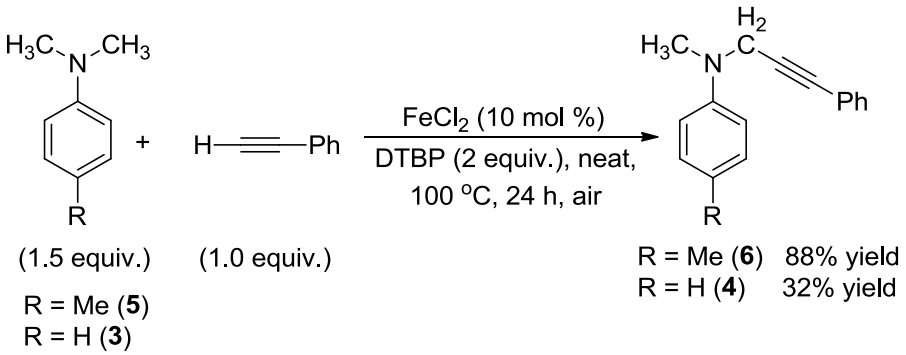

The success of the oxidative Mannich reaction depends on the method of generation of iminium ion. The mild conditions of transition metal catalyzed oxidation of *N*,*N*-dialkylanilines to iminium ions with TBHP enable the utilization of selected nucleophiles such as siloxyfurans,[32] enol silanes,[75b,80] allyl silanes,[76b] indoles,[74b,75c,76d,81] cyanides,[73,74c,76a,77,78b,82] alkynes,[43,72b] ketones,[74a,75c,75e,78a,83] nitroalkanes,[74d,77,84] 1,3-dicarbonyl compounds,[84b,85] electron-rich arenes,[86] heterarenes,[75a,76d,86] boronic acids,[87] and heteroatom nucleophiles[39,88] in the oxidative Mannich reaction. However, the majority of these nucleophiles were employed in the copper(I) catalyzed oxidative Mannich reaction of *N*-aryl-tetrahydroisoquinolines.[43,72b,75a] The use of Rh[32] and Ru[39,74b] complexes, on the other hand, provides a broader scope of *N*,*N*-dilakylanilines but has a limited scope of employed nucleophiles. This comparison raises a question whether the scopes of *N*,*N*-dialkylanilines and nucleophiles in the oxidative Mannich reaction are catalyst-specific or could be generalized among different catalysts and conditions. An understanding of the role of the transition metal in the *N*,*N*-dialkylaniline oxidation step and in the subsequent Mannich reaction would provide an answer to this question. The detailed understanding of each step of the process could also improve existing protocols of the oxidative Mannich reaction with TBHP that often require an excess of *N*,*N*-dialkylanilines to achieve high yields.[32,74b] Finally, the knowledge of factors

controlling *N*,*N*-dialkylaniline oxidation step and the Mannich reaction step might facilitate the development of new catalytic systems that utilizes inexpensive catalysts and more atom economical oxidants, such as O_2.

As stated above, the oxidative Mannich reaction consists of two independent steps – oxidation of *N*,*N*-dialkylaniline to the iminium ion and the reaction of the iminium ion or the associated intermediate with a nucleophile (Scheme 3-5). A few systematic mechanistic studies of the catalyzed *N*,*N*-dialkylaniline oxidations by TBHP have been reported.[39,74b] Investigations of possible intermediates leading to the Mannich adduct and factors controlling the selectivity *N*,*N*-dialkylaniline oxidation by TBHP have received more attention.[32,74b,75a]

Scheme 3-5. General scheme of oxidative Mannich reaction with TBHP.

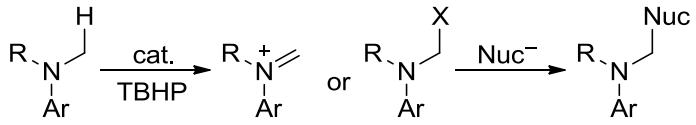

Our research group reported a dirhodium caprolactamate [$Rh_2(cap)_4$] catalyzed oxidative Mannich reaction of *N*,*N*-alkylanilines and siloxyfurans using 70% aqueous solution of TBHP (T-HYDRO) as the oxidant.[32] Butenolide products were formed in 53-89% yields (Scheme 3-6a).

In the case of *N*-methyl-*N*-ethylaniline (**7**) functionalization occurred exclusively at the less substituted *N*-alkyl group (Scheme 3-6b). The oxidative Mannich reaction of **1** and siloxyfuran **8** furnished the addition product at the benzylic position adjacent to nitrogen (Scheme 3-6c). No explanation of the observed selectivity was provided.[32]

Scheme 3-6. The $Rh_2(cap)_4$ catalyzed Mannich reaction of *N*,*N*-dialkylanilines and siloxyfurans.[32]

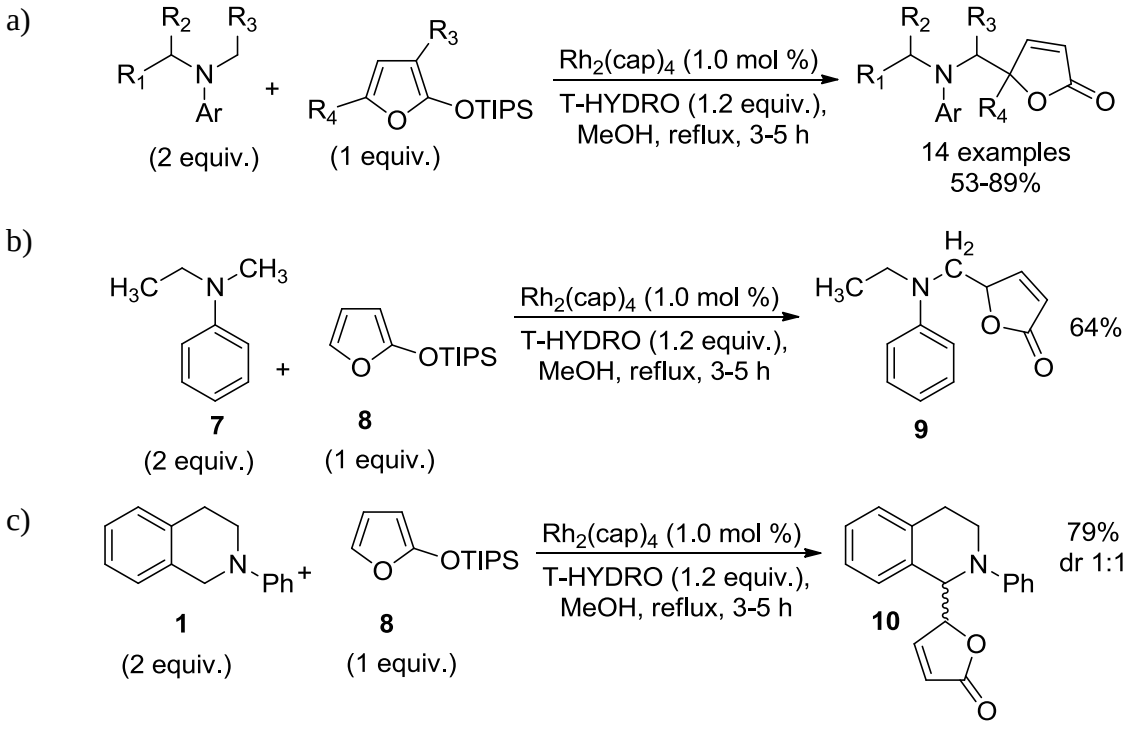

The formation of an iminium ion **12** from *N*,*N*-dialkylaniline **11** followed by a competition of capture of **12** by siloxyfuran **8** and methanol (Scheme 3-7) were postulated by Doyle for the $Rh_2(cap)_4$ catalyzed oxidative Mannich reaction with T-HYDRO.[32] In methanol, but in the absence of a nucleophile other than the solvent, methoxy hemiaminal **15** was isolated in 62% from *N*,*N*-dimethylaniline **3** (Scheme 3-8a). The *N*,*N*-dialkylaniline oxidation with anhydrous TBHP in non-nucleophilic DCM catalyzed by $Rh_2(cap)_4$ afforded the peroxy hemiaminal **16** in 60% yield (Scheme 3-8b). Dissolution of **16** in methanol revealed the equilibrium between **15** and **16** with the equilibrium constant of about 3×10^{-2} favoring **16** (Scheme 3-8c). Thus, Doyle concluded that the preferential formation of less thermodynamically stable methoxy hemiaminal **15** in the oxidation of *N*,*N*-dimethylaniline by T-HYDRO in methanol is a kinetically

controlled reaction. Consequently, methoxy hemiaminal **15** is a side-product that is formed in competition with siloxyfuran for the iminium ion under the conditions of the oxidative Mannich reaction.

Scheme 3-7. Proposed mechanism the $Rh_2(cap)_4$ catalyzed oxidative Mannich reaction with T-HYDRO.

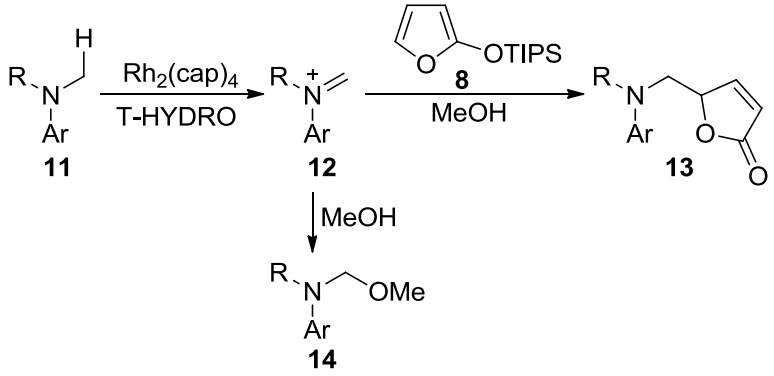

Scheme 3-8. Preparation and interconversion of **15** and **16**.

a)

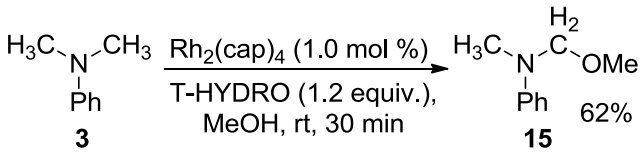

b)

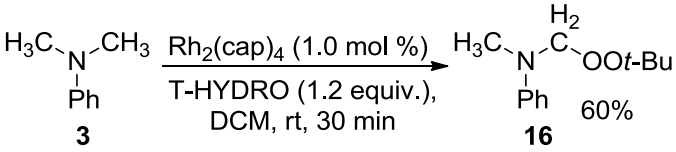

c)

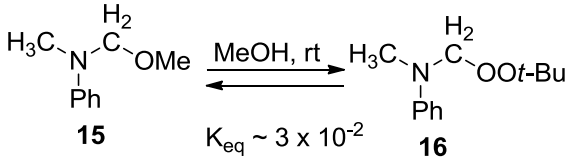

Murahashi first reported the $RuCl_2(PPh_3)_3$ catalyzed *N*,*N*-dialkylaniline oxidation by anhydrous TBHP.[39] The observed preferential oxidation of the less substituted *N*-alkyl

group of the unsymmetrical *N*,*N*-dialkylanilies is the same as for the $Rh_2(cap)_4$ catalyzed oxidative Mannich reaction with T-HYDRO. Mechanistic investigations by Murahashi of Ru-catalyzed *N*,*N*-dialkylanilines oxidations by TBHP revealed a linear correlation of the natural logarithm (log_e) of the relative initial rates of the oxidations of 4-methoxy- (**17**), 4-methyl- (**5**), unsubstituted (**3**), and 4-chloro-*N*,*N*-dimethylanilines (**18**) by anhydrous TBHP against σ values on a Hammett plot ($\gamma = 0.974$) with $\rho = -0.84$. The negative ρ value indicates the formation of an electron deficient intermediate from *N*,*N*-dimethylaniline on a rate-determining step. Kinetic and product isotope effects of demethylations of a 1:1 mixture of **3** and d_6-**3** and demethylation of d_3-**3** were 1.64 and 3.53, respectively (Scheme 3-8). The ruthenium trichloride catalyzed demethylation of the same substrates by H_2O_2, however, showed $\rho = -3.26$ for the same parameters in Hammett LFER analysis and kinetic and product isotope effects of 3.47 and 3.72, respectively (Scheme 3-9).[89] The large difference between the isotope effects of ruthenium-catalyzed demethylation by TBHP and H_2O_2 is surprising because the ruthenium oxo-complex mechanistic proposal of Murahashi is expected to be independent of the oxidant.

Scheme 3-9. Kinetic and product isotope effects of *N*,*N*-dimethylanilines oxidations by anhydrous TBHP catalyzed $RuCl_2(PPh_3)_3$ and by H_2O_2 catalyzed by $RuCl_3$.

a) Kinetic Isotope Effect

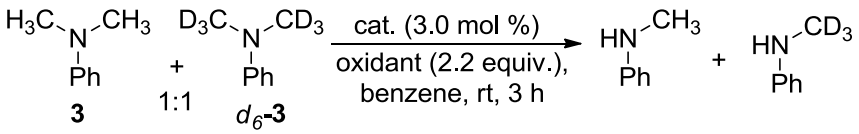

$RuCl_2(PPh_3)_3$ / TBHP	1.64
$RuCl_3$ / H_2O_2	3.47

b) Product Isotope Effect

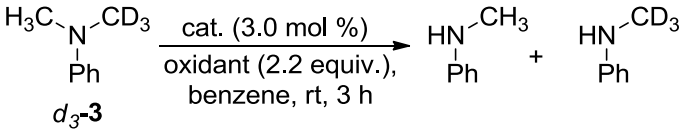

$RuCl_2(PPh_3)_3$ / TBHP	3.53
$RuCl_3$ / H_2O_2	3.72

Murahashi adopted the mechanistic model proposed by Sligan and Bruice[90] and by Guengerich and MacDonald[91] for the cytochrome P450 catalyzed demethylation of 4-substituted *N*,*N*-dimethylanilines in the presence of O_2 that postulated the formation of iron porphyrin oxo-complex and its role in abstraction of electron and hydrogen atom from *N*,*N*-dimethylanilines (Scheme 3-9).[39,92] According to the initial report by Murahashi,[39] the similarity of the kinetic and product isotope effects measured for the Ru-catalyzed (1.64 and 3.53, respectively) and Fe-catalyzed demethylations (1.0-1.1 and 1.6-3.1)[90,93] served as evidence for the proposed role of ruthenium oxo-complex in the Ru-catalyzed demethylation of *N*,*N*-dimethylaniline by TBHP. Murahashi suggested that the greater values measured for the Ru-catalyzed reactions imply that there is more

radical character in the C-H breaking step than for the step occurring in the Fe-porphyrin catalyzed reaction. According to this adopted mechanism, $RuCl_2(PPh_3)_3$ forms an oxo-complex **19** upon the reaction with TBHP (Scheme 3-10).[39] Complex **19** subsequently undergoes single electron transfer (SET) from the nitrogen lone pair of *N*,*N*-dialkylaniline followed by hydrogen atom transfer (HAT) from the corresponding cation-radical to yield the iminium ion. Although Murahashi stated that "it was premature to discuss the precise mechanism",[39] the oxo-ruthenium hypothesis was invoked in the mechanism of Ru-catalyzed the benzylic oxidation[94] and peroxidation of phenol by anhydrous TBHP.[36] Since the ruthenium oxo-complex is unstable in the presence of water, the anhydrous conditions were postulated for the Ru-catalyzed oxidative Mannich reaction by TBHP.[36]

Scheme 3-10. The adopted mechanism of $RuCl_2(PPh_3)_3$ catalyzed *N*,*N*-dialkylaniline oxidation by TBHP.

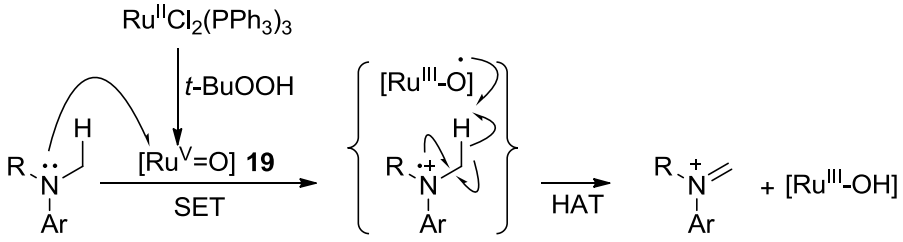

Che employed Ru-porphyrin complex **20** and, alternatively, $RuCl_3$ for catalysis of the oxidative Mannich reaction of *N*,*N*-dialkylanilines and indoles with T-HYDRO (Scheme 3-11a).[74b] A series of experiments were conducted to determine the role of **20** and to search for any intermediates under conditions of the oxidative Mannich reaction. The formation of Ru porphyrin oxo-complex **21** from **20** and TBHP was a working

hypothesis based on analogy with the previous Murahashi report.[39] Similar to a sequence of SET and HAT step presented in Scheme 3-9, complex **21**, acting as a sole oxidant, furnished the iminium ion from *N*,*N*-dialkylanilines (Scheme 3-11b).

Scheme 3-11. The oxidative Mannich reaction of *N*,*N*-dialkylanilines and indoles with T-HYDRO catalyzed by ruthenium complex **20**.

a)

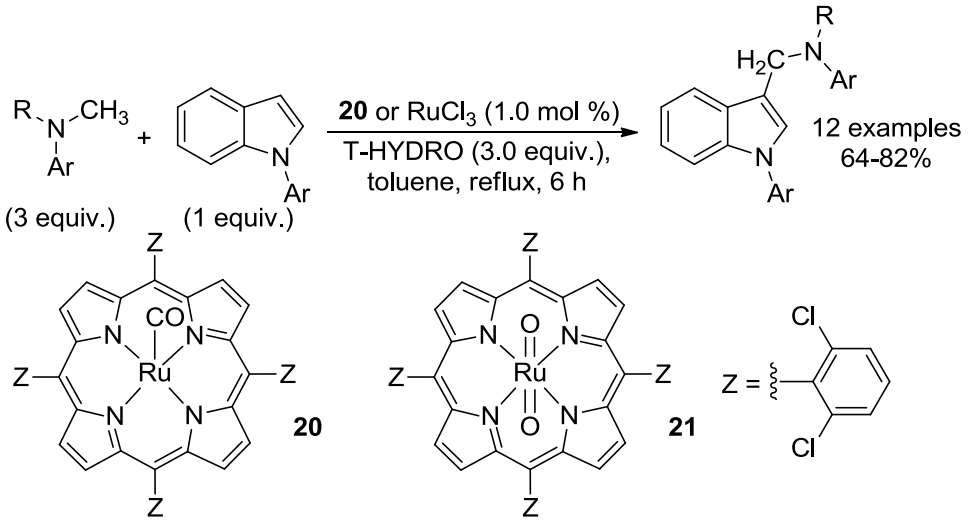

b)

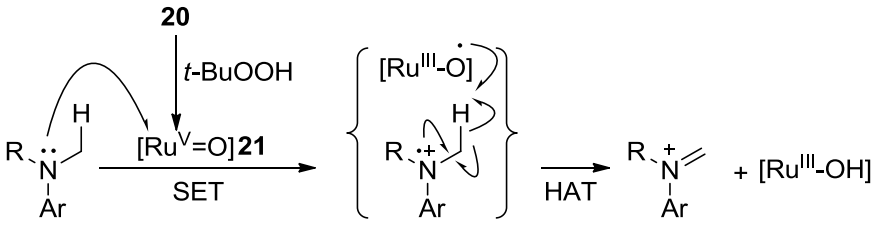

Che referenced the indirect detection by Balch[95] of the iron oxo-complex formation **23** with TBHP (Scheme 3-12) as a precedent of transition metal oxo-complex formation with TBHP to support the formation of ruthenium oxo-complex in the oxidative Mannich reaction by TBHP. Balch concluded that the complex formed from **22**

upon treatment with TBHP is iron oxo-complex **23** by excluding of known iron hydroxy- and peroxy-complexes in a series of comparisons of paramagnetic ^{1}H NMR spectra.

It is important to note, however, that the formation of one mole of Fe oxo-complex **23** from **22** generates two moles of *tert*-butylperoxy radical (Scheme 3-12). These radicals may contribute to the oxidation process according to the findings discussed in Chapter 1 for the ruthenium catalyzed phenol oxidation by T-HYDRO.[1,19] The detection of di-*tert*-butyl peroxide (DTBP), a product of dimerization of *tert*-butylperoxy radicals, supports the radical character of the Fe oxo-complex formation.[95]

Scheme 3-12. The proposed mechanism for the formation of Fe oxo-complex **23** from **22** with TBHP.

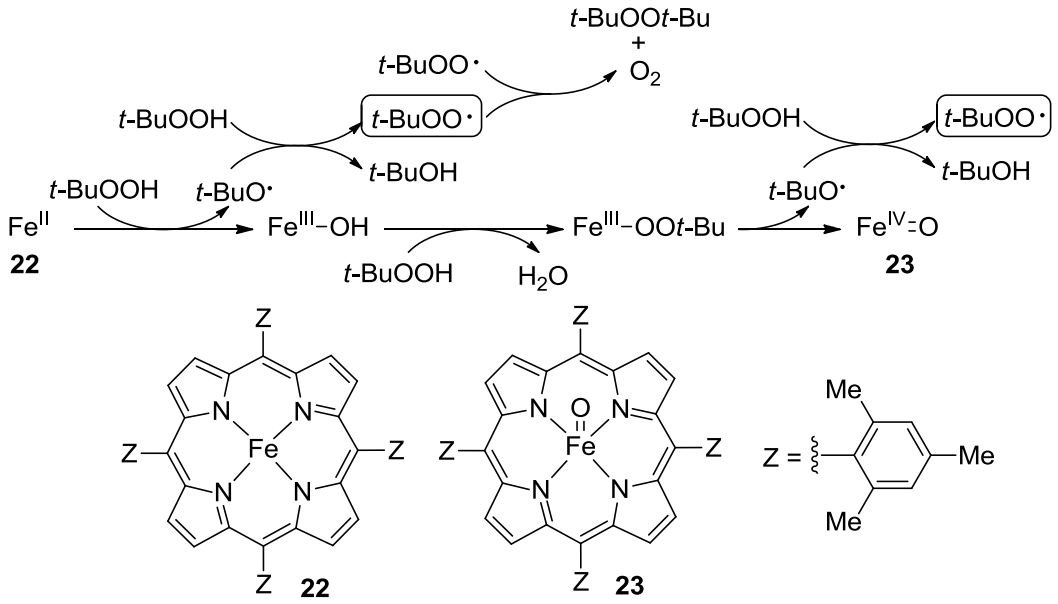

Che prepared ruthenium oxo-complex **21** by treatment of **20** with TBHP and unambiguously characterized it by X-Ray analysis. A stoichiometric amount of **21** afforded demethylation of *N*,*N*-dimethylaniline in 36% yield, however, the fate of the

ruthenium oxo-complex **21** was not reported (Scheme 3-13a). Che concluded that this result supports Ru-porphyrin oxo-complexes as kinetically feasible species in the oxidation of *N*,*N*-dialkylanilines. Furthermore, the replacement of TBHP for *N*-oxide **25** afforded the oxidative Mannich reaction of **3** and indole **24** in 75% yield and 95% conversion (Scheme 3-13b). Since the oxidative Mannich reaction catalyzed by **20** afforded the same product **26** with two different oxidants, TBHP and *N*-oxide **25**, Che postulated that Ru porphyrin oxo-complexes are the sole oxidants in *N*,*N*-dialkylaniline oxidation.

Scheme 3-13. Demethylation of *N*,*N*-dimethylaniline by stoichiometric Ru oxo-complex **21** and the oxidative Mannich reaction of **3** and indole **24** with *N*-Oxide **25** catalyzed complex **20**.

a)

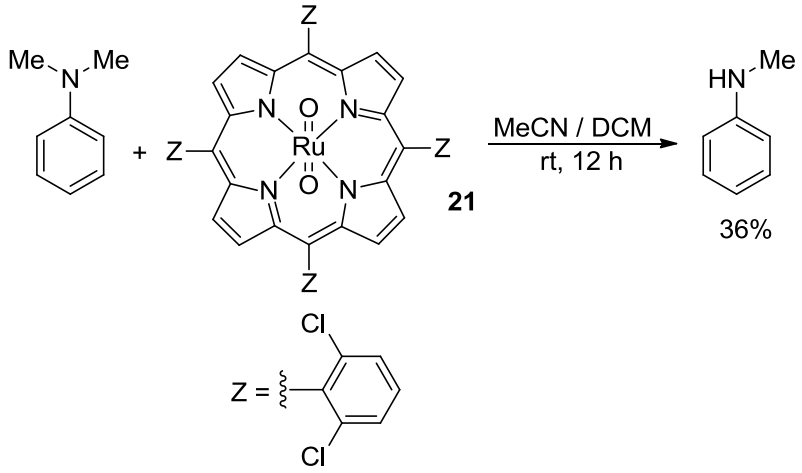

b)

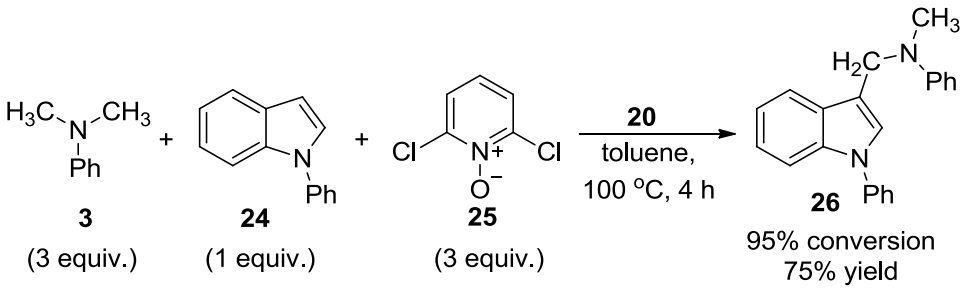

Che conducted the LFER analysis for the Mannich reaction of 4-substituted *N*,*N*-dimethylanilines and indole **24** with T-HYDRO catalyzed by **20** (Scheme 3-14). The Hammett plot of natural logarithm (ln) of relative initial reaction rates measured for 4-methoxy- (**17**), 4-methyl- (**5**), unsubstituted (**3**), and 4-bromo-*N*,*N*-dimethylanilines (**27**) showed a linear correlation ($R^2 = 0.989$) with σ^+ parameters and a ρ value of - 1.09. Che used the negative ρ value as evidence for the build-up of positive charge on nitrogen in the transition state of a rate-determining step. Although LFER analysis of Che supports the mechanism presented in Scheme 3-11b, this conclusion has to be considered with caution. Che measured the initial reaction rates as the rates of product formation and extrapolated the rates of Mannich adduct formations to the rates of *N*,*N*-dialkylaniline oxidations. However, no evidence was reported supporting *N*,*N*-dialkylaniline oxidation rather than Mannich addition (Scheme 3-5) as the rate-determining step of the oxidative Mannich reaction. Furthermore, the dependence of temperature in the copper(I) halide catalyzed oxidative Mannich reaction by TBHP on the activity of nucleophiles and not *N*,*N*-dialkylanilines led Li to conclusion that Mannich addition is the rate-determining step.[43]

Scheme 3-14. The reaction employed for LFER analysis.

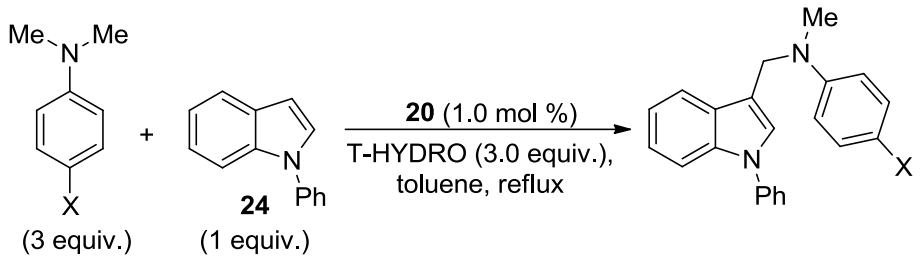

Kinetic isotope effects were measured by Che for a series of oxidative Mannich reaction of 4-substituted *N*,*N*-dimethylanilines and *N*-phenylindole (Table 3-1). The ratio of the deuterium labeled methylene group to the unlabeled methylene group determined for the Mannich adduct decreased on going from electron-rich to electron-poor *N*,*N*-dimethylanilines. Che concluded that the difference between kinetic and product isotope effects is due to an early transition state of the rate-determining electron-transfer from *N*,*N*-dialkylaniline to the ruthenium oxo-complex (Scheme 3-11b). Surprisingly, the change of the kinetic isotope effects with the electron donating ability of 4-substituent of *N*,*N*-dimethylaniline is opposite to the one observed for demethylation of *N*,*N*-dimethylanilines with iron-porphyrin oxo-complexes (Table 3-1).[93a]

Table 3-1. Kinetic and product isotope effects of oxidative Mannich reaction of 4-substituted *N*,*N*-dimethylanilines and *N*-phenylindole with T-HYDRO catalyzed complex **20**[74b] and with complex **23**.[93a]

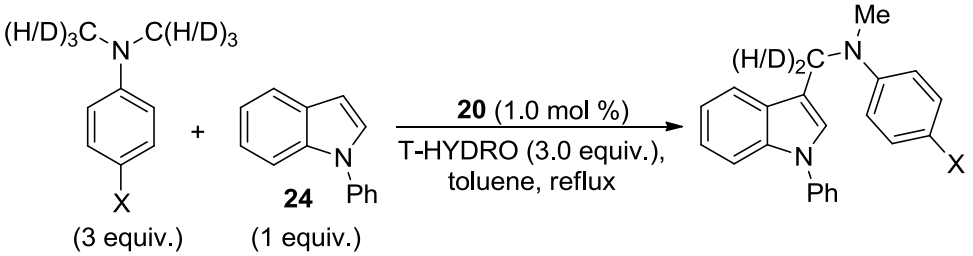

entry	isotope effect	X			
		OMe	Me	H	Br
1	KIE	2.5	2.1	1.7	nd[a]
2	PIE	3.8	3.2	2.2	1.2

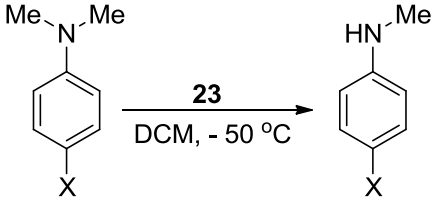

entry	isotope effect	X			
		OMe	Me	H	Br
3	KIE	1.3	1.5	1.9	2.0
4	PIE	3.9	3.8	2.8	3.4

[a] nd - not determined.

Similar to the report of Doyle,[32] Che detected peroxy hemiaminal **16** in the oxidative Mannich reaction of **3** and **24** catalyzed by **20** that led him to conclusion of a competition between nucleophile and TBHP for the iminium ion. Peroxy hemiaminal **16** was isolated in 90% yield by conducting the **3** oxidation with T-HYDRO catalyzed by **20** in the absence of another nucleophile. The refluxing of peroxy hemiaminal **16** and **24** for four hours in toluene in the presence of one mole % of **20** afforded the Mannich adduct in

85% yield (Scheme 3-15). Hence, Che postulated that compound **16** is "a reactive intermediate"[74b] regenerating the iminium ion under the reaction conditions and not a side product. However, no kinetic data were provided to answer whether **16** is an intermediate in the formation of a Mannich adduct or a side-product of competing pathway that can be converted to a Mannich adduct under the reaction conditions.

Scheme 3-15. Mannich reaction of hemiaminal **16** with indole **24**.

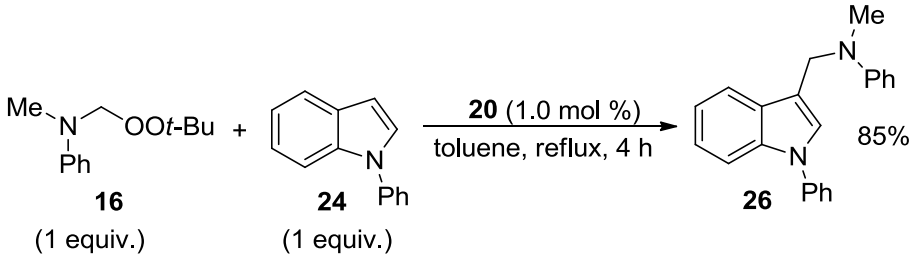

Li first reported the use of copper salts as catalysts for the oxidative Mannich reaction of *N*-aryl-tetrahydroisoquinolines and monosubstituted alkynes.[96] Further elaboration of the scope of nucleophiles led Li to an observation that the optimal reaction temperatures correlated with the reactivity of the nucleophiles and not *N*,*N*-dialkylanilines.[43] The oxidative Mannich reactions with more nucleophilic nitroalkanes and malonates occurred at room temperature overnight, while the use of the less nucleophilic indole requires a temperature of 50 °C for the reaction to be completed in the same period of time (Scheme 3-16). Hence, Li suggested that the formation of Mannich adduct rather than *N*-dialkylaniline oxidation is the rate-determining step of the copper halide catalyzed oxidative Mannich reaction with TBHP.

Scheme 3-16. The oxidative Mannich reaction isoquinoline **1** and indole.

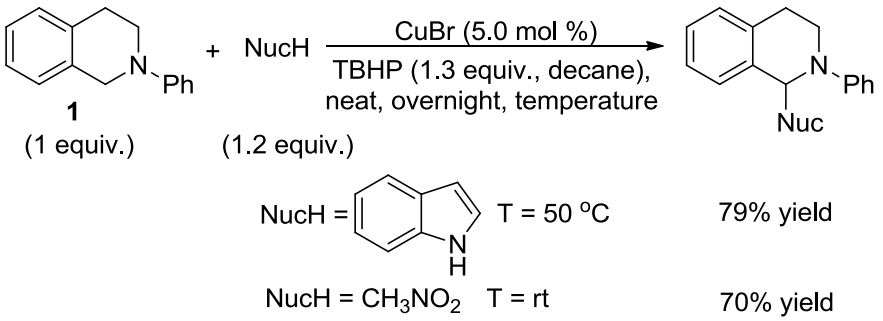

The copper(I) bromide catalyzed oxidative Mannich reaction of tetrahydroisoquinoline **1** and nitromethane furnished the addition product in 70% yield according to ^{1}H NMR spectroscopy when the reaction was conducted with one equivalent of TBHP and two equivalents of **28** (BHT) as a radical scavenger (Scheme 3-17a).[43] Li concluded that the decrease from 84% to 70% yield of the Mannich adduct with and without the radical scavenger, respectively, suggests a non-radical mechanism of the Cu-catalyzed *N*,*N*-dialkylaniline oxidation. Recently, however, Huang reported contradictory of Li results on the effect of an addition of BHT to the CuBr catalyzed oxidative Mannich reaction of *N*,*N*-dimethylaniline and an acetone derived enamine (Scheme 3-17b) or indole using anhydrous TBHP as an oxidant.[75c] Addition of BHT eroded yields of the Mannich adducts with enamine and indole to 18% and 0%, respectively. Furthermore, Klussmann found that BHT decelerated the oxidation of tetrahydroisoquinoline **1** at the conversion below 45% and suggested that the isolated Mannich adduct could arise from the CuBr-catalyzed oxidation by air rather than by TBHP.[75a]

Scheme 3-17. The CuBr catalyzed oxidative Mannich reaction of tetrahydroisoquinoline **1** and nitromethane with TBHP in the presence of radical scavenger **28**.

a)

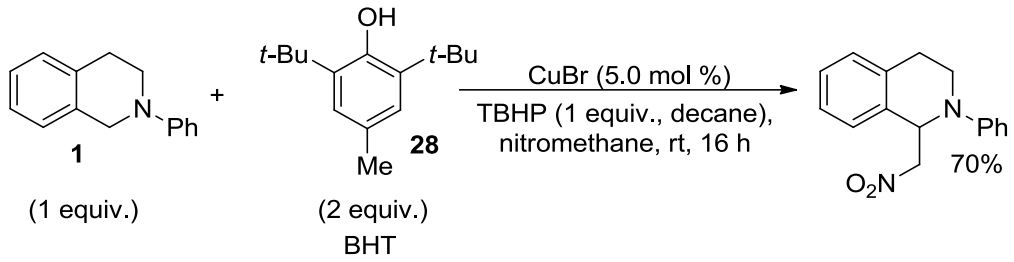

b)

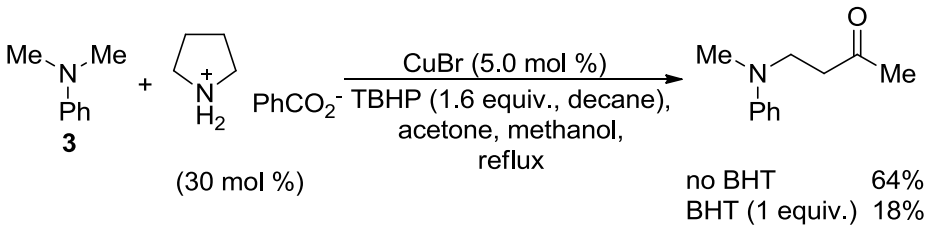

Additionally, Li invoked literature precedents to support two tentative non-radical mechanisms of the copper(I) halide catalyzed oxidative Mannich reaction with TBHP.[43] The first mechanism adopted the Murahashi mechanistic model proposed for the Ru-catalyzed oxidative Mannich reaction with TBHP.[92] According to this mechanistic model, the oxo-copper complex coordinates to the nitrogen atom of *N*,*N*-dialkylaniline and forms a copper bound intermediate **29** after the elimination of water in a five-membered transition state (Scheme 3-18a).[43] The formation of intermediate **29**, however, has no experimental evidence when TBHP was used as the oxidant. Likewise, the literature precedent of oxo-copper complex formation was reported for only H_2O_2 and O_2.[97] According to the second mechanism (Scheme 3-18b), the initial single-electron transfer (SET) to a copper complex is followed by a hydrogen atom abstraction by the *tert*-butoxy radical.[43] The precedented SET from *N*,*N*-dialkylaniline to a Cu(II) complex was reported for $(batho)_2Cu$ (batho = 2,9-dimethyl-4,7-diphenyl-1,10-

phenanthrolinedisulfonate) and the extrapolation of oxidative ability of this complex to CuBr and CuCl is questionable.[98]

Scheme 3-18. Two proposed mechanisms for the CuBr catalyzed oxidative Mannich reaction with TBHP as the oxidant.

a)

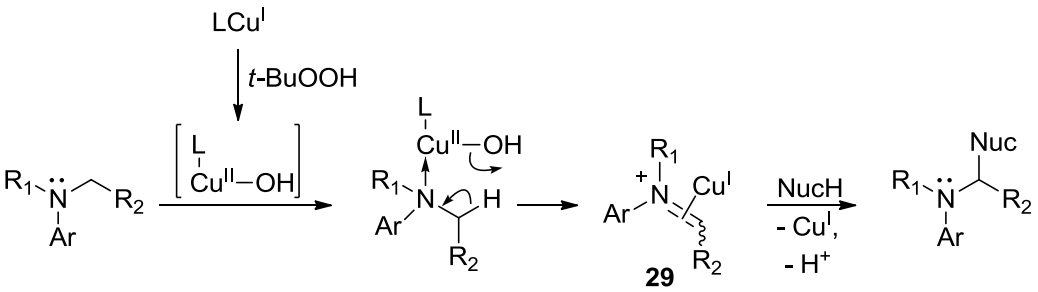

b)

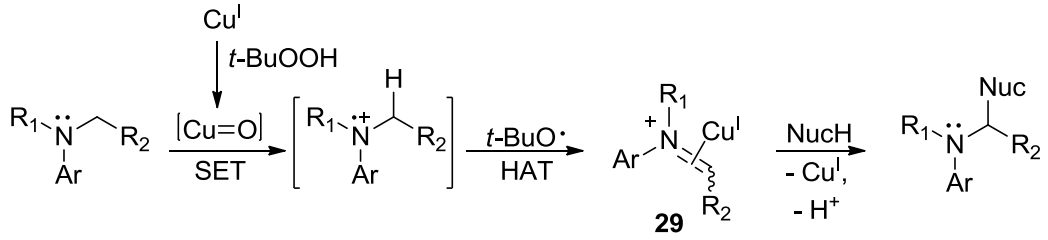

The mechanistic proposal of Li was recently adopted by Kumaraswami for the $FeCl_3$-catalyzed oxidative Mannich reaction of *N*,*N*-dialkylanilines with allyltributylstannane using T-HYDRO as an oxidant[76b] and by Schnuerch for the Cu-catalyzed oxidative functionalization of tetrahydroisoquinolines by TBHP.[76c] In the latter work, stoichiometric amounts of CuCl and $CuCl_2$ failed to oxidize the isoquinoline derivatives. Schnuerch used this result as an evidence to propose the necessity of Cu coordination with the nitrogen of isoquinoline (Scheme 3-19). According to the

mechanistic proposal by Schuerch, the oxidation of the complex **30** by TBHP affords intermediate **31** that eliminates water to yield copper-bound iminium ion followed by the release of catalytic Cu(II) species after the reaction with indole.

Scheme 3-19. The mechanism of CuBr oxidative Mannich reaction of isoquinoline and indole with TBHP.

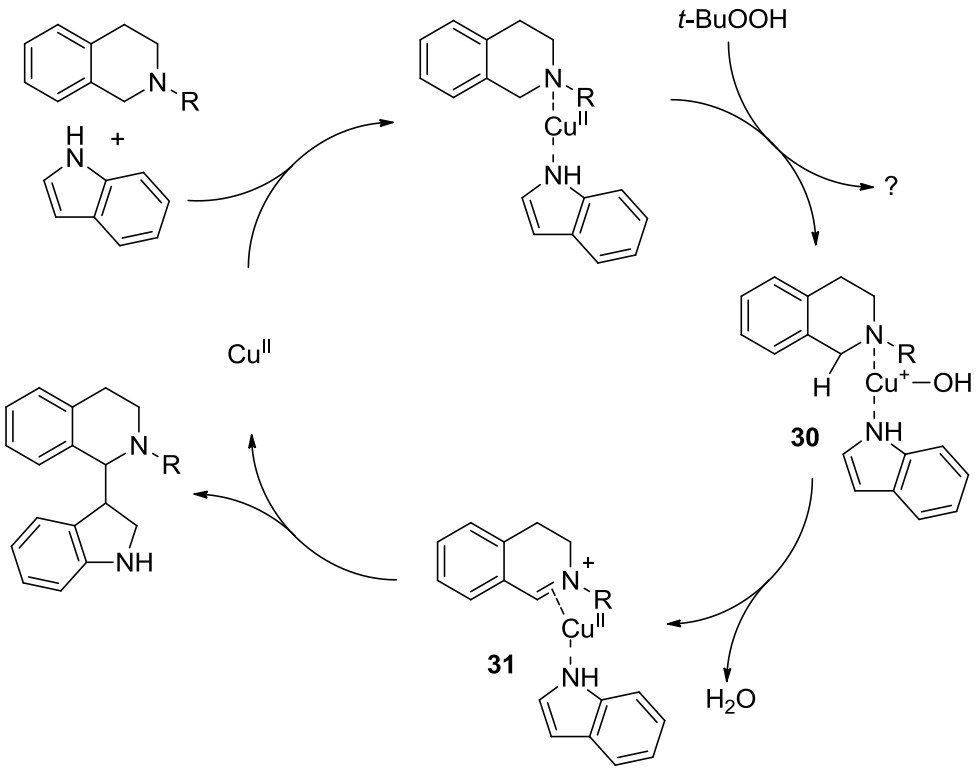

Detailed mechanistic studies of the Cu-catalyzed oxidative Mannich reaction by TBHP were conducted by Klussmann.[75a] Peroxy hemiaminal **32** was the only product of oxidation tetrehydroisoquinoline **1** by TBHP in the absence of other nucleophiles without solvent (Scheme 3-2a). The yield of peroxy hemiaminal **32** reached 65% with nitromethane, 55% with dimethylmalonate, and 70% with *N*-methylindole in the CuBr catalyzed oxidative Mannich reaction 30 to 60 minutes after the addition of TBHP. The respective Mannich adducts were formed in 35%, 30%, and 8% yields in the same

reaction mixture and at the same time. At the higher conversions of the reaction, however, peroxy hemiaminal **32** was almost completely consumed, while growth of the Mannich adducts had a sigmoidal shape. Thus, Klussmann suggested that peroxy hemiaminal **32** is the direct precursor of the Mannich adduct in the oxidative Mannich reaction with TBHP catalyzed by CuBr; and the term "iminium ion reservoir" was coined to describe the role of **32**. To verify this proposal, the peroxy hemiaminal **32** was isolated and its treatment with three equivalents of nitromethane overnight in decane afforded product in quantitative yield (Scheme 3-20b).

Scheme 3-20. Preparation of peroxy hemiaminal **35** and its reaction with nitromethane.

a)

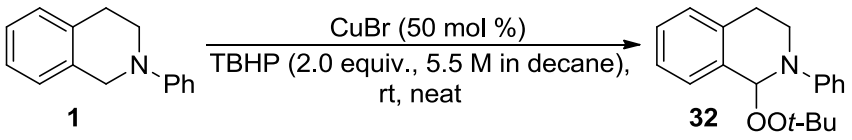

b)

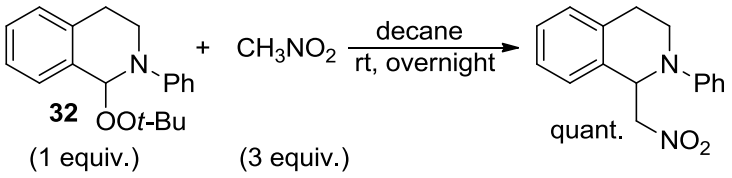

Klussmann adopted the mechanism for CuBr catalyzed oxidation of tetrahydroisoquinoline **1** by TBHP from the work of Minisci[99] and Doyle.[19] According to the Klussmann proposal, CuBr undergoes oxidation to CuBr(OH) and forms the *tert*-butoxy radical from TBHP (Scheme 3-21). The *tert*-butoxy radical subsequently reacts either with TBHP to afford the *tert*-butylperoxy radical or abstracts a hydrogen atom from the α-position of the tertiary amine according to the literature precedent.[100] Copper(II) bromohydroxide, on the other hand, undergoes a ligand exchange with TBHP to form **33** that, in turn, undergoes reaction with α-amino radical **34** to furnish peroxy

hemiaminal **32** and recycles the catalyst. The deceleration of the CuBr catalyzed oxidation of tetrahydroisoquinoline **1** by TBHP in presence of BHT (discussed above) supports the radical nature of the mechanism. A kinetic isotope effect measured for the 1-d_1-tetrahydroisoquinoline **1** oxidation was found to be 3.4, which is consistent with C-H bond cleavage in the rate-determining step. Klussmann suggested the generality of this mechanistic model of the oxidative Mannich reaction with TBHP for Rh, Cu, V, and Fe catalysts although no comparative studies of these metal complexes were conducted.

Scheme 3-21. Proposed mechanism for the CuBr catalyzed oxidation of tetrahydroisoquinoline by TBHP.

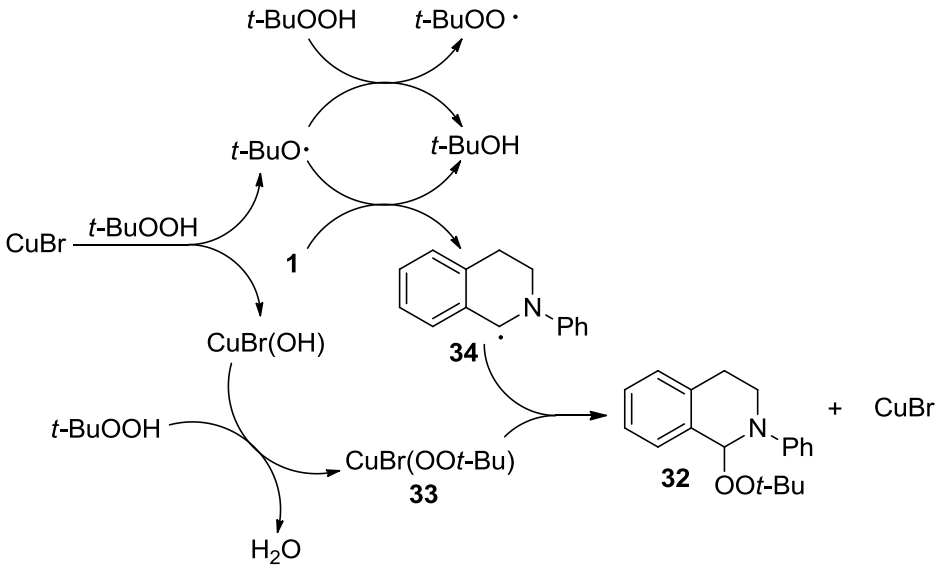

The reported data provide evidence for the formation of ruthenium oxo-complexes and several authors invoked the formation of transition metal oxo-complexes as general intermediates in *N*,*N*-dialkylaniline oxidations by TBHP catalyzed by the transition metal salts. Do the literature results indicate the formation of a novel dirhodium oxo-complex in the successful $Rh_2(cap)_4$ catalyzed oxidative Mannich reaction by

T-HYDRO? A positive answer to this question, however, contradicts the mechanistic investigations discussed in Chapter 1, that are consistent the role of $Rh_2(cap)_4$ in generating a flux of *tert*-butylperoxy radicals. Hence, I envisioned that the investigation of a detailed mechanism of the $Rh_2(cap)_4$ catalyzed oxidative Mannich reaction with TBHP and a comparative study of Rh, Ru, Cu, Fe, and Co complexes would be an important step for the advancement of the oxidative Mannich reaction and the design of new catalytic systems for this transformation.

Results and Discussion

Mechanistic Studies of the Transition Metal Salt Catalyzed Mannich Reaction with T-HYDRO

N,*N*-Dimethylanilines have higher oxidation potentials[101] than similar tetrahydroisoquinolines[102] (Scheme 3-22). Mechanistic details elaborated for less reactive substrates provide more certainty for generalization of mechanistic proposals to the entire scope of *N*,*N*-dialkylanilines. Consequently, *N*,*N*-dimethylanilines were model substrates of choice in a number of mechanistic investigations of the oxidative Mannich reaction.[39,74b,93a] *N*,*N*-dimethylanilines were selected for the mechanistic investigations of the $Rh_2(cap)_4$ catalyzed oxidative Mannich reaction with T-HYDRO because these results could be compared with the previous mechanistic models and could be extrapolated on more reactive tetraisoquinolines.

Scheme 3-22. Oxidation potentials of **1** and **3**.

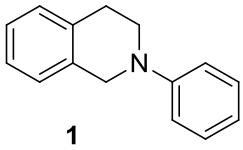

1

0.51 V vs. SCE

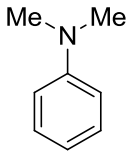

3

0.84 V vs. SCE

Investigations of the $Rh_2(cap)_4$ catalyzed oxidative Mannich reaction with T-HYDRO consists of two parts that resemble the general model of the oxidative Mannich reaction (Scheme 3-5). The first part will include the investigations of the *N*,*N*-dimethylaniline oxidation intermediates that lead to the Mannich adducts. An understanding of the role of methoxy hemiaminal **15** and peroxy hemiaminal **16** and criteria for their formation will be a basis for the second part that will include the mechanistic studies of the transformation of *N*,*N*-dimethylanilines to the corresponding iminium ions with T-HYDRO.

Conditions developed in our lab[32] were adopted for the oxidative Mannich reaction (1 mol % of $Rh_2(cap)_4$ as a catalyst, two equivalents of T-HYDRO in methanol at 60 °C, and biphenyl as an internal standard). The initial experiments were conducted using *N*,*N*-dimethylaniline as the substrate in the absence of an added nucleophile in methanol to obtain data on the rate of exchange between **15** and **16** (Scheme 3-23). Doyle reported the exclusive formation of **15** in the *N*,*N*-dimethylaniline oxidation by T-HYDRO in methanol and an equilibrium between **15** and **16**.[32]

Scheme 3-23. Dirhodium caprolactamate catalyzed *N*,*N*-dimethylaniline oxidation by T-HYDRO.

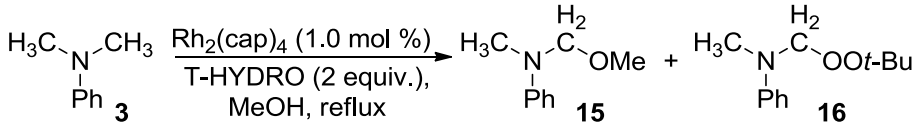

^{1}H NMR analysis was selected to monitor the kinetics of the $Rh_2(cap)_4$ catalyzed *N*,*N*-dimethylaniline oxidation by T-HYDRO because this method makes measurements with sufficient frequency for the measurement of detailed kinetics for this transformation. The preliminary experiments showed that boiling methanol created inhomogeneity in the NMR sample. Thus, the temperature of the reaction was decreased to room temperature which afforded 70% conversion after 30 minutes for the 1.0 M solution of *N*,*N*-dimethylaniline in methanol with 0.5 mole % of $Rh_2(cap)_4$ and two equivalents of T-HYDRO.

The oxidation of *N*,*N*-dimethylaniline by T-HYDRO in methanol catalyzed by $Rh_2(cap)_4$ furnished **15** [4.75 ppm (s, 2H), 3.10 ppm (s, 3H)] and **16** [5.15 ppm (s, 2H), 3.14 ppm (s, 3H)].[32] As was previously reported by Doyle,[32] **15** was formed as a major product after 5 minutes; and the ratio of **15** to **16** was 12.0 (Figure 3-1). The ratio of methanol and TBHP in this reaction mixture, on the other hand, was 12.4. Thus, nearly identical ratios of hemiaminal products and methanol to TBHP suggested that an iminium ion **35** preferentially reacted with the nucleophilic solvent, methanol (Scheme 3-24a). This conclusion is similar to the kinetic control postulated by Doyle for the $Rh_2(cap)_4$ catalyzed oxidative Mannich reaction with siloxyfurans.[32] The larger amount of **15** at the initial stages of *N*,*N*-dimethylaniline oxidation by TBHP eliminates the possibility of

reaction between the α-amino radical **36** and the *tert*-butylperoxy radical leading to **16** in the last step of the $Rh_2(cap)_4$ catalyzed *N*,*N*-dialkylaniline oxidation by T-HYDRO (Scheme 3-24b).

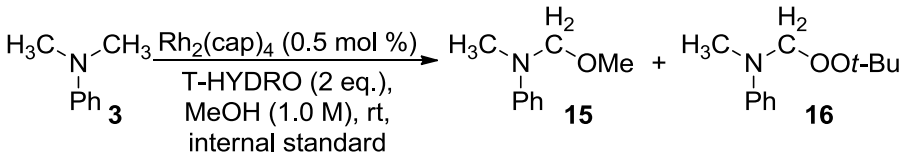

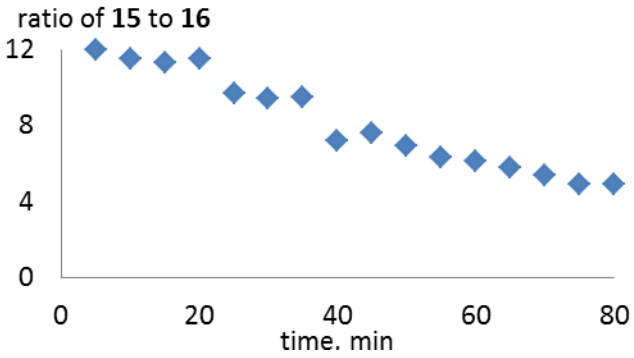

Figure 3-1. The change of **15** to **16** ratio with time in the oxidation of *N*,*N*-dimethylaniline by 2 equivalents of T-HYDRO catalyzed by 0.5 mole % of $Rh_2(cap)_4$.

Scheme 3-24. Mechanistic implications of the observed ratio of **15** to **16** at the initial stages of the $Rh_2(cap)_4$ catalyzed N,N-dimethylaniline oxidation by T-HYDRO.

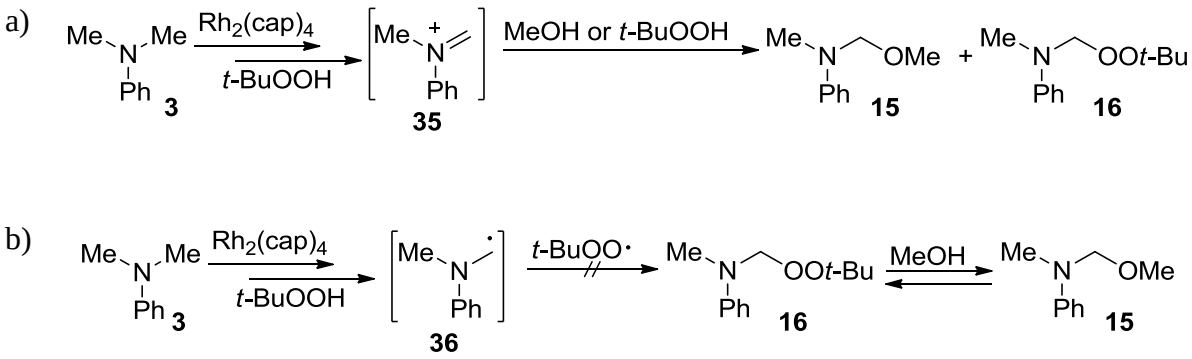

The ratio of **15** to **16** decreased from 12.0 to 4.9 over 80 minutes that the T-HYDRO oxidation of *N,N*-dimethylaniline was followed (Figure 3-1). A dynamic equilibrium of **15** and **16** favoring **16** could cause this exchange. To evaluate this hypothesis, peroxy hemiaminals **16** was prepared according to the reported procedure[32] and the kinetics of its conversion to **15** in methanol at 0.14 M concentration of **16** was monitored by ^{1}H NMR spectroscopy (Figure 3-2). Identical ratios of **15** and **16** measured after 8 and 24 h were used to calculate the equilibrium constant of 11.7 that favors **16** (Scheme 3-25). Thus, the less thermodynamically stable methoxy hemiaminal **15** is formed under kinetic control at the initial stage and serves a resting state for the iminium ion **35** that is an immediate result of oxidation of **3** (Scheme 3-24b).

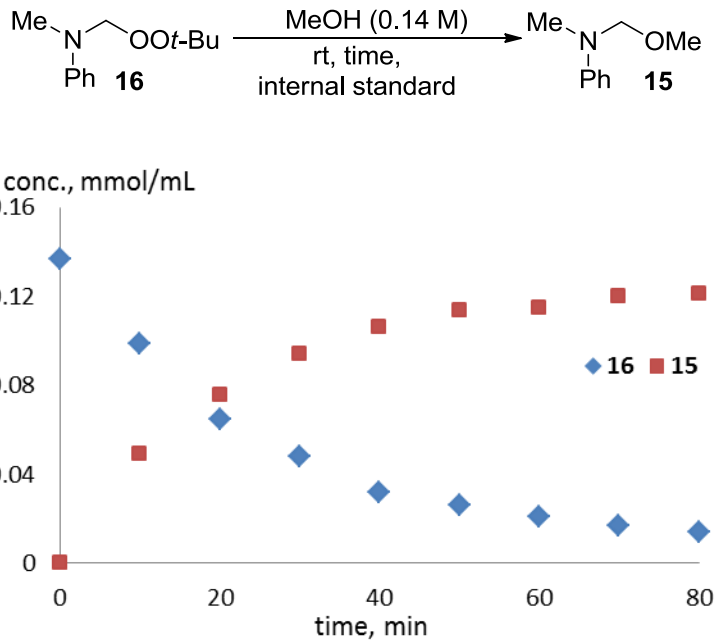

Figure 3-2. Equilibration of **16** to **15** in 0.14 M solution of methanol.

Scheme 3-25. The equilibrium of **15** and **16** in methanol.

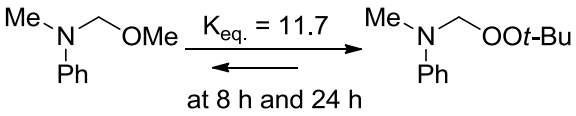

Determination of the reactive intermediates for the $Rh_2(cap)_4$ catalyzed *N*,*N*-dimethylaniline oxidation by T-HYDRO raised the question whether **15** and **16** are side products[32,43,72b,73] or iminium ion reservoirs.[75a] To distinguish two roles of **15** and **16**, the kinetic data were obtained for the $Rh_2(cap)_4$ catalyzed oxidative Mannich reaction in methanol by T-HYDRO of **3** and siloxyfuran **8** at 40 °C. In this study, 15% conversion based on siloxyfuran **8** was achieved in one hour. The mechanistic model of Li suggested that under these conditions **8** should outcompete the less nucleophilic methanol and TBHP to yield **37** without the formation of peroxy or methoxy hemiaminals. However, this hypothesis was not confirmed by experimental data of Li. The initial rate of

consumption of *N*,*N*-dimethylaniline was greater than the initial rate of siloxyfuran **8** consumption (Figure 3-3a). Furthermore, methoxy hemiaminal **15** was the major product at low conversion (Figure 3-3b). The accumulation of **15** in the reaction mixture at low conversion was followed by a decrease in its concentration. A noticeable rate of formation of **37** is evident only after the concentration of **15** reaches its maximum (Figure 3-3b). Interestingly, the concentration of **16** remained below the concentration of **37** indicating the preferential trapping by **8** of an iminium ion formed from **15**.

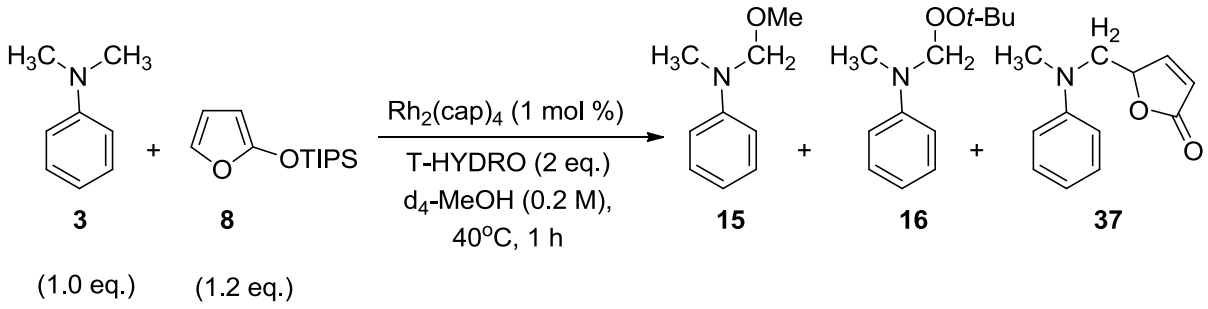

a) Rate of consumption of **3** and **8**. b) Rate of formation of **15**, **16**, and **37**.

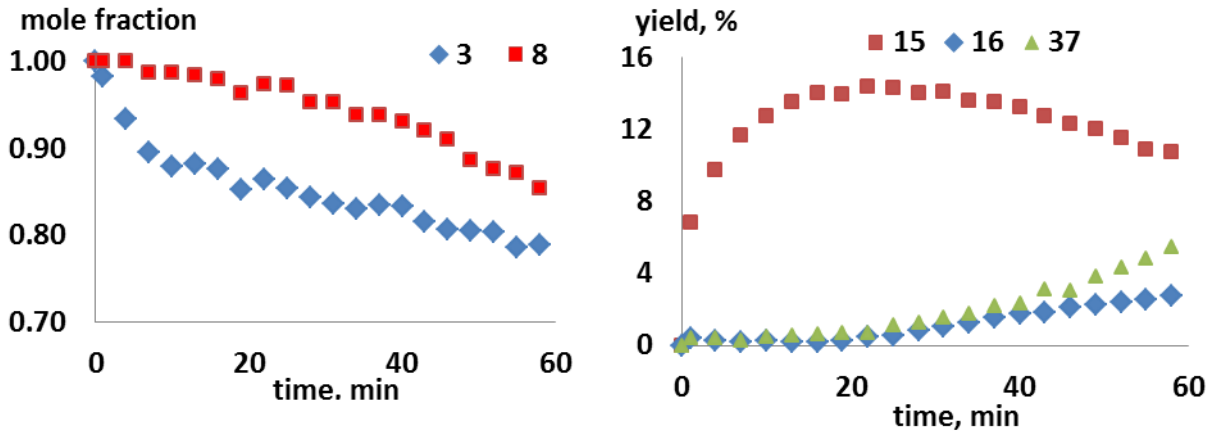

Figure 3-3. Kinetics of the $Rh_2(cap)_4$ catalyzed oxidative Mannich reaction in methanol by T-HYDRO of *N*,*N*-dimethylaniline and siloxyfuran **8.**

The role of **15** and **16** as intermediates was evaluated with an isotopic scrambling experiment. The $Rh_2(cap)_4$ catalyzed oxidative Mannich reaction of d_6-**5** and **8** was conducted in the presence of an excess of 37% aqueous solution of formaldehyde (Scheme 3-26). The isolated product lacked any deuterium labeling in methylene group that unequivocally showed **39** and **40** reached equilibrium faster than siloxyfuran **8** trapped an iminium ion (Scheme 3-27). In other words, this experiment demonstrated that the formation of the Mannich adduct of iminium ion and **8** was a thermodynamic sink for this transformation.

Scheme 3-26. Isotope scrambling experiment.

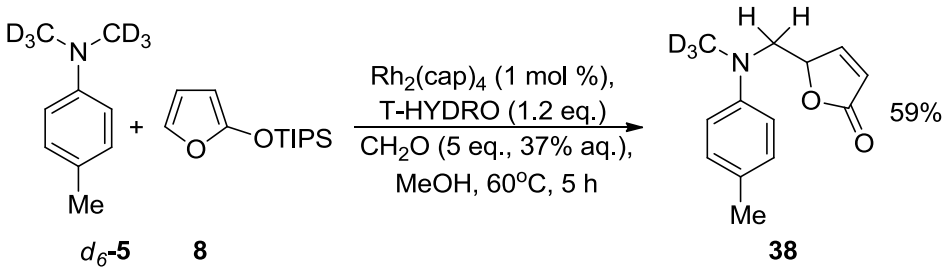

d_6-**5** **8** **38**

Scheme 3-27. Mechanism of the loss of deuterium labeling.

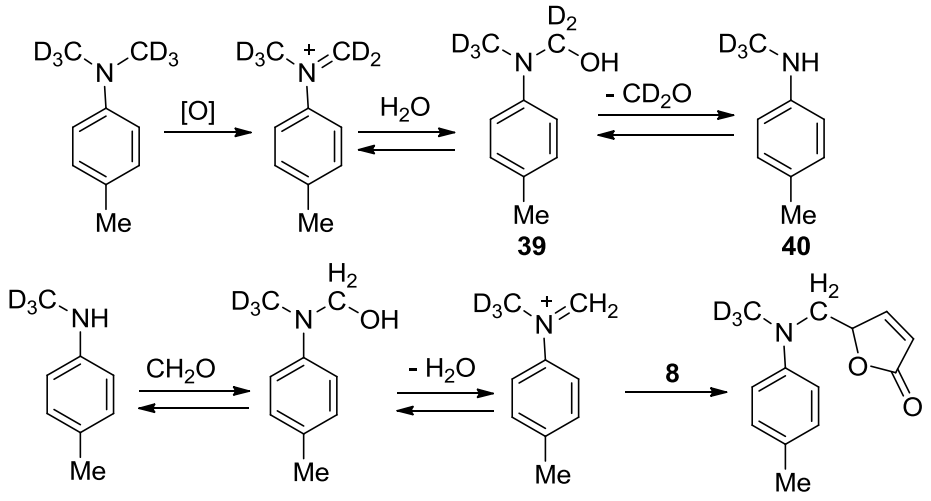

Having proposed a mechanistic model of the oxidative Mannich reaction with T-HYDRO in a nucleophilic solvent, the oxidative Mannich reaction by T-HYDRO in non-nucleophilic toluene was investigated. Che showed the viability of these conditions for the Ru-catalyzed oxidative Mannich reaction of *N*,*N*-dialkylanilines and indoles.[74b] According to the Che proposal, non-nucleophilic media should facilitate the capture of an iminium ion by indoles in the oxidation of *N*,*N*-dialkylanilines. The oxidative Mannich reaction of **3** and *N*-methylindole (**41**) using $Rh_2(cap)_4$ as a catalyst afforded intermediate **16** and **42** [4.78 ppm, s, 2H] preferentially over 20 minutes (Scheme 3-28). The continuation of this reaction for 3 hours quantitatively converted **16** and **42** into the final adduct **43** (Scheme 3-28). Thus, even in non-nucleophilic media hemiaminals are the precursors to the Mannich adducts.

Scheme 3-28. The $Rh_2(cap)_4$ catalyzed oxidative Mannich reaction of **3** and *N*-methylindole (**41**) in toluene.

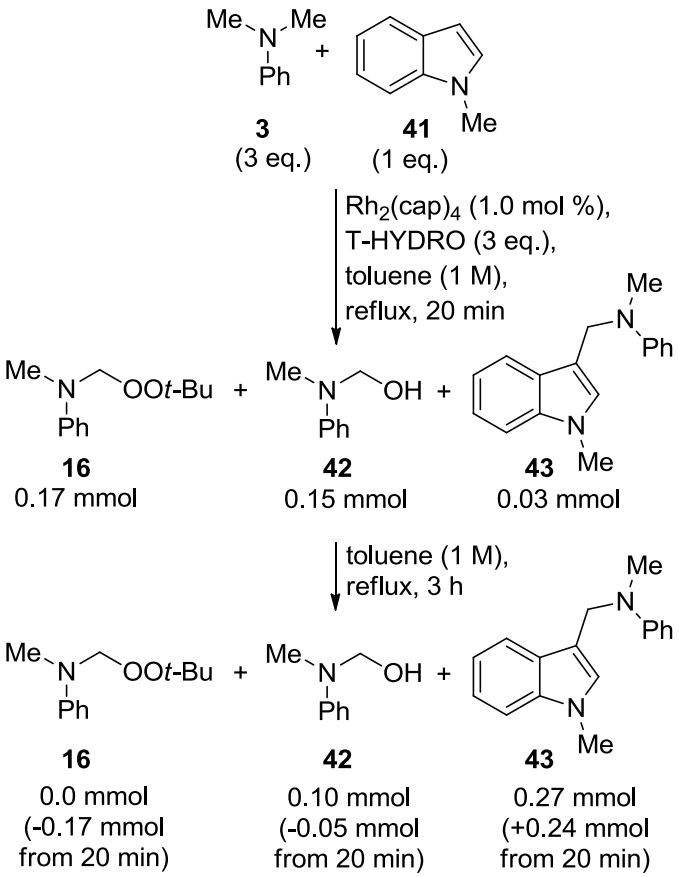

In summary, the transition metal salts catalyzed oxidation of *N*,*N*-dimethylanilines by T-HYDRO forms an iminium ion that is initially trapped by either nucleophilic solvent or TBHP. The resulting methoxy and peroxy hemiaminals exist in the equilibrium with an iminium ions that irreversibly form Mannich adducts with siloxyfurans or indoles (Scheme 3-29).

Scheme 3-29. Summary of conversion of an iminium ion formed in the oxidation of *N*,*N*-dialkylanilines to the final Mannich adduct.

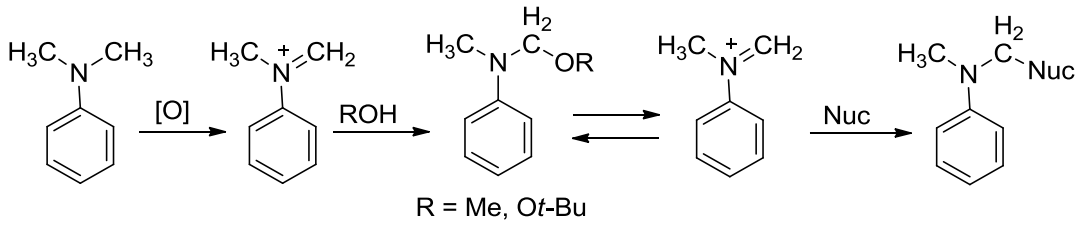

After proposing the mechanism of conversion of an iminium ion into a Mannich adduct consistent with experimental data, investigations of the mechanism of transition metal salts catalyzed *N*,*N*-dimethylaniline oxidation by T-HYDRO were begun. Previous studies suggested SET from *N*,*N*-dialkylaniline to ruthenium oxo-complex (Schemes 3-10 and 3-11b),[39,74b] hydrogen atom transfer (HAT) from the 1-position of 4-aryl-tetrahydroisoquinoline by the *tert*-butoxy radical (Scheme 3-21),[75a] and oxidation of copper atom followed elimination of water (Schemes 3-18a and 3-19).[43,76c] The work of Doyle,[1,19] on the other hand, suggested the only role of $Rh_2(cap)_4$ is in generation of a flux of the *tert*-butylperoxy radicals. Hence, the initial focus of mechanistic investigation was on determining whether the rate-determining step is electron-neutral (Schemes 3-30a-b) or generates electron deficient species (Scheme 3-30c). The ρ value of the Hammett analysis close to 0 would suggest HAT (Scheme 3-30a) or oxidation of a metal center by TBHP as the rate-determining step (Scheme 3-30b); positive ρ value would indicate elimination of water elimination as the rate-determining step (Scheme 3-30b); finally, negative ρ would be consistent with the SET step (Scheme 3-30c).[93a]

Scheme 3-30. Two potential rate-determining steps of the *N*,*N*-dimethylanilines oxidations by T-HYDRO.

a)

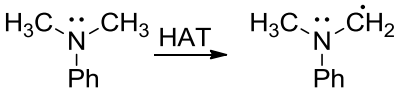

b)

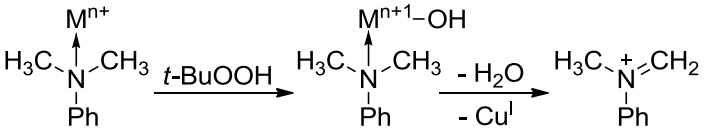

c)

The Hammett LFER analysis was conducted for a series of competition experiments of the $Rh_2(cap)_4$ catalyzed oxidations by T-HYDRO of 4-methoxy- (**17**), 4-methyl- (**5**), 4-fluoro- (**44**), 4-bromo- (**27**), 4-ethylcaboxylato- (**45**), 4-trifluoromethyl- (**46**), and 4-cyano-*N*,*N*-dimethylanilines (**47**) against **3**. The initial competition experiments were performed under the conditions used for monitoring of the oxidative Mannich reaction of **27** and **2** in methanol (0.5 mole % of $Rh_2(cap)_4$, 2 equivalent of T-HYDRO, 40 °C, methanol as a solvent). However, the concentrations of 4-substituted *N*,*N*-dimethylanilines were decreased from 1.0 M to 0.1 M because the oxidation of 1.0 M solution 4-methoxy-*N*,*N*-dimethylaniline in methanol reached over 50% conversion in just 10 minutes. The correlation of natural logarithms of the relative initial rates was higher with σ^+ Hammett parameters ($R^2 = 0.975$) than with σ_{para} Hammett parameters ($R^2 = 0.909$). The linear correlation from 4-methoxy- to 4-cyano- groups was observed that indicated no change in the nature of the rate-determining step for the studied range of 4-substituents (Figure 3-4). Additionally, the measured ρ value of -2.63 was consisted with SET in the rate-determining step.[39,93a,102]

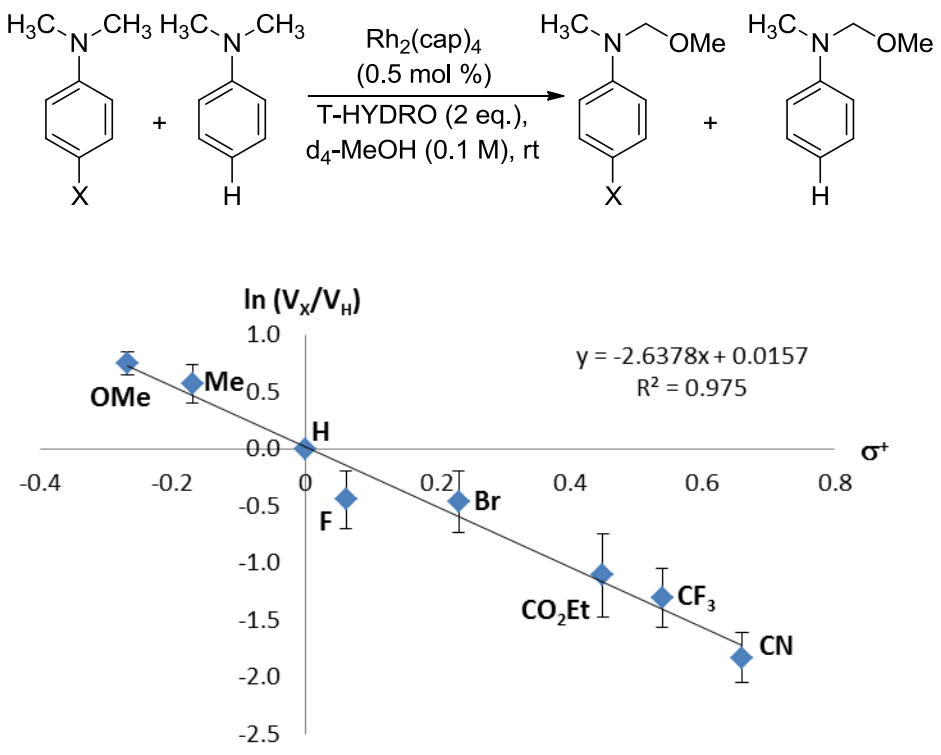

Figure 3-4. Hammett LFER analysis of the $Rh_2(cap)_4$ catalyzed oxidations by T-HYDRO of 4-substituted *N*,*N*-dimethylanilines at 40 °C in methanol. Each reaction rate was measured at least three times, and the error margins were calculated as a standard deviation of the reaction rates.

The Hammett analysis was consistent with the SET mechanism but did not provide information regarding the nature of the single electron acceptor. Higher oxidation potential of the *tert*-butylperoxy radical (0.52 V vs. SCE)[103] relative to the *tert*-butoxy radical (-0.30 V vs. SCE)[104] and $[Rh_2(cap)_4]^+$ (11 mV vs. SCE)[23a] suggests that the peroxy radical is a thermodynamically preferred oxidant (Scheme 3-31).

Scheme 3-31. The rate-determining step of the $Rh_2(cap)_4$ catalyzed *N*,*N*-dimethylaniline oxidation by T-HYDRO.

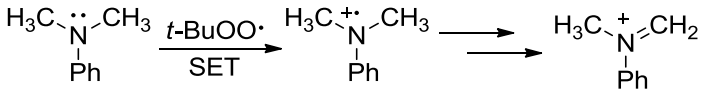

The nature of the C-H cleavage step was investigated by kinetic and product isotope effects (KIE and PIE, respectively). The kinetic isotope effects for $Rh_2(cap)_4$ catalyzed oxidation by T-HYDRO were determined from the deuteration level of adjacent to nitrogen methylene and methyl groups of corresponding methoxy hemiaminals in oxidation of 1:1 mixture of *N*,*N*-dimethylanilines and *N*,*N*-bis(trideuteromethyl)anilines (Scheme 3-32a). The product isotope effects were determined from the ratio of integration of peaks in ^{1}H NMR spectra that corresponded to methylene and methyl groups of methoxy hemiaminals in oxidation of *N*-methyl-*N*-(trideuteromethyl)anilines (Scheme 3-32b). Each measurement of KIE and PIE was repeated at least three times and the average value along with error margins are reported. The measured values of KIE and PIE values remained on the level of 1.61 ± 0.08 and 2.39 ± 0.24, respectively, from **5** to **27** (Figure 3-5). The KIE values start to increase for the **45** and approach PIE values for **47**.

Scheme 3-32. KIE and PIE experiments of the $Rh_2(cap)_4$ catalyzed oxidations of 4-substituted *N*,*N*-dimethylanilines by T-HYDRO.

a) Reaction used to determine kinetic isotope effect.

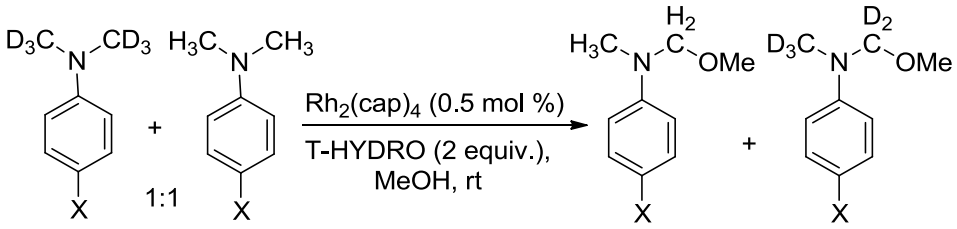

b) Reaction used to determine product isotope effect.

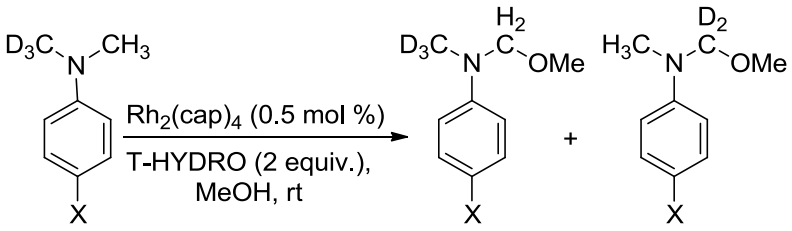

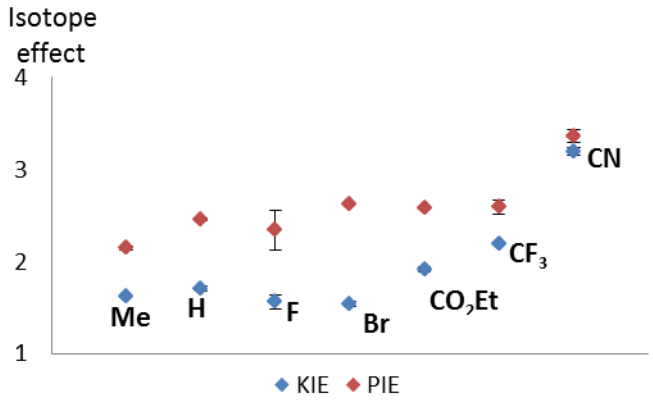

Figure 3-5. KIE and PIE measured for the $Rh_2(cap)_4$ catalyzed oxidative Mannich reaction by T-HYDRO. Each isotope effect measurement was repeated at least three times, and the error margins were calculated as a standard deviation of the measured isotope effects.

The characteristic gap between KIE and PIE values, previously reported by Watanabe[93a] for the enzymatic demethylations of *N*,*N*-dimethylanilines by cytochrome P450, was also observed for the $Rh_2(cap)_4$ catalyzed oxidations of 4-substituted *N*,*N*-dimethylanilines by T-HYDRO. According to the steady-state model of Watanabe,[93a] a rate determining forward SET forms a constant concentration of cation-radical that is consumed by competing backward SET and an irreversible C-H bond cleavage (Scheme 3-33a). The relationship between KIE and PIE was derived by Watanabe[93a] from this kinetic model and is presented in Scheme 3-33b. The PIE value depends only on the C-H bond cleavage step and is determined by the late transition state. On the other hand, KIE values also depend on the backward SET (k_{-SET}). Thus, KIE values approach 1.0 if the rate of backward SET is slower than the rate of the irreversible C-H cleavage ($k_{PIE} < k_{-SET}$). On the other hand, the higher rate of backward SET relative to the rate of the irreversible step ($k_{PIE} > k_{-SET}$) leads to higher KIE value. Oxidation of **47** is the limiting case of $k_{-SET} >> k_{PIE}$ where the KIE value (3.20) approached PIE value (3.26).

Scheme 3-33. Kinetic model of the $Rh_2(cap)_4$ catalyzed oxidations of 4-substituted *N*,*N*-dimethylanilines by T-HYDRO.

a)

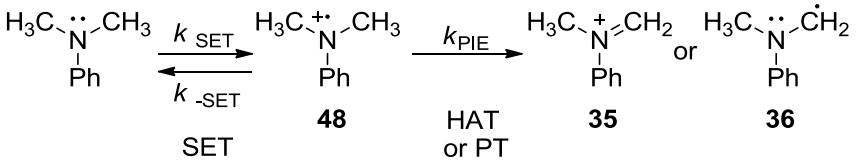

b)

$$\frac{k^H_{KIE}}{k^D_{KIE}} = \frac{k^H_{PIE}}{k^D_{PIE}} \times \frac{(k_{-SET} + k^D_{PIE})}{(k_{-SET} + k^H_{PIE})}$$

KIE and PIE values measured for the $Rh_2(cap)_4$ catalyzed oxidation of 4-substituted *N,N*-dimethylanilines by T-HYDRO were two independent experimental measurements that would allow to answer whether $RuCl_2(PPh_3)_3$, CuBr, $FeCl_3$, and $Co(OAc)_2$ form under the same conditions oxo-complexes that act as sole oxidant. *N,N*-Dimethylanilines **5** (σ^+ = -0.311), **3** (σ^+ = 0.00), and **27** (σ^+ = 0.150) were chosen to represent substrates of different electronic properties. The KIE and PIE values were determined in the same fashion as KIE and PIE of the $Rh_2(cap)_4$ catalyzed oxidations (Scheme 3-32). Thus, the measurements of KIE and PIE values for three different substrates would account for total of six independent measurements of transition metal salt catalyzed oxidation of *N,N*-dimethylanilines by T-HYDRO and would lead to a conclusion with a high degree of confidence.

The comparison of KIE (Table 3-2) and PIE (Table 3-3) shows the identical trends. The identical isotope effects in each Table are above the dotted line (Tables 3-2 and 3-3). The KIE and PIE numbers determined for oxidations of three *N,N*-dimethylanilines by T-HYDRO catalyzed by $Rh_2(cap)_4$ and $RuCl_3$ show identical values within experimental error that suggests the same operating mechanism for $RuCl_3$ as for $Rh_2(cap)_4$. Thus, the role of $Rh_2(cap)_4$ and $RuCl_3$ is to convert TBHP into *tert*-butylperoxy radicals. The copper(I) bromide catalyzed oxidation shows identical values as those determined for $Rh_2(cap)_4$ catalyzed oxidation of **3** and **5**, but not for **27** which shows slightly higher values. Iron(III) and cobalt(II) salts catalyzed oxidations have consistently higher KIE and PIE values than those measured for the $Rh_2(cap)_4$ catalyzed oxidation.

Table 3-2. Kinetic isotope effects of the $Rh_2(cap)_4$ catalyzed oxidations of 4-substituted *N*,*N*-dimethylanilines by T-HYDRO.

entry	catalyst	catalyst loading, %	KIE		
			4-Me (**5**)	4-H (**3**)	4-Br (**27**)
1	$Rh_2(cap)_4$	1.0	1.63 ± 0.03[a]	1.71 ± 0.08	1.54 ± 0.02
2	$RuCl_3$	1.0	1.69 ± 0.16	1.66 ± 0.18	1.55 ± 0.06
3	CuBr	5.0	1.58 ± 0.07	1.79 ± 0.01	1.71 ± 0.15
4	$FeCl_3$	2.0	1.91 ± 0.01	1.95 ± 0.02	1.67 ± 0.02
5	$Co(OAc)_2$	10.0	1.94 ± 0.03	2.42 ± 0.16	1.69 ± 0.02

[a] Error margins are calculated as a standard deviation of measured kinetic isotope effects.

Table 3-3. Product isotope effects of the $Rh_2(cap)_4$ catalyzed oxidations of 4-substituted *N*,*N*-dimethylanilines by T-HYDRO.

entry	catalyst	catalyst loading, %	PIE		
			4-Me (**5**)	4-H (**3**)	4-Br (**27**)
1	$Rh_2(cap)_4$	1.0	2.15 ± 0.02[a]	2.46 ± 0.22	2.63 ± 0.01
2	$RuCl_3$	1.0	2.20 ± 0.06	2.37 ± 0.06	2.55 ± 0.08
3	CuBr	5.0	2.21 ± 0.10	2.36 ± 0.04	3.04 ± 0.14
4	$FeCl_3$	2.0	2.46 ± 0.07	3.16 ± 0.20	2.62 ± 0.07
5	$Co(OAc)_2$	10.0	4.84 ± 0.16	4.42 ± 0.23	2.93 ± 0.12

[a] Error margins are calculated as a standard deviation of measured kinetic isotope effects.

The storage of methanol solutions opened to air of **5** and d_6-**5** in the presence of $Co(OAc)_2$ and **3** and d_6-**3** in the presence of $RuCl_3$ offered a clue to the explanation of the

observed deviations of KIE and PIE for CuBr, $FeCl_3$, and $Co(OAc)_2$ (Table 3-4, entries 6-7). *N*,*N*-Dimethylanilines underwent partial oxidation by dioxygen in air with 2.09 ± 0.11 and 3.36 ± 0.33 KIE values overnight at room temperature in the presence $RuCl_3$ and $Co(OAc)_2$, respectively. Noteworthy, the value measured for the $Co(OAc)_2$ catalyzed *N*,*N*-dimethylaniline oxidation by T-HYDRO was between the extreme KIE values of *tert*-butylperoxy radical oxidative pathway (entry 1) and the dioxygen oxidative pathway (entry 6). This fact indicated that the values measured for CuBr, $FeCl_3$, and $Co(OAc)_2$ catalyzed oxidations of 4-substituted *N*,*N*-dimethylanilines could be a combination of the competing *tert*-butylperoxy radical oxidative pathway and a dioxygen oxidative pathway. If this is the case, bubbling N_2 through the reaction mixture would decrease the contribution from the of dioxygen oxidative pathway by removal of dioxygen originating from air and from dimerization of the *tert*-butylperoxy radicals (Scheme 3-34). Indeed, N_2 flow decreased KIE values for Co-catalyzed oxidation of **3** to 2.17 ± 0.05 and CuBr catalyzed oxidation of **27** to 1.58 ± 0.06. Consequently, dioxygen interference was confirmed for the Cu(I), Fe(III), and Co(II) salts catalyzed oxidations of 4-substituted *N*,*N*-dimethylanilines by T-HYDRO. Furthermore, KIE value of 1.58 ± 0.06 is identical within an experimental error to the KIE values obtained for $Rh_2(cap)_4$ and $RuCl_3$ thus indicating the same operating mechanism for $Rh_2(cap)_4$, $RuCl_3$, and CuBr.

Table 3-4. Kinetic isotope effects of the $Rh_2(cap)_4$ catalyzed oxidations of 4-substituted *N*,*N*-dimethylanilines by T-HYDRO with and without N_2 flow and by O_2.

entry	catalyst	catalyst loading, %	oxidant	N_2 flow	KIE		
					Me	H	Br
1	$RuCl_3$	1.0	T-HYDRO	no	1.69 ± 0.16[a]	1.66 ± 0.18	1.55 ± 0.06
2	CuBr	5.0	T-HYDRO	no	1.58 ± 0.07	1.79 ± 0.01	1.71 ± 0.15
3	$Co(OAc)_2$	10.0	T-HYDRO	no	1.94 ± 0.03	2.42 ± 0.16	1.69 ± 0.02
4	CuBr	5.0	T-HYDRO	yes	nd[b]	nd	**1.58 ± 0.06**
5	$Co(OAc)_2$	10.0	T-HYDRO	yes	nd	**2.17 ± 0.05**	nd
6	$RuCl_3$	1.0	O_2	no	nd	2.09 ± 0.11	nd
7	$Co(OAc)_2$	10.0	O_2	no	3.36 ± 0.33	nd	nd

[a] Error margins are calculated as a standard deviation of measured kinetic isotope effects. [b] nd - not determined.

Scheme 3-34. Dimerization of the *tert*-butylperoxy radicals.

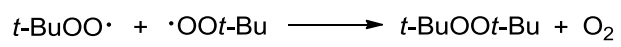

The two possible pathways for the irreversible C-H cleavage step include proton transfer (PT) forming an α-amino radical **36** (Scheme 3-35a) and HAT leading directly to the iminium ion **35** (Scheme 3-35b). Radical trap substituents were employed to test the possible formation of a transient α-amino radical. These substituents do not undergo ring opening in the presence of adjacent onium cations,[105] but they show high rates of intramolecular ring opening when they are adjacent to a carbon radical center (Scheme 3-36).[106]

Scheme 3-35. Possible mechanisms of the irreversible C-H cleavage in transition metal salt catalyzed oxidation of *N*,*N*-dimethylanilines.

a)

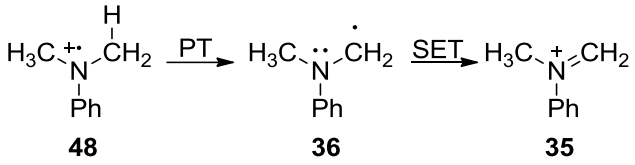

48 **36** **35**

b)

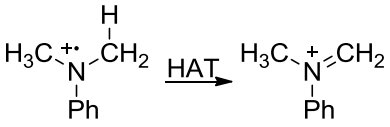

48 **35**

Scheme 3-36. Rate of cyclopropane opening rates of radical trap substituents.

a)

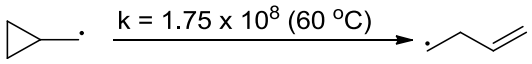

b)

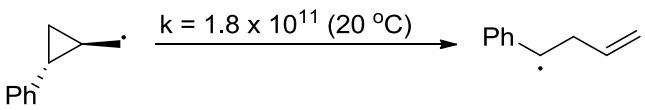

Compounds **50** was synthesized from aniline **49** and cyclopropyl aldehyde in 85% yield via reductive elimination according to the adopted procedure[107] (Scheme 3-37a). Aniline **52** was prepared by a 3-step synthesis in 62% overall yield from **51** (Scheme 3-37b).

Scheme 3-37. Synthesis of **50** and **52** for radical trap experiments.

a)

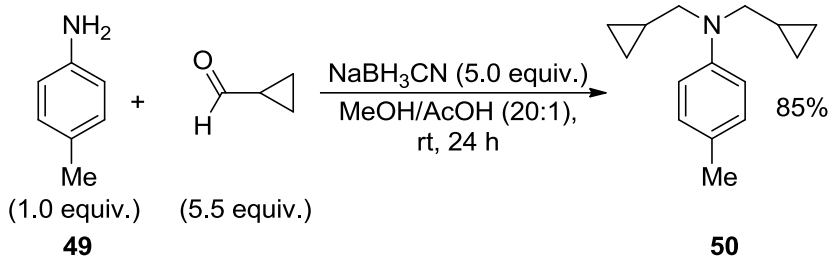

b)

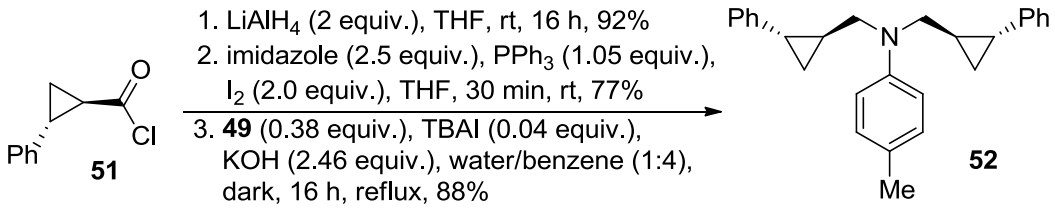

Conditions developed in our lab[32] for the oxidative Mannich reaction were chosen for the radical trap experiments (Scheme 3-38). The $Rh_2(cap)_4$ catalyzed oxidation by T-HYDRO of **50** formed methoxy hemiaminal in 65% yield without cyclopropane ring opening (Scheme 3-38a) that was seemingly consistent with the HAT step (Scheme 3-35b). However, the oxidation of **52** that had more sensitive radical trap substituent (Scheme 3-36b) led to decomposition of an aniline with the formation of unknown products with high molecular weight. *p*-Cymene was added as a hydrogen atom donor to minimize possible radical side reactions of the resulting benzyl radical (Scheme 3-36b). Indeed, the oxidation of **52** in 1:1 mixture of methanol and *p*-cymene furnished a number of aldehyde peaks according to the ^{1}H NMR spectrum of the reaction mixture. A free 4-phenylbutanal was trapped with 2,4-dinitrophenylhydrazine (**53**) and was isolated in 15% yield as **55** along 12 % of hydrazone **56**.

Scheme 3-38. The $Rh_2(cap)_4$ catalyzed oxidations by T-HYDRO of *N*,*N*-dialkylanilines bearing radical trap substituents.

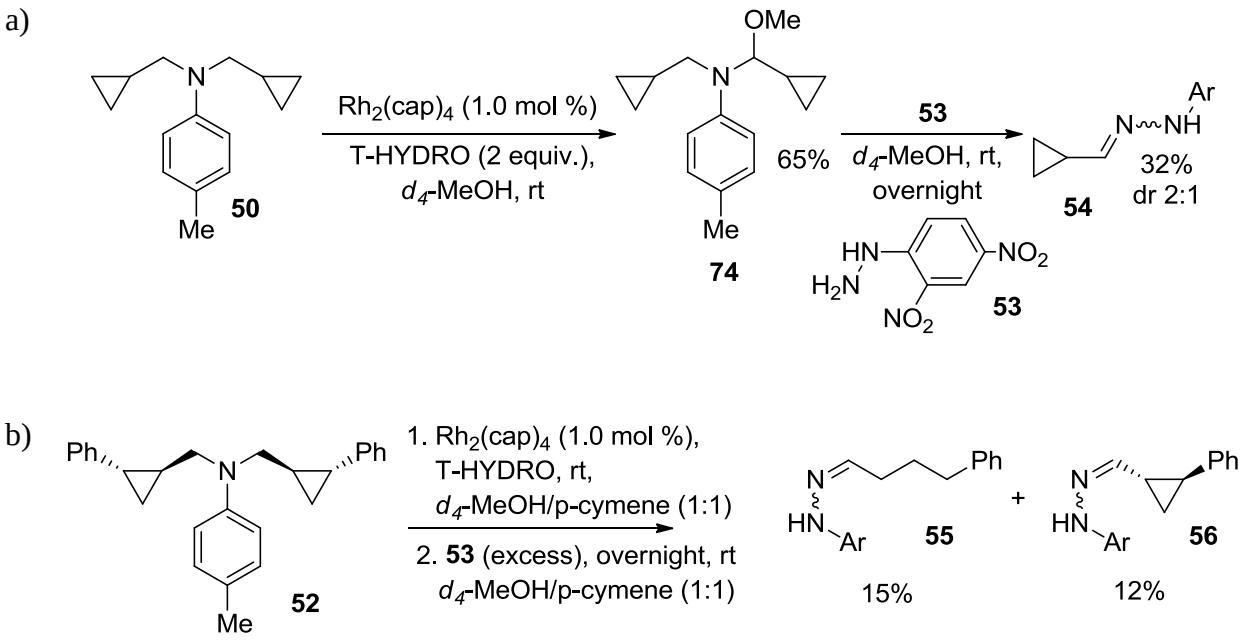

Opening of the cyclopropane ring is consistent with the formation of a transient α-amino radical (Scheme 3-35a) in the transition metal salts catalyzed *N*,*N*-dialkylaniline oxidation by T-HYDRO. Proton transfer should occur at the most acidic carbon of unsymmetrical *N*,*N*-dialkylaniline cation-radicals. According to report of Albini, Falvey, and Mariano,[108] the acidity of carbon adjacent to nitrogen decreases in order presented in Table 3-5. Thus, irreversible PT offers the first explanation of the observed regioselectivity of the oxidation of unsymmetrical *N*,*N*-dialkylanilines by T-HYDRO.[32] Steric factor may also play a role in regioselectivity because the oxidative Mannich reaction of *N*-methyl-*N*-ethylaniline (**7**) with siloxyfuran **8** occurs only at the *N*-methyl group (Scheme 3-6b) although the acidity ratio suggest 3:1 regioselectivity.

Table 3-5. Relative acidities of substituted carbon adjacent to nitrogen in *N*,*N*-dialkylaniline cation-radicals.[108]

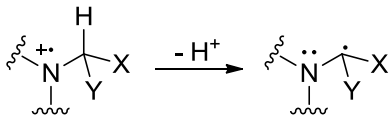

entry	X	Y	relative deprotonation rate
1	H	H	0.3
2	H	CH_3	0.1
3	CH_3	CH_3	0.05
4	H	Ph	1.0
5	H	$CHCH_2$	0.8
6	H	CCH	22

Oxidative Mannich Reaction by O_2 Catalyzed by $FeCl_3 \times 6\ H_2O$

The variable KIE and PIE values for CuBr, $FeCl_3 \times 6\ H_2O$, and $Co(OAc)_2$ catalyzed oxidation of *N*,*N*-dimethylanilines by T-HYDRO (Tables 3-2 and 3-3) suggested that *N*,*N*-dimethylanilines could be oxidized in methanol to corresponding methoxy hemiaminals by O_2. If so, CuBr, $FeCl_3$, and $Co(OAc)_2$ could catalyze in the oxidative Mannich reaction of *N*,*N*-dialkylanilines and siloxyfurna **8**. This protocol, if successful, would be very attractive due to the use of a commodity catalyst and an atom efficient oxidant.

4-Methyl-*N*,*N*-dimethylaniline (**5**) was chosen as the initial substrate. One atmosphere of O_2 was used instead of air to increase the partial pressure of dioxygen and

increase the rate of oxidation of **5**. The solvent, concentration, temperature, and the reaction time were kept the same as in the KIE experiments. Evaluation of CuBr, $FeCl_3 \times 6\ H_2O$, and $Co(OAc)_2$ catalyzed oxidations **5** by O_2 showed that ferric chloride afforded the highest yield of the corresponding methoxy hemiaminal **57** and the highest catalyst turnover rate (Table 3-6). Thus, $FeCl_3$ was chosen for the following oxidative Mannich reaction with dioxygen.

Table 3-6. Catalyst optimization of transition metal salt catalyzed oxidation of **5** by O_2.

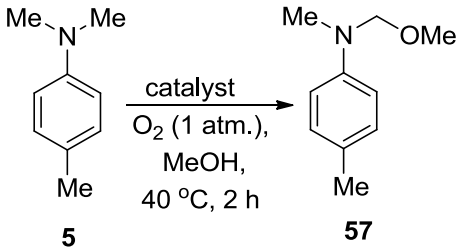

5 **57**

entry	catalyst	catalyst loading, mole %	conversion, %[a]	yield, %[b]
1	CuBr	5.0	75	32
2	$FeCl_3 \times 6\ H_2O$	2.0	71	50
3	$Co(OAc)_2$	10	61	42

[a] Determined by ^{1}H NMR spectroscopy from the ratio of peak (2.89 ppm, s, 6H) corresponding to **5** and biphenyl peak (7.60 ppm, d, J = 7.2 Hz, 4H) that was used as an internal standard. [b] Determined by ^{1}H NMR spectroscopy from the ratio of peaks [4.74 ppm (s, 2H) and 3.06 ppm (s, 3H)] corresponding to **57** and biphenyl peak (7.60 ppm, d, J = 7.2 Hz, 4H).

Siloxyfuran **8** was chosen due to the expertise of our research group in the oxidative Mannich reaction of *N*,*N*-dialkylanilines with this nucleophile.[32] The Mannich adduct **58** was isolated in 72% yield using one atmosphere of O_2 and 2.0 mole % of $FeCl_3$

(Scheme 3-39). The initial success prompted elaboration of the *N*,*N*-dialkylaniline scope of the ferric chloride oxidative Mannich reaction by O_2.

Scheme 3-39. The $FeCl_3 \times 6\ H_2O$ catalyzed oxidative Mannich reaction by O_2 of **5** and **8**.

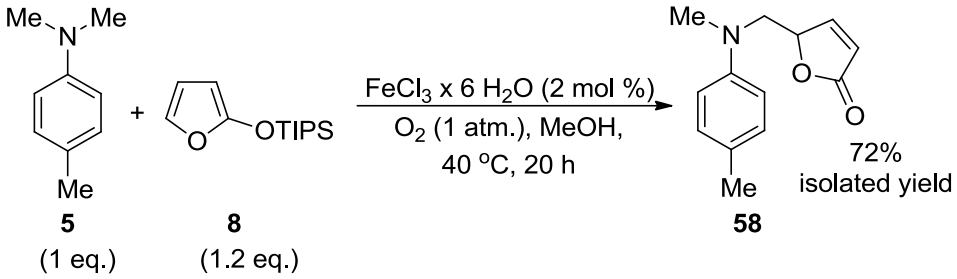

Optimization of $FeCl_3$ loading for the oxidative Mannich reaction of **5** and **8** in methanol showed that higher than 90% conversion could be achieved even with 2.0 mole % of catalyst, and the yield of Mannich adduct is about 65% for reactions catalyzed by both 2.0 and 5.0 mole % of $FeCl_3$ (Table 3-7, entries 1-2). However, further increase of $FeCl_3$ loading to 10 mole % led to a rapid $FeCl_3$ promoted methanolysis of siloxyfuran **8** that decreased the yield of Mannich adduct to 10% (entry 3). Reflux methanol decreased conversion of **58** to 60% (entry 4). Presumably, the concentration of O_2 was reduced in methanol at the boiling point, and these conditions also facilitated siloxyfuran **8** methanolysis leading to trace amounts of the Mannich adducts (entry 4). The use of air as the source of the oxidant formed the **58** in only 28% yield (entry 5). In ethanol the oxidative Mannich reaction of **5** and **8** catalyzed 2.0 mole % of $FeCl_3$ afforded 80% conversion and 75% yield (entry 6). The use of 5 mole % of $FeCl_3$ furnished only 5% yield of **58** because of rapid ethanolysis of the siloxyfuran **8** (entry 7). In summary, two complimentary protocols of were identified: first, 2.0 mole % of $FeCl_3$ in ethanol (method A) and 5.0 mol % of $FeCl_3$ in methanol (method B).

Table 3-7. Conditions optimization for the $FeCl_3$ catalyzed oxidative Mannich reaction by O_2 of 4-methyl-*N*,*N*-dimethylaniline and **2**.

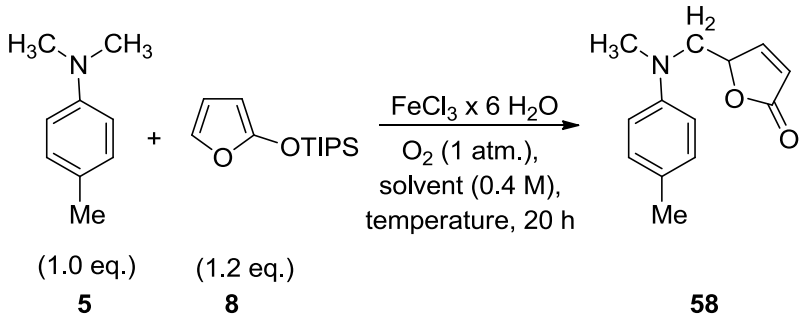

(1.0 eq.) **5** (1.2 eq.) **8** **58**

entry	catalyst loading, mole %	conditions	conversion[a]	yield[b]	adjusted yield[c]
1	2.0	—	92	65	70
2	**5.0**	—	**96**	**69**	**72**
3	10	—	94	10	10
4	2.0	reflux	60	3	5
5	2.0	air	76	28	36
6	**2.0**	**EtOH**	**80**	**75**	**94**
7	5.0	EtOH	100	5	5

[a] Determined by ^{1}H NMR spectroscopy from the ratio of peak (2.89 ppm, s, 6H) corresponding to **5** and biphenyl peak (7.60 ppm, d, J = 7.2 Hz, 4H) that was used as an internal standard. [b] Isolated yield after column chromatography on silica gel. [c] Yield calculated based on the amount of consumed **5**.

The scope of the oxidative Mannich reaction was examined with several *N*,*N*-dialkylanilines that afforded the butenolide products in 49-87% yield (Table 3-8). *N*,*N*-Dimethylanilines **3**, **5**, and **17** formed Mannich adducts in higher than 84% yield (entries 1-3). Electron deficient **44** afforded **61** in 66% yield (entry 4). The presence of two methyl groups in the ortho positions of the aromatic ring of **62** furnished butenolide

63 in 66% yield (entry 5). Unsymmetrical **7** underwent a selective reaction at the *N*-methyl group (entry 6). The oxidative Mannich reaction of tetrahydroisoquinoline **1** occurred at the 1-position and a 50% yield of **10** was isolated.

Table 3-8. The $FeCl_3$ catalyzed oxidative Mannich reaction by O_2 of *N*,*N*-dialkylanilines and **8**.

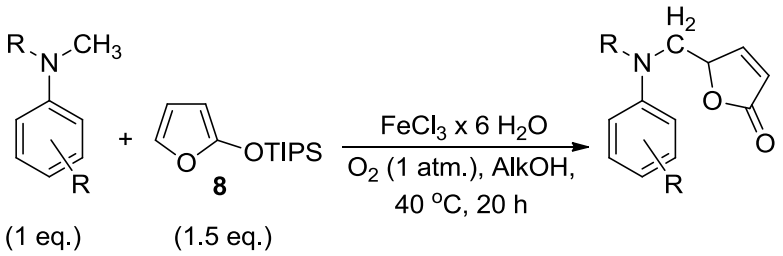

entry	N,N-dialkylaniline	method[a]	product	isolated yield[b]
1	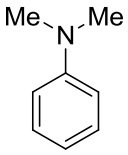 **3**	A	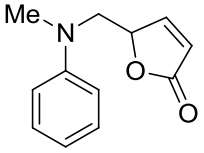 **59**	87
2	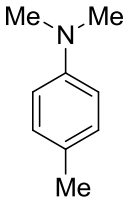 **5**	A	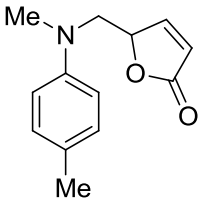 **58**	85
3	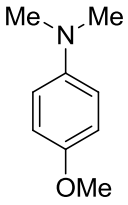 **17**	A	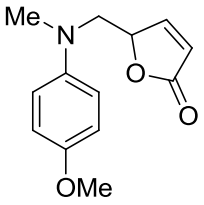 **60**	84

4	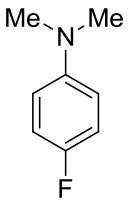 **44**	B	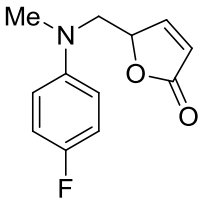 **61**	66
5	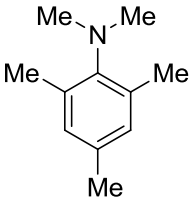 **62**	A	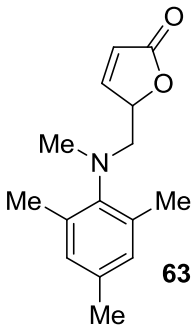 **63**	66
6	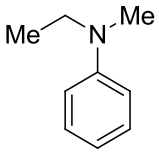 **7**	A	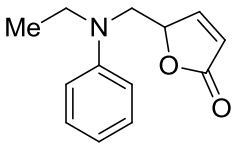 **9**	49
7	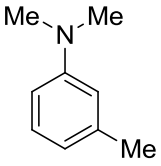 **64**	B	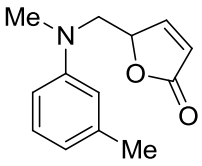 **65**	72
8	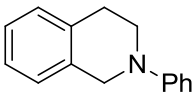 **1**	A	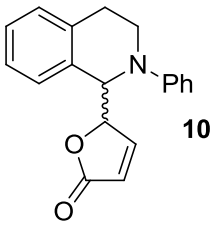 **10**	50[c]

[a] **Method A:** 2.0 mole % of $FeCl_3$ in ethanol. **Method B:** 5.0 mol % of $FeCl_3$ in methanol. [b] Isolated yields after column chromatography on silica gel. [c] Diastereomer ratio is 3:1.

Conclusion

In conclusion, the mechanistic models of Murahashi,[39] Che,[74b] Li,[43] and Klussmann[75a] of the transition metal salts catalyzed oxidative Mannich reaction of *N*,*N*-dialkylaniline with TBHP were evaluated, and a new mechanistic scheme was proposed (Scheme 3-1).

A combination of LFER analysis and the oxidation potentials of $[Rh_2(cap)_4]$ and the *tert*-butyl radical suggests that unlike Li[43] and Klussmann[75a] proposed *N*,*N*-dialkylanilines undergo SET to *tert*-butylperoxy radical in the rate determining step that is uniform between 4-methoxy- and 4-cyano-substituted *N*,*N*-dimethylanilines. The difference between KIE and PIE of *N*,*N*-dimethylaniline oxidations by THBP was first explained by the competition between backward SET and irreversible proton transfer after the rate-determining SET. The formation of a transient α-amino radical is consistent with the cyclopropane ring opening in the radical trap experiments. Unlike earlier models involving ruthenium[39,74b] and copper[43] oxo-complexes, the general role of $Rh_2(cap)_4$, $RuCl_3$, CuBr, $FeCl_3$, and $Co(OAc)_2$ in converting TBHP to the *tert*-butylperoxy radical is consistent with the identical within experimental error KIE and PIE values for oxidations of **5**, **3**, and **27** by T-HYDRO in methanol and the decrease of KIE and PIE values of CuBr and $Co(OAc)_2$ catalyzed oxidations with N_2 flow. The role of hemiaminals as precursors to Mannich adducts and not side-products[32] was determined by monitoring the initial stage of the $Rh_2(cap)_4$ catalyzed oxidative Mannich reaction of **3** and **8** in methanol and **3** and *N*-methylindole in toluene.

The interference of the dioxygen pathway in the copper, iron, and cobalt salts catalyzed oxidations of *N*,*N*-dimethylanilines by T-HYDRO was developed into a new catalytic system for the oxidative Mannich reaction with siloxyfuran **8**.

Experimental

General Information. All reactions were performed under atmospheric conditions unless the conditions are specified. ^{1}H NMR spectra were recorded on 400 MHz and 600 MHz spectrometers. Tetramethylsilane (TMS) (0.00 ppm) was used as an internal reference for all spectra. Data are reported as follows: chemical shift (in ppm, δ), integration, multiplicity (s = singlet, d = doublet, t = triplet, q = quartet, sept = septet, br = broad, m = multiplet, comp = composite), and coupling constants (in Hz). ^{13}C NMR spectra were recorded on a 125 MHz spectrometer operated with complete proton decoupling. Chemical shifts are reported in ppm using central peak of $CDCl_3$ as a reference (77.0 ppm). Thin layer chromatography was performed on silica gel coated glass plates (250 μm, F-254), and spots were visualized with either 254 nm ultraviolet light or $KMnO_4$ stain. Flash chromatography used silica gel (32-63 μm). High resolution mass spectra (HRMS) were acquired on a ESI-TOF spectrometer using CsI as a standard.

Dirhodium caprolactamate [$Rh_2(cap)_4$] was prepared by the method of Doyle.[67] *N*,*N*-Dimethylanilines **17**, **5**, **44**, **3,** d_6-**17**, d_6-**5**, d_6-**44**, and d_6-**3** were prepared by alkylation method adapted from the literature.[109] 4-Methoxy- (**66**), 4-methyl- (**67**), 4-fluoro- (**68**), 4-bromo- (**69**) and unsubstituted (**70**) derivatives of *N*-(trideuteromethyl)anilines and *N*-methyl-*N*-(trideuteromethyl)anilines were prepared

by the procdure adapted from the literature.[110] Siloxyfuran **8** was prepared according to the procedure of Martin.[111] Commercial cyclopropyl aldehyde and **51** were used as received.

***N*-(Methoxymethyl)-*N*-methylaniline (15).** *N*,*N*-dimethylaniline (1.2 mmol, 145 mg), $Rh_2(cap)_4$ (4 μmol, 2.9 mg), and methanol (2.0 mL) were placed in a 25-mL round-bottomed flask. The mixture was heated to reflux and T-HYDRO (0.72 mmol, 0.6 equiv., 100 μL) was added all once via syringe. The flask was equipped with a condenser and refluxed for 5 hours. The solvent was removed under reduced pressure, and the residual oil was purified by column chromatography [silica gel, AcOEt:hexanes (20:1)] to yield a light yellow oil of **15** (72 mg, 40%) that matched the reported ^{1}H NMR spectrum.[89]

***N*-[(*tert*-Butylperoxy)methyl]-*N*-methylaniline (16).** *N*,*N*-dimethylaniline (1.2 mmol, 145 mg), $Rh_2(cap)_4$ (4 μmol, 2.9 mg), and toluene (0.4 mL) were placed in a 4 dram screw-cap vial. The mixture was heated to 60 °C and 5 M TBHP solution in decane (2.4 mmol, 2 equiv., 0.48 mL) was added all once via syringe. The reaction was stirred for 1.5 hour at 60 °C, cooled, then the solvent removed under reduced pressure; and the residual oil was purified by column chromatography [silica gel, AcOEt:hexanes (20:1)] to yield a light yellow oil of **16** (108 mg, 43%) that matched the reported ^{1}H NMR spectrum.[39]

Kinetics of 3 Oxidation in Deuterated Methanol. *N*,*N*-dimethylaniline (0.5 mmol, 60 mg), $Rh_2(cap)_4$ (2.5 μmol, 1.8 mg), biphenyl (65 μmol, 10 mg) as an internal standard, and d_4-methanol (0.5 mL) were mixed in a 2 dram vial and sonicated until the

mixture became homogeneous. The solution was transferred into a NMR tube, and T-HYDRO (1.0 mmol, 2 equiv., 138 µL) was added all at once via syringe. The reaction mixture was shaken to ensure sample homogeneity, and the tube inserted into the probe of NMR spectrometer at room temperature. ^{1}H NMR spectra were obtained every 5 minutes for 80 minutes. The concentrations of **15** (4.75 ppm, s, 2H) and **16** (5.15 ppm, s, 2H) were calculated from the relative integration of the absorption of the internal standard (7.60 ppm, d, J = 7.2 Hz, 4H).

Kinetics of Equilibration of 16 to 15 in Deuterated Methanol. Biphenyl (65 µmol, 10 mg) as an internal standard followed by peroxy hemiaminal **16** (0.10 mmol, 21 mg) were dissolved in d_4-methanol (0.50 mL) at room temperature in an NMR tube. The reaction mixture was shaken to ensure sample homogeneity and the tube was inserted into the probe of NMR spectrometer at room temperature. ^{1}H NMR spectra were obtained every 10 minutes for 80 minutes, then at 8 and 24 hours. The concentrations of **15** (4.75 ppm, s, 2H) and **16** (5.15 ppm, s, 2H) were calculated from the relative integration of the absorption of the internal standard (7.60 ppm, d, J = 7.2 Hz, 4H).

Oxidative Mannich Reaction of 3 and 41 in Toluene. *N*,*N*-Dimethylaniline (**3**) (0.60 mmol, 3 equiv., 73 mg), *N*-methylindole (**41**) (0.20 mmol, 26 mg), $Rh_2(cap)_4$ (2 µmol, 1.0 mole %, 1.5 mg), and toluene (1.0 mL) were added to a 5-mL round bottom flask at room temperature. T-HYDRO (0.6 mmol, 3 equiv., 83 µL) was added all at once via syringe at room temperature. The reaction mixture immediately became red, and $Rh_2(cap)_4$ completely dissolved. The flask was placed in an oil bath, equipped with a condenser, and the reaction mixture was refluxed for 6 hours. The reaction mixture was concentrated under reduced pressure. Product **43** was purified by column

chromatography [silica gel, AcOEt:hexanes (1:10), R_f = 0.31]. Fractions containing the product were combined, and the solvent was evaporated under reduced pressure. The colorless oil was dried under high vacuum for 20 minutes (0.09 Torr, room temperature) to yield **43** (41 mg, 82%) that matched the reported ^{1}H NMR spectrum.[75c]

Kinetic Studies of Oxidative Mannich Reaction of 3 and 41 in Toluene. *N*,*N*-Dimethylaniline (1.20 mmol, 3 equiv., 145 mg), *N*-methylindole (0.40 mmol, 52 mg), $Rh_2(cap)_4$ (4 μmol, 1.0 mole %, 2.9 mg), toluene (0.4 mL), and 4-nitro-1-bromobenzene as the internal standard (0.1 mmol, 20 mg) were mixed in a 5-mL round bottom flask at room temperature. T-HYDRO (1.2 mmol, 3 equiv., 166 μL) was added all at once via syringe at room temperature. The reaction mixture immediately became red, and $Rh_2(cap)_4$ completely dissolved. The flask was placed in an oil bath, equipped with a condenser, and the reaction mixture was refluxed. Small aliquots (about 100 μL) were taken from the organic layer of the reaction mixture after 20 minutes and 3 hours, diluted with $CDCl_3$, and their ^{1}H NMR spectra were acquired. The concentrations of **16** (5.15 ppm, s, 2H), **42** (4.76 ppm, s, 2H), **43** (4.67 ppm, s, 2H) were calculated from the relative integration of the absorption of the internal standard (8.10 ppm, d, J = 8.8 Hz, 2H).

Kinetic Studies of Oxidative Mannich Reaction of 3 and Siloxyfuran 8 in *d_4*-Methanol. *N*,*N*-dimethylaniline (0.10 mmol, 12 mg), siloxyfuran **8** (0.12 mmol, 1.2 equiv., 29 mg), biphenyl (33 μmol, 5 mg) as an internal standard, a 3.5 mg/mL solution of $Rh_2(cap)_4$ in *d_4*-methanol (1.0 μmol, 1.0 mole %, 0.20 mL), and *d_4*-methanol were mixed in a 1 dram screw-cap vial at room temperature. The solution was transferred to a NMR tube. T-HYDRO (0.12 mmol, 1.2 equiv., 16 μL) was added all at once via syringe, and the tube was shaken to ensure sample homogeneity and immediately inserted into the

probe of NMR spectrometer at room temperature. ^{1}H NMR spectra were obtained every 3 minutes for 66 minutes. The concentrations of *N*,*N*-dimethylaniline (2.87 ppm, s, 6H), siloxyfuran **8** (5.10, dd, *J* = 3.2, 1.0 Hz, 1H) were calculated from the relative integration of the absorption of the internal standard (7.60 ppm, d, *J* = 7.2 Hz, 4H). The integration values per proton for **15** (4.75 ppm, s, 2H; 3.04 ppm, s, 3H), **16** (5.15 ppm, s, 2H; 3.08 ppm, s, 2H), and the Mannich adduct **37** (5.35-5.30 ppm, m, 1H; 3.80 ppm, dd, *J* = 15.6, 4.6 Hz, 1H, 3.59 ppm, dd, *J* = 15.6, 4.9, 1H; 2.95, s 3H) were averaged for the respective peaks. The amounts of **15**, **16**, and the Mannich adduct **37** were calculated from the relative integration of the peak of the internal standard (7.60 ppm, d, *J* = 7.2 Hz, 4H) using these averaged values.

Deuterium Scrambling in the formation of 38. T-HYDRO (0.65 mmol, 1.2 equiv.) was added all at once to a stirring solution of 4-methyl-*N*,*N*-di(trideuteromethyl)aniline (0.54 mmol), siloxyfuran **8** (0.54 mmol), 37% aqueous solution of formaldehyde (2.72 mmol, 5.0 equiv.) and $Rh_2(cap)_4$ (5.4 μmol, 1.0 mole %) in methanol (2.0 mL). The reaction mixture was refluxed for 5 hours. The solvent was removed under reduced pressure, and the crude oil was purified by column chromatography [silica gel, AcOEt:hexanes (1:5 to 1:1)] to yield a tan oil of **38** (66 mg, 59%) that was consistent with the reported characterization.[32] ^{1}H NMR (400 MHz, $CDCl_3$) δ 7.47 (dd, *J* = 5.8, 1.5 Hz, 2H), 7.07 (d, *J* = 8.4 Hz, 2H), 6.64 (d, *J* = 8.8 Hz, 1H), 6.11 (d, *J* = 6.0 Hz, 1H), 5.24-5.27 (m, 1H), 3.65 (d, *J* = 6.0 Hz, 1.98H); ^{13}C NMR (100 MHz, $CDCl_3$) δ 172.7, 154.5, 146.2, 129.9, 126.7, 122.1, 112.6, 82.0, 55.3, 39.1, 20.2. Deuterium enrichment was calculated from the integration of a peak at 3.65 ppm (d, *J* = 6.0 Hz, 1.98H) against the ideal value of 2.00.

Preparation of 46. Methyl iodide (18.0 mmol, 3.0 equiv., 2.56 g) was added in a single portion to a mixture of 4-(trifluoromethyl)aniline (6.0 mmol, 0.96 g) and K_2CO_3 (12.0 mmol, 2 equiv., 1.66 g) in acetone (20 mL). The mixture containing partially undissolved K_2CO_3 was stirred for 20 minutes at room temperature and then refluxed overnight. The reaction mixture was allowed to cool to room temperature, the solution was diluted by Et_2O (50 mL) and washed with water (50 mL), saturated $NaHCO_3$ (50 mL), and brine (50 mL). The solvent was evaporated, and the residue was purified by column chromatography [silica gel, AcOEt/hexanes (1:1), R_f = 0.20]. Fractions containing product were combined, and the solvent was removed under reduced pressure to yield **46** (580 mg, 51%) as a colorless liquid that matched the reported ^{1}H NMR spectrum.[112]

Preparation of *d_6*-27. The procedure is the same as that for **46** preparation except the use of 4-bromoaniline and trideuteromethyl iodide. R_f = 0.48 (EtOAc/hexane (1:1)); colorless solid; ^{1}H NMR (500 MHz, $CDCl_3$) δ 7.30 (d, *J* = 9.1 Hz, 2H), 6.58 (d, *J* = 9.0 Hz, 2H); ^{13}C NMR (126 MHz, $CDCl_3$) δ 149.5, 131.7, 114.0, 108.4; EI-HRMS: calculated for $C_8H_4D_6NBr$ (M+H) 206.04516, found 206.04632.

General Procedure for the Preparation of 17 and 44. A 50-mL round-bottomed flask was equipped with a magnetic stirring bar and a reflux condenser and was charged with 4-substituted aniline (5.0 mmol), tetra-*n*-butylammonium iodide (0.50 mmol, 10 mole %, 185 mg), potassium hydroxide (32.0 mmol, 6.4 equiv., 1.79 g), benzene (8.0 mL), and water (2.0 mL). The mixture was stirred for 10 minutes at room temperature, and methyl iodide (13 mmol, 2.6 equiv., 1.85 g) was added dropwise over 2 minutes. The reaction mixture containing organic and aqueous phases was stirred for 20 minutes at

room temperature and then refluxed for 24 hours. After cooling the reaction mixture to room temperature, the organic layer was taken up by Et_2O (100 mL), washed with water (20 mL), saturated Na_2CO_3 (20 mL), and brine (20 mL), and dried over anhydrous Na_2SO_4. The solution was concentrated, and the products were purified with column chromatography [silica gel, AcOEt:hexanes (1:10)]. Fractions containing product were combined, and the solvent was removed under reduced pressure. The ^{1}H NMR spectra of **17** [318 mg, 42% yield, R_f = 0.20 in AcOEt:hexanes (1:10)][113] and **44** [439 mg, 63% yield, R_f = 0.40 in AcOEt:hexanes (1:10)][114] matched the reported data.

General Procedure for Preparation of *d*$_6$-3, *d*$_6$-5, and *d*$_6$-44. The procedure is the same as that for **44** preparation except in the use of 4-methyl-, 4-fluoro- or unsubstituted anilines and trideuteromethyl iodide. The ^{1}H NMR spectra of *d*$_6$-**5** [423 mg, 60% yield, R_f = 0.42 in AcOEt:hexanes (1:10)] and *d*$_6$-**3** [440 mg, 69% yield, R_f = 0.48 in AcOEt:hexanes (1:10)] matched the reported data.[74b]

4-Fluoro-*N*,*N*-di(trideuteromethyl)aniline: 506 mg, 59% yield, R_f = 0.40 (EtOAc/hexane (1:1)); colorless liquid; ^{1}H NMR (500 MHz, $CDCl_3$) δ 7.07 – 6.84 (m, 1H), 6.81 – 6.46 (m, 1H); ^{13}C NMR (126 MHz, $CDCl_3$) δ 155.57 (d, *J* = 235.2 Hz), 147.53 (s), 115.35 (d, *J* = 22.0 Hz), 113.85 (d, *J* = 7.3 Hz), 40.44 (hept, *J* = 20.5 Hz); EI-HRMS: calculated for $C_8H_4D_6NF$ (M+H) 146.12522, found 146.12407.

General Procedure for the Preparation of 4-Methyl, 4-Fluoro, 4-Bromo and Unsubstituted *N*-(Trideuteromethyl)anilines. A 125-mL separatory funnel was charged with a saturated solution of Na_2CO_3 in water (8.0 mL), AcOEt (20.0 mL), and aniline (5.0 mmol). Isobutyl chloroformate (5.3 mmol, 1.06 equiv., 724 mg) was added portion-wise

over 20 minutes. Isobutyl chloroformate was shaken after the addition of each portion until the aniline was completely consumed according to TLC analysis. The organic layer was washed with water (20 mL) and brine (20 mL). The solvent was evaporated under reduced pressure to yield an oil that was dissolved in dry THF in 250-mL round-bottomed flask. The solution was cooled to 0 °C in an ice bath, and $LiAlD_4$ (10.0 mmol, 2 equiv., 420 mg) was added portion-wise to minimize gas evolution. The resulting suspension was purged with nitrogen and refluxed overnight. After allowing the reaction mixture to cool to room temperature, Et_2O (50 mL) was added, and the flask was placed in an ice bath. Excess $LiAlD_4$ was quenched with aqueous saturated Na_2SO_4. The resulting suspension was filtered through Celite, dried over anhydrous $MgSO_4$, and the solvent was evaporated under reduced pressure. The crude product was purified by flash chromatography on silica gel. The ^1H NMR spectra of 4-methyl-*N*-(trideuteromethyl)aniline (**67**) [87 mg, 14% yield, R_f = 0.26 in AcOEt:hexanes (1:10)] and *N*-(trideuteromethyl)aniline (**70**) [411 mg, 75% yield, R_f = 0.42 in AcOEt:hexanes (1:10)] matched the reported data.[110]

4-Fluoro-*N*-(trideuteromethyl)aniline (68): 621 mg, 97% yield, R_f = 0.33 (EtOAc/hexane (1:1)); pale yellow liquid; ^1H NMR (500 MHz, $CDCl_3$) δ 6.90 (t, *J* = 8.7 Hz, 1H), 6.61 – 6.43 (m, 1H); ^{13}C NMR (126 MHz, $CDCl_3$) δ 155.8 (d, *J* = 234.4 Hz), 145.7, 115.6 (d, *J* = 22.3 Hz), 113.1 (d, *J* = 7.4 Hz); EI-HRMS: calculated for $C_7H_5D_3NF$ (M+H) 129.09075, found 129.09047.

4-Bromo-*N*-(trideuteromethyl)aniline (69): 840 mg, 89% yield, R_f = 0.37 (EtOAx/hexane (1:1)); pale yellow liquid; ^1H NMR (500 MHz, $CDCl_3$) δ 7.25 (d, *J* = 8.6

Hz, 2H), 6.48 (d, J = 8.6 Hz, 2H), 3.70 (s, 1H); ^{13}C NMR (126 MHz, $CDCl_3$) δ 148.3, 131.8, 113.9, 108.7; EI-HRMS: calculated for $C_7H_5D_3NBr$ (M+H) 189.01069, found 189.00975.

General Procedure for Preparation of *d*$_3$-3, *d*$_3$-5, *d*$_3$-27,and *d*$_3$-44.[115] A solution of $ZnCl_2$ (2.00 mmol, 0.50 equiv., 272 mg) and $NaBH_3CN$ (2.40 mmol, 0.60 equiv., 151 mg) in methanol (20 mL) was added portion-wise to a stirring solution of 4-substituted aniline (4.0 mmol) and 37% aqueous solution of formaldehyde (7.4 mmol, 1.85 equiv., 0.30 mL) in methanol (20 mL). The reaction mixture was stirred at room temperature until there was no aniline remaining according to TLC analysis. The resulting solution was poured into a 250-mL separatory funnel containing a 2 M solution of NaOH (120 mL) and the aqueous layer was extracted with Et_2O (2 × 40 mL). The combined ethereal solutions were washed with brine (2 × 80 mL). The solution was concentrated under reduced pressure, and the residue was purified by flash chromatography on silica gel. The ^{1}H NMR spectra of *d*$_3$-**5** [436 mg, 79% yield, R_f = 0.42 in AcOEt:hexanes (1:10)],[74b] *d*$_3$-**27** [690 mg, 85% yield, R_f = 0.48 in AcOEt:hexanes (1:10)],[74b] and *d*$_3$-**3** [352 mg, 71% yield, R_f = 0.48 in AcOEt:hexanes (1:10)][110] matched the reported data.

4-Fluoro-*N*-methyl-*N*-(trideuteromethyl)aniline (*d*$_3$-44): R_f = 0.40 (EtOAc/hexane (1:1)); pale yellow liquid; ^{1}H NMR (500 MHz, $CDCl_3$) δ 6.94 (t, J = 8.8 Hz, 2H), 6.73 – 6.62 (comp, 2H), 2.89 (s, 3H); ^{13}C NMR (126 MHz, $CDCl_3$) δ 155.6 (d, J = 235.2 Hz), 147.5, 115.4 (d, J = 22.0 Hz), 113.9 (d, J = 7.4 Hz), 41.3; EI-HRMS: calculated for $C_8H_7D_3NF$ (M+H) 143.10641, found 143.10599.

General Procedure for Preparation of 4-Ethylcarboxylato (71), 4-Trifluoromethyl (72), and 4-Cyano- (73) derivatives of *N*-(Trideutero)methylanilines and *d*$_6$-45, *d*$_6$-46, and *d*$_6$-47. Trideuteromethyl iodide (3.2 mmol, 1.6 equiv., 464 mg) was added in a single portion to a mixture of 4-substituted aniline (2.0 mmol) and K_2CO_3 (4.0 mmol, 2.0 equiv., 552 mg) in acetone (7.0 mL). The mixture was stirred for 20 minutes at room temperature and refluxed overnight. The reaction mixture was allowed to cool to room temperature, and then the organic layer was taken by Et_2O (20 mL) and washed with water (15 mL), saturated $NaHCO_3$ (15 mL), and brine (15 mL). The solvent was evaporated, and mono- and di(trifluoromethylated) products were separated by column chromatography (silica gel, AcOEt/hexanes). Fractions containing product were combined, and the solvent was removed under reduced pressure. The ^{1}H NMR spectra of *d*$_6$-**45** [61 mg, 15% yield, R_f = 0.20 in AcOEt:hexanes (1:1)][116] and *d*$_6$-**47** [19 mg, 6% yield, R_f = 0.25 in AcOEt:hexanes (1:5)][110] matched the reported data.

4-Ethylcarboxylato-*N*-(trideuteromethyl)aniline (71): 118 mg, 33% yield, R_f = 0.06 (EtOAc/hexane (1:1)); colorless solid; ^{1}H NMR (500 MHz, $CDCl_3$) δ 7.89 (d, *J* = 8.8 Hz, 2H), 6.58 (d, *J* = 8.7 Hz, 2H), 4.55 (br s, 1H), 4.32 (q, *J* = 7.1 Hz, 2H), 1.36 (t, *J* = 7.1 Hz, 3H); ^{13}C NMR (126 MHz, $CDCl_3$) δ 166.9, 152.5, 131.4, 118.9, 111.3, 60.2, 14.4; EI-HRMS: calculated for $C_{10}H_{10}D_3O_2N$ (M+H) 183.12132, found 183.12165

4-Trifluoromethyl-*N*-(trideuteromethyl)aniline (72): 226 mg, 64% yield, R_f = 0.23 (EtOAc/hexane (1:1)); colorless solid; ^{1}H NMR (500 MHz, $CDCl_3$) δ 7.41 (d, *J* = 8.7 Hz, 1H), 6.59 (d, *J* = 8.7 Hz, 1H); ^{13}C NMR (126 MHz, $CDCl_3$) δ 151.6, 126.5 (q, *J* =

3.8 Hz), 125.0 (q, *J* = 270.2 Hz), 118.6 (q, *J* = 32.6 Hz), 111.4; EI-HRMS: calculated for $C_8H_5D_3NF_3$ (M+H) 179.08755, found 19.08599.

4-Cyano-*N*-(trideuteromethyl)aniline (73): 105 mg, 39% yield, R_f = 0.15 (EtOAc/hexane (1:5)); colorless solid; ^{1}H NMR (500 MHz, $CDCl_3$) δ 7.41 (d, *J* = 8.8 Hz, 2H), 6.56 (d, *J* = 8.8 Hz, 2H), 4.32 (s, 1H); ^{13}C NMR (126 MHz, $CDCl_3$) δ 152.2, 133.5, 120.6, 111.8, 98.2, 29.1 (hept, *J* = 20.8 Hz); EI-HRMS: calculated for $C_8H_5D_3N_2$ (M+H) 136.09542, found 136.09587.

4-Trifluoromethyl-*N*-di(trideuteromethyl)aniline (*d_6*-46): 48 mg, 12% yield, R_f = 0.46 (EtOAc/hexane (1:1)); colorless solid; ^{1}H NMR (500 MHz, $CDCl_3$) δ 7.45 (d, *J* = 8.5 Hz, 1H), 6.69 (d, *J* = 8.5 Hz, 1H); ^{13}C NMR (126 MHz, $CDCl_3$) δ 152.3, 126.3 (q, *J* = 3.8 Hz), 125.2 (q, *J* = 270.0 Hz), 117.4 (q, *J* = 32.6 Hz), 111.1, 39.2 (hept, *J* = 20.4 Hz); EI-HRMS: calculated for $C_9H_4D_6NF_3$ (M+H) 196.12202, found 196.12349.

General Procedure for Preparation of *d_3*-45, *d_3*-46, and *d_3*-47. Trideuteromethyl iodide (1.2 mmol, 1.2 equiv., 170 mg) was added in a single portion to a mixture of 4-substituted aniline (1.0 mmol) and K_2CO_3 (2.0 mmol, 2.0 equiv., 276 mg) in acetone (4.0 mL). The mixture containing partially undissolved $K_2CO_3$was stirred for 20 minutes at room temperature and then refluxed overnight. The reaction mixture was allowed to cool to room temperature, the organic layer was diluted by Et_2O (10 mL) and washed with water (8 mL), saturated $NaHCO_3$ (8 mL), and brine (8 mL). The solvent was evaporated, and mono- and di(trifluoromethylated) products were separated by column chromatography (silica gel, AcOEt/hexanes). Fractions containing product were combined, and the solvent was removed under reduced pressure.

4-Ethylcarboxylato-*N*-methyl-*N*-(trideuteromethyl)aniline: 207 mg, 88% yield R_f = 0.20 (EtOAc/hexane (1:1)); colorless solid; ^{1}H NMR (500 MHz, MeOD) δ 7.83 (d, *J* = 9.0 Hz, 2H), 6.69 (d, *J* = 9.0 Hz, 2H), 4.28 (q, *J* = 7.1 Hz, 2H), 3.02 (s, 3H), 1.35 (t, *J* = 7.1 Hz, 3H); ^{13}C NMR (126 MHz, MeOD) δ 167.5, 153.7, 130.7, 116.4, 110.4, 59.9, 38.6, 13.3; EI-HRMS: calculated for $C_{11}H_{12}D_3O_2N$ (M+H) 197.13692, found 197.13543.

4-Trifluoromethyl-*N*-methyl-*N*-(trideuteromethyl)aniline: 164 mg, 71% yield R_f = 0.46 (EtOAc/hexane (1:1)); colorless solid; ^{1}H NMR (500 MHz, MeOD) δ 7.42 (d, *J* = 8.9 Hz, 2H), 6.77 (d, *J* = 8.8 Hz, 2H), 3.00 (s, 3H); ^{13}C NMR (126 MHz, MeOD) δ 152.7, 125.7 (q, *J* = 3.7 Hz), 125.3 (q, *J* = 269.2 Hz), 116.8 (q, *J* = 32.5 Hz), 110.9, 38.7; EI-HRMS: calculated for $C_9H_7D_3NF_3$ (M+H) 193.10321, found 193.10232.

4-Cyano-*N*-methyl-*N*-(trideuteromethyl)aniline: 105 mg, 59% yield R_f = 0.25 (EtOAc/hexane (1:5)); colorless solid; ^{1}H NMR (500 MHz, MeOD) δ 7.47 (d, *J* = 9.1 Hz, 2H), 6.75 (d, *J* = 9.1 Hz, 2H), 3.03 (s, 3H); ^{13}C NMR (126 MHz, MeOD) δ 153.0, 132.9, 120.2, 111.2, 96.2, 38.4; EI-HRMS: calculated for $C_9H_7D_3N_2$ (M+H) 150.11108, found 150.11113.

General Procedure for Determining Initial Rates. *N*,*N*-Dimethylaniline (0.15 mmol, 18.0 mg), 4-substituted *N*,*N*-dimethylaniline (0.15 mmol), a 1.75 mg/mL solution of $Rh_2(cap)_4$ in *d*$_4$-methanol (1.5 μmol, 0.5 mole %, 0.60 mL), *d*$_4$-methanol (0.90 mL), and biphenyl as an internal standard (0.097 mmol, 15 mg) were mixed in a 2 dram vial at room temperature and the resulting solution was divided between 3 NMR tubes (0.55 mL of solution in each NMR tube). T-HYDRO (0.20 mmol, 2.0 equiv., 28 μL) was added all once via syringe at room temperature. The NMR tube was shaken to ensure homogeneity

of the solution and was then immediately inserted into the probe of NMR spectrometer. The ^{1}H NMR spectra were obtained every 66 seconds for 12.5 minutes and 136 seconds for 21.5 minutes (Table 3-9). The rate of oxidation was measured as the decrease of the integration value of absorptions corresponding to 4-substituted anilines with respect to the internal standard (7.60 ppm, d, J = 7.2 Hz, 4H).

Table 3-9. Monitored peak pairs ^{1}H NMR peaks for the reaction rate determination.

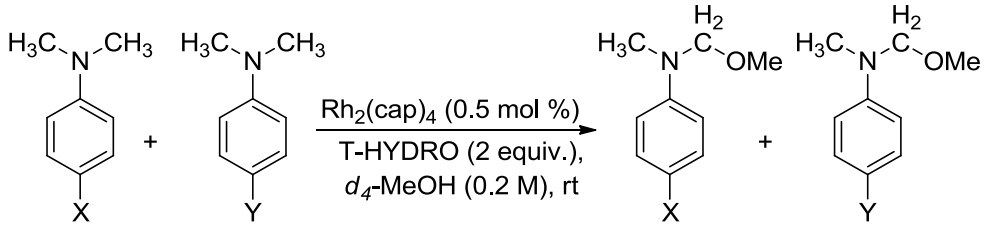

Entry	X	Y	Monitored peak pair, ppm	Reaction time, min	Sampling rate, sec/spectrum
1	OMe	H	2.81 (s, 6H) 2.90 (s, 6H)	12.5	66
2	Me	H	2.85 (s, 6H) 2.90 (s, 6H)	12.5	66
3	F	H	2.87 (s, 6H) 2.90 (s, 6H)	12.5	66
4	Br	H	6.65 (d, J = 8.8 Hz, 2H) 6.70 (t, J = 7.3 Hz, 1H)	12.5	66
5	CO_2Et	H	3.02 (s, 6H) 2.90 (s, 6H)	12.5	66
6	CF_3	H	3.01 (s, 6H) 2.90 (s, 6H)	21.5	136
7	CN	CF_3	3.01 (s, 6H) 3.03 (s, 6H)	21.5	136

General Procedure for Measuring Kinetic Isotope Effect of $Rh_2(cap)_4$ Catalyzed Oxidation of 4-substituted *N,N*-Dimethylaniline by T-HYDRO. 4-Substituted *N,N*-dimethylaniline (0.15 mmol), 4-substituted *N,N*-bis(trideuteromethyl)aniline (0.15 mmol), a 1.75 mg/mL solution of $Rh_2(cap)_4$ in d_4-methanol (0.5 µmol; 0.5 mole %, 0.60 mL), and d_4-methanol (0.90 mL) were mixed in a 2 dram vial at room temperature; and the resulting solution was divided between three 2 dram vials (0.55 mL of solution in each vial). T-HYDRO (20 µmol, 2.0 equiv., 3.0 µL) was added in each vial all at once via syringe at room temperature. The vials were shaken to ensure homogeneity of the solution and kept at room temperature (Table 3-10). The kinetic isotope effect ratio was determined as the ratio of average of two normalized to a single proton integrations of *N*-CH_3 and *N*-CH_2 absorptions of corresponding methoxy hemiaminals relative to normalized to a single proton integration of aromatic hydrogens at the 2- and 4-positions (Table 3-10).

Table 3-10. ^{1}H NMR peaks monitored for kinetic isotope effect.

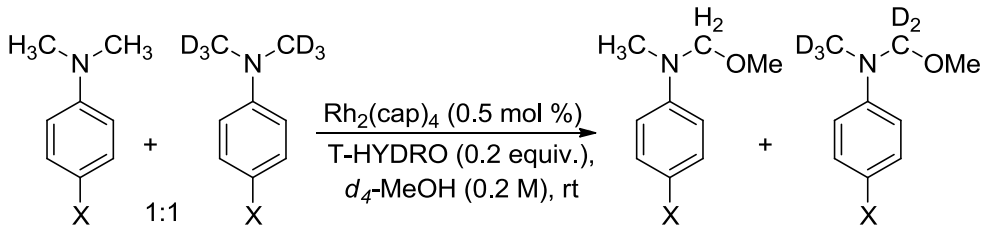

Entry	X	Monitored peaks, ppm	Reaction time, min
1	Me	3.06 (s, *N*-CH_3) 4.74 (s, *N*-CH_2) 6.82-6.77 (m, 2H)	15
2	H	3.09 (s, *N*-CH_3) 4.78 (s, *N*-CH_2) 6.89 (dd, *J* = 8.5, 3.5 Hz, 2H)	20
3	F	3.07 (s, *N*-CH_3) 4.74 (s, *N*-CH_2) 6.87 (dd, *J* = 9.1, 4.4 Hz, 2H)	30
4	Br	3.07 (s, *N*-CH_3) 4.74 (s, *N*-CH_2) 6.82-6.77 (m, 2H)	30
5	CO_2Et	3.16 (s, *N*-CH_3) 4.83 (s, *N*-CH_2) 6.95-6.88 (m, 2H)	60
6	CF_3	3.16 (s, *N*-CH_3) 4.83 (s, *N*-CH_2) 6.98 (dd, *J* = 8.7, 4.3 Hz, 2H)	60
7	CN	3.17 (s, *N*-CH_3) 4.83 (s, *N*-CH_2) 7.54 (d, *J* = 9.0 Hz, 2H)	60

General Procedure for Measuring Product Isotope Effects of $Rh_2(cap)_4$ Catalyzed Oxidations of 4-Substituted *N,N*-Dimethylaniline by T-HYDRO. 4-Substituted *N*-methyl-*N*-(trideuteromethyl)aniline (0.30 mmol), a 1.75 mg/mL solution of $Rh_2(cap)_4$ in d_4-methanol (0.5 μmol; 0.5 mole %, 0.60 mL), and d_4-methanol (0.90 mL) were mixed in a 2 dram vial at room temperature and the resulting solution was divided between three 2 dram vials (0.55 mL of solution in each vial). T-HYDRO (20 μmol, 2.0 equiv., 3.0 μL) was added in each vial all at once via syringe at room temperature. The vials were shaken to ensure homogeneity of the solution and kept at room temperature for the same time as in kinetic isotope effect measurements. The product isotope effect ratio was determined as a ratio of normalized to a single proton integration of *N*-CH_3 absorption relative to normalized to a single proton to a single proton integration of *N*-CH_2 peak of corresponding methoxy hemiaminals (Table 3-10).

General Procedure for Measuring Kinetic Isotope Effect of Transition Metal Salt Catalyzed Oxidation of 4-Substituted *N,N*-Dimethylaniline by T-HYDRO. The same procedure was used for measurements of the kinetic isotope effects of $RuCl_3$ (1.0 mole %), CuBr (5.0 mol %), $FeCl_3$ (2.0 mole %), $Co(OAc)_2$ (10 mol %) catalyzed oxidations of **3**, **5**, **27** by T-HYDRO as was used for $Rh_2(cap)_4$. The reaction mixtures were kept at room temperature for 1-2 hours. After copper, iron, and cobalt catalyzed reaction mixtures were concentrated under reduced pressure, and then filtered through a silica plug as a $CDCl_3$ solution to remove paramagnetic metal salts. The kinetic isotope effect was calculated as a ratio of normalized to a single proton integrations of *N*-CH_3 and *N*-CH_2 peaks of corresponding methoxy and *tert*-butylperoxy hemiaminals relative to

normalized to a single proton integration of aromatic hydrogens at the 2- and 4-positions (Table 3-11).

Table 3-11. ^{1}H NMR chemical shifts of methoxy and *tert*-butylperoxy hemiaminals.

Entry	X	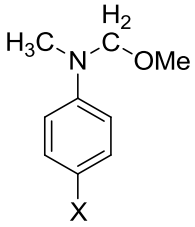	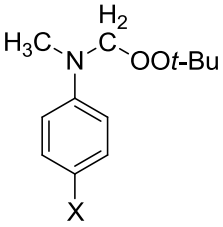
1	Me	3.06 (s, *N*-CH_3) 4.74 (s, *N*-CH_2) 6.82-6.77 (m, 2H)	3.13 (s, *N*-CH_3) 5.14 (s, *N*-CH_2) 6.80 (dd, *J* = 8.7, 2.4 Hz, 2H)
2	H	3.09 (s, *N*-CH_3) 4.78 (s, *N*-CH_2) 6.89 (dd, *J* = 8.5, 3.5 Hz, 2H)	3.16 (s, *N*-CH_3) 5.14 (s, *N*-CH_2) 6.89 (dd, *J* = 8.5, 3.5 Hz, 2H)
3	Br	3.07 (s, *N*-CH_3) 4.74 (s, *N*-CH_2) 6.87 (dd, *J* = 9.1, 4.4 Hz, 2H)	3.12 (s, *N*-CH_3) 5.12 (s, *N*-CH_2) 6.86-6.67 (m, 2H)

General Procedure for Measuring Product Isotope Effect of Transition Metal Salt Catalyzed *N,N*-Dimethylaniline Oxidation by T-HYDRO. The same procedure was used for measurements of the product isotope effects of $RuCl_3$ (1.0 mole %), CuBr (5.0 mol %), $FeCl_3$ (2.0 mole %), $Co(OAc)_2$ (10 mol %) catalyzed oxidations of **3**, **5**, **27** by T-HYDRO as was used for $Rh_2(cap)_4$. The reaction mixtures were kept at room temperature for 1-2 hours. After copper, iron, and cobalt catalyzed reaction mixtures were concentrated under reduced pressure, and then filtered through a silica plug as a

$CDCl_3$ solution to remove paramagnetic metal salts. The product isotope effects were calculated as a ratio of normalized to a single proton integration of *N*-CH_3 peak relative to normalized to a single proton integration of *N*-CH_2 peak of corresponding methoxy and *tert*-butylperoxy hemiaminals (Table 3-11).

Procedure for Measurement of Kinetic Isotope Effects for the Oxidations of 3 and 27 by T-HYDRO in Presence of Dinitrogen. 4-Substituted *N*,*N*-dimethylaniline (0.15 mmol), 4-substituted *N*,*N*-bis(trideuteromethyl)aniline (0.15 mmol), a solution of transition metal salt in methanol [0.60 mL; CuBr (5.0 mol %) or $Co(OAc)_2$ (10 mol %)] and methanol (0.90 mL) were mixed in a 2 dram vial at room temperature, and the resulting solution was divided between three 2 dram vials (0.55 mL of solution in each vial). Each vial was equipped with a septum, a needle open to the air and a balloon containing N_2 with a long needle going below the surface of the liquid. T-HYDRO (20 μmol, 2 equiv., 3.0 μL) was added in each vial all at once via syringe at room temperature, and the solutions were stirred at room temperature for 1 hour. Methanol (2 × 0.5 mL) was added after 25 and 50 minutes to replenish the evaporated solvent. The reaction mixtures were concentrated under reduced pressure and filtered through a silica plug as a $CDCl_3$ solution to remove paramagnetic metal salts. The kinetic isotope effect ratio was determined as a ratio of averaged normalized to a single proton integrations of *N*-CH_3 and *N*-CH_2 peaks of corresponding methoxy and *tert*-butylperoxy hemiaminals relative to normalized to a single proton integration of aromatic hydrogens at the 2- and 4-positions (Table 3-11).

Preparation of 50. Cyclopropyl aldehyde (2.75 mmol, 5.5 equiv., 193 mg) was added to a solution of *p*-toluidine (0.5 mmol, 54 mg) in methanol (5.0 mL) followed by

$NaBH_3CN$ (2.5 mmol, 5.0 equiv., 158 mg) and acetic acid (0.25 mL). The solution was kept overnight at room temperature under an atmosphere of N_2. A saturated solution of Na_2CO_3 (10 mL) was added to the reaction mixture, and the product was extracted with Et_2O (3 × 12 mL). The organic layer was dried, the solvent was evaporated under reduced pressure, and the residue was purified by flash chromatography on silica gel [EtOAc/hexane (1:10)] to yield the desire product as a colorless liquid (91 mg, 85% yield). R_f = 0.71 (EtOAc/hexane (1:10)); colorless liquid; ^{1}H NMR (500 MHz, $CDCl_3$) δ 7.03 (d, *J* = 8.6 Hz, 2H), 6.75 (d, *J* = 8.6 Hz, 2H), 3.23 (d, *J* = 6.1 Hz, 4H), 2.25 (s, 3H), 1.13 – 0.96 (m, 2H), 0.55 – 0.42 (m, 4H), 0.20 (q, *J* = 5.0 Hz, 4H); ^{13}C NMR (126 MHz, $CDCl_3$) δ 147.1, 129.6, 125.3, 113.3, 55.3, 20.2, 9.4, 3.8; EI-HRMS: calculated for $C_{15}H_{21}N$ (M+H) 216.17533, found 216.17533.

Preparation of 52. Lithium aluminium hydride (7.10 mmol, 2.0 equiv., 270 mg) was added over 10 minutes under N_2 to a dry solution of *trans*-2-Phenyl-1-cyclopropanecarbonyl chloride (**51**) (3.55 mmol, 640 mg) in THF (15 mL) in a 25-mL round-bottomed flask. The suspension was stirred overnight at room temperature, then poured into a 100-mL beaker containing water (35 mL). The resulting suspension was stirred at room temperature for 20 minutes. The organic material was extracted by DCM (3 × 75 mL). The extracts were combined, dried over anhydrous Na_2SO_4, and concentrated under reduced pressure to yield (2-phenylcyclopropyl)methanol (483 mg, 92% yield) that was used on the next step without purification.

Imidazole (5.0 mmol, 2.5 equiv., 340 mg), PPh_3 (2.1 mmol, 1.05 equiv., 550 mg), and iodine (4.0 mmol, 2 equiv., 1.02 g) were successively added to a solution of (2-phenylcyclopropyl)methanol (2.0 mmol, 296 mg) in THF (7.0 mL). The reaction

mixture was stirred for 30 minutes at room temperature, then aqueous saturated $Na_2S_2O_3$ (20 mL) was added. The resulting mixture was extracted with Et_2O (3 × 30 mL). The ethereal extracts were combined and washed with brine (20 mL). The solvent was removed under reduced pressure to yield [2-(iodomethyl)cyclopropyl] a light sensitive colorless liquid (91 mg, 77% yield): R_f = 0.43 (EtOAc/hexane (1:20)); cololess liquid;^{1}H NMR (500 MHz, $CDCl_3$) δ 7.26 (m, 2H), 7.17 (t, *J* = 7.9 Hz, 1H), 7.10 (d, *J* = 7.9 Hz, 2H), 3.36 (dd, *J* = 9.6, 7.5 Hz, 1H), 3.21 (t, *J* = 9.6 Hz, 1H), 1.95 – 1.83 (m, 1H), 1.68 – 1.57 (m, 1H), 1.29 (dd, *J* = 13.7, 5.5 Hz, 1H), 0.96 (dt, *J* = 10.6, 5.4 Hz, 1H); ^{13}C NMR (126 MHz, $CDCl_3$) δ 141.5, 128.4, 126.0, 125.9, 29.3, 27.1, 20.5, 12.2. EI-HRMS: calculated for $C_{10}H_{11}I$ (M+H) 258.99844, found 258.99866.

A 25-mL round-bottomed flask containing a magnetic stirring bar was charged with *p*-toluidine (0.63 mmol, 68 mg), [2-(iodomethyl)cyclopropyl]benzene (1.65 mmol, 2.6 equiv., 426 mg), tetra-*n*-butylammonium iodide (0.07 mmol, 0.1 equiv., 26 mg), potassium hydroxide (4.0 mmol, 6.4 equiv., 226 mg), water (0.3 mL), and benzene (1.2 mL). The flask was place in an oil bath, equipped with a condenser, and covered with aluminium foil. The reaction was refluxed for 20 hours, was allowed to cool to room temperature, and the residue was diluted by Et_2O (40 mL). The organic layer was washed with water (10 mL), saturated Na_2CO_3 (10 mL), and brine (10 mL). The solution was concentrated under reduced pressure, and the residue was purified by flash chromatography on silica gel to give a colorless oil (202 mg, 87% yield): R_f = 0.49 (EtOAc/hexane (1:10)); cololess liquid; ^{1}H NMR (500 MHz, $CDCl_3$) δ 7.22 (t, *J* = 7.5 Hz, 4H), 7.12 (t, *J* = 7.3 Hz, 2H), 7.03 (d, *J* = 8.3 Hz, 2H), 6.97 (d, *J* = 8.1 Hz, 4H), 6.76 (d, *J* = 8.3 Hz, 2H), 3.57 – 3.27 (comp, 4H), 2.25 (s, 3H), 1.87 – 1.73 (comp, 2H), 1.37

(dt, *J* = 14.4, 5.0 Hz, 2H), 1.03 – 0.82 (comp, 4H); ^{13}C NMR (126 MHz, $CDCl_3$) δ 142.8, 129.7, 128.3, 125.9, 125.7, 125.7, 125.4, 113.7, 54.8, 54.8, 22.5, 22.4, 21.9, 21.8, 20.2, 15.0; EI-HRMS: calculated for $C_{27}H_{29}N$ (M+H) 368.23797, found 368.23654.

Dirhodium Caprolactamate Oxidation of 50 by T-HYDRO. A 2 dram vial was charged with **50** (0.10 mmol, 22 mg), a 3.4 mg/mL solution of $Rh_2(cap)_4$ in *d*$_4$-methanol (1.0 µmol, 1.0 mol %, 0.20 mL), biphenyl (5 mg, 32.5 µmol) as the internal standard, and *d*$_4$-methanol (0.30 mL). The solution was stirred, and T-HYDRO (0.20 mmol, 2.0 equiv., 28 µL) was added all at once. After 40 minutes the reaction mixture was transferred into a NMR tube to assess the yield and conversion. A 65 % yield of **74** and 72% conversion of **50** was calculated from the integration of peaks corresponding to **50** (3.20 ppm, d, J = 6.2 Hz, 4H), **74** (4.18 ppm, d, *J* = 6.8 Hz, 1H), and an absorption at 8.84 ppm (d, *J* = 6.0 Hz, 1H) consistent with cyclopropyl aldehyde relative to the internal standard (7.60 ppm, d, *J* = 7.2 Hz, 4H). To assess the formation of cyclopropyl aldehyde, an excess 2,4-dinitrophenylhydrazine (1.0 mmol, 10.0 equiv., 198 mg) was added to the reaction mixture and the solution was kept at room temperature overnight. The hydrazone was isolated by column chromatography as a mixture of diastereoisomers (8 mg, 32% yield, dr 2:1).

Major diastereomer: R_f = 0.35 (EtOAc/hexane (1:5)); yellow oil; ^{1}H NMR (500 MHz, $CDCl_3$) δ 11.03 (s, 1H), 9.11 (d, *J* = 2.6 Hz, 1H), 8.29 (dd, *J* = 9.6, 2.6 Hz, 1H), 7.91 (d, *J* = 9.6 Hz, 1H), 7.08 (d, *J* = 7.6 Hz, 1H), 1.83 (qd, *J* = 7.9, 3.9 Hz, 1H), 1.07 (td, *J* = 7.0, 4.7 Hz, 3H), 0.88 – 0.81 (m, 4H).

Minor diastereomer: R_f = 0.35 (EtOAc/hexane (1:5)); yellow oil; ^{1}H NMR (500 MHz, $CDCl_3$) δ 11.53 (s, 1H), 9.14 (d, *J* = 2.6 Hz, 1H), 8.32 (dd, *J* = 9.6, 2.6 Hz, 1H), 7.92 (d, *J* = 9.6 Hz, 4H), 6.41 (d, *J* = 8.1 Hz, 1H), 1.79 – 1.70 (m, 2H), 1.20 (dt, *J* = 6.8, 4.6 Hz, 4H), 0.88 – 0.81 (m, 11H).

Mixture of diastereomers: ^{13}C NMR (126 MHz, $CDCl_3$) δ 155.5, 153.5, 145.4, 144.8, 137.6, 130.0, 129.9, 129.7, 128.6, 123.6, 123.5, 116.4, 29.7, 20.4, 13.9, 9.1, 7.4, 7.0; EI-HRMS: calculated for $C_{10}H_{10}O_4N_4$ (M+H) 251.07805, found 251.07823.

Dirhodium Caprolactamate Oxidation of 52 by T-HYDRO. A 2 dram vial was charged with **52** (0.10 mmol, 37 mg), a 3.4 mg/mL solution of $Rh_2(cap)_4$ in *d*$_4$-methanol (1.0 μmol, 1.0 mol %, 0.20 mL), *p*-cymene (0.30 mL), and *d*$_4$-methanol (0.10 mL). T-HYDRO (0.40 mmol, 4.0 equiv., 56 μL) was added all at once, and the solution was stirred for 1.5 hour at 40 °C. An excess of 2,4-dinitrophenylhydrazine (1.0 mmol, 10.0 equiv., 198 mg) was added to the reaction mixture and the solution was kept at room temperature overnight. The hydrazones **55** (yellow oil, 5 mg, 15% yield) and **56** (yellow oil, 4 mg, 12% yield) were isolated by preparative TLC.

55: R_f = 0.41 (EtOAc/hexane (1:5)); yellow oil; ^{1}H NMR (400 MHz, $CDCl_3$) δ 11.00 (s, 1H), 9.13 (d, *J* = 2.6 Hz, 1H), 8.30 (dd, *J* = 9.6, 2.6 Hz, 1H), 7.92 (d, *J* = 9.6 Hz, 1H), 7.51 (t, *J* = 5.2 Hz, 1H), 7.31 (t, *J* = 7.7 Hz, 2H), 7.22 (t, *J* = 7.7 Hz, 3H), 2.74 (t, *J* = 7.5 Hz, 2H), 2.47 (dd, *J* = 12.8, 7.5 Hz, 2H), 2.03 – 1.91 (m, 2H); ^{13}C NMR (126 MHz, $CDCl_3$) δ 169.7, 151.9, 145.1, 137.9, 130.0, 129.0, 128.5, 128.5, 126.2, 123.5, 116.5, 35.3, 32.0, 27.9; EI-HRMS: calculated for $C_{16}H_{16}O_4N_4$ (M+H) 329.12503, found 329.12269.

56: R_f = 0.48 (EtOAc/hexane (1:5)); yellow oil; ^{1}H NMR (400 MHz, $CDCl_3$) δ 11.00-10.85 (m, 1H), 9.17-9.09 (m, 1H), 8.33-8.29 (m, 1H), 7.37-7.16 (comp, 5H), 2.43-2.39 (m, 1H), 2.12-2.07 (m, 1H), 1.60-1.53 (comp, 2H); EI-HRMS: calculated for $C_{16}H_{16}O_4N_4$ (M+H) 329.12503, found 329.12319.

General Procedure for $FeCl_3$ catalyzed Oxidative Mannich Reaction in Ethanol. To a solution of *N*,*N*-dialkylaniline (0.5 mmol) and siloxyfuran **8** (0.25 mmol, 0.5 equiv, 60 mg) in ethanol (1.5 mL), $FeCl_3 \times 6\ H_2O$ (10 μmol, 2.0 mole %, 2.7 mg) was added at room temperature. The vial was equipped with a balloon containing only O_2 and the solution was stirred at 40 °C for 5 hours. The second portion of siloxyfuran **8** (0.50 mmol, 1 equiv., 120 mg) was added to the solution and the reaction mixture was stirred overnight at 40 °C under the atmosphere of O_2. The reaction mixture was concentrated under reduced pressure, and the product was isolated by column chromatography on silica gel.

General Procedure for $FeCl_3$ catalyzed Oxidative Mannich Reaction in Methanol. The same procedure as for the oxidation in ethanol except the use of $FeCl_3 \times 6\ H_2O$ (25 μmol, 5.0 mole %, 6.8 mg) as a catalyst and methanol as a solvent.

5-[[Mesityl(methyl)amino]methyl]furan-2(5*H*)-one (63): R_f = 0.38 (EtOAc/hexane (1:2)); colorless liquid; ^{1}H NMR (500 MHz, $CDCl_3$) δ 7.47 (dd, *J* = 5.7, 1.6 Hz, 1H), 6.84 (s, 1H), 6.82 (s, 1H), 6.12 (dd, *J* = 5.7, 1.9 Hz, 1H), 5.07 (tt, *J* = 6.1, 1.6 Hz, 1H), 3.40 (dd, *J* = 14.0, 6.1 Hz, 1H), 3.27 (dd, *J* = 14.0, 6.1 Hz, 1H), 2.82 (s, 3H), 2.28 (s, 3H), 2.23 (s, 6H); ^{13}C NMR (126 MHz, $CDCl_3$) δ 173.0, 155.4, 145.9, 136.5,

136.4, 135.1, 129.7, 129.6, 121.9, 83.7, 59.1, 42.0, 20.6, 18.8, 18.8; EI-HRMS: calculated for $C_{15}H_{19}O_2N$ (M+H) 246.14949, found 246.14853.

5-[[Methyl(3-methylphenyl)amino]methyl]furan-2(5*H*)-one (65): R_f = 0.29 (EtOAc/hexane (1:2)); colorless liquid; ^{1}H NMR (500 MHz, $CDCl_3$) δ 7.48 (dd, *J* = 5.7, 1.5 Hz, 1H), 7.14 (t, *J* = 7.4 Hz, 1H), 6.60 (d, *J* = 7.4 Hz, 1H), 6.54 (comp, 2H), 6.13 (dd, *J* = 5.7, 1.5 Hz, 1H), 5.26 (tt, *J* = 5.9, 1.5 Hz, 1H), 3.67 (dd, *J* = 5.9, 1.5 Hz, 2H), 3.01 (s, 3H), 2.32 (s, 3H); ^{13}C NMR (126 MHz, $CDCl_3$) δ 172.6, 154.5, 148.3, 139.2, 129.2, 122.1, 118.4, 113.1, 109.5, 81.9, 55.1, 39.6, 21.9.

5-[[(4-Fluorophenyl)(methyl)amino]methyl]furan-2(5*H*)-one (61): R_f = 0.19 (EtOAc/hexane (1:2)); colorless liquid; ^{1}H NMR (500 MHz, $CDCl_3$) δ 7.48 (d, *J* = 5.7 Hz, 1H), 6.95 (t, *J* = 8.6 Hz, 2H), 6.74 – 6.62 (m, 2H), 6.16 – 6.10 (m, 1H), 5.25 (td, *J* = 5.8, 1.4 Hz, 1H), 3.67 (dd, *J* = 15.3, 5.4 Hz, 1H), 3.59 (dd, *J* = 15.4, 6.0 Hz, 1H), 2.97 (s, 3H); ^{13}C NMR (126 MHz, $CDCl_3$) δ 172.5, 157.1, 154.7, 154.2, 145.1, 122.4, 115.9, 115.7, 113.8, 113.7, 82.0, 55.9, 40.0; EI-HRMS: calculated for $C_{12}H_{12}O_2NF$ (M+H) 222.09308, found 222.09324.

^{1}H and ^{13}C Spectra of New Compounds

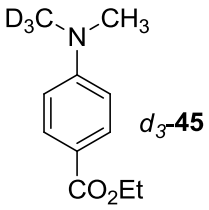

d$_3$-**45**

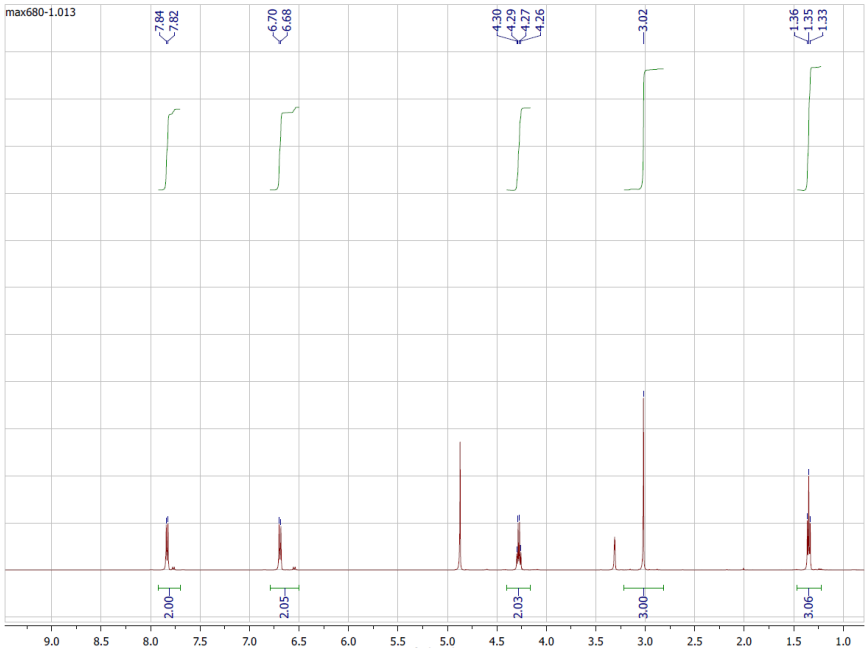

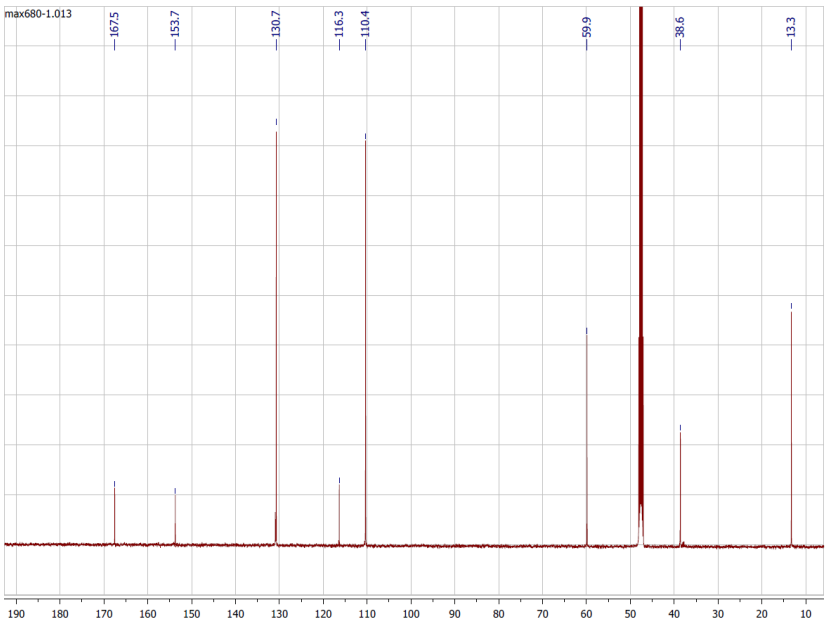

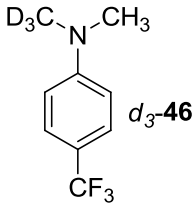
D3C
N
CH3
CF3

d$_3$-**46**

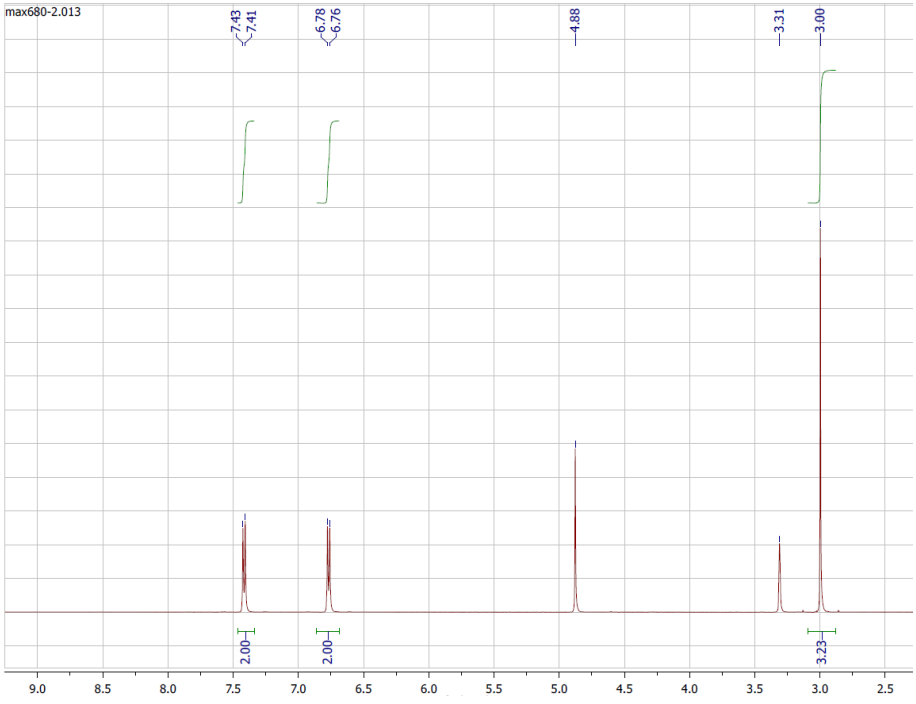
max680-2.013
7.43
7.41
6.78
6.76
4.88
3.31
3.00
2.00
2.00
3.23
9.0
8.5
8.0
7.5
7.0
6.5
6.0
5.5
5.0
4.5
4.0
3.5
3.0
2.5

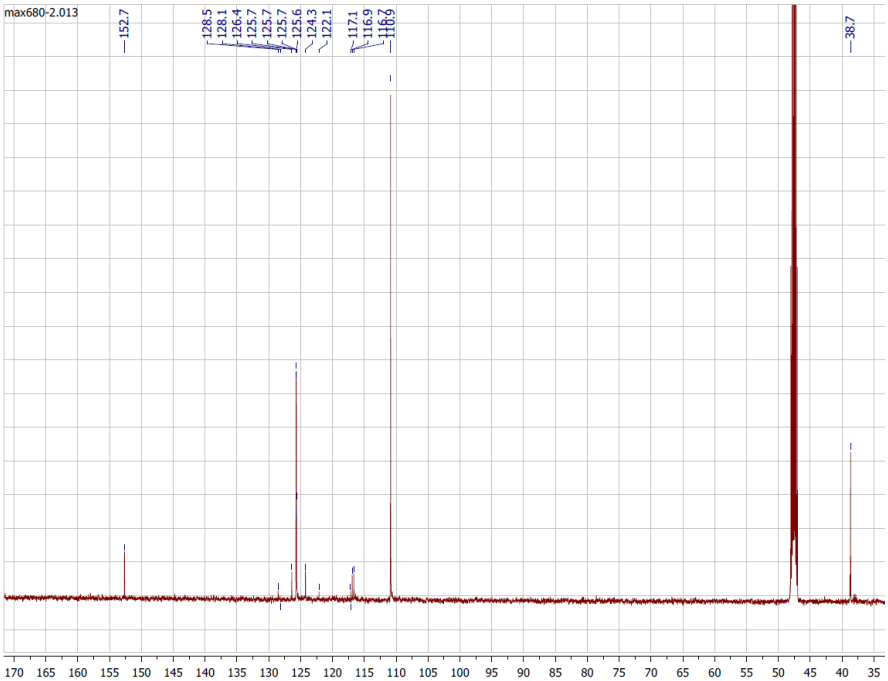
max680-2.013
152.7
128.5
128.1
126.4
125.7
125.7
125.7
125.6
124.3
122.1
117.1
116.9
116.7
116.5
38.7
170
165
160
155
150
145
140
135
130
125
120
115
110
105
100
95
90
85
80
75
70
65
60
55
50
45
40
35

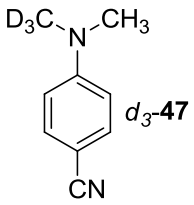
D3C
N
CH3
CN

d$_3$-**47**

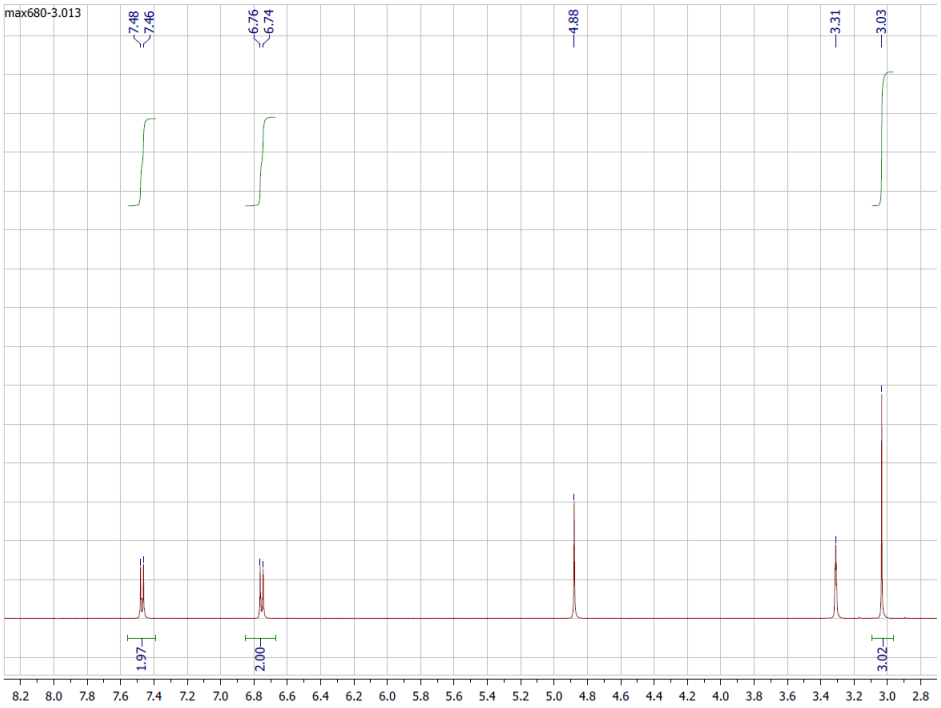
max680-3.013
7.48
7.46
6.76
6.74
4.88
3.31
3.03
1.97
2.00
3.02

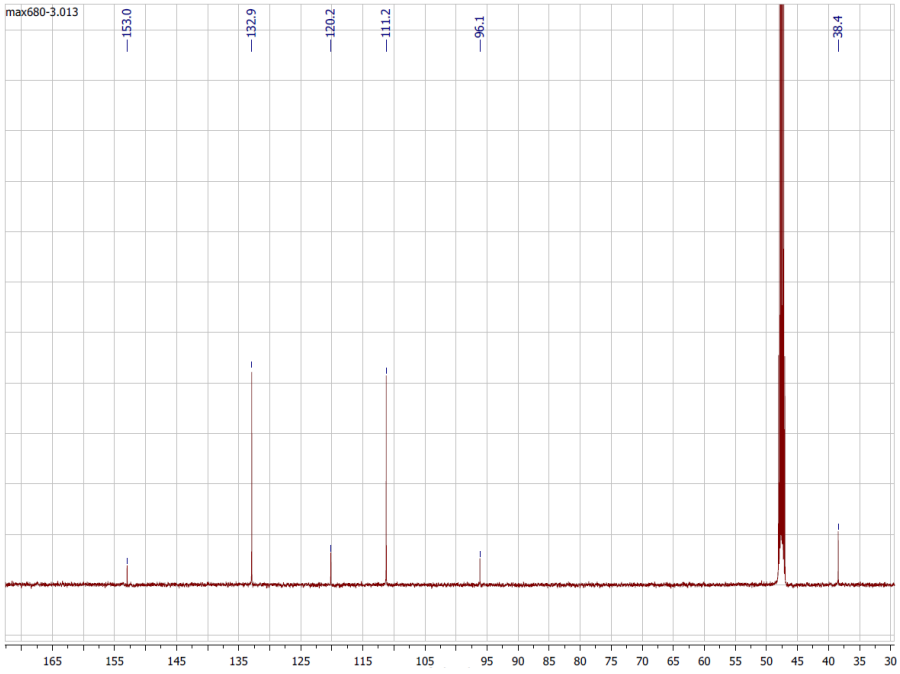
max680-3.013
153.0
132.9
120.2
111.2
96.1
38.4

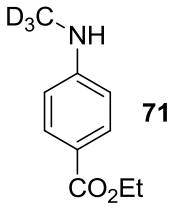
D3C
NH
CO2Et

71

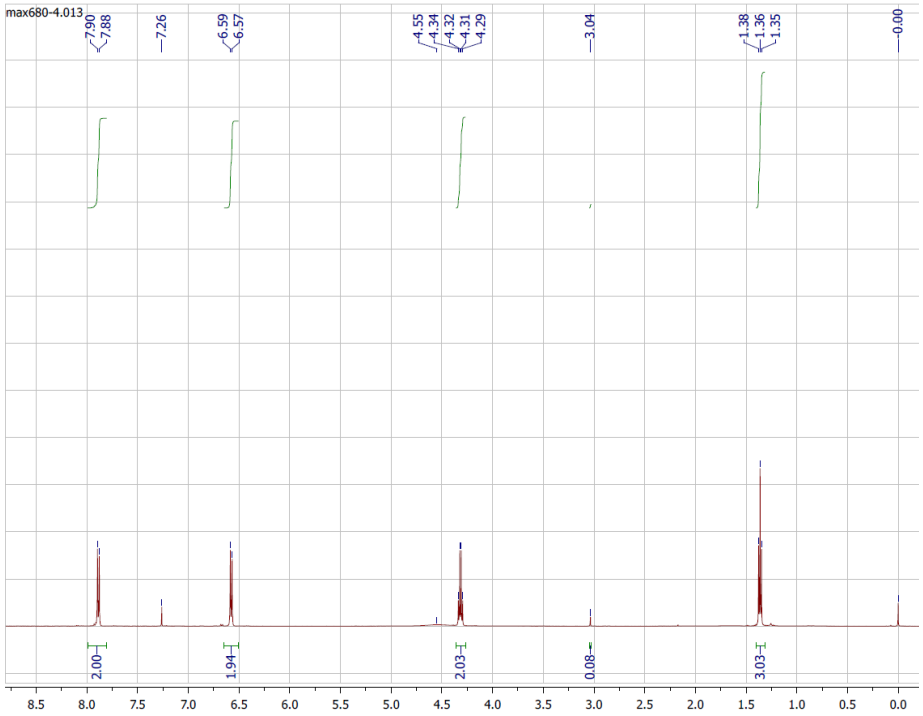
max680-4.013
7.90
7.88
7.26
6.59
6.57
4.55
4.34
4.32
4.31
4.29
3.04
1.38
1.36
1.35
0.00
2.00
1.94
2.03
0.08
3.03
8.5
8.0
7.5
7.0
6.5
6.0
5.5
5.0
4.5
4.0
3.5
3.0
2.5
2.0
1.5
1.0
0.5
0.0

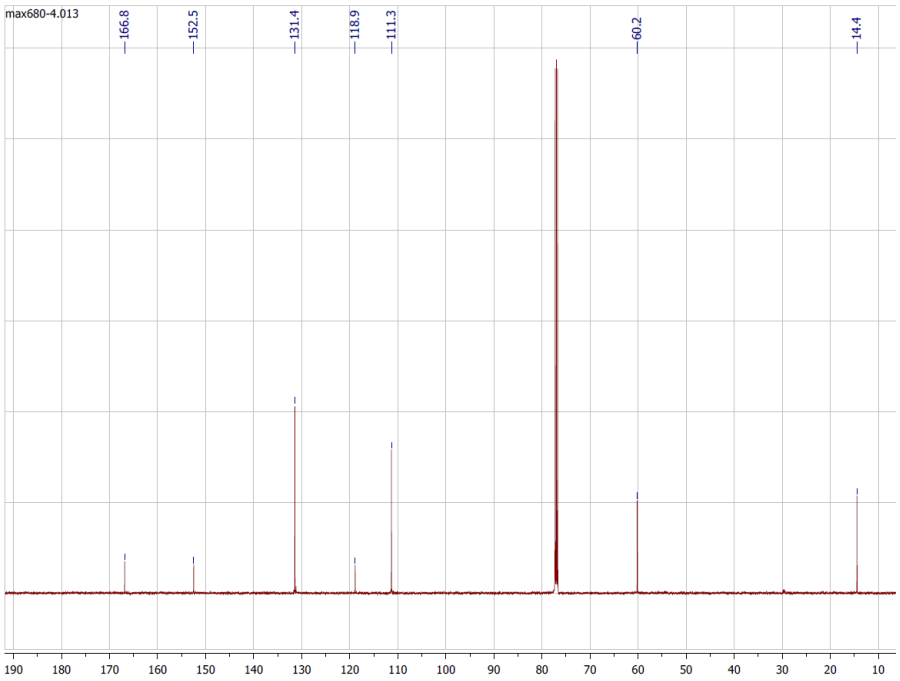
max680-4.013
166.8
152.5
131.4
118.9
111.3
60.2
14.4
190
180
170
160
150
140
130
120
110
100
90
80
70
60
50
40
30
20
10

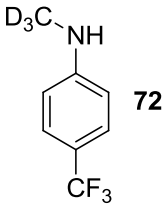
D3C
NH
CF3

72

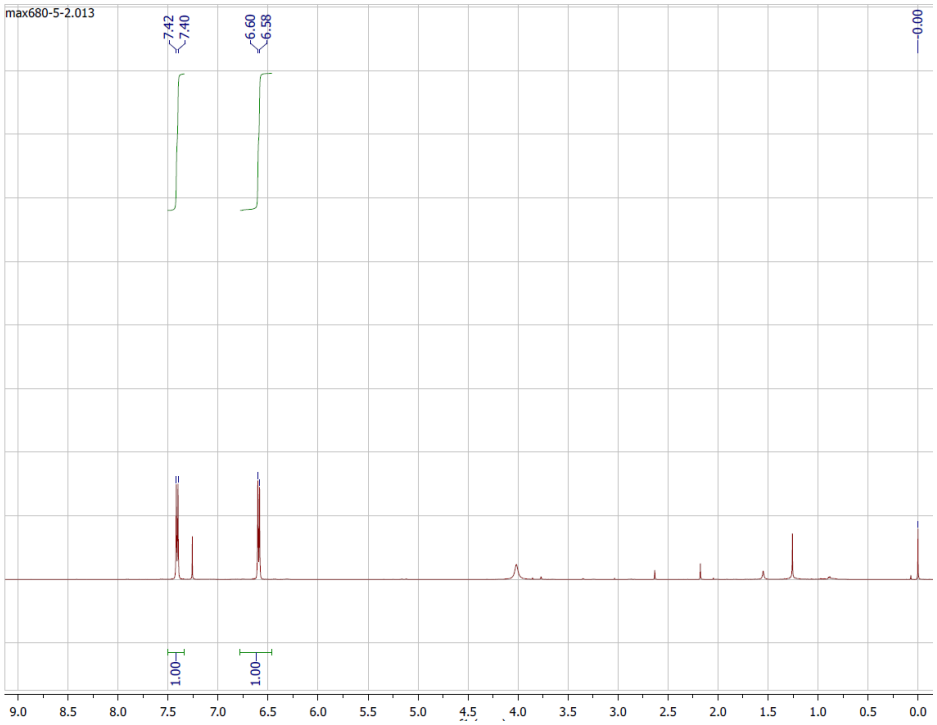
max680-5-2.013
7.42
7.40
6.60
6.58
0.00
1.00
1.00
9.0 8.5 8.0 7.5 7.0 6.5 6.0 5.5 5.0 4.5 4.0 3.5 3.0 2.5 2.0 1.5 1.0 0.5 0.0

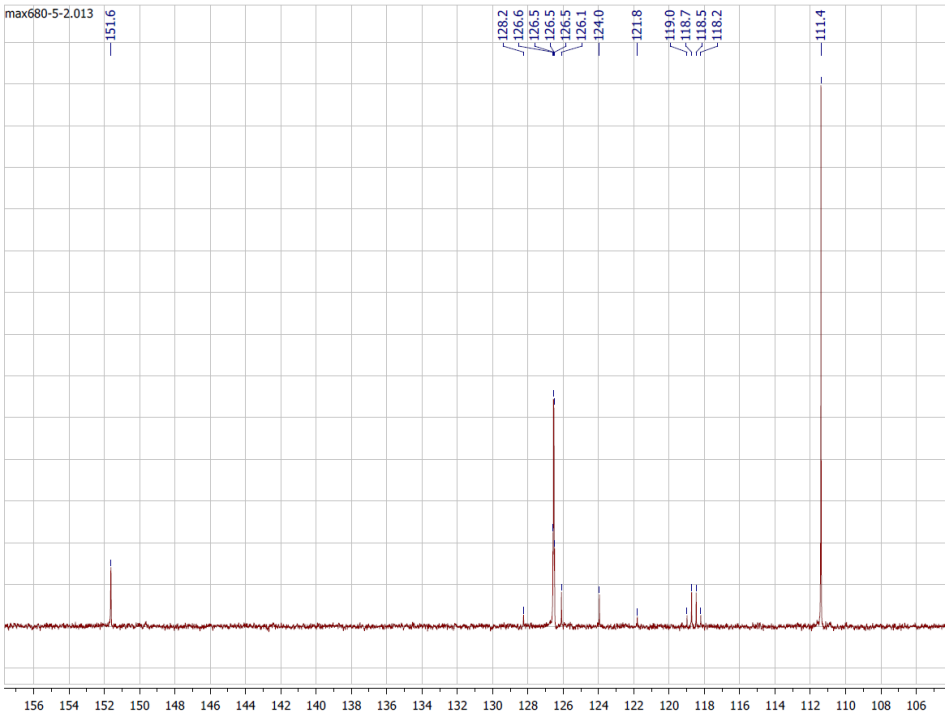
max680-5-2.013
151.6
128.2
126.6
126.5
126.5
126.5
126.1
124.0
121.8
119.0
118.7
118.5
118.2
111.4
156 154 152 150 148 146 144 142 140 138 136 134 132 130 128 126 124 122 120 118 116 114 112 110 108 106

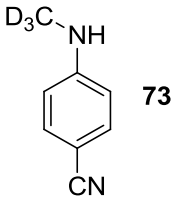
D3C
NH
CN

73

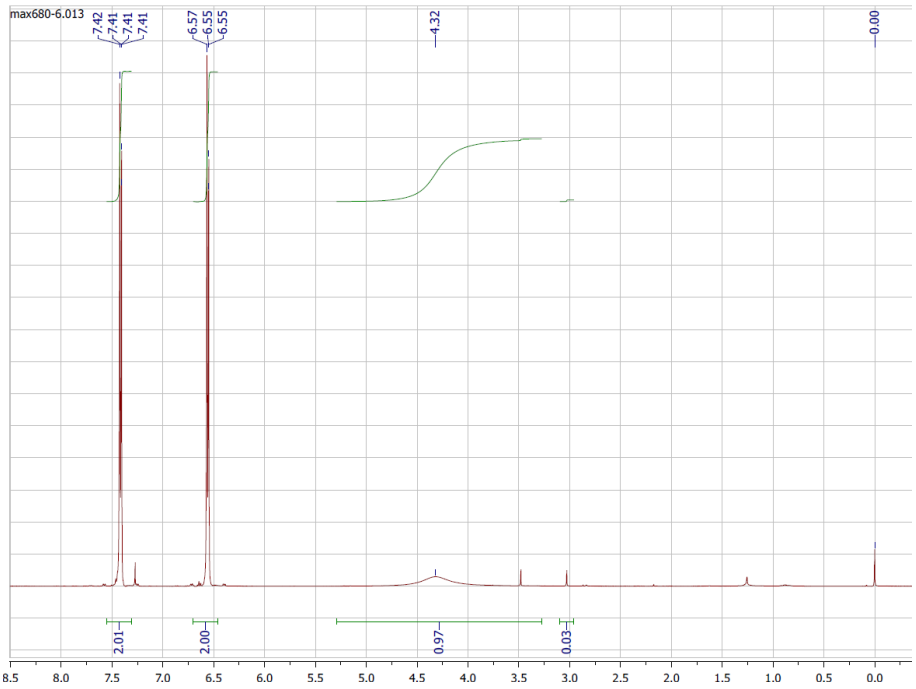
max680-6.013
7.42
7.41
7.41
7.41
6.57
6.55
6.55
4.32
0.00
2.01
2.00
0.97
0.03
8.5
8.0
7.5
7.0
6.5
6.0
5.5
5.0
4.5
4.0
3.5
3.0
2.5
2.0
1.5
1.0
0.5
0.0

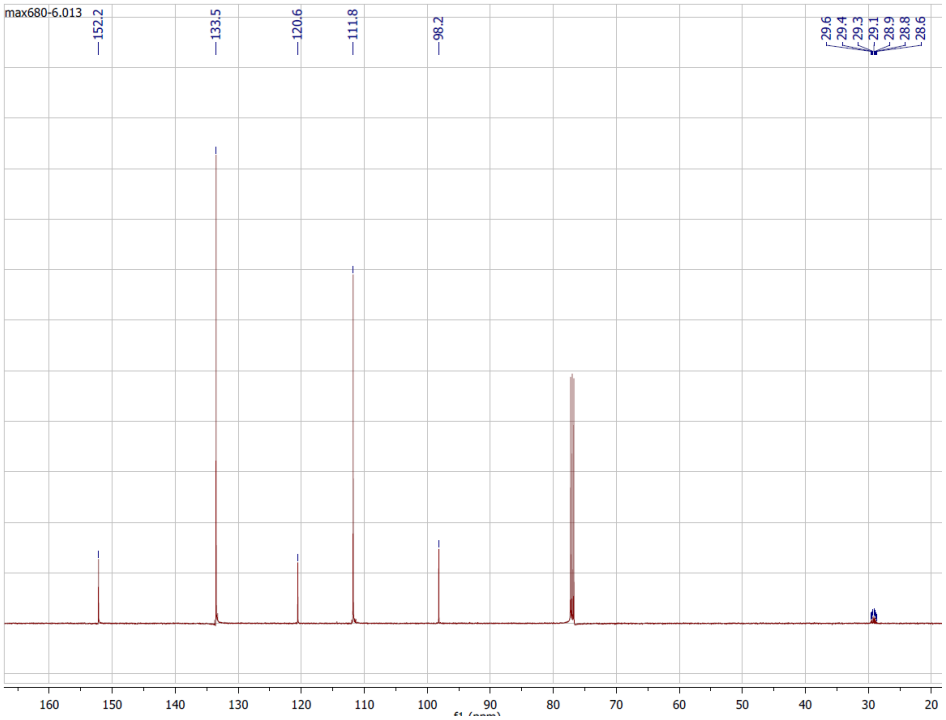
max680-6.013
152.2
133.5
120.6
111.8
98.2
29.6
29.4
29.3
29.1
28.9
28.8
28.6
160
150
140
130
120
110
100
90
80
70
60
50
40
30
20

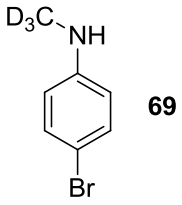
D3C
NH
Br

69

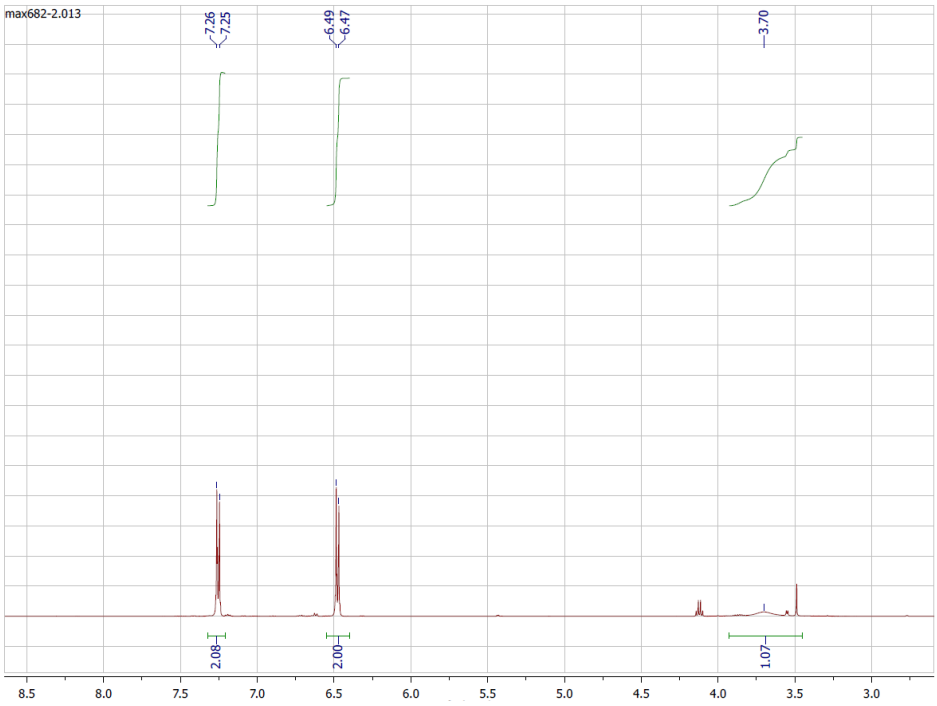
max682-2.013
7.26
7.25
6.49
6.47
3.70
2.08
2.00
1.07
8.5
8.0
7.5
7.0
6.5
6.0
5.5
5.0
4.5
4.0
3.5
3.0

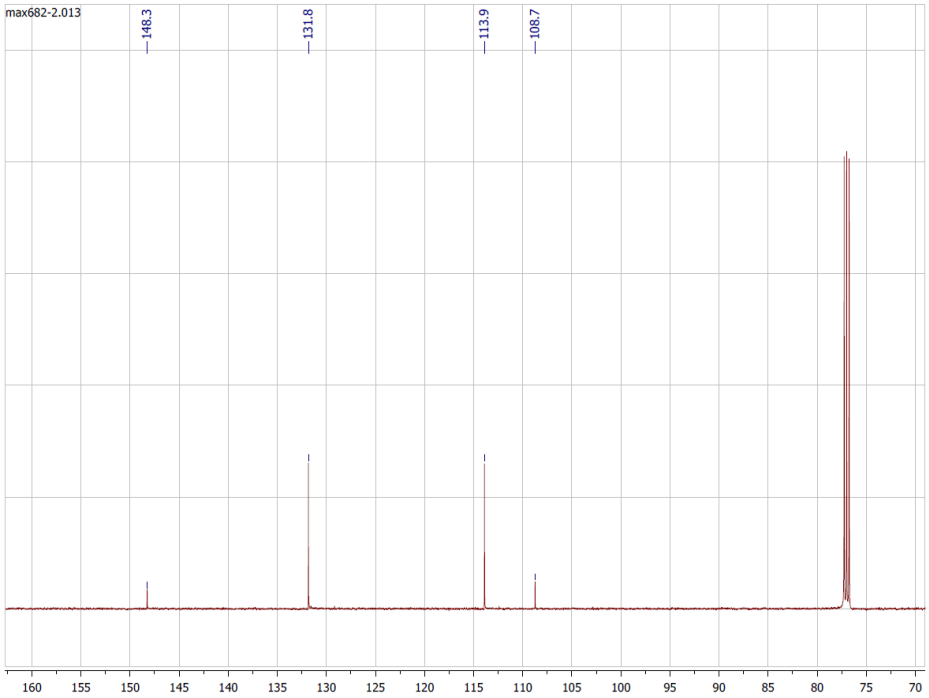
max682-2.013
148.3
131.8
113.9
108.7
160
155
150
145
140
135
130
125
120
115
110
105
100
95
90
85
80
75
70

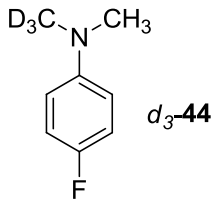
D3C
N
CH3
F

d_3-**44**

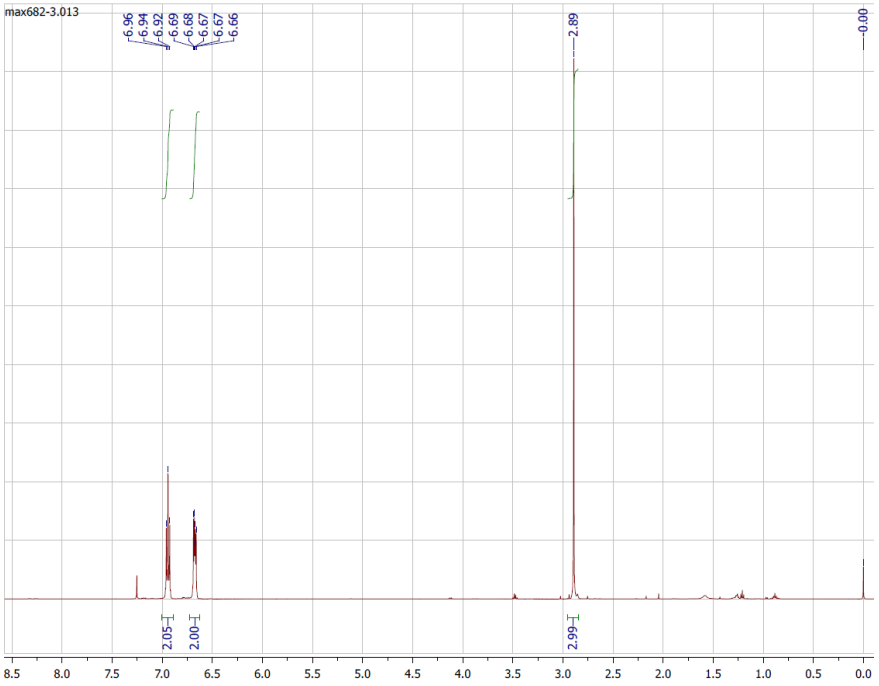
max682-3.013
6.96
6.94
6.92
6.69
6.68
6.67
6.67
6.66
2.89
0.00
2.05
2.00
2.99

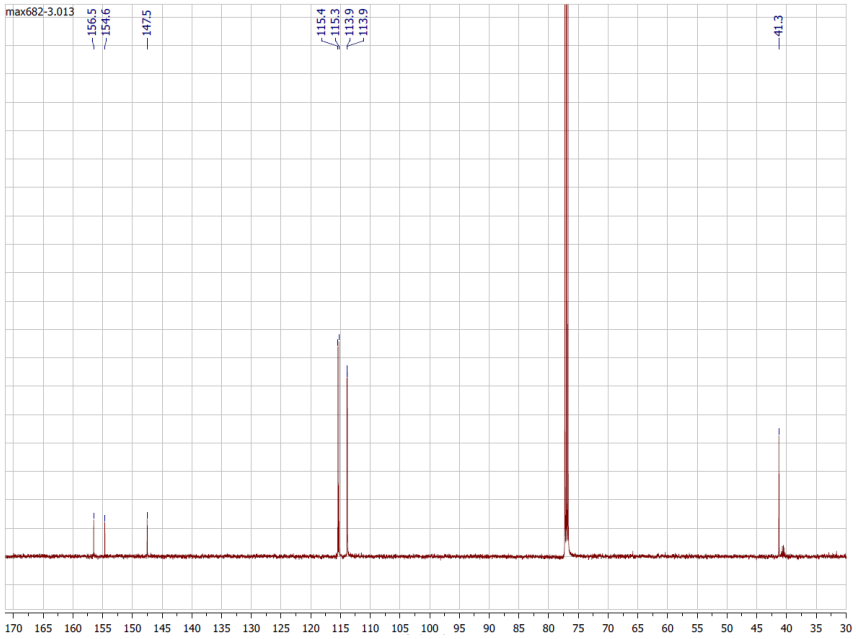
max682-3.013
156.5
154.6
147.5
115.4
115.3
113.9
113.9
41.3

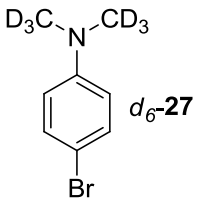
D3C
N
CD3
Br

d$_6$-**27**

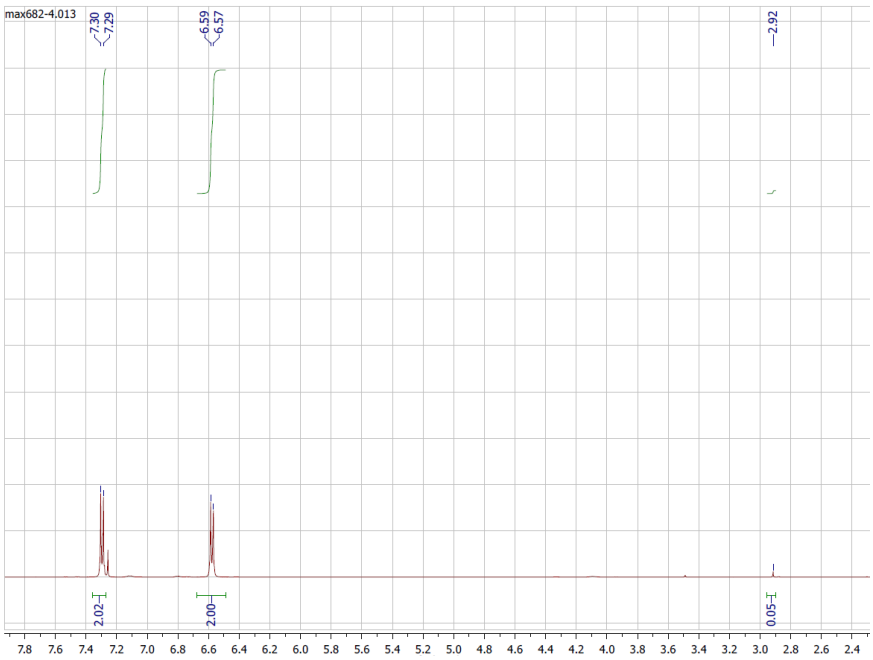
max682-4.013
7.30
7.29
6.59
6.57
2.92
2.02
2.00
0.05

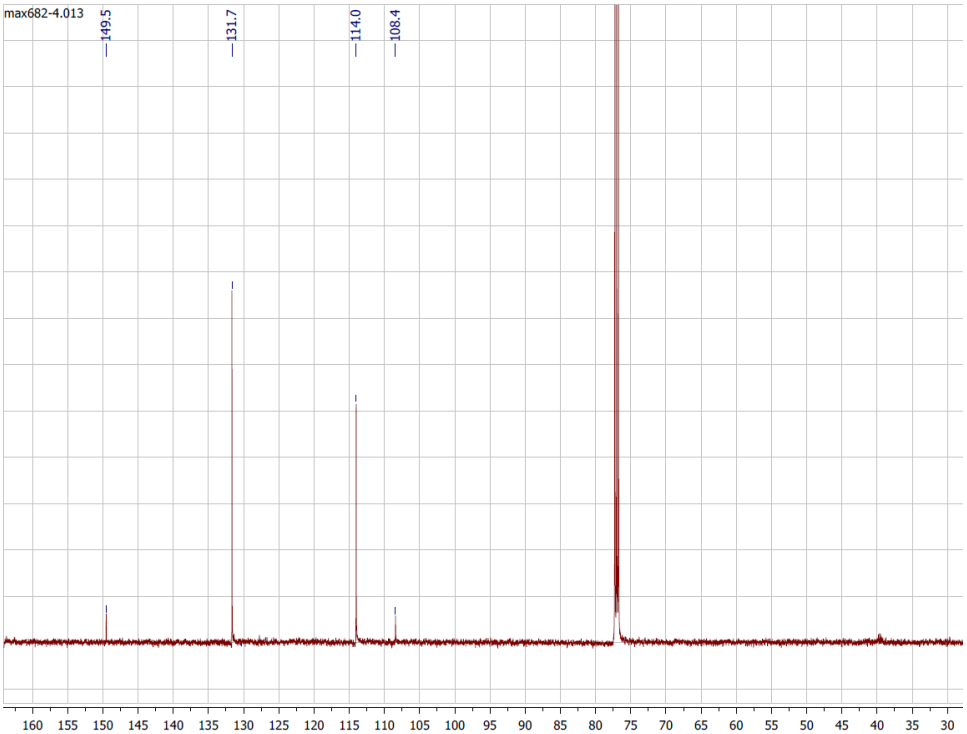
max682-4.013
149.5
131.7
114.0
108.4

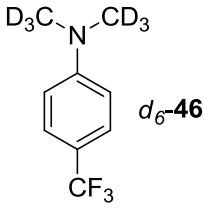
D3C
N
CD3
CF3

d$_6$-**46**

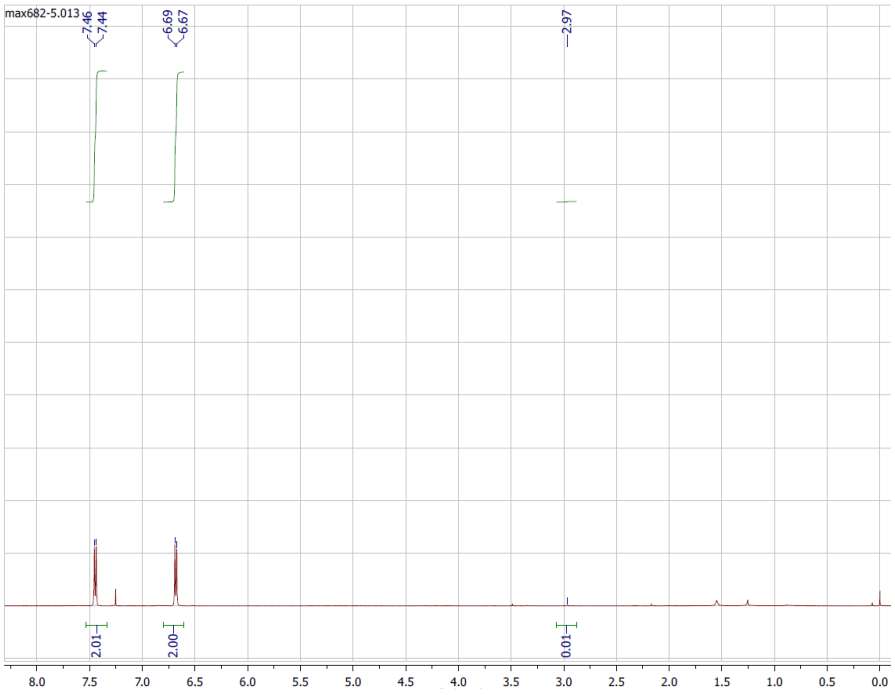
max682-5.013
7.46
7.44
6.69
6.67
2.97
2.01
2.00
0.01
8.0 7.5 7.0 6.5 6.0 5.5 5.0 4.5 4.0 3.5 3.0 2.5 2.0 1.5 1.0 0.5 0.0

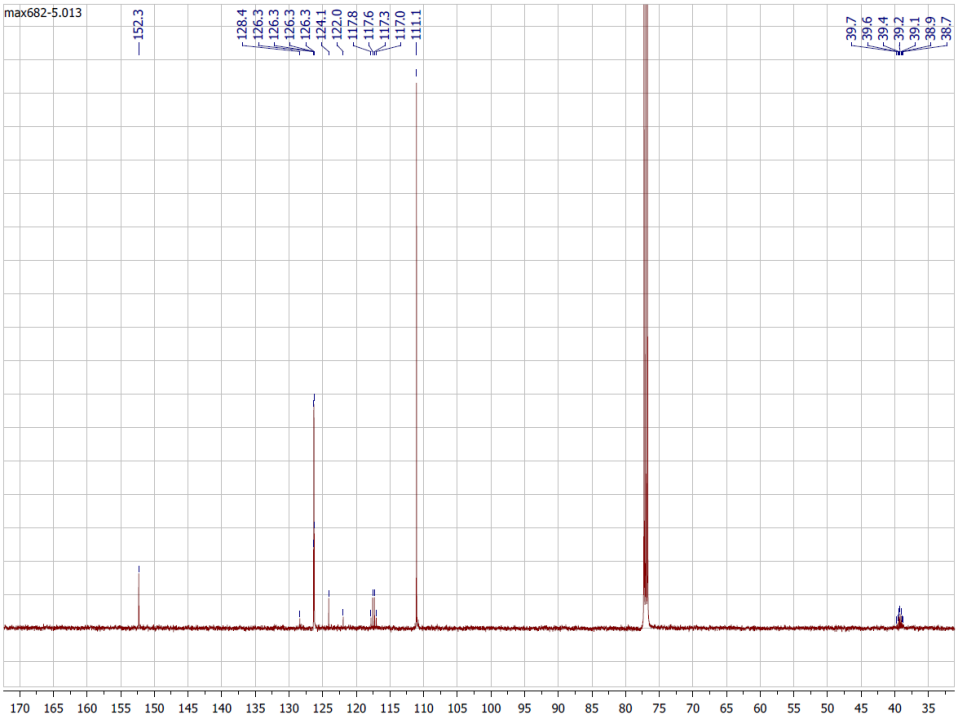
max682-5.013
152.3
128.4
126.3
126.3
126.3
126.3
124.1
122.0
117.8
117.6
117.3
117.0
111.1
39.7
39.6
39.4
39.2
39.1
38.9
38.7
170 165 160 155 150 145 140 135 130 125 120 115 110 105 100 95 90 85 80 75 70 65 60 55 50 45 40 35

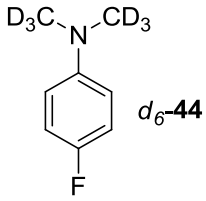
D3C
N
CD3
F

d$_6$-**44**

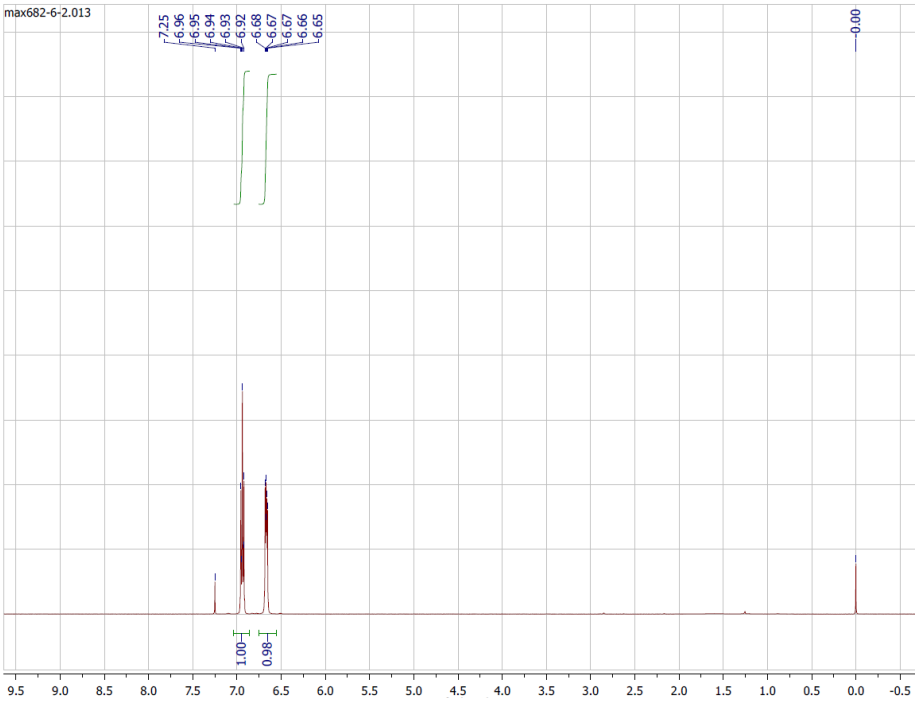
max682-6-2.013
7.25
6.96
6.95
6.94
6.93
6.92
6.68
6.67
6.67
6.66
6.65
0.00
1.00
0.98
9.5
9.0
8.5
8.0
7.5
7.0
6.5
6.0
5.5
5.0
4.5
4.0
3.5
3.0
2.5
2.0
1.5
1.0
0.5
0.0
-0.5

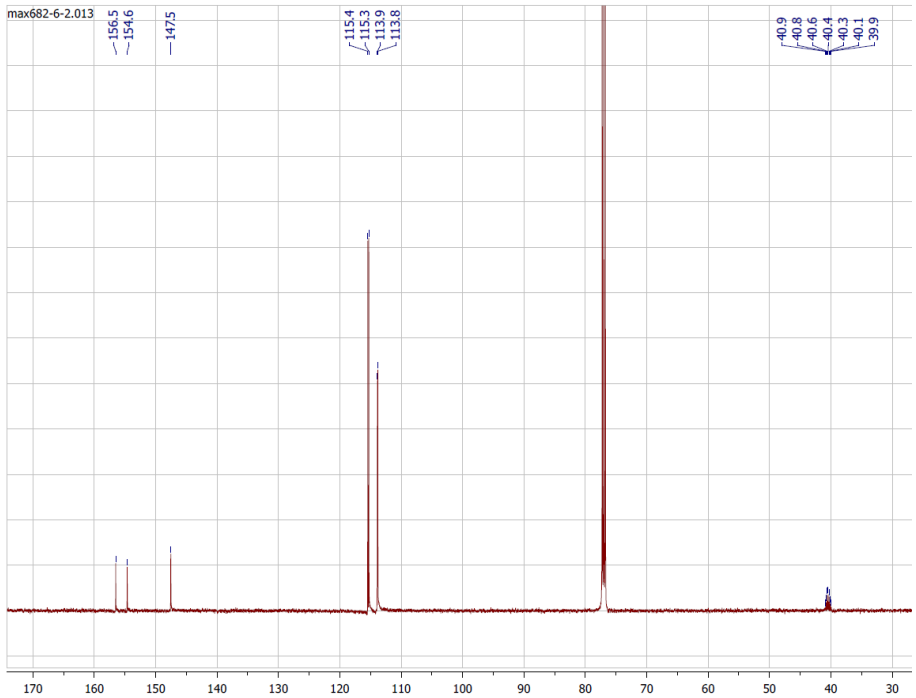
max682-6-2.013
156.5
154.6
147.5
115.4
115.3
113.9
113.8
40.9
40.8
40.6
40.4
40.3
40.1
39.9
170
160
150
140
130
120
110
100
90
80
70
60
50
40
30

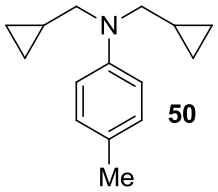
N
Me

50

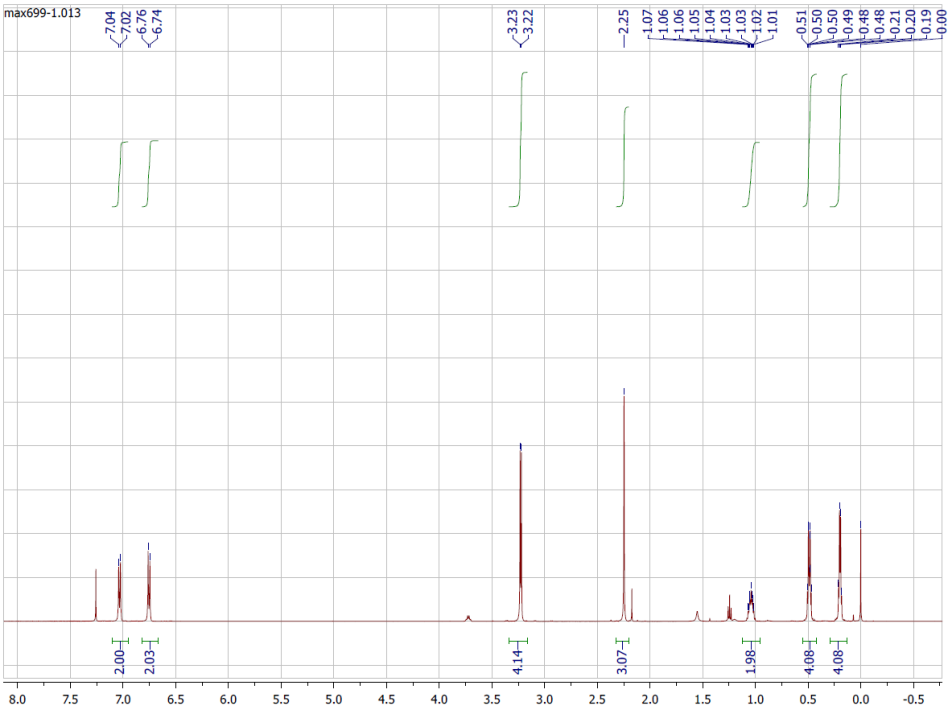
max699-1.013
7.04
7.02
6.76
6.74
3.23
3.22
2.25
1.07
1.06
1.06
1.05
1.04
1.03
1.03
1.02
1.01
0.51
0.50
0.50
0.49
0.48
0.48
0.21
0.20
0.19
0.00
2.00
2.03
4.14
3.07
1.98
4.08
4.08
8.0
7.5
7.0
6.5
6.0
5.5
5.0
4.5
4.0
3.5
3.0
2.5
2.0
1.5
1.0
0.5
0.0
-0.5

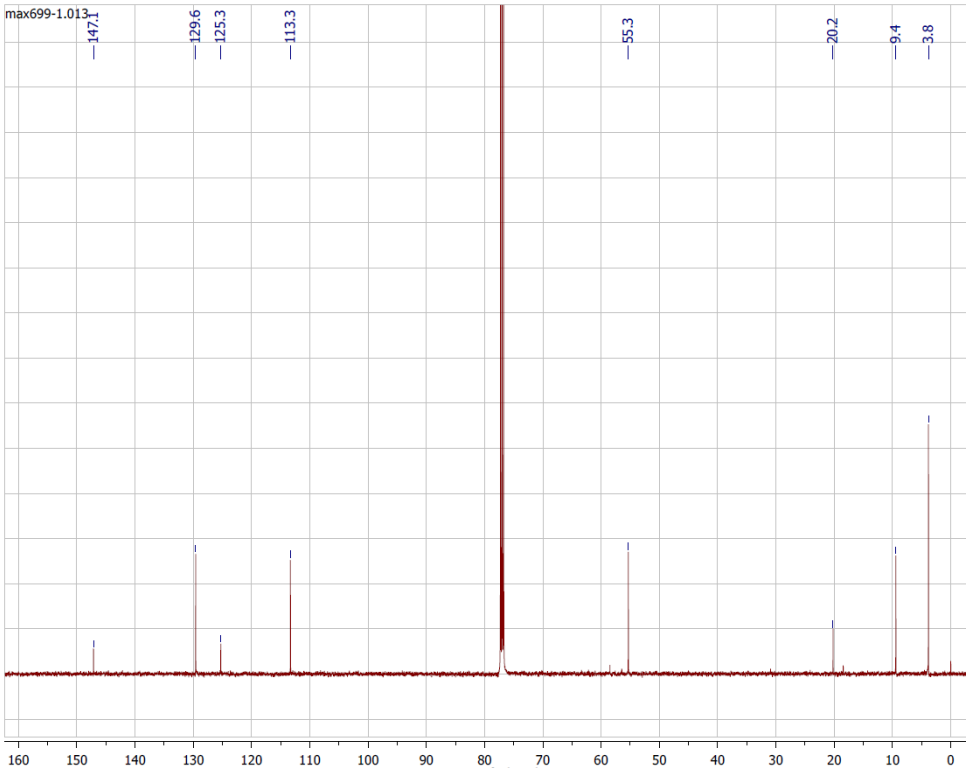
max699-1.013
147.1
129.6
125.3
113.3
55.3
20.2
9.4
3.8
160
150
140
130
120
110
100
90
80
70
60
50
40
30
20
10
0

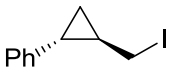
Ph
I

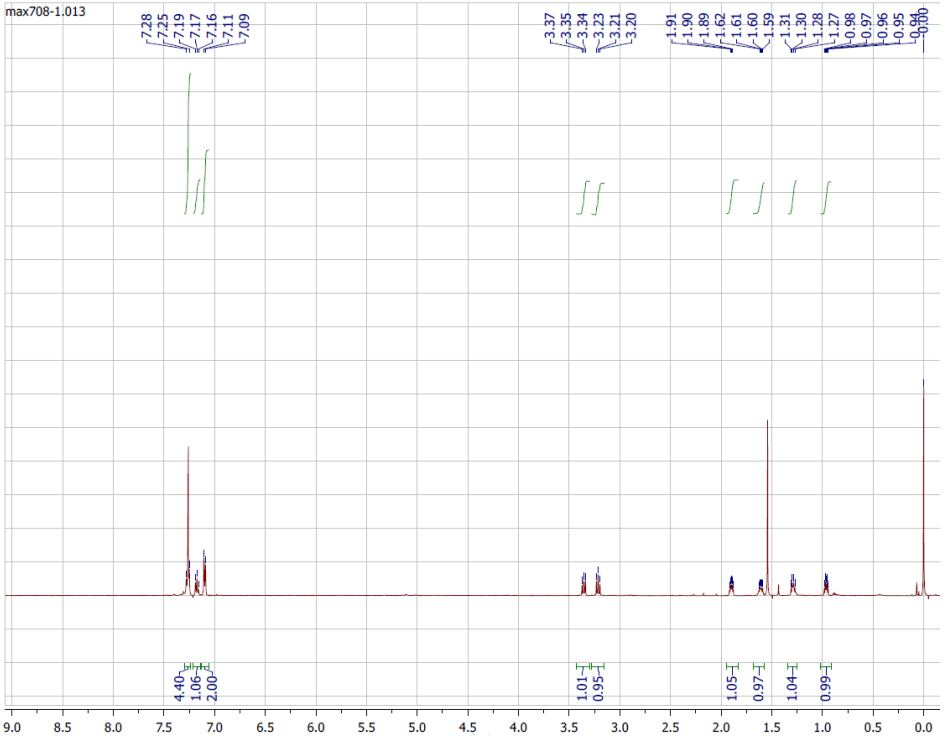
max708-1.013
7.28
7.25
7.19
7.17
7.16
7.11
7.09
3.37
3.35
3.34
3.23
3.21
3.20
1.91
1.90
1.89
1.62
1.61
1.60
1.59
1.31
1.30
1.28
1.27
0.98
0.97
0.96
0.95
0.00
4.40
1.06
2.00
1.01
0.95
1.05
0.97
1.04
0.99
9.0
8.5
8.0
7.5
7.0
6.5
6.0
5.5
5.0
4.5
4.0
3.5
3.0
2.5
2.0
1.5
1.0
0.5
0.0


max708-1.013
141.5
128.4
126.0
125.9
29.3
27.1
20.5
12.2
160
150
140
130
120
110
100
90
80
70
60
50
40
30
20
10

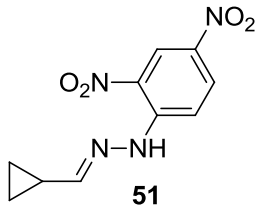
NO2
O2N
N–NH

51

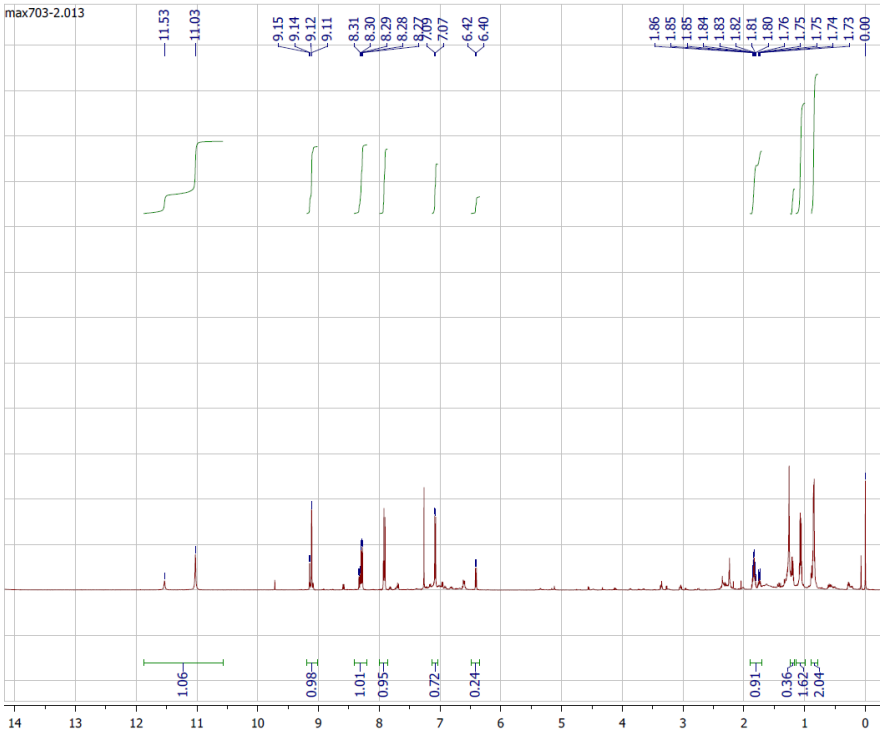
max703-2.013
11.53
11.03
9.15
9.14
9.12
9.11
8.31
8.30
8.29
8.28
8.27
8.26
7.07
6.42
6.40
1.86
1.85
1.85
1.84
1.83
1.82
1.81
1.80
1.76
1.75
1.75
1.74
1.73
0.00
1.06
0.98
1.01
0.95
0.72
0.24
0.91
0.36
1.62
2.04
14
13
12
11
10
9
8
7
6
5
4
3
2
1
0

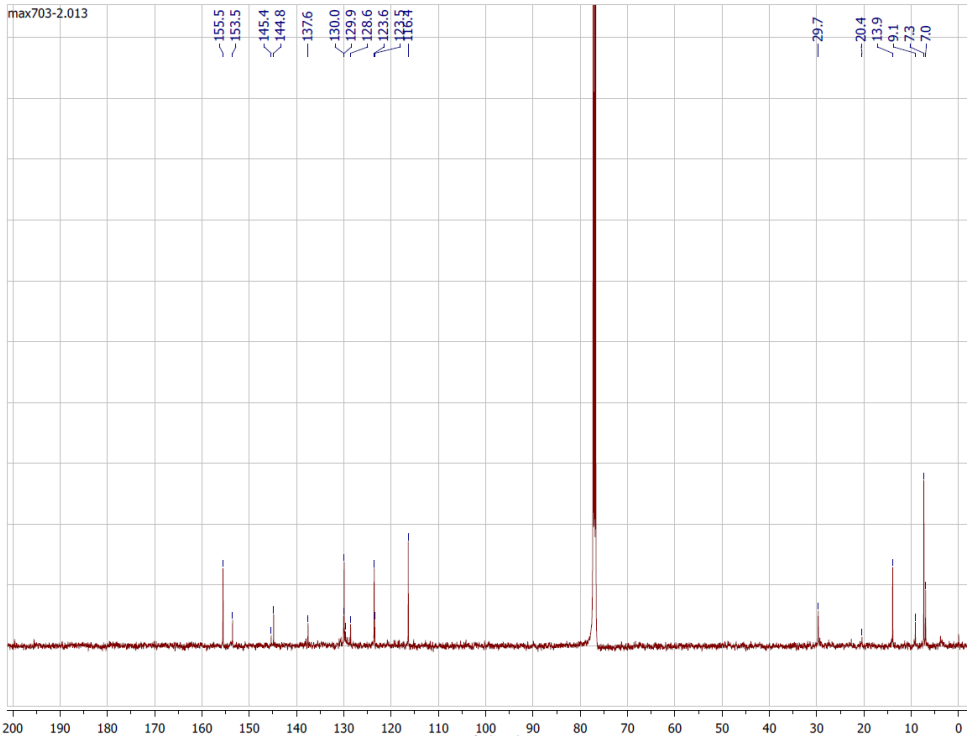
max703-2.013
155.5
153.5
145.4
144.8
137.6
130.0
129.9
128.6
123.6
123.5
116.4
29.7
20.4
13.9
9.1
7.3
7.0
200
190
180
170
160
150
140
130
120
110
100
90
80
70
60
50
40
30
20
10
0

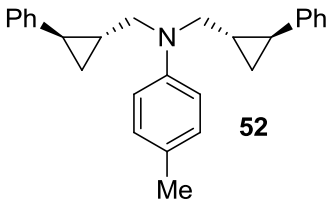
Ph
N
Ph
Me

52

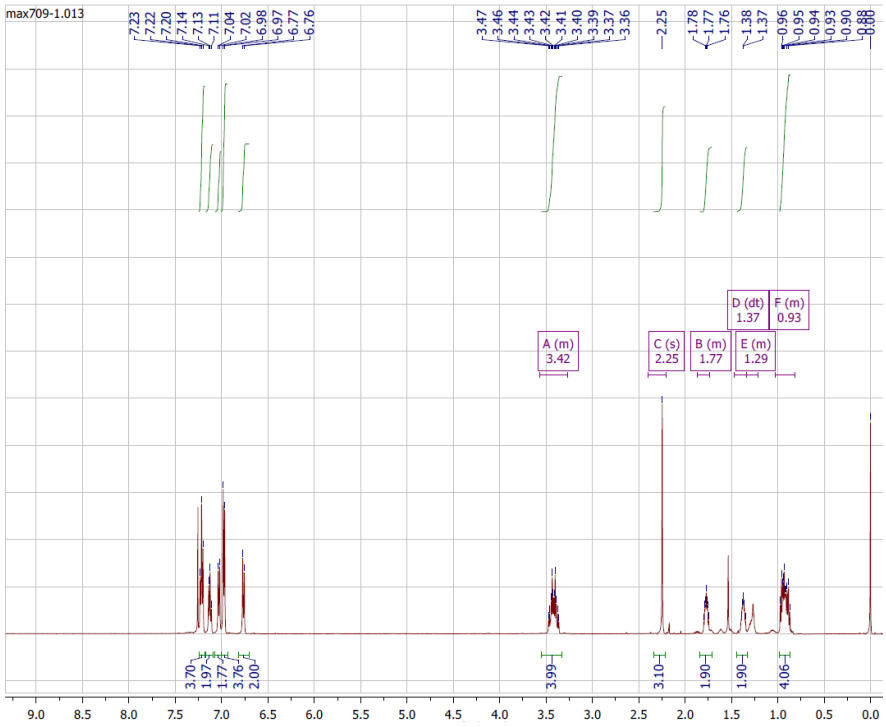
max709-1.013
A (m) 3.42
C (s) 2.25
B (m) 1.77
E (m) 1.29
D (dt) 1.37
F (m) 0.93

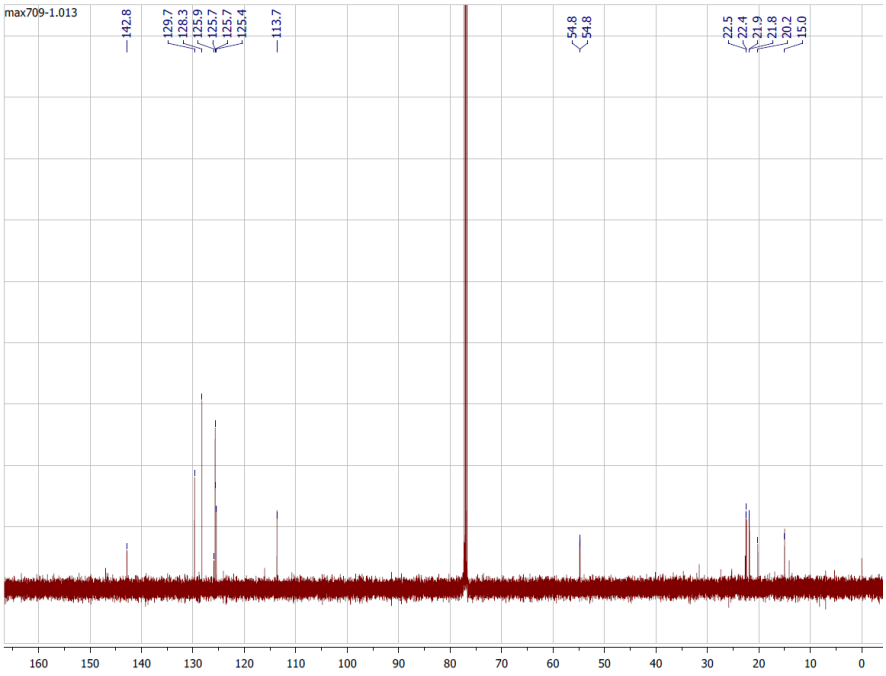
max709-1.013

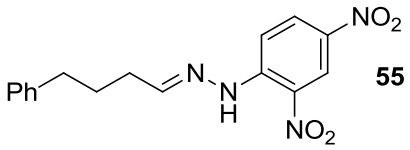

55

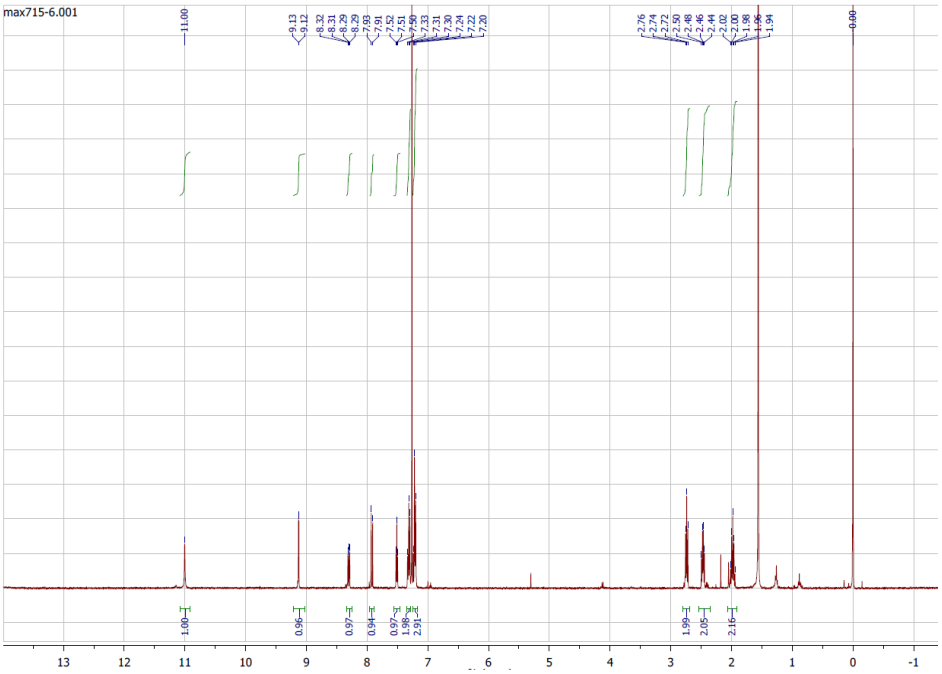

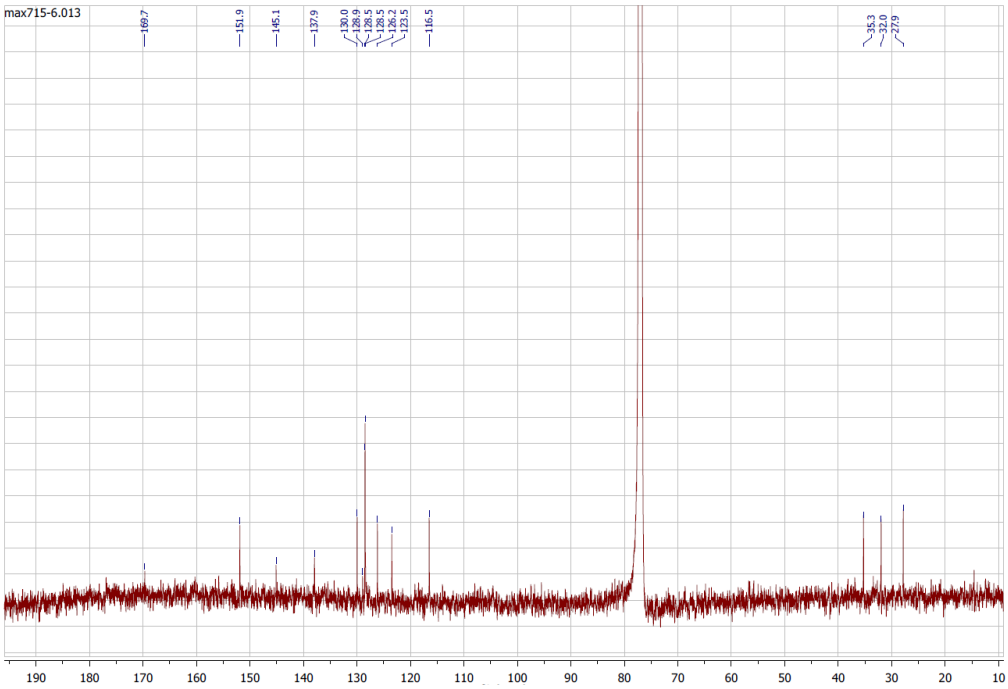

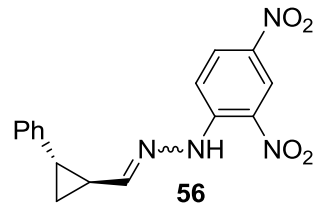
NO2
Ph
N
NH
NO2

56

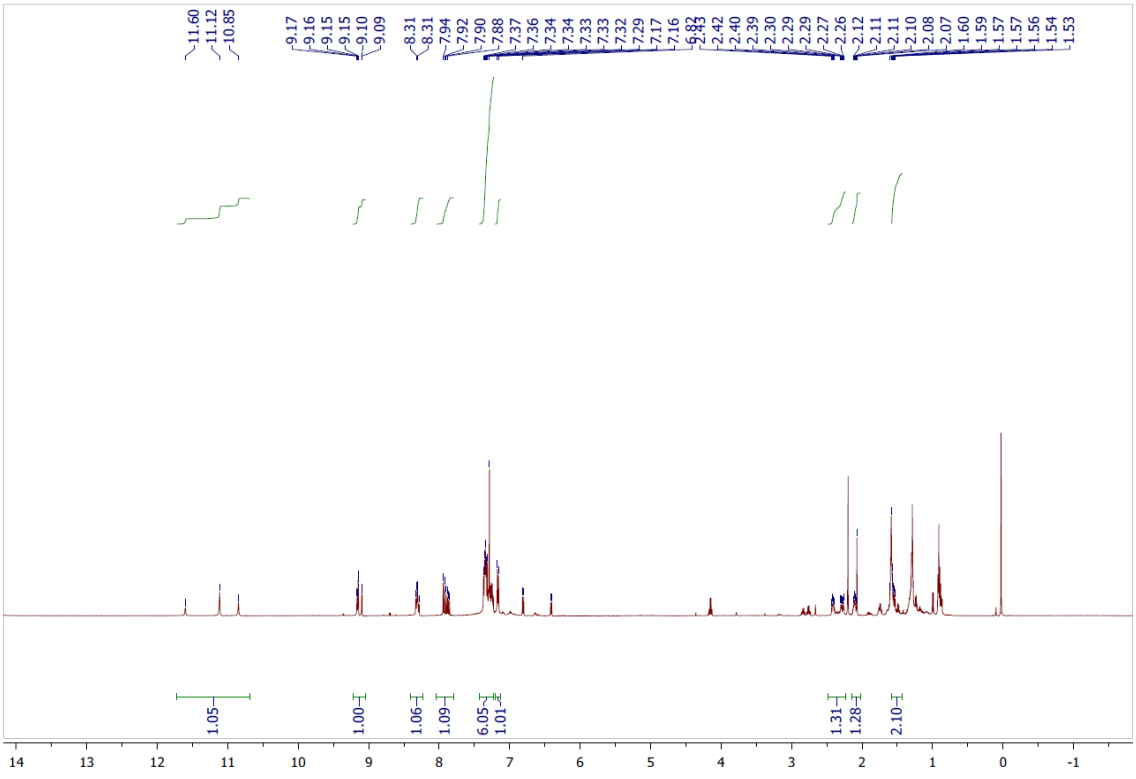
11.60
11.12
10.85
9.17
9.16
9.15
9.15
9.10
9.09
8.31
8.31
7.94
7.92
7.90
7.88
7.37
7.36
7.34
7.34
7.33
7.33
7.32
7.29
7.17
7.16
2.42
2.40
2.39
2.30
2.29
2.29
2.27
2.26
2.12
2.11
2.11
2.10
2.08
2.07
1.60
1.59
1.57
1.57
1.56
1.54
1.53
1.05
1.00
1.06
1.09
6.05
1.01
1.31
1.28
2.10
14
13
12
11
10
9
8
7
6
5
4
3
2
1
0
-1

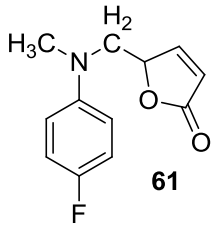
H2
H3C
N
C
O
O
F

61

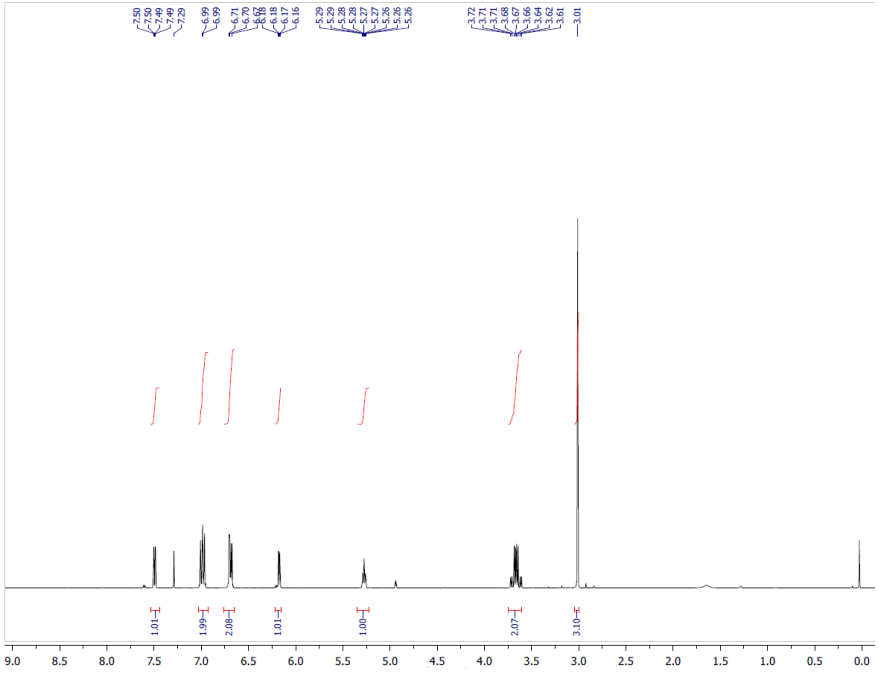
7.50
7.50
7.49
7.49
7.29
6.99
6.99
6.71
6.70
6.67
6.68
6.18
6.17
6.16
5.29
5.29
5.28
5.28
5.27
5.27
5.26
5.26
3.72
3.71
3.71
3.68
3.67
3.66
3.64
3.62
3.61
3.01
1.01
1.99
2.08
1.01
1.00
2.07
3.10
9.0
8.5
8.0
7.5
7.0
6.5
6.0
5.5
5.0
4.5
4.0
3.5
3.0
2.5
2.0
1.5
1.0
0.5
0.0

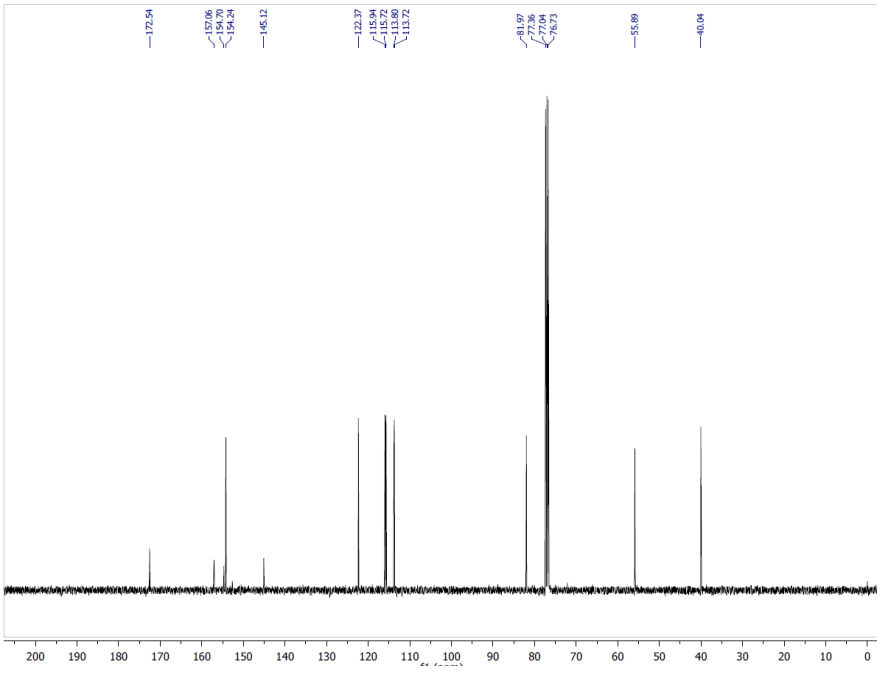
172.54
157.06
154.70
154.24
145.12
122.37
115.94
115.72
113.80
113.72
81.97
77.36
77.04
76.73
55.89
40.04
200
190
180
170
160
150
140
130
120
110
100
90
80
70
60
50
40
30
20
10
0

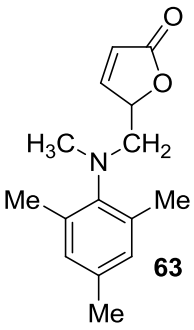
O
O
H3C
N
CH2
Me
Me
Me

63

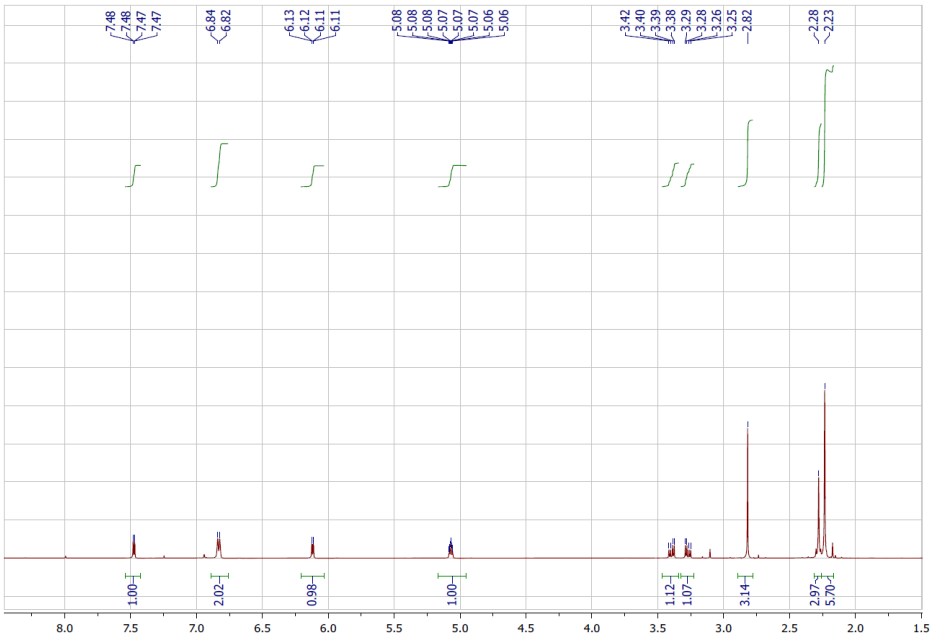
7.48
7.48
7.47
7.47
6.84
6.82
6.13
6.12
6.11
6.11
5.08
5.08
5.08
5.07
5.07
5.07
5.06
5.06
3.42
3.40
3.39
3.38
3.29
3.28
3.26
3.25
2.82
2.28
2.23
1.00
2.02
0.98
1.00
1.12
1.07
3.14
2.97
5.70
8.0
7.5
7.0
6.5
6.0
5.5
5.0
4.5
4.0
3.5
3.0
2.5
2.0
1.5

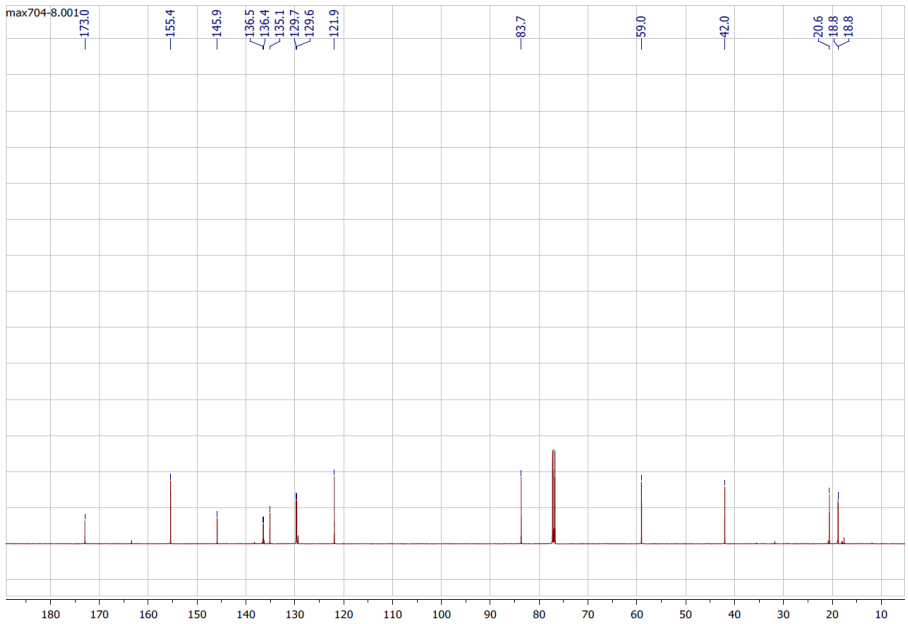
max704-8.001
173.0
155.4
145.9
136.5
136.4
135.1
129.7
129.6
121.9
83.7
59.0
42.0
20.6
18.8
18.8
180
170
160
150
140
130
120
110
100
90
80
70
60
50
40
30
20
10

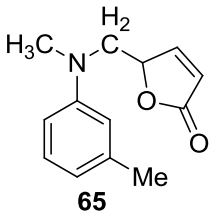
H2
H3C
N
C
O
O
Me

65

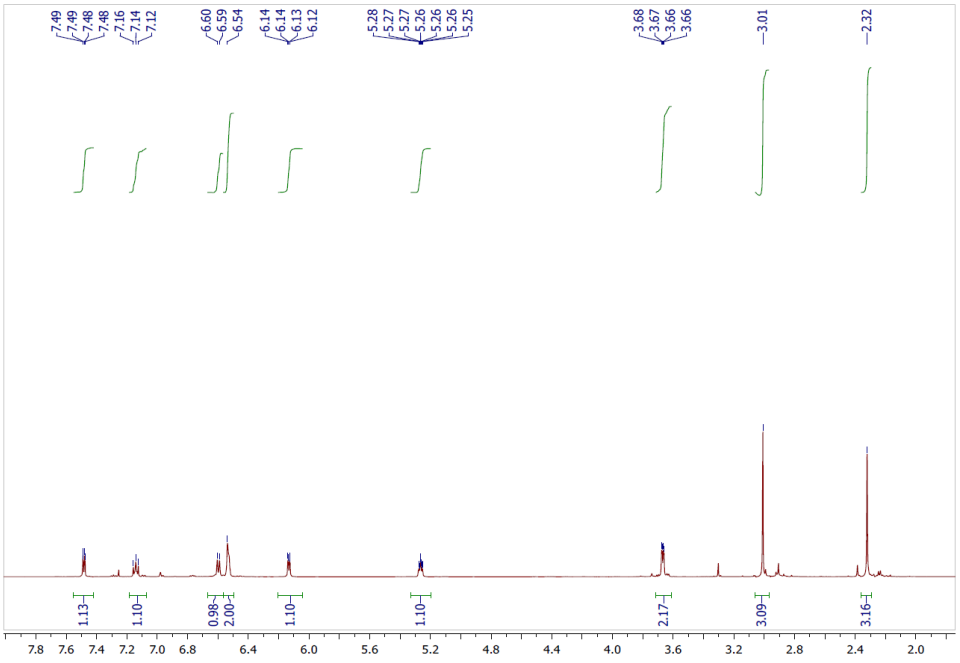
7.49
7.49
7.48
7.48
7.16
7.14
7.12
6.60
6.59
6.54
6.14
6.14
6.13
6.12
5.28
5.27
5.27
5.26
5.26
5.26
5.25
3.68
3.67
3.66
3.66
3.01
2.32
1.13
1.10
0.98
2.00
1.10
1.10
2.17
3.09
3.16
7.8 7.6 7.4 7.2 7.0 6.8 6.4 6.0 5.6 5.2 4.8 4.4 4.0 3.6 3.2 2.8 2.4 2.0

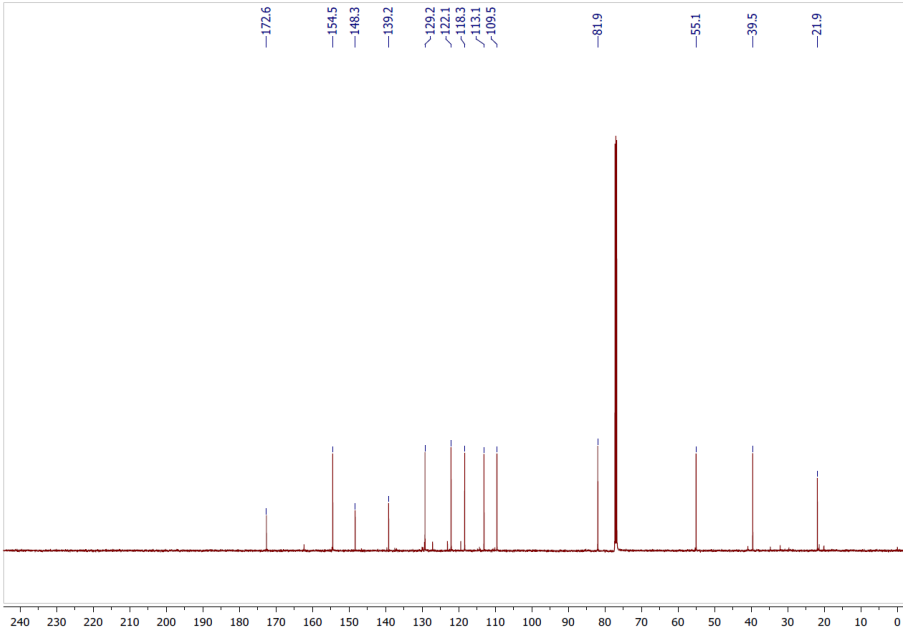
172.6
154.5
148.3
139.2
129.2
122.1
118.3
113.1
109.5
81.9
55.1
39.5
21.9
240 230 220 210 200 190 180 170 160 150 140 130 120 110 100 90 80 70 60 50 40 30 20 10 0

Bibliography

(1) Ratnikov, M. O.; Farkas, L. E.; McLaughlin, E. C.; Chiou, G.; Choi, H.; El-Khalafy, S. H.; Doyle, M. P. *J. Org. Chem.* **2011**, *76*, 2585.

(2) Ratnikov, M. O.; Doyle, M. P. *Handb. Reagents Org. Synth.* **2012**, accepted.

(3) Bregeault, J.-M. *Dalton Trans.* **2003**, 3289.

(4) Uyanik, M.; Okamoto, H.; Yasui, T.; Ishihara, K. *Science* **2010**, *328*, 1376.

(5) (a) Lu, X.; Liu, Y.; Sun, B.; Cindric, B.; Deng, L. *J. Am. Chem. Soc.* **2008**, *130*, 8134. (b) Wu, W.; Su, W. *J. Am. Chem. Soc.* **2011**, *133*, 11924. (c) Tian, J.-S.; Loh, T.-P. *Chem. Commun.* **2011**, *47*, 5458. (d) Jiang, H.-F.; Huang, H.-W.; Cao, H.; Qi, C.-R. *Org. Lett.* **2010**, *12*, 5561. (e) Chen, S.; Xu, Y.; Wan, X. *Org. Lett.* **2011**, *13*, 6152.

(6) (a) Blanc, A.; Toste, F. D. *Angew. Chem., Int. Ed.* **2006**, *45*, 2096. (b) Davies, I. R.; Cheeseman, M.; Green, R.; Mahon, M. F.; Merritt, A.; Bull, S. D. *Org. Lett.* **2009**, *11*, 2896. (c) Weiss, K. M.; Wei, S.; Tsogoeva, S. B. *Org. Biomol. Chem.* **2011**, *9*, 3457. (d) Liu, Y.; Tsunoyama, H.; Akita, T.; Tsukuda, T. *Chem. Commun.* **2010**, *46*, 550.

(7) (a) Michel, B. W.; Camelio, A. M.; Cornell, C. N.; Sigman, M. S. *J. Am. Chem. Soc.* **2009**, *131*, 6076. (b) Michel, B. W.; McCombs, J. R.; Winkler, A.; Sigman, M. S. *Angew. Chem., Int. Ed.* **2010**, *49*, 7312.

(8) (a) Yoo, W.-J.; Li, C.-J. *J. Am. Chem. Soc.* **2006**, *128*, 13064. (b) Ji, Y.; Brueckl, T.; Baxter, R. D.; Fujiwara, Y.; Seiple, I. B.; Su, S.; Blackmond, D. G.; Baran, P. S. *Proc. Natl. Acad. Sci. U. S. A.* **2011**, *108*, 14411.

(9) (a) Zheng, W.; Wojtas, L.; Antilla, J. C. *Angew. Chem., Int. Ed.* **2010**, *49*, 6589. (b) Baj, S.; Chrobok, A.; Derfla, S. *Green Chem.* **2006**, *8*, 292. (c) Liu, W.; Li, Y.; Liu, K.; Li, Z. *J. Am. Chem. Soc.* **2011**, *133*, 10756.

(10) (a) Guinaudeau, A.; Mazieres, S.; Wilson, D. J.; Destarac, M. *Polym. Chem.* **2012**, *3*, 81. (b) Tanaka, N.; Sato, E.; Matsumoto, A. *Org. Biomol. Chem.* **2011**, *9*, 3753.

(11) Srinivasan, K.; Perrier, S.; Kochi, J. K. *J. Mol. Catal.* **1986**, *36*, 297.

(12) (a) Baptistella, L. H. B.; Sousa, I. M. O.; Gushikem, Y.; Aleixo, A. M. *Tetrahedron Lett.* **1999**, *40*, 2695. (b) Fousteris, M. A.; Koutsourea, A. I.; Nikolaropoulos, S. S.; Riahi, A.; Muzart, J. *J. Mol. Catal. A Chem.* **2006**, *250*, 70. (c) Pearson, A. J.; Chen, Y. S.; Han, G. R.; Hsu, S. Y.; Ray, T. *J. Chem. Soc., Perkin Trans. 1* **1985**, 267.

(13) Shing, T. K. M.; Yeung, Y.-Y.; Su, P. L. *Org. Lett.* **2006**, *8*, 3149.

(14) Miller, R. A.; Li, W.; Humphrey, G. R. *Tetrahedron Lett.* **1996**, *37*, 3429.

(15) (a) Yu, J.-Q.; Corey, E. J. *J. Am. Chem. Soc.* **2003**, *125*, 3232. (b) Yu, J.-Q.; Corey, E. J. *Org. Lett.* **2002**, *4*, 2727.

(16) Salvador, J. A. R.; Silvestre, S. M. *Tetrahedron Lett.* **2005**, *46*, 2581.

(17) Marwah, P.; Marwah, A.; Lardy, H. A. *Green Chem.* **2004**, *6*, 570.

(18) Silvestre, S. M.; Salvador, J. A. R. *Tetrahedron* **2007**, *63*, 2439.

(19) McLaughlin, E. C.; Choi, H.; Wang, K.; Chiou, G.; Doyle, M. P. *J. Org. Chem.* **2009**, *74*, 730.

(20) (a) Kotani, E.; Takeya, T.; Egawa, H.; Tobinaga, S. *Chem. Pharm. Bull.* **1997**, *45*, 750. (b) Takeya, T.; Egawa, H.; Inoue, N.; Miyamoto, A.; Chuma, T.; Kotani, E. *Chem. Pharm. Bull.* **1999**, *47*, 64.

(21) (a) Li, Y.; Wu, X.; Lee, T. B.; Isbell, E. K.; Parish, E. J.; Gorden, A. E. V. *J. Org. Chem.* **2010**, *75*, 1807. (b) Arsenou, E. S.; Koutsourea, A. I.; Fousteris, M. A.; Nikolaropoulos, S. S. *Steroids* **2003**, *68*, 407. (c) Salvador, J. A. R.; Sa e Melo, M. L.; Campos Neves, A. S. *Tetrahedron Lett.* **1997**, *38*, 119.

(22) Catino, A. J.; Forslund, R. E.; Doyle, M. P. *J. Am. Chem. Soc.* **2004**, *126*, 13622.

(23) (a) Das, K.; Kadish, K. M.; Bear, J. L. *Inorg. Chem.* **1978**, *17*, 930. (b) Zhu, T. P.; Ahsan, M. Q.; Malinski, T.; Kadish, K. M.; Bear, J. L. *Inorg. Chem.* **1984**, *23*, 2.

(24) Moyer, B. A.; Thompson, M. S.; Meyer, T. J. *J. Am. Chem. Soc.* **1980**, *102*, 2310.

(25) Bokare, A. D.; Choi, W. *Environ. Sci. Technol.* **2011**, *45*, 9332.

(26) Catino, A. J.; Nichols, J. M.; Choi, H.; Gottipamula, S.; Doyle, M. P. *Org. Lett.* **2005**, *7*, 5167.

(27) (a) Barrett, A. G. M.; Hamprecht, D.; Meyer, T. *Chem. Commun.* **1998**, 809. (b) Ragot, J. P.; Steeneck, C.; Alcaraz, M.-L.; Taylor, R. J. K. *J. Chem. Soc., Perkin Trans. 1* **1999**, 1073.

(28) Barrett, A. G. M.; Blaney, F.; Campbell, A. D.; Hamprecht, D.; Meyer, T.; White, A. J. P.; Witty, D.; Williams, D. J. *J. Org. Chem.* **2002**, *67*, 2735.

(29) Choi, H.; Doyle, M. P. *Org. Lett.* **2007**, *9*, 5349.

(30) McLaughlin, E. C.; Doyle, M. P. *J. Org. Chem.* **2008**, *73*, 4317.

(31) (a) Waddell, M. K.; Bekele, T.; Lipton, M. A. *J. Org. Chem.* **2006**, *71*, 8372. (b) Zhang, X.; Sarkar, S.; Larock, R. C. *J. Org. Chem.* **2006**, *71*, 236. (c) Wang, C.; Forsyth, C. J. *Org. Lett.* **2006**, *8*, 2997.

(32) Catino, A. J.; Nichols, J. M.; Nettles, B. J.; Doyle, M. P. *J. Am. Chem. Soc.* **2006**, *128*, 5648.

(33) Choi, H.; Doyle, M. P. *Chem. Commun.* **2007**, 745.

(34) (a) Gu, Q.; Rong, Z.-Q.; Zheng, C.; You, S.-L. *J. Am. Chem. Soc.* **2010**, *132*, 4056. (b) Vo, N. T.; Pace, R. D. M.; O'Hara, F.; Gaunt, M. J. *J. Am. Chem. Soc.* **2008**, *130*, 404. (c) Barradas, S.; Carreno, M. C.; Gonzalez-Lopez, M.; Latorre, A.; Urbano, A. *Org. Lett.* **2007**, *9*, 5019.

(35) (a) Kirste, A.; Elsler, B.; Schnakenburg, G.; Waldvogel, S. R. *J. Am. Chem. Soc.* **2012**, *134*, 3571. (b) Kholdeeva, O. A.; Ivanchikova, I. D.; Zalomaeva, O. V.; Sorokin, A. B.; Skobelev, I. Y.; Talsi, E. P. *J. Phys. Chem. B* **2011**, *115*, 11971. (c) Owton, W. M. *J. Chem. Soc., Perkin Trans. 1* **1999**, 2409.

(36) Murahashi, S.-I.; Naota, T.; Miyaguchi, N.; Noda, S. *J. Am. Chem. Soc.* **1996**, *118*, 2509.

(37) Murahashi, S.-I.; Fujii, A.; Inubushi, Y.; Komiya, N. *Tetrahedron Lett.* **2010**, *51*, 2339.

(38) Murahashi, S.-I.; Zhang, D. *Chem. Soc. Rev.* **2008**, *37*, 1490.

(39) Murahashi, S.; Naota, T.; Yonemura, K. *J. Am. Chem. Soc.* **1988**, *110*, 8256.

(40) Seok, W. K.; Meyer, T. J. *J. Am. Chem. Soc.* **1988**, *110*, 7358.

(41) (a) Snelgrove, D. W.; Lusztyk, J.; Banks, J. T.; Mulder, P.; Ingold, K. U. *J. Am. Chem. Soc.* **2001**, *123*, 469. (b) MacFaul, P. A.; Arends, I. W. C. E.; Ingold, K. U.; Wayner, D. D. M. *J. Chem. Soc., Perkin Trans. 2* **1997**, 135.

(42) Blanksby, S. J.; Ellison, G. B. *Acc. Chem. Res.* **2003**, *36*, 255.

(43) Li, Z.; Bohle, D. S.; Li, C.-J. *Proc. Natl. Acad. Sci. U. S. A.* **2006**, *103*, 8928.

(44) Miyamoto, S.; Martinez, G. R.; Medeiros, M. H. G.; Di Mascio, P. *J. Am. Chem. Soc.* **2003**, *125*, 6172.

(45) (a) Zalomaeva, O. V.; Ivanchikova, I. D.; Kholdeeva, O. A.; Sorokin, A. B. *New J. Chem.* **2009**, *33*, 1031. (b) Beyrhouty, M.; Sorokin, A. B.; Daniele, S.; Hubert-Pfalzgraf, L. G. *New J. Chem.* **2005**, *29*, 1245. (c) Wong, W.-K.; Chen, X.-P.; Guo, J.-P.; Chi, Y.-G.; Pan, W.-X.; Wong, W.-Y. *J. Chem. Soc., Dalton Trans.* **2002**, 1139. (d) Pathak, R.; Rao, G. N. *J. Mol. Catal. A Chem.* **1998**, *130*, 215. (e) Ghera, E.; Ben-David, Y. *Tetrahedron Lett.* **1985**, *26*, 6253.

(46) (a) Villa, C.; Baldassari, S.; Gambaro, R.; Mariani, E.; Loupy, A. *Int. J. Cosmet. Sci.* **2005**, *27*, 11. (b) Mizuba, S.; Sheikh, W. *J. Ind. Microbiol.* **1987**, *1*, 363.

(47) (a) Amorati, R.; Pedulli, G. F.; Guerra, M. *Org. Biomol. Chem.* **2010**, *8*, 3136. (b) Foti, M. C.; Daquino, C.; Mackie, I. D.; DiLabio, G. A.; Ingold, K. U. *J. Org. Chem.* **2008**, *73*, 9270.

(48) Foerster, S.; Rieker, A.; Maruyama, K.; Murata, K.; Nishinaga, A. *J. Org. Chem.* **1996**, *61*, 3320.

(49) Doyle, M. P.; Westrum, L. J.; Wolthuis, W. N. E.; See, M. M.; Boone, W. P.; Bagheri, V.; Pearson, M. M. *Journal of the American Chemical Society* **1993**, *115*, 958.

(50) Crich, D.; Zou, Y. *J. Org. Chem.* **2005**, *70*, 3309.

(51) Iida, T.; Ogawa, S.; Hosoi, K.; Makino, M.; Fujimoto, Y.; Goto, T.; Mano, N.; Goto, J.; Hofmann, A. F. *J. Org. Chem.* **2007**, *72*, 823.

(52) Sato, K.; Tarui, A.; Matsuda, S.; Omote, M.; Ando, A.; Kumadaki, I. *Tetrahedron Lett.* **2005**, *46*, 7679.

(53) Xing, D.; Guan, B.; Cai, G.; Fang, Z.; Yang, L.; Shi, Z. *Org. Lett.* **2006**, *8*, 693.

(54) Yin, W.-P.; Shi, M. *J. Chem. Res.* **2006**, 549.

(55) Stylianides, N.; Danopoulos, A. A.; Pugh, D.; Hancock, F.; Zanotti-Gerosa, A. *Organometallics* **2007**, *26*, 5627.

(56) Caron, L.; Campeau, L.-C.; Fagnou, K. *Org. Lett.* **2008**, *10*, 4533.

(57) (a) Pitsinos, E. N.; Cruz, A. *Org. Lett.* **2005**, *7*, 2245. (b) Mendelsohn, B. A.; Ciufolini, M. A. *Org. Lett.* **2009**, *11*, 4736.

(58) (a) You, Z.; Hoveyda, A. H.; Snapper, M. L. *Angew. Chem., Int. Ed.* **2009**, *48*, 547. (b) Cha, J. Y.; Huang, Y.; Pettus, T. R. R. *Angew. Chem., Int. Ed.* **2009**, *48*, 9519.

(59) (a) Evans, D. A.; Wu, J. *J. Am. Chem. Soc.* **2003**, *125*, 10162. (b) Takagi, R.; Miyanaga, W.; Tojo, K.; Tsuyumine, S.; Ohkata, K. *J. Org. Chem.* **2007**, *72*, 4117.

(60) Redondo, M. C.; Ribagorda, M.; Carreno, M. C. *Org. Lett.* **2010**, *12*, 568.

(61) Hayashi, Y.; Gotoh, H.; Tamura, T.; Yamaguchi, H.; Masui, R.; Shoji, M. *J. Am. Chem. Soc.* **2005**, *127*, 16028.

(62) Tello-Aburto, R.; Kalstabakken, K. A.; Volp, K. A.; Harned, A. M. *Org. Biomol. Chem.* **2011**, *9*, 7849.

(63) Gu, Q.; You, S.-L. *Org. Lett.* **2011**, *13*, 5192.

(64) (a) Wenderski, T. A.; Huang, S.; Pettus, T. R. R. *J. Org. Chem.* **2009**, *74*, 4104. (b) Yang, H.; Hou, A.-J.; Mei, S.-X.; Sun, H.-D.; Che, C.-T. *J. Asian Nat. Prod. Res.* **2002**, *4*, 165. (c) Tian, J.; Zhao, Q.-S.; Zhang, H.-J.; Lin, Z.-W.; Sun, H.-D. *J. Nat. Prod.* **1997**, *60*, 766. (d) Hase, T.; Kawamoto, Y.; Ohtani, K.; Kasai, R.; Yamasaki, K.; Picheansoonthon, C. *Phytochemistry* **1995**, *39*, 235.

(65) (a) Shchepin, R.; Moller, M. N.; Kim, H.-y. H.; Hatch, D. M.; Bartesaghi, S.; Kalyanaraman, B.; Radi, R.; Porter, N. A. *J. Am. Chem. Soc.* **2010**, *132*, 17490. (b) Masuda, T.; Akiyama, J.; Fujimoto, A.; Yamauchi, S.; Maekawa, T.; Sone, Y. *Food Chem.* **2010**, *123*, 442.

(66) Robinson, T. V.; Taylor, D. K.; Tiekink, E. R. T. *J. Org. Chem.* **2006**, *71*, 7236.

(67) Doyle, M. P.; Westrum, L. J.; Wolthuis, W. N. E.; See, M. M.; Boone, W. P.; Bagheri, V.; Pearson, M. M. *J. Am. Chem. Soc.* **1993**, *115*, 958.

(68) (a) Terada, M.; Toda, Y. *J. Am. Chem. Soc.* **2009**, *131*, 6354. (b) Cheon, C. H.; Yamamoto, H. *J. Am. Chem. Soc.* **2008**, *130*, 9246.

(69) Nakamura, K.; Nakajima, T.; Kayahara, H.; Nomura, E.; Taniguchi, H. *Tetrahedron Lett.* **2004**, *45*, 495.

(70) Ray, S.; Das, A. K.; Banerjee, A. *Chem. Commun.* **2006**, 2816.

(71) (a) Casiraghi, G.; Battistini, L.; Curti, C.; Rassu, G.; Zanardi, F. *Chem. Rev.* **2011**, *111*, 3076. (b) Toure, B. B.; Hall, D. G. *Chem. Rev.* **2009**, *109*, 4439.

(72) (a) Murahashi, S.-i.; Komiya, N. In *Modern Oxidation Methods*; 2nd ed.; Baeckvall, J.-E., Ed.; Wiley-VCH: Weinheim, Germany, 2010. (b) Li, C.-J. *Acc. Chem. Res.* **2009**, *42*, 335. (c) Arend, M.; Westermann, B.; Risch, N. *Angew. Chem., Int. Ed.* **1998**, *37*, 1045.

(73) Murahashi, S.-I.; Nakae, T.; Terai, H.; Komiya, N. *J. Am. Chem. Soc.* **2008**, *130*, 11005.

(74) (a) Rueping, M.; Vila, C.; Koenigs, R. M.; Poscharny, K.; Fabry, D. C. *Chem. Commun.* **2011**, *47*, 2360. (b) Wang, M.-Z.; Zhou, C.-Y.; Wong, M.-K.; Che, C.-M. *Chem.--Eur. J.* **2010**, *16*, 5723. (c) Murahashi, S.; Komiya, N.; Terai, H.; Nakae, T. *J. Am. Chem. Soc.* **2003**, *125*, 15312. (d) Condie, A. G.; Gonzalez-Gomez, J. C.; Stephenson, C. R. J. *J. Am. Chem. Soc.* **2010**, *132*, 1464.

(75) (a) Boess, E.; Schmitz, C.; Klussmann, M. *J. Am. Chem. Soc.* **2012**, *134*, 5317. (b) Boess, E.; Sureshkumar, D.; Sud, A.; Wirtz, C.; Fares, C.; Klussmann, M. *J. Am. Chem. Soc.* **2011**, *133*, 8106. (c) Yang, F.; Li, J.; Xie, J.; Huang, Z.-Z. *Org. Lett.* **2010**, *12*, 5214. (d) Zhao, L.; Li, C.-J. *Angew. Chem., Int. Ed.* **2008**, *47*, 7075. (e) Xie, J.; Huang, Z.-Z. *Angew. Chem., Int. Ed.* **2010**, *49*, 10181.

(76) (a) Han, W.; Ofial, A. R. *Chem. Commun.* **2009**, 5024. (b) Kumaraswamy, G.; Murthy, A. N.; Pitchaiah, A. *J. Org. Chem.* **2010**, *75*, 3916. (c) Ghobrial, M.; Schnuerch, M.; Mihovilovic, M. D. *J. Org. Chem.* **2011**, *76*, 8781. (d) Liu, P.; Zhou, C.-Y.; Xiang, S.; Che, C.-M. *Chem. Commun.* **2010**, *46*, 2739.

(77) Alagiri, K.; Prabhu, K. R. *Org. Biomol. Chem.* **2012**, *10*, 835.

(78) (a) Sud, A.; Sureshkumar, D.; Klussmann, M. *Chem. Commun.* **2009**, 3169. (b) Singhal, S.; Jain, S. L.; Sain, B. *Chem. Commun.* **2009**, 2371.

(79) Volla, C. M. R.; Vogel, P. *Org. Lett.* **2009**, *11*, 1701.

(80) (a) Sureshkumar, D.; Sud, A.; Klussmann, M. *Synlett* **2009**, 1558. (b) Chu, L.; Zhang, X.; Qing, F.-L. *Org. Lett.* **2009**, *11*, 2197.

(81) Li, Z.; Li, C.-J. *J. Am. Chem. Soc.* **2005**, *127*, 6968.

(82) Murata, S.; Teramoto, K.; Miura, M.; Nomura, M. *Bull. Chem. Soc. Jpn.* **1993**, *66*, 1297.

(83) Shen, Y.; Li, M.; Wang, S.; Zhan, T.; Tan, Z.; Guo, C.-C. *Chem. Commun.* **2009**, 953.

(84) (a) Li, Z.; Li, C.-J. *J. Am. Chem. Soc.* **2005**, *127*, 3672. (b) Basle, O.; Li, C.-J. *Green Chem.* **2007**, *9*, 1047. (c) Zeng, T.; Song, G.; Moores, A.; Li, C.-J. *Synlett* **2010**, 2002.

(85) Li, Z.; Li, C.-J. *Eur. J. Org. Chem.* **2005**, 3173.

(86) Ohta, M.; Quick, M. P.; Yamaguchi, J.; Wuensch, B.; Itami, K. *Chem.--Asian J.* **2009**, *4*, 1416.

(87) Basle, O.; Li, C.-J. *Org. Lett.* **2008**, *10*, 3661.

(88) (a) Zhang, Y.; Fu, H.; Jiang, Y.; Zhao, Y. *Org. Lett.* **2007**, *9*, 3813. (b) Basle, O.; Li, C.-J. *Chem. Commun.* **2009**, 4124. (c) Han, W.; Ofial, A. R. *Chem. Commun.* **2009**, 6023.

(89) Murahashi, S.; Naota, T.; Miyaguchi, N.; Nakato, T. *Tetrahedron Lett.* **1992**, *33*, 6991.

(90) Heimbrook, D. C.; Murray, R. I.; Egeberg, K. D.; Sligar, S. G.; Nee, M. W.; Bruice, T. C. *J. Am. Chem. Soc.* **1984**, *106*, 1514.

(91) Burka, L. T.; Guengerich, F. P.; Willard, R. J.; Macdonald, T. L. *J. Am. Chem. Soc.* **1985**, *107*, 2549.

(92) Murahashi, S.-I. *Angew. Chem., Int. Ed. Engl.* **1995**, *34*, 2443.

(93) (a) Goto, Y.; Watanabe, Y.; Fukuzumi, S.; Jones, J. P.; Dinnocenzo, J. P. *J. Am. Chem. Soc.* **1998**, *120*, 10762. (b) Shono, T.; Toda, T.; Oshino, N. *J. Am. Chem. Soc.* **1982**, *104*, 2639. (c) Miwa, G. T.; Garland, W. A.; Hodshon, B. J.; Lu, A. Y. H.; Northrop, D. B. *J. Biol. Chem.* **1980**, *255*, 6049. (d) Miwa, G. T.; Walsh, J. S.; Kedderis, G. L.; Hollenberg, P. F. *J. Biol. Chem.* **1983**, *258*, 14445.

(94) (a) Murahashi, S.-I.; Komiya, N.; Oda, Y.; Kuwabara, T.; Naota, T. *J. Org. Chem.* **2000**, *65*, 9186. (b) Murahashi, S.; Oda, Y.; Naota, T. *J. Am. Chem. Soc.* **1992**, *114*, 7913.

(95) Arasasingham, R. D.; Cornman, C. R.; Balch, A. L. *J. Am. Chem. Soc.* **1989**, *111*, 7800.

(96) Li, Z.; Li, C.-J. *Org. Lett.* **2004**, *6*, 4997.

(97) Barton, D. H. R.; Beviere, S. D.; Chavasiri, W.; Csuhai, E.; Doller, D. *Tetrahedron* **1992**, *48*, 2895.

(98) Wang, F.; Sayre, L. M. *J. Am. Chem. Soc.* **1992**, *114*, 248.

(99) Minisci, F.; Fontana, F.; Araneo, S.; Recupero, F.; Banfi, S.; Quici, S. *J. Am. Chem. Soc.* **1995**, *117*, 226.

(100) Griller, D.; Howard, J. A.; Marriott, P. R.; Scaiano, J. C. *J. Am. Chem. Soc.* **1981**, *103*, 619.

(101) Dombrowski, G. W.; Dinnocenzo, J. P.; Zielinski, P. A.; Farid, S.; Wosinska, Z. M.; Gould, I. R. *J. Org. Chem.* **2005**, *70*, 3791.

(102) Basle, O.; Borduas, N.; Dubois, P.; Chapuzet, J. M.; Chan, T.-H.; Lessard, J.; Li, C.-J. *Chem.--Eur. J.* **2010**, *16*, 8162.

(103) Das, T. N.; Dhanasekaran, T.; Alfassi, Z. B.; Neta, P. *J. Phys. Chem. A* **1998**, *102*, 280.

(104) Bietti, M.; Di Labio, G. A.; Lanzalunga, O.; Salamone, M. *J. Org. Chem.* **2010**, *75*, 5875.

(105) Barrett, A. G. M.; Doubleday, W. W.; Tustin, G. J.; White, A. J.; Williams, D. J. *J. Chem. Soc., Chem. Commun.* **1994**, 1783.

(106) (a) Beckwith, A. L. J.; Bowry, V. W. *J. Org. Chem.* **1989**, *54*, 2681. (b) Newcomb, M.; Manek, M. B. *J. Am. Chem. Soc.* **1990**, *112*, 9662.

(107) van Oeveren, A.; Motamedi, M.; Mani, N. S.; Marschke, K. B.; Lopez, F. J.; Schrader, W. T.; Negro-Vilar, A.; Zhi, L. *J. Med. Chem.* **2006**, *49*, 6143.

(108) Zhang, X.; Yeh, S.-R.; Hong, S.; Freccero, M.; Albini, A.; Falvey, D. E.; Mariano, P. S. *J. Am. Chem. Soc.* **1994**, *116*, 4211.

(109) Karki, S. B.; Dinnocenzo, J. P.; Jones, J. P.; Korzekwa, K. R. *J. Am. Chem. Soc.* **1995**, *117*, 3657.

(110) Dinnocenzo, J. P.; Karki, S. B.; Jones, J. P. *J. Am. Chem. Soc.* **1993**, *115*, 7111.

(111) Martin, S. F.; Barr, K. J.; Smith, D. W.; Bur, S. K. *J. Am. Chem. Soc.* **1999**, *121*, 6990.

(112) Gupton, J. T.; Idoux, J. P.; Baker, G.; Colon, C.; Crews, A. D.; Jurss, C. D.; Rampi, R. C. *J. Org. Chem.* **1983**, *48*, 2933.

(113) Seim, K. L.; Obermeyer, A. C.; Francis, M. B. *J. Am. Chem. Soc.* **2011**, *133*, 16970.

(114) Dvornikova, K. V.; Platonov, V. E.; Yakobson, G. G. *J. Fluorine Chem.* **1978**, *11*, 1.

(115) Shearer, J.; Zhang, C. X.; Hatcher, L. Q.; Karlin, K. D. *J. Am. Chem. Soc.* **2003**, *125*, 12670.

(116) Loeppky, R. N.; Singh, S. P.; Elomari, S.; Hastings, R.; Theiss, T. E. *J. Am. Chem. Soc.* **1998**, *120*, 5193.